Local Adaptation Portends Tradeoffs Between Leaf Cooling and Hydraulic Risk in an

Arid Land Riparian Tree Species (*Populus Fremontii*)

by

Davis Blasini

A Dissertation Presented in Partial Fulfillment
of the Requirements for the Degree
Doctor of Philosophy

Approved November 2022 by the
Graduate Supervisory Committee:

Kevin Hultine, Co-Chair
Thomas Day, Co-Chair
Roberto Gaxiola
Kiona Ogle
Heather Throop

ARIZONA STATE UNIVERSITY

December 2022

ABSTRACT

Climate change is making the arid southwestern U.S. ("Southwest") warmer and

drier. Decreases in water availability coupled with increases in episodic heat waves can

pose extraordinary challenges for native riparian tree species to persist in their current

ranges. However, the morpho-physiological mechanisms that these species deploy to

cope with extreme temperature events are not well understood. Specifically, how do these

species maintain leaf temperatures within a safe operational threshold in the extreme

conditions found across the region? Morpho-physiological mechanisms influencing

intraspecific local adaptation to thermal stress were assessed in *Populus fremontii* using

two experimental common gardens. In a common garden located near the mid-point of

this species' thermal distribution, I studied coordinated traits that reflect selection for leaf

thermal regulation through the measurement of 28 traits encompassing four different trait

spectra: phenology, whole-tree architecture, and the leaf and wood economic spectrum.

Also, I assessed how these syndromes resulted in more acquisitive and riskier water-use

strategies that explained how warm-adapted populations exhibited lower leaves

temperatures than cool-adapted populations. Then, I investigated if different water-use

strategies are detectable at inter-annual temporal scales by comparing tree-ring growth,

carbon, and oxygen isotopic measurements of cool- versus warm-adapted populations in

a common garden located at the extreme hottest edge of *P. fremontii's* thermal

distribution. I found that *P. fremontii's* adaptation to the extreme temperatures is

explained by a highly intraspecific specialized trait coordination across multiple trait

scales. Furthermore, I found that warmer-adapted populations displayed 39% smaller

leaves, 38% higher midday stomatal conductance, reflecting 3.8 °C cooler mean leaf

i

temperature than cool-adapted populations, but with the tradeoff of having 14% lower minimum leaf water potentials. In addition, warm-adapted genotypes at the hot edge of *P. fremontii's* distribution had 20% higher radial growth rates, although no differences were detected in either carbon or oxygen isotope ratios indicating that differences in growth may not have reflected seasonal differences in photosynthetic gas exchange. These studies describe the potential effect that extreme climate might have on *P. fremontii's* survival, its intraspecific responses to those events, and which traits will be advantageous to cope with those extreme environmental conditions.

DEDICATION

I would like to dedicate this work to my childhood hero, Alexander Von Humboldt, for inspiring me to explore and study our natural world and the most important of all the living organisms in this planet, photosynthesizers. My native and adopted countries, Venezuela, and the United States of America, for giving me the opportunity to fall in love with nature and pursue my dreams of becoming an advocate of the study of our natural world. I also dedicate this work to my mother, Eddy, and wife, Natalie, for being there for me throughout this entire doctorate program.

ACKNOWLEDGMENTS

TABLE OF CONTENTS

v

LIST OF TABLES

1. DISSERTATION INTRODUCTION

Ecosystems across the southwestern United States ("Southwest") have been experiencing significant increases of annual temperatures, more frequent and longer extreme heatwaves, and drought severity intensification because of anthropogenic climate change (Diffenbaugh et al. 2011; Seager et al. 2015; Garfin et al. 2013, Williams et al. 2013). During the first two decades of the present century, the Southwest has experienced the most profound megadrought in over a millennium (Williams et al. 2022). Consequently, dominant plant species in the region could become increasingly maladapted to changing environmental conditions in the near future (Allen and Breshears 1998, Adams et al. 2009; Gitlin et al. 2006; Hultine et al. 2013). The abundance, composition, and distribution of riparian tree species in the Southwest are expected to be especially susceptible to climate change because these species already live near their physiological limits for temperature and water stress (Archer and Predick 2008; Hultine et al. 2019, 2020). In particular, the foundation tree species Fremont cottonwood (*Populus fremontii*) has experienced extensive reduction of its historical habitat due to land use change, alteration of flow regimes, climate change, and exotic species invasions during the last century (Merritt and Poff, 2010; Noss et al. 1995; Hultine et al. 2020). In this dissertation, I examine the morpho-physiological mechanisms that the native riparian tree species, *Populus fremontii*, express to cope with extreme thermal stress.

Air temperature directly impacts plant physiology by the influence it has on the rates of photosynthesis and respiration (Fauset et al. 2018) and indirectly by increasing the atmospheric moisture-holding capacity, or ambient vapour pressure deficit (VPD) (Weiss et al. 2009, Breshears et al. 2013; Williams et al. 2013). Increases in air

temperature and its associated VPD have the potential to simultaneously lower soil moisture and increase evapotranspiration demand in plants (Breshears et al. 2009; McDowell et al. 2010; Meddens et al. 2014). Because higher VPD increases the water potential gradient along the soil – plant – atmospheric continuum, plants that use stomatal regulation to maintain a near constant minimum leaf water potential regardless of the environmental conditions (isohydric) do so by closing their stomata to avoid excessive water loss (Addington et al. 2004; McDowell et al. 2008; Oren et al. 1999). Consequently, isohydric plants, like *P. fremontii*, are expected to become more susceptible to hydraulic failure or carbon starvation as a consequence of climate change (McDowell et al. 2010). Additionally, exposure to extreme temperatures can negatively disrupt cell membrane integrity and photosynthetic metabolism (Hazel, 1995). Therefore, the ability to regulate leaf temperature near its optima for photosynthesis and avoid thermal damage is increasingly becoming crucial for plant survival under future climate change scenarios (Fauset et al. 2018).

Stomatal conductance plays a key role in plant water and carbon fluxes because it regulates the partial pressure of CO_2 at the site of carboxylation and the transpiration rates (Farquhar and Sharkey 1982). Simultaneously, changes in stomatal conductance provide a way for plants to modify the water potential and temperature of their leaves (Drake et al. 2018; Sack et al. 2003; Urban et al. 2017). Specifically, leaf temperature can be maintained at optimal and safe levels for photosynthesis and thermal damage through the influence that stomatal conductance has on transpiration and latent cooling (Horton et al. 2001; Urban et al. 2017; Drake et al. 2018). Besides stomatal conductance, there are other leaf functional traits that can help maintain leaf temperatures within a safe range of

2

variation around metabolic optima (Fauset et al. 2018; Michaletz et al. 2015). Because of its influence on the leaf boundary layer and its sensible heat exchange with the surrounding air, leaf size is a morphological trait that can display a great control on leaf temperatures (Wright et al. 2017). For instance, smaller leaves exhibit faster sensible heat exchange with the surrounding air because of their thinner boundary layers (Leigh et al. 2017, Wright et al. 2017). Therefore, smaller leaves display smaller leaf-to-air temperature differences than larger leaves (Leigh et al. 2017). Consequently, most plant species found in arid-hot ecosystems around the world have smaller leaves (Wright et al. 2017). Under projected climate change scenarios, broad-leaved plants will face an increasing risk of their leaves reaching extreme temperature that would result in significant structural and functional damage, especially under water limited conditions.

Analysis of morpho-physiological functional traits from individual organs to whole-plant scales can help us better understand the key mechanisms behind the trade-offs between life span and productivity and therefore local climatic adaptation in tree species (Chapin et al. 1993; Wright et al. 2004; Chave et al. 2009). Extensive analyses of numerous functional traits in a wide variety of plants representing most terrestrial ecosystems of the world have led to the identification of consistent associations of plant functional traits known as trait spectra. Key trait spectra include the leaf economic spectrum (LES) (Wright et al. 2004), the wood economic spectrum (WS) (Chave et al. 2009), Corner's Rules (CR) (Corner 1949), the fast-slow economics spectra (Wright et al. 2004), and more recently the whole plant economic spectrum (Diaz et al. 2016). These different trait spectra pool traits in ways that reveal the physiological relationships and trade-offs among traits that underlie plant performance in terms of growth and survival

3

from single organs to whole-plants (Chave et al. 2009; Diaz et al. 2016; Freschet et al. 2010; Reich, 2014).

Although it is known that species with wide geographic distributions can display significant functional trait variation across environmental gradients, single species investigations on trait variability at the whole-tree level has been limited. Because variations in specific functional traits are caused by the complex relationship among physiologically related traits and local environmental pressures, many traits can be expressed differently at the intraspecific level (Laforest-Lapointe, Martinez-Vilalta, and Retana, 2014). Accordingly, single species can display significant differences in particular suite of traits (an adaptive trait syndrome) that make different populations adapted to their unique local environments (Sartori et al. 2019). There is evidence suggesting that climate change-driven maladaptation may vary among populations within the same species (O'Neill et al. 2008). This can be especially true for plant species with wide range distributions (Walther et al. 2002). By identifying the coordinated set of functional traits at the whole-plant level, we might be able to develop better ways to predict how a species will be affected by climate change throughout its entire geographic range.

Experimental common gardens can be an extremely powerful tool to identify intraspecific trait characteristics in species with wide geographic and climatic distributions because they homogenize the influence that the environment has on the physiology and performance of plants (Schwinning et al. 2022). Because common garden studies accurately identify the relationships between climate of source populations and their functional traits (Schwinning et al. 2022), these studies have played a crucial role in

the study of climate adaptation in plants. Consequently, these types of investigations can help us to gain a better understanding of the impact that climate change will have on locally-adapted populations because they allow the transfer of populations from their source sites to a warmer climate garden site (Franks et al. 2014; Huxman et al. 2021). The use of experimental common gardens experiments with species exhibiting wide geographic distribution provides extraordinary opportunities to evaluate intraspecific differences in adaptive trait syndromes. Thus, we can identify the specific mechanistic forces guiding climatic adaptation at the population level.

This investigation explores the role that morpho-physiological traits at multiple scales have on climate adaptation in *P. fremontii*. Specifically, this dissertation uses such trait data to investigate the challenges of maintaining leaf temperature within an optimal range for photosynthesis under predicted climate change. Thus, this dissertation consists of three research chapters (Chapters 2 - 4) and a summary that integrates across chapters (Chapter 5). Following is a brief introduction of each of these chapters.

Chapter 2 ("Adaptive trait syndromes along multiple economic spectra define cold and warm adapted ecotypes in a widely distributed foundation tree species") was published in the *Journal of Ecology* (Blasini et al. 2020). In this study, I used an experimental common garden located near the mid-point of *P. fremontii's* thermal distribution. I studied the quantifiable trait syndromes that reflect selection for leaf thermal regulation through the measurement of a wide suite of traits. In the case of *P. fremontii*, its climate gradient comprises both extreme high temperatures experienced by the Sonoran Desert ecotype and freezing temperatures in the high-desert Mogollon Rim ecotype. Therefore, in this study, I completed a comprehensive investigation of the

intraspecific differences in functional trait coordination at multi-organ levels through the measurements of 28 traits encompassing four different trait spectra: phenology, whole-tree architecture, and the leaf and wood economic spectrum. The results from this study revealed highly specialized trait spectra coordination that explain *P. fremontii's* adaptation to the two very distinct regional climate conditions of the two ecotypes present in this study. On one hand, the high-desert Mogollon Rim ecotype exhibited a coordinated set of traits that avoids damage from freezing temperatures and maximizes growth, while the Sonoran Desert ecotype displays a combination of traits that support greater water transport efficiency to reduce foliar thermal loads via enhanced evaporative cooling. Additionally, this investigation detected finer differences at the population level that reflect gradual adaptation strategies to more local environmental conditions.

Chapter 3 ("Tradeoffs between leaf cooling and hydraulic safety in a dominant arid land riparian tree species") was published in *Plant, Cell, and Environment* (Blasini et al. 2022). In this study, I used the same experimental common garden from chapter 2, but I analyzed the intraspecific differences in leaf thermoregulation strategies between warm-(>40°C maximum summer temperature) and cool-adapted (<40°C maximum summer temperature) genotypes of *P. fremontii*. Through measurements of leaf temperatures, I evaluated three potential methods of leaf thermoregulation: leaf morphology (sensible heat loss), midday canopy stomatal conductance (latent heat loss) and stomatal sensitivity to vapor pressure deficit (latent heat loss under dry atmospheric conditions). It was found that warm-adapted genotypes exhibited a suite of morpho-physiological traits and hydraulic strategies that simultaneously reduce leaf radiative load gain while increasing evaporative cooling. However, these results also suggest that to maintain leaf temperature

within optimal levels, warm-adapted genotypes display high stomatal conductance during extreme hot and dry conditions. By doing this, warm-adapted genotypes could undergo dangerous declines in their leaf turgor and xylem conductivity even under optimal soil moisture conditions. Thus, the results from this study indicate that warm-adapted genotypes might become highly vulnerable to episodic soil water deficits due to their risky hydraulic strategy to maximize leaf cooling. Accordingly, warm-adapted *P. fremontii* genotypes would be strictly limited to occupy locations with perennial water access to survive.

In Chapter 4 ("Radial growth decreases with enhanced heat stress while canopy stomatal conductance, inferred from $\delta^{13}C$ and $\delta^{18}O$ of tree-ring cellulose does not in a warm-desert riparian tree species"), I investigated multi-year tree growth and physiological responses to extreme temperatures in *P. fremontii* genotypes in a common garden located at the hot edge of this species thermal distribution. Radial growth and $\delta^{13}C$ in tree-ring holocellulose were measured to assess plant water status, and $\delta^{18}O$ in tree-ring α-cellulose was used to estimate the physiological adjustments in stomatal conductance at the population level. I found that populations sourced from provenances with cooler mean annual maximum temperature (MAMT) than the garden displayed lower radial growth rates than populations with similar MAMT of the garden. However, contrary to my expectations, I did not find a meaningful correlation between growth and either of the two isotopic tree-ring measurements, $\delta^{13}C$ or $\delta^{18}O$. These results underline the potential adverse effect that warming climate will have on aboveground productivity on *P. fremontii* regardless of its impacts on stomatal conductance.

In Chapter 5 ("Dissertation summary"), I conclude by discussing the contribution that this work (from Chapters 2, 3, and 4) provides to our current understanding of leaf thermoregulation and functional trait ecology and how my investigations contribute to future research involving these topics.

References

Adams HD, Guardiola-Claramonte M, Barron-Gafford GA, Villegas JC, Breshears DD, Zou CB, Troch PA, Huxman TE (2009) Temperature sensitivity of drought-induced tree mortality portends increased regional die-off under global-change-type drought. Proceedings of the National Academy of Sciences of the United States of America 106:7063–6. https://doi.org/10.1890/ES15-00203.1

Addington RN, Mitchell RJ, Oren R, Donovan LA (2004) Stomatal sensitivity to vapor pressure deficit and its relationship to hydraulic conductance in *Pinus palustris*. Tree Physiology 24:561–569. https://doi.org/10.1093/treephys/24.5.561

Allen CD, Breshears DD (1998) Drought-induced shift of a forest-woodland ecotone: rapid landscape response to climate variation. Proceedings of the National Academy of Science of the United States of America 95:14839–42. https://doi.org/10.1073/pnas.95.25.14839

Archer SR, Predick KI (2008). Climate Change and Ecosystems of the Southwestern. United States Rangelands 30(3):23–28. https://doi.org/10.2111/1551-501X(2008)30[23:CCAEOT]2.0.CO;2

Blasini, DE, Koepke DF, Bush, SE, Allan GJ, Gehring CA, Whitham TG, Day T, Hultine KR (2022) Tradeoffs between leaf cooling and hydraulic safety in a dominant arid land riparian tree species. Plant, Cell and Environment 1–18. https://doi.org/10.1111/pce.14292

Blasini DE, Koepke DF, Grady KC, Allan GJ, Gehring CA, Whitham TG, Cushman SA, Hultine KR (2020) Adaptive trait syndromes along multiple economic spectra define cold and warm adapted ecotypes in a widely distributed foundation tree species. Journal of Ecology 1–21. https://doi.org/10.1111/1365-2745.13557

Breshears DD, Adams HD, Eamus D, McDowell NG, Law DJ, Will RE, Williams AP, Zou CB (2013) The critical amplifying role of increasing atmospheric moisture demand on tree mortality and associated regional die-off. Frontiers in Plant Science 4, 266. https://doi.org/10.3389/fpls.2013.00266

Breshears DD, Myers OB, Meyer CW, Barnes FJ, Zou CB, Allen CD, McDowell NG, Pockman, WT (2009) Tree die-off in response to global change-type drought: mortality insights from a decade of plant water potential measurements. Frontiers in Ecology and the Environment 7, 185-189. https://esajournals.onlinelibrary.wiley.com/doi/abs/10.1890/080016

Chapin FS, Autumn K, Pugnaire S (1993) Evolution of Suites of Traits in Response to Environmental Stress. The American Naturalist 142: S78-S92. https://doi.org/10.1086/285524

Chave J, Coomes D, Jansen S, Lewis SL, Swenson NG, Zanne AE (2009) Towards a worldwide wood economics spectrum. Ecology Letters 12(4), 351–366. https://doi.org/10.1111/j.1461-0248.2009.01285.x

Corner EJH (1949) The Durian theory or the origin of the modern tree. Annals of Botany 13(4), 367–414. https://doi.org/10.1093/oxfordjournals.aob.a083225

Diaz S, Kattge K, Cornelissen JH, Wright IJ, Lavorel S, Dray S, Reu B, Kleyer M, Wirth C, Prentice IC, Garnier E, Bonisch G, Westoby M, Poorter H, Reich PB, Moles AT, Dickie J, Gillison AN, Zanne AE, Chave J, Wright SJ, Sheremet'ev SN, Jactel H, Baraloto C, Cerabolini B, Pierce S, Shipley B, Kirkup D, Casanoves F, Joswig JS, Gunther A, Falczuk V, Ruger N, Mahecha MD, Gorne LD (2016) The global spectrum of plant form and function. Nature 529, 167–171. https://doi.org/10.1038/nature16489

Diffenbaugh NS, Ashfaq M, Scherer M (2011) Transient regional climate change: Analysis of the summer climate response in a high-resolution, century-scale ensemble experiment over the continental United States. Journal of geophysical research 116, D24111. https://doi.org/10.1029/2011JD016458

Drake JE, Tjoelker MG, Vårhammar A, Medlyn BE, Reich PB, Leigh A, Pfautsch S, Blackman CJ, López R, Aspinwall MJ, Crous KY, Duursma RA, Kumarathunge D, De Kauwe MG, Jiang M, Nicotra AB, Tissue DT, Choat B, Atkin OK, Barton CVM (2018) Trees tolerate an extreme heatwave via sustained transpirational cooling and increased leaf thermal tolerance. Global Change Biology 24(6), 2390–2402. https://doi.org/10.1111/gcb.14037

Fauset S, Freitas HC, Galbraith DR, Sullivan MJP, Aidar MPM, Joly CA (2018) Differences in leaf thermoregulation and water use strategies between three co-occurring Atlantic forest tree species: leaf energy balance of Atlantic forest trees. Plant, Cell and Environment 41, 1618–1631. https://doi.org/10.1111/pce.13208

Farquhar GD, Sharkey TD (1982) Stomatal conductance and photosynthesis. Annual Review of Plant Physiology 33, 317–345. https://doi.org/10.1146/annurev.pp.33.060182.001533

Franks SJ, Weber JJ, Aitken SN (2014) Evolutionary and plastic responses to climate change in terrestrial plant populations. Evolutionary Applications 7, 123–139. https://doi.org/10.1111/eva.12112

Freschet GT, Cornelissen JHC, van Logtestijn RSP, Aerts R (2010) Evidence of the 'plant economics spectrum' in a subarctic flora. Journal of Ecology 98(2), 362 373. https://doi.org/10.1111/j.1365-2745.2009.01615.x

Garfin G, Jardine A, Merideth R, Black M, LeRoy S (Eds.) (2013) Assessment of Climate Change in the Southwest United States. Natl Clim Assess Reg Tech Input Rep Ser Assess 531. https://doi.org/10.5822/978-1-61091-484-0

Gitlin AR, Sthultz CM, Bowker MA, Stumpf S, Paxton KL, Kennedy K, Muñoz A, Bailey JK, Whitham TG (2006) Mortality gradients within and among dominant plant populations as barometers of ecosystem change during extreme drought. Conservation Biology 20, 1477–86. https://doi.org/10.1111/j.1523-1739.2006.00424.x

Hazel JR (1995) Thermal adaptation in biological membranes: is home viscous adaptation the explanation? Annual Review of Physiology 57, 19–42. https://doi.org/10.1146/annurev.ph.57.030195.000315

Horton R, Buck T, Waterson P (2001) Explaining intranet use with the technology acceptance model. J Inf Technol 16, 237–249. https://doi.org/10.1080/02683960110102407

Hultine KR, Allan GJ, Blasini DE, Bothwell HM, Cadmus A, Cooper HF, Doughty CE, Gehring CA, Gitlin AR, Grady KC, Keith AR, Koepke DF, Markovchick L, Corbin Parker JM, Sankey TT, Whitham TG (2020) Adaptive capacity in the foundation tree species *Populus fremontii:* implications for resilience to climate change and non-native species invasion in the American Southwest. Conservation Physiology 8(1), coaa061. https://doiorg.ezproxy1.lib.asu.edu/10.1093/conphys/coaa061

Hultine KR, Burtch KG, Ehleringer JR (2013). Gender specific patterns of carbon uptake and water use in a dominant riparian tree species exposed to a warming climate. Global Change Biology 19(11), 3390–3405. https://onlinelibrary.wiley.com/doi/10.1111/gcb.12230

Hultine KR, Froend R, Blasini D, Bush SE, Karlinski M, Koepke DF (2019) Hydraulic traits that buffer deep-rooted plants from changes in hydrology and climate. Hydrological Processes, 1–14. https://doi.org/10.1002/hyp.13587

Huxman TE, Winkler DE, Mooney KA (2022) A common garden super-experiment: An impossible dream to inspire possible synthesis. Journal of Ecology 110, 997–1004. https://doi.org/10.1111/1365-2745.13793

Ikeda DH, Max TL, Allan GJ, Lau MK, Shuster SM, Whitham TG (2017) Genetically informed ecological niche models improve climate change predictions. Global Change Biology 23, 164–176. https://doi.org/10.1111/gcb.13470

Laforest-Lapointe I, Martínez-Vilalta J, Retana J (2014) Intraspecific variability in functional traits matters: case study of Scots pine. Oecologia 175(4):1337–48. https://doi.org/10.1007/s00442-014-2967-x

Leigh A, Sevanto S, Close JD, Nicotra AB (2017) The influence of leaf size and shape on leaf thermal dynamics: does theory hold up under natural conditions? Plant Cell Environ 40(2):237–248. https://doi.org/10.1111/pce.12857

McDowell NG, Allen C, Marshall L (2010) Growth, carbon isotope discrimination, and mortality across a ponderosa pine elevation transect. Global Change Biology 16, 399–415. https://doi.org/10.1111/j.1365-2486.2009.01994.x

McDowell NG, White S, Pockman WT (2008) Transpiration and stomatal conductance across a steep climate gradient in the southern Rocky Mountains. Ecohydrology 1, 193–204. https://doi.org/10.1002/eco.20

Meddens AJH, Hicke JA, Macalady AK, Buotte PC, Cowles TR, Allen CD (2014) Patterns and causes of observed piñon pine mortality in the southwestern United States. New Phycologist 206, 91–97. https://doi.org/10.1111/nph.13193

Merritt DM, Poff NL (2010) Shifting dominance of riparian *Populus* and *Tamarix* along gradients of flow alteration in western North American rivers. Ecol App 20, 135–152. https://doi.org/10.1890/08-2251.1

Michaletz ST, Weiser MD, McDowell NG, Zhou J, Kaspari M, Helliker BR, Enquist BJ (2015) Plant thermoregulation, energetics, trait-environment interactions, and carbon economics. Trends in Ecology & Evolution 30, 714–724. https://doi.org/10.1016/j.tree.2015.09.006

Noss RF, Laroe ET III, Scott JM (1995) Endangered ecosystems of the United States: a preliminary assessment of loss and degradation. Restoration & Management Notes 14.

O'Neill GA, Hamann A, Wang T (2008) Accounting for population variation improves estimates of the impact of climate change on species growth and distribution. Journal of Applied Ecology 45(4), 1040–1049. https://doi.org/10.1111/j.1365-2664.2008.01472.x

Oren R, Sperry JS, Katul G, Pataki DE, Ewers BE, Phillips N (1999) Survey and synthesis of intra- and interspecific variation in stomatal sensitivity to vapour pressure deficit. Plant, Cell and Environment 22, 1515–1526. https://doi.org/10.1046/j.1365-3040.1999.00513.x

Reich PB (2014) The world-wide 'fast–slow' plant economics spectrum: A traits manifesto. Journal of Ecology 102(2), 275–301. https://doi.org/10.1111/1365-2745.12211

Sartori K, Vasseur F, Violle C, Baron E, Gerard M, Rowe R, Ayala-Garay O, Christophe A, Garcia de Jalón L, Masclef D, Harscouet E, del Rey Granado M, Chassagneux A, Kazakou E, Vile D (2019) Leaf economics and slow-fast adaptation across the geographic range of *Arabidopsis thaliana*. Sci Rep 9, 10758. https://doi.org/10.1038/s41598-019-46878-2

Sack L, Cowan PD, Jaikumar N, Holbrook NM (2003) The 'hydrology' of leaves: Co-ordination of structure and function in temperate woody species. Plant, Cell and Environment 26(8), 1343–1356. https://doi.org/10.1046/j.0016-8025.2003.01058.x

Seager R, Goddard L, Nakamura J, Henderson N, Lee DE (2014) Dynamical Causes of the 2010/11 Texas–Northern Mexico Drought. Journal of Hydrometeorology 15, 39–68. https://doi.org/10.1175/JHM-D-13-024.1

Seager R, Hooks A, Williams AP, Cook B, Nakamura J, Henderson N (2015) Climatology, Variability, and Trends in the U.S. Vapor Pressure Deficit, an Important Fire-Related Meteorological Quantity, Journal of Applied Meteorology and Climatology 54(6), 1121–1141. https://journals.ametsoc.org/view/journals/apme/54/6/jamc-d-14-0321.1.xml

Schwinning S, Lortie CJ, Esque TC, DeFalco LA (2022) What common-garden experiments tell us about climate responses in plants. Journal of Ecology 110, 986–996. https://doi.org/10.1111/1365-2745.13887

Urban J, Ingwers M, McGuire MA, Teskey RO (2017) Stomatal conductance increases with rising temperature. Plant Signaling & Behavior 12, 1–3. https://doi.org/10.1080/15592324.2017.1356534

Walther GR, Post E, Convey P, Menzel A, Parmesan C, Beebee TJ, Fromentin JM, Hoegh-Guldberg O, Bairlein F (2002) Ecological responses to recent climate change. Nature 416(6879):389-95. https://doi.org/10.1038/416389a

Weiss JL, Castro CL, Overpeck JT (2009) Distinguishing pronounced droughts in the southwestern United States: Seasonality and effects of warmer temperatures. Climate 22, 5918–5932. https://doi.org/10.1175/2009JCLI2905.1

Williams AP, Allen CD, Macalady AK, Griffin D, Woodhouse CA, Meko DM, Swetnam TW, Rauscher SA, Seager R, Grissino-Mayer HD (2013) Temperature as a potent driver of regional forest drought stress and tree mortality. Nature Climate Change 3, 292-297. https://doi.org/10.1038/nclimate1693

Williams AP, Cook BI, Smerdon JE (2022) Rapid intensification of the emerging southwestern North American megadrought in 2020–2021. Nat. Clim. Chang. 12, 232–234. https://doi-org.ezproxy1.lib.asu.edu/10.1038/s41558-022-01290-z

Wright IJ, Dong N, Maire V, Prentice IC, Westoby M, Díaz S (2017) Global climatic drivers of leaf size. Plant Ecology, 357, 917–920. https://doi.org/10.1126/science.aal4760

Wright IJ, Reich PB, Westoby M, Ackerly DD, Baruch Z, Bongers F, Cavender-Bares J, Chapin T, Cornelissen JHC, Diemer M, Flexas J, Garnier E, Groom PK, Gulias J, Hikosaka K, Lamont BB, Lee T, Lee W, Lusk C, … Villar R (2004) The worldwide leaf economics spectrum. Nature 428(6985), 821–827. https://doi.org/10.1038/nature02403

2. ADAPTIVE TRAIT SYNDROMES ALONG MULTIPLE TRAIT SPECTRA DEFINE COLD AND WARM ADAPTED ECOTYPES IN A WIDELY DISTRIBUTED TREE SPECIES

Abstract

The coordination of traits from individual organs to whole plants is under strong selection because of environmental constraints on resource acquisition and use. However, the tight coordination of traits may provide underlying mechanisms of how locally adapted plant populations can become maladapted because of climate change. To better understand local adaptation in intraspecific trait coordination, I studied trait variability in the widely distributed foundation tree species, *Populus fremontii* using a common garden near the mid-elevational point of this species distribution. I examined 28 traits encompassing four spectra: phenology, leaf economic spectrum (LES), whole-tree architecture (Corner's Rule), and wood economic spectrum (WES). Based on adaptive syndrome theory, I hypothesized that trait expression would be coordinated among and within trait spectra, reflecting local adaptation to either exposure to freeze-thaw conditions in genotypes sourced from high-elevation populations or exposure to extreme thermal stress in genotypes sourced from low-elevation populations. High-elevation genotypes expressed traits within the phenology and WES that limit frost exposure and tissue damage. Specifically, genotypes sourced from high elevations had later mean budburst, earlier mean budset, higher wood densities, higher bark fractions, and smaller xylem vessels than their low-elevation counterparts. Conversely, genotypes sourced from low elevations expressed traits within the LES that prioritized hydraulic efficiency and canopy thermal regulation to cope with extreme heat exposure, including 40% smaller

15

leaf areas, 67% higher stomatal densities and 34% higher mean theoretical maximum stomatal conductance. Low-elevation genotypes also expressed a lower stomatal control over leaf water potentials that subsequently dropped to pressures that could induce hydraulic failure. My results suggest that *P. fremontii* expresses a high degree of coordination across multiple trait spectra to adapt to local climate constraints on photosynthetic gas exchange, growth, and survival. These results, therefore, increase our mechanistic understanding of local adaptation and the potential effects of climate change that in turn, improves our capacity to identify genotypes that are best suited for future restoration efforts.

Keywords: Plant-Climate interaction, Physiology, experimental common garden, foliage phenology, leaf economic spectrum, Corner's Rule, wood economic spectrum, xylem anatomy, ecotype.

Introduction

Functional trait expression in plants underlies their performance in relation to local environmental conditions (Chapin et al. 2012; Lambers et al. 2008). However, the coordination of traits across multiple scales from individual organs to whole plants has only recently been addressed in the study of organisms and communities across broad environmental gradients (Freschet et al. 2010; Kleyer and Minden 2015; Messier et al. 2017; Reich et al. 2003; Reich 2014; Rosas et al. 2019). Two classic examples of how trait variability relates to environmental gradients are captured in the leaf economic spectrum (LES) and in Corner's Rules (CR). While LES describes how leaf traits govern the acquisition and utilization of carbon and nutrients at various inter-specific scales (Wright et al. 2004), CR defines the adaptive significance of whole-plant morphology (e.g., organ size), architecture (e.g., branching patterns), and function (e.g., hydraulics and biomechanics) across resource gradients (Lauri 2019; Messier et al. 2017; Valladares et al. 2002). More recently, the "world-wide fast-slow plant economic spectrum" and "wood economic spectrum (WES)" have shown that the principles of LES and CR can be applied to other plant organs such as stems and roots (Chave et al. 2009; Reich 2014). The whole-plant economic spectrum provides a potentially robust integrative description of the coordination among traits and resource-fluxes within and among plants (Freschet et al. 2010; Reich 2014). Accordingly, there are whole-plant or multi-organ coordinated trade-offs between the rate of resource acquisition and conservation that explain the performance of a plant in terms of growth and survival (Chave et al. 2009; Freschet et al. 2010; Reich 2014). For example, plants with higher wood densities also often have more compact and smaller xylem vessels. Although higher wood densities often reflect lower

17

maximum hydraulic conductivity, it provides greater mechanical and protective features that enhance survival when faced with environmental stress (Chave et al. 2009; Reich 2014; Sperry and Sullivan 1992). Conversely, plants with acquisitive or exploitative traits characteristically display higher maximum resource uptake and transport efficiency such as higher maximum hydraulic conductivity, higher photosynthetic capacity and higher growth rates at the risk of having reduced tolerance to environmental stress (Lambers and Poorter 1992; Reich 2014).

Studying the adaptive significance of coordinated traits along a broad climatic gradient is critical for predicting whether a specific population that is locally adapted to a narrow range of climate conditions will become maladapted under rapid climate shifts. Common gardens are a powerful tool for studying patterns of local adaptation to evaluate adaptive variation among populations in individual traits, and the coordination of multiple traits over broad climate gradients (Clausen et al. 1940; Cooper et al. 2019; de Villemereuil et al. 2016; Germino et al. 2019; Kawecki and Ebert 2004; Mooney and Billings 1961). Common gardens can eliminate the confounding effects of the corresponding environment, and thus uncover adaptive variation in trait expression among widely dispersed populations. However, common garden studies of long-lived woody plants can be challenging to implement, and consequently only a relatively small fraction of woody plant species have been critically evaluated within common garden studies.

Populus fremontii, Sarg. (Fremont cottonwood), is among the most dominant riparian tree species in the southwestern US and northern Mexico and is an ideal species to evaluate adaptive trait syndromes for a number of reasons. First, *P. fremontii* is

distributed across an extremely broad climate gradient that encompasses regular freezing

temperatures in high-desert locations to extreme heat exposure in low-desert locations.

Second, *P. fremontii* shares many morphological and ecological features with relatives

within the genus that includes 29 species broadly distributed throughout North America,

Africa, Asia and Europe (Eckenwalder 1996). Third, like many species within the genus,

P. fremontii is recognized as a foundation species that supports numerous communities

through genetically-based functional trait variation (Whitham et al. 2008). Finally, many

Populus species, including *P. fremontii* has experienced a substantial decline in its

historical distribution due to climate change and other environmental changes (Hultine

and Bush 2011; Hultine et al. 2010; Stromberg 1993; Worrell et al. 2008; 2013; Zhou et

al. 2020). Consequently, *P. fremontii* and other similar tree species are rapidly becoming

maladapted to their local environmental conditions (Grady et al. 2011; Hultine et al.

2019, 2020; Merritt and Leroy Poff 2010).

There is evidence suggesting that climate change-driven maladaptation may vary

among populations within the same species (Ikeda et al. 2014; O'Neill et al. 2008). For

instance, populations with certain physiological and morphological traits (e.g., high-water

use efficiency, low specific leaf area) may be better equipped to withstand drier and

hotter conditions than other populations (Chapin et al. 2012; Lambers et al. 1998; Smith

and Allen 1996). This can be especially critical for *P. fremontii* because recent landscape

genetic studies across the species entire geographical distribution have identified

genetically distinct ecotypes that are distributed across geographically distinct ecoregions

(Ikeda et al. 2017). These ecotypes occur within the Sonoran Desert region in southern

Arizona and northern Mexico (Sonora Desert, SD), the Mogollon Rim in Northern

Arizona (Mongollon Rim, MR), the Colorado Plateau and northern Great Basin region from southern Utah to western Colorado (Utah High-Plateaus, UHP), and the Central Valley and coastal regions of California (California Central Valley, CCV (Cushman et al. 2014; Ikeda et al. 2017) (Bothwell et al. unpublished data). Although previous common garden experiments have uncovered intraspecific trait variation in *P. fremontii* (Grady et al. 2011; 2013) these studies have mainly investigated adaptive variation of leaf traits measured in populations sourced exclusively from the SD ecotype that only represent the warmest edge of the climatic gradient of this species' distribution. Thus, the adaptive trait coordination among multiple trait spectrums, and their potential significance to potential maladaptation to climate shifts remain an open question.

In this study, I used an experimental common garden located near the thermal and elevational mid-point of *P. fremontii's* distribution (988 m) (Fig. 2.1, Table. 2.1) to study trait variability in relation to elevation and the mean annual temperature (MAT) transfer distance, defined as the MAT of the source population location subtracted from the MAT of the common garden location (Grady et al. 2011). I studied contrasts in morpho-physiological coordination in functional trait expression among eight *P. fremontii* populations spanning two ecotypes (SD and MR) and an approximate 12 °C mean annual temperature gradient (Wang et al. 2012). I analyzed four trait spectra including: foliage phenology (spring budburst and budset), trait variability across a leaf economic spectrum, including petiole traits (LES), trait variability across a wood and xylem economic spectrum (WES), and trait variability in aboveground architecture, including traits related to Corner's Rule (CR) (Cornelissen 1999; Corner 1949; Lauri 2019; Messier et al. 2017). Combined, these trait spectra represent coordinated strategies at multi-organ levels for

coping with climate stress exposure from intense freezing events at higher latitudes and elevations to episodic heat waves at lower latitudes and elevations.

I hypothesized that the combined intraspecific coordination of traits across all trait spectra reflect local adaptation to both the extreme high temperatures in the SD ecotype as well as exposure to freeze-thaw events in the MR ecotype. I argue that this hypothesis can be generalized as the economic spectrum similarity rule in which plants with functionally related traits at low trait level (epidermal and vascular tissue) scale up to functionally related traits at higher (organ to whole-tree) trait level. Because phenology, leaf, whole-tree architecture, and wood traits are, in part, genetically based (Bailey et al. 2004; Barbour et al. 2015; Cooper et al. 2019; Preston et al. 2006), My findings provide a genetic mechanism for the potential evolution of a general adaptive plant stress syndrome in which many traits would be accumulated in each ecotype to best survive their specific environments (Rueda et al. 2018). The same logic applies to my proposed economic spectrum similarity rule. Tests of this hypothesis are reflected in the following sub hypotheses. 1. At the leaf level, warm-adapted SD ecotype trees should possess a suite of traits that maximize stomatal conductance and transpirational cooling while reducing foliar exposure to radiation and thermal load. MR ecotype trees, on the other hand, should possess characteristics reflecting shorter growing season duration and a more conservative hydraulic strategy to cope with episodic freezing events. 2. Aboveground architecture in SD ecotype trees should be constructed to prioritize leaf water supply relative to demand while the MR ecotype trees should maximize leaf sun-exposure over their shorter growing season. 3. At the wood trait level, intraspecific differences in xylem hydraulic traits should reflect a trade-off between maximizing hydraulic efficiency in the

21

SD ecotype trees to reducing vulnerability to cavitation during freeze-thaw cycles in MR ecotype trees by constructing smaller and hydraulically less efficient xylem vessels. 4. In addition to expecting differences in these traits across levels of organization between ecotypes, I also expected finer levels of local adaptation within ecotypes. Information derived from this research will help shape our understanding of local adaptation related to climate-induced resource limitation in *P. fremontii*, and other widely distributed *Populus* species threatened with climate change.

Methods

Study site and plant material

An experimental common garden was established in October 2014 with ~4100 propagated cuttings from 16 populations that represent the entire climatic gradient of *P. fremontii* within the state of Arizona. The garden is located on a 1.2 Ha portion of historic cropland within the Agua Fria National Monument (N 34.2567, -112.0661, elevation 988 m). To avoid using clones within each population, all cuttings were collected randomly from trees at least 20 meters apart during the 2013-2014 winter. Individual cuttings were grown in pots in the Northern Arizona University greenhouse for four months and then transplanted to the common garden when saplings were approximately 0.3 meters in height. During the growing season, the garden was drip irrigated with approximately 20 liters per tree, 2-3 times per week. In this study, 10 genotypes were randomly selected from five Arizona Sonoran Desert (SD) ecotype populations and from three Mogollon Rim (MR) ecotype populations (n = 80 total ecotypes). Climatic variables from each sampling location were obtained using the platform ClimateWNA (Wang et al. 2012);

22

Table 2.1). For climatic data regarding number of days with temperatures above/below freezing and above 40 °C, I used modelled estimates of temperature from PRISM data. Copyright © <2020>, PRISM Climate Group, Oregon State University, http://prism.oregonstate.edu. The eight population were chosen because they collectively represent the broadest possible range in mean annual temperature from 10.7 °C to 22.6 °C, and an elevation gradient from 72 m to 1940 m (Table 2.1, Fig. 2.1) Likewise, the eight populations selected for this study had a mean annual temperature transfer distance to the common garden of 3.3 °C to 6.7 °C in the MR populations and a -5.2 °C to 5.0 °C in the SD populations (Table 2.1).

Measured traits

Between the 2016-18 growing seasons, I measured 28 traits on 48-80 genotypes representing the eight populations described above. These traits were categorized according to their respective trait spectrum which include foliage phenology, LES, CR and WES (Table 2.2).

Foliage phenology - From February 13th to May 9th and from October 4th to 30th of 2017, I evaluated phenophase status on spring budburst and fall budset every 15 days following the USA National Phenology Network protocol (Denny et al. 2014). Repeated observational assessment of presence or absence of the two phenological events of interest were monitored in all eight populations on (n=10 genotypes). I recorded the date of the emergence of new leaves, budburst status, per individual ecotypes as zero, less than 50, and greater than 50 budburst occurrences. For budset, I noted the dates of the appearance of the first 20 terminal buds in each genotype.

LES Traits

Stomatal anatomy - In 2016, fully expanded leaves were collected from outer leaves on the south facing side of mid-canopy height to assess stomatal density, length, width, and area. Following the nail polish impression method (Hilu and Randall 1984), 160 impressions on both the abaxial and adaxial sides of the leaves (n = 640 images) were obtained to be observed under an Olympus CX41light microscope and images were taken with a Moticam Pro 282A camera (Motic, Richmond, BC, Canada). Stomatal density was estimated as the number of stomata in eighty 0.59 mm2 digital images at 10× magnification. Stomatal sizes (length × width) were estimated on 800 stomata from digital images at 40× magnification (n= 100 per population) using an open-source imaging program, ImageJ (https://imagej.nih.gov/ij/). Maximum theoretical stomatal conductance to water vapor (mmol m-2 s-1) was calculated from Franks and Farquhar (2001):

$$G_{smax} = \frac{dw * Ds * a_{max}}{v\left(l + \frac{\pi}{2}\sqrt{\frac{a_{max}}{\pi}}\right)} \tag{1}$$

Where dw is the diffusivity of water in air (2.43×10^{-5} m^2 s^{-1}), v is the molar volume of air (0.024 m^3 mol-1) (Jones 2014), D_s is the stomatal density, a_{max} is the maximum area of the open stomatal pore, approximated as $\pi(p/2)^2$, where p is stomatal pore length, assumed to be stomatal length divided by two (Franks and Farquhar 2007).

Leaf traits - Specific leaf area (SLA) was calculated as the one-sided area of a fresh leaf, divided by its oven-dry mass (Wright and Westoby 2002). SLA was measured in June, July, and September of 2017. A subset of 12-20 collected leaves per tree were scanned with a high-resolution computer scanner, and one-sided leaf area was measured

with ImageJ. The scanned leaves were then oven-dried for 72 hours at 75 °C and weighed

to calculate SLA ($cm^2 g^{-1}$). Individual leaf area (A_{il}) was derived from the average

individual leaf area from these measurements (Ackerly et al. 2002).

Petiole traits - In September 2017, three to four leaves located at the mid-canopy

level and south-facing side were collected from six trees per population to study petiole

traits. Leaf samples were stored in a cooler at approximately 7-10 °C and transported to

the Imaging and Histology Core Facility at Northern Arizona University. Individual

petioles were cut with a razor blade and their mid-portions were sectioned to fit within

embedding cassettes (28.5 x 41.0 x 6.7 mm). The samples were prepped using an

automated fixation and paraffin embedding process. Specifically, the samples were fixed

with formalin, dehydrated with increasing concentrations of undenatured alcohol, cleared

with xylene to then be infiltrated with paraffin, and then embedded into the cassette.

Cassette blocks were then sliced into transverse sections approximately 5-10 µm thick

with a microtome and molded onto positively charged slides, deparaffinized with xylene

and rehydrated with decreasing concentrations of undenatured alcohol until rinsing with

only DI water, and then stained with 0.1% toluidine blue. Images were produced on a

digital light microscope that were subsequently analyzed using ImageJ. Several petiole

characteristics were recorded, including the length, width, and area of the entire petiole

(A_p). Additionally, I measured petiole xylem vessel diameter (d), vessel density (D_{pv}),

mean and total lumen area of all of the vessels contained in the petiole (A_{pl}), the

hydraulically weighted mean vessel diameter (Hd_p) was calculated as $\sum d^5/\sum d^4$ (Scholz et

al. 2013; Sperry and Saliendra 1994). Petiole flatness (L_{pf}) – a distinct characteristic of

Populus species – was quantified from the petiole width to length ratio at the mid-rib of

the petiole (Lindtke et al. 2013). The petiole lumen fraction (F_{pl}) was calculated as total

A_{pl} per petiole transverse area (A_p) at the mid-rib.

Mean petiole theoretical hydraulic conductivity (K_p; mg m MPa $^{-1}$ s $^{-1}$) was

calculated from total petiole vessel lumen diameter using the Hagen–Poiseuille equation

(Eguchi et al. 2008; Nobel 2009; Tyree and Zimmermann 2002):

$$K_p = \Sigma \frac{d_i^4 \pi \rho}{128 \eta_w} \tag{2}$$

where d_i is the diameter of a single vessel (m), ρ is water density at 25 °C (998 kg m -3)

and ηw is viscosity of water at 25 °C (8.9 ×10–10 MPa s) (Eguchi et al. 2008).

Theoretical hydraulic conductivity per unit leaf area (K_l, mg m-1 s-1 MPa-1)

(Sack et al. 2003; Sack and Frole 2006), was calculated as:

$$K_l = \Sigma \frac{K_p}{A_{il}} \tag{3}$$

where A_{il} is the area of the leaf (m^2) attached to the petiole and K_p is the mean petiole

theoretical hydraulic conductivity. Additionally, I estimated differences in water use

strategies at the population and ecotype levels by dividing leaf area normalized

theoretical hydraulic conductivity of the petiole (K_l, mg m^{-1} s^{-1} MPa^{-1}) by G_{smax}.

CR traits

In July 2017, I estimated whole-tree leaf area (A_l) and sapwood area (A_s) using

population-specific allometric relationships between stem diameter to leaf area through a

branch summation approach (Jones et al. 2015; Kenefic and Seymour 1999). Thus,

whole-tree leaf area was estimated per branch by multiplying the mass of all leaves by

their respective SLA. Canopy diameters (4 to 8 measurements per tree) and their

respective canopy areas together with whole-tree height (H) were measured five times

during the 2016 and 2017 growing seasons with a telescoping measuring pole. Canopy area (A_c) was determined using the ellipse equation, πab, where a is the mean radius of longest canopy axes and b is the radius of two perpendicular canopy axes (Ansley et al. 2012). Leaf area index (LAI) was estimated by the equation from (Hultine et al. 2013):

$$LAI = \frac{A_i}{A_c} \tag{4}$$

WES Traits

In May to June 2018, I collected one-year-old stem samples to measure wood and xylem traits. I collected branch cuttings approximately 1 cm diameter and cut the segment to a length of 30 cm. The segments were placed into a plastic bag with a moist paper towel and kept in a cooler until being transferred to a lab refrigerator kept at 4 °C. Specific wood density (D_{stem}) was determined using Archimedes' principle of water displacement (Cornelissen et al. 2003; Hacke et al. 2000; Preston et al. 2006). The outer bark was removed from a 1 cm diameter stem segment. The segments were cut to a length of approximately 15 cm with no obvious side branches and total stem volume with the bark was measured. Specifically, a graduated cylinder with water was tared on a scale with 0.01 g accuracy, and the segment was submerged just below the meniscus; the weight was recorded and converted to volume. After the whole stem volume was initially measured, the bark was removed, and the sapwood volume was measured using the same method. The samples were then over-dried at 70° C for 48 h, and a dry weight was recorded. D_{stem} was determined as the ratio of dry weight to volume displaced of the sapwood. The whole stem volume was measured to assess the stem bark fraction (F_b). Xylem vessel area was determined from the 1 cm diameter segments used for density by first removing 2 cm length segments to mount in a GSL1 sledge microtome (Gärtner et

al. 2014). The samples were moistened with a Strasburger solution (Eilmann et al. 2011) before being shaved into 100-150 µm slices. The fresh cut slices were transferred to a dye solution of 0.1% toluidine blue for 1-2 minutes (Sridharan and Shankar 2012) before being dehydrated by increasing concentrations of undenatured alcohol (50, 70, 95, and 99.5% EtOH; KOPTEC 200 proof, VWR) (Buesa and Peshkov 2009). At the end of this process, I used the synthetic mounting medium Permount (Mayr et al. 2014; Ravikumar et al. 2014) to embed the samples. Slides were photographed with a Moticam Pro 282A camera (Motic, Richmond, BC, Canada) mounted to an Olympus CX41light microscope. The region of interest included a subset of the previous year's growth ring to include both the early wood and late wood. Vessel lumen area was measured using ImageJ software, and individual images were stitched together (Preibisch et al. 2009) to analyze xylem vessels of the entire growth year. The number of vessels measured per genotype ranged from 153 to 941 (mean = 460). From the images I quantified mean stem lumen area (A_{sl}), mean stem hydraulic diameter (Hd_s) and stem vessel density (D_{sv}). Stem lumen fraction (F_{sl}) was calculated as the total A_{sl} per D_{sv}.

Water potential - Monthly measurements of leaf water potential (Ψ) were taken from June to October of 2017 using the Scholander pressure chamber (Cochard et al. 2001; Scholander et al. 1965). Pre-dawn and midday Ψ measurements were taken to assess possible differences in water potential gradients at the population and ecotype levels. A single shoot tip from each of the 64 trees was cut with a sharp razor blade to measure water potential at predawn (Ψ_{pd}) between 0300 and 0500 h, and at midday (Ψ_{md}) between 1100 and 1300 h.

Statistical analysis

      All statistical analyses were conducted in R version 3.6.2 (R Development Core

Team 2011). Prior to analyzing the data, I examined whether each variable met the

assumptions of normality and homogeneity of variance, using a Shapiro and Barlett test.

When the data were not normally distributed, they were normalized by log10, square

root, or box-cox transformations. Once the basic requirements were met, functional traits

were analyzed statistically using a linear regression with provenance elevation as the

predictor and traits as the responses. I also used analysis of variance (ANOVA) to

analyze differences among populations. When a trait showed significant variation, I used

a Tukey's HSD post-hoc test to detect differences at the elevation level (Sokal and Rohlf,

1995). Trait contrasts at the ecotype level were analyzed using a student's t-test. Ecotype

differences in traits measured several times during the growing season (A_{il}, SLA, A_c, H,

and Ψ_{pd} , Ψ_{md}) were analyzed by individual mixed-model repeated measures ANOVA

(type III with Satterthwaite's method) in the lmer R package (Bates, Mächler, Bolker, and

Walker, 2015; Kuznetsova, Brockhoff, and Christensen, 2017). In this test, individual

traits were represented as response variables while the ecotype and month were treated as

fixed effects with two and three levels, respectively. Individual genotype nested within

ecotype was the random effect.

      I conducted separated principal component analyses (PCAs) on the three trait

spectra (leaf, architecture, and wood) and all traits pooled together using the factoextra

and FactoMineR packages (Kassambara and Mundt 2017; Lê et al. 2008). Because G_{smax}

is autocorrelated with D_{stom} and S_{stom}, it was excluded from these analyses. Thus, I

simultaneously assessed what traits explained most of the variation within each trait

spectrum and among all the remaining 27 *P. fremontii* traits together. For each PCA

analysis, the variables showing the highest loading in each PCA were selected as

indicators of local climatic adaptability. I initially determined the number of meaningful

PCA axes using the Kaiser criterion. This criterion recommends using axes with

eigenvalues above 1.0 exclusively. However, because the Kaiser criterion is not

recommended to be used as the only cut-off criterion for estimating the number of factors

(Freeman and Jackson 1992; Grossman et al. 1991; Jackson 2016; Peres-Neto et al.

2005), I also used the Broken Stick Model in the vegan and biodiversity R package to

determine significant components. This model randomly divided a stick of components

into the same number of elements found in the PCA axis. Then, these elements were

rearranged in decreasing order according to their length to be compared to the

eigenvalues. Axes with larger eigenvalues than their corresponding stick of components

were considered significant (Borcard et al. 2011).

In each principal component graph (biplot), trait representation was based on the

magnitude of the correlation (loadings) between traits and the given principal component.

Thus, in each biplot, traits were represented as vectors with a length and direction

indicating the strength and trend of a given trait's relationship among other traits.

Specific location of the vector in the biplot indicates the positive or negative impact that a

trait has on each of the two components x-axis, first component (PC1) and y-axis, second

component (PC2). Additionally, to assess the relationship between the two ecotypes and

the traits distribution in every PCA biplot, I constructed two 95% confidence ellipses

based on the PCA scores of each of the two ecotype means. Subsequently, linear

regressions between significant principal components and elevation of source populations

were constructed. Additionally, I performed t-tests and ANOVA Tukey's HSD tests to assess significant differences in PC axes scores at ecotype and population levels. Because PC scores mainly described dominant traits in each axis, I evaluated population differences in all traits included in each PCA simultaneously by using a permutational multivariate analysis of variance (PERMANOVA; (Anderson 2001) in the vegan R package. Population differences in all 27 traits PCA were further analyzed with pairwise comparisons using permutation MANOVAs on a Pillai test and distance matrix in the vegan and RVAideMemoire R packages.

Redundancy Analysis (RDA) (Borcard et al. 2011)) was used to determine how environmental (e.g., provenance latitude, longitude, mean annual precipitation, MAT transfer distance and ecotype) and genetic (e.g., ecotype) descriptors influence multi-spectra trait variance in *P. fremontii*. I also used forward stepwise selection of descriptor variables to determine the significance of each variable to the RDA. Forward selection determines the successive contribution of each descriptor to explaining trait variation and adds only those variables with significant contribution.

Results

Foliage phenology

Consistent with my hypothesis of local adaptation to extreme high summer temperatures in the SD ecotype and early spring and fall freeze-thaw exposure in the MR ecotype, I found large differences in foliage phenology between these two groups. Thus, I found that budburst of the SD ecotype occurred on average 46 days earlier than the MR ecotype (t = 15.65, df = 78, p < 0.001, Table 2.3, Fig. 2.2a). Similarly, on average budset

31

occurred 13 days later in the SD ecotype compared to the MR ecotype (t = 8.63, df = 78, P < 0.001, Table 2.3, Fig. 2.2b).

Leaf economic spectrum traits

I found remarkable differences in leaf structural traits between the extreme hot adapted SD ecotype and the cold-adapted MR ecotype. Specifically, I found that the MR ecotype had 30% larger leaves (t = 8.98, df = 78, P < 0.001, Table 2.3) while SLA in the SD ecotype was on average 22% higher than the MR ecotype (t = -8.42, df = 78, P < 0.001, Table 2.3). Repeated measures analysis showed that A_{il} increased (F = 126.4, df = 2, P < 0.001, Table S2.1) and SLA decreased (F = 70.9, df = 1, P < 0.001, Table S2.1) over the course of the growing season. Likewise, there was a significant interaction between time of year and ecotype in both A_{il} (F = 15.8, df = 1, P < 0.001, Table S2.1) and SLA (F = 6.3, df = 1, P < 0.01, Table S2.1), indicating that differences between ecotypes depended on the time of year and therefore might have different adaptive responses to seasonal conditions.

From June to September, I found a more pronounced increase in leaf sizes in the MR ecotype (66%) than the SD ecotype (46%). Over the same time, the SD ecotype displayed similar SLA values while the MR ecotype exhibited a 17% decrease (Table S2.1). Combined, the higher A_{il} and lower SLA results suggest that the MR leaves have higher construction costs and longer lifespans than the SD leaves.

Stomatal traits supported my hypothesis regarding selection for transpirational cooling in genotypes sourced from the SD region. Stomata in the SD ecotype were on average 37% smaller (t = -14.22, df = 78, P < 0.001, Table 2.3) but mean stomatal densities of the SD ecotype were 40% higher (t = 12.81, df = 77.6, P < 0.001, Table 2.3).

The higher stomatal densities yielded a 34% higher G_{smax} in the SD ecotype (t = 9.24, df = 77.1, P < 0.001, Table 2.3), despite having smaller mean stomatal size.

Differences in leaf structure were accompanied by differences in petiole structure. The MR ecotypes had on average 63% larger petioles (t = -4.64, df = 46, P < 0.001, Table 2.3) that were 13% more elliptical (i.e., flatter) than the SD ecotypes (t = -3.25, df = 46, P < 0.001, Table 2.3). Conversely, none of the xylem vessel traits of the petioles differed between SD and MR ecotypes (Table 2.3). However, calculated petiole hydraulic conductivity was 80% higher (t = -4.81, df = 46, P < 0.001, Table 2.3) in the MR ecotypes, reflecting their larger petiole sizes and larger total lumen area compared to the SD ecotypes. Despite the higher K_p in the MR ecotype, the larger leaves in this ecotype resulted in K_l being similar between the two ecotypes. (Table 2.3).

To better understand leaf functional variation in water supply versus demand in relation to climate, I analyzed petiole theoretical K_p , K_l and G_{smax} in relation to source population MAT transfer distance. Theoretical K_p increased with elevation and positive MAT transfer distance (R2 = 0.31, F = 17.0, P < 0.001, Fig. 2.3a), although MAT transfer distance did not have a significant effect on K_l (Fig. 2.3b). On the other hand, G_{smax} decreased with positive MAT transfer distance (R2 = 0.41, F = 27.9, P < 0.001, Fig. 2.3c) with the regression explaining 41% of the variation. I found that the ratio between leaf-level water supply (K_l) and the leaf-level demand (G_{smax}) increased moderately with positive MAT transfer distance (R2 = 0.15, F = 7.47, P < 0.01, Fig. 2.3d), indicating that the low elevation (negative MAT transfer distance) genotypes may take on a riskier hydraulic strategy regarding the supply of water to the leaves relative to demand.

According to the Broken-Stick Model (Borcard et al. 2011), only the first two principal components significantly explained the variance within the leaf trait spectrum in *P. fremontii.* Together, these two principal components accounted for 55.7% of the variance. The first principal component axis, PC1 (accounting for 37.1% of the variance) showed a significant positive relationship with S_{stom}, A_{il}, A_p, K_p, L_{pf}, K_l, Hd_p, A_{pl} while showing opposite trends with D_{stom}, SLA, and D_{pv} (Fig. 2.4). The second axis, PC2 (which explained 18.6 % of the variance) displayed significant positive correlations with SLA, A_{pl}, Hd_p, and K_l and negative correlations with D_{pv}, F_{pl}, A_{il} and S_{stom} (Fig. 2.4). Thus, the MR ecotype 95% confidence ellipse was found in the positive half of PC1 axis encompassing A_{il}, S_{stom}, K_p, A_p, and L_{pf} trait vectors. The SD ecotype displayed a larger 95% confidence ellipse mainly located in the negative side of the PC1 axis (Fig. 2.4). Accordingly, D_{stom}, SLA, D_{pv}, A_{pl} and K_l traits were found within this SD ecotype ellipse. Simultaneously, PC1 and PC2 displayed positive and negative significant relationships with the *P. fremontii* climatic range ($R^2 = 0.51$, $P < 0.001$, R2 = 0.14, $P < 0.01$; Fig S2.1). I found PC1 and PC2 scores significantly differed between the two ecotypes (t = -10.2, df = 46, p-value < 0.001; t = 3.21, df = 45.3, p-value < 0.01). ANOVA and Tukey's HSD detected that the three populations with the negative MAT transfer distances displayed significantly lower PC1 scores than the three highest elevation populations with the most positive MAT transfer distances (Fig. S2.1). Simultaneous evaluation of all leaf traits through PERMANOVA and pairwise permutation MANOVAs identified similar significant differences at ecotype and population level (F = 17.97, df = 1, P > 0.001; F = 3.85, df = 7, P > 0.001; Fig. S2.1).

Whole-plant architecture spectrum

Traits within the architecture spectrum mostly diverged between ecotypes (Table 2.3). As hypothesized, tree architecture in the MR ecotype enhanced leaf sun-exposure while the SD ecotype prioritized transpiration rates of individual leaves. Specifically, A_l and A_c were 20% (t = -2.26, df = 62, P < 0.01, Table 2.3) and 34% (t = -4.02, df = 46.83, P < 0.001, Table 2.3) larger in the MR ecotype, respectively while A_s:A_l and H were 38% (t = 10.9, df = 43.5, P < 0.001, Table 2.3) and 34% larger (t = 2.34, df = 78, P < 0.05, Table 2.3) in the SD ecotype, respectively (Table 2.3). However, LAI did not differ between ecotypes due to the higher A_l occurring in more spreading canopies (i.e., higher A_c) of the MR ecotypes. Repeated measures showed that the MR ecotype maintained a larger A_c throughout the growing season (F = 24.5, df = 1, P < 0.001, Table S2.1), that was independent of the time of year (i.e., the interaction, ecotype*time was not significant). Similarly, the repeated measures analysis revealed a significant difference between the taller SD and the shorter MR trees (F = 7.50, df = 2, P < 0.001, Table S2.1), that was also independent of time of year (ecotype*time was not significant).

I found that PC1 and PC2, explained 35.3% and 25.8% of the variance and were the only significant components in the architecture trait spectrum (Fig. 2.5). However, because PC1 was the only component showing a significant relationship with the *P. fremontii* elevational gradient (R^2 = 0.57, P < 0.001, Fig S2.2), I focused my analysis on this axis exclusively. PC1 displayed simultaneous positive relationships with trait characteristics of the MR ecotype (A_l, A_c and LAI) and negative relationship with the two architectural trait characteristics of the SD ecotype (A_s:A_l and H; Fig.2.5). Although the 95% confidence ellipses of both ecotypes overlapped in the biplot (Fig. 2.5), I found a

significant difference between the two ecotype PC1scores (t = 6.42, df = 62, p-value > 0.001). Interestingly, ANOVA and Tukey's HSD tests detected significant differences between the four highest elevation populations with positive MAT transfer distance, including the only SD population with positive MAT transfer distance, with the four populations having zero or negative MAT transfer distance (Fig. S2.2). Simultaneous analysis of all architecture traits confirmed these significant differences between ecotypes and populations (F = 14.81, df = 1, P > 0.001; F = 5.54, df = 7, P > 0.001; Fig. S2.2).

Wood economic spectrum traits

Wood traits related to structural support and frost protection including D_{stem} and F_b were 8% (t = -4.06, df = 46, P < 0.001, Table 2.3) and 35% (t = -5.91, df = 46, P < 0.001, Table 2.3) greater in the MR ecotype, respectively. Conversely, in wood traits related to water transport efficiency, I found that Hd_s and F_{sl} were 8% (t = 2.28, df = 46, P < 0.05, Table 2.3), and 17% (t = -2.66, df = 46, P < 0.05, Table 2.3) greater in the SD ecotype, respectively. A_{sl} and D_{sv} values did not significantly differ between these two ecotypes (Table 2.3). As expected in an irrigated common garden, I did not find differences in mean Ψ_{pd} throughout the growing season (Table 2.3). However, I found the SD ecotype displayed more negative mean Ψ_{md} throughout the growing season (t = -0.56, df = 46, P < 0.001, Table 2.3). Repeated measures detected significant Ψ_{pd} differences among the five measurement periods (F = 15.8, df = 1, P < 0.001, Table S2.1), but no differences were detected in Ψ_{pd} between ecotypes or the interaction ecotype*time (Table S2.1). On the other hand, Ψ_{md} exhibited significant differences between ecotypes (F = 23.6, df = 1, P < 0.001, Table S2.1) and time (F = 112.7, df = 4, P < 0.001, Table S2.1) while the interaction ecotype*time was not significant.

In the wood spectrum PCA, three principal components which together explained 64% of the variation were significant. However, only PC1, accounting for 29.7% of the variation, was correlated with MAT transfer distance ($R^2 = 0.37$, $P < 0.001$; Fig. S2.3). PC1 also exhibited significant positive correlations with D_{stem}, Ψ_{md} and F_b while showing negative correlations with F_{sl}, Hd_s and A_{sl} (Fig. 2.6). Like the architecture trait PCA, the 95% confidence ellipses of both ecotypes overlapped but contrasts between ellipses were still detected ($t = 6.86$, $df = 46$, p-value < 0.001). Nevertheless, ANOVA and Tukey's HSD tests only detected differences between the lowest elevation population with the most negative MAT transfer distance (-5.2 °C) and the three populations with the most positive MAT transfer distance (Fig. S2.3). PERMANOVA and pairwise permutation MANOVAs tests revealed significant differences between ecotypes ($F = 9.31$, $df = 1$, $P > 0.001$; Fig. S2.3) and among populations ($F = 2.42$, $df = 7$, $P > 0.001$; Fig. S2.3).

PCA analysis of pooled traits

A PCA of all 27 traits measured required eight components with eigenvalues greater than 1 to reach 78% of total variance. However, PC1 was the only axis of the PCA that was significant accounting for 32% of the total variance. Likewise, PC1 yielded a significant correlation with MAT transfer distance of source populations ($R^2 = 0.84$, $P < 0.001$; Fig. S2.4). Additionally, I found PC1 displaying significant negative correlations with traits characteristic of the SD ecotype while observing the opposite trend with traits associated with the MR ecotype (Fig. 2.7). Therefore, the SD ecotype 95% confidence ellipse was found in the negative half of PC1 axis enclosing the vectors representing BS, $A_s:A_l$, D_{stom}, SLA, H, F_{sl}, D_{pv}, A_{sl}, and Hd_s. In the positive half of the biplot, I observed the MR ellipse enclosing the BB, S_{stom}, A_{il}, K_p, Ψ_{md} and F_b, L_{pf}, D_{stem}, Hd_p, A_c and A_l

37

vectors (Fig. 2.7). Differences between the ecotypes along the PC1 axis were highly significant (t = -17.03, df = 46, P < 0.001), and a PERMANOVA test confirmed these differences (F = 17.84, df = 1, P > 0.001).

Although the relationships between the two ecotypes and the 27 different traits elucidate important features regarding climate adaptation at the regional scale, trait differentiation at the population-level can increase our understanding of adaptation at the local level. I found that the SD population with the largest mean warmest monthly temperature (MWMT), elevation 161 m (Table S2.3), displayed A_{il}, SLA, S_{stom}, L_{pf}, A_l, A_s:A_l, A_c, H, K_p, and D_{stem} with the most extreme values within the ecotype (Tables. S2.2, S2.3, S2.4, S2.5). Similar results were obtained in the MR ecotype. Specifically, the population with the lowest mean coldest monthly temperature (MCMT), elevation 1940 (Table 2.3), exhibited the most extreme A_{il}, SLA, D_{stem}, A_l, A_c, and Ψ_{md} within the ecotype (Tables. S2.3, S2.5, S2.6). Additionally, I found significant positive relationships between elevation and A_{il}, S_{stom}, A_p, L_{pf}, A_l, A_c, D_{stem}, and F_b (Tables. S2.2, S2.3, S2.4, S2.5). Likewise, source population elevation had a negative relationship with D_{stom}, G_{smax}, SLA, K_p, H, A_s:A_l, A_{sl}, and Ψ_{md} (Tables. S2.2, S2.3, S2.4, S2.5).

To gain a better understanding of trait variability in each ecotype, I constructed 95% confidence ellipses for the eight populations that made up the two ecotypes in the same PCA of all 27 traits (Fig. 2.8). As expected, I found low elevation – negative MAT transfer distance -populations ellipses (SD ecotype) were mainly placed in the negative half of the PC1 axis while the three high elevation populations (MR ecotype) remained in the right half of PC1 (Fig. 2.8). However, as suggested by the larger size SD ecotype ellipses in the leaf, architecture and all 27 traits PCA biplots, I observed larger variability

38

in the locations occupied by the five SD populations' ellipses. Particularly, I found that

the San Pedro Riparian National Conservation Area (TSZSAN) population in southern

Arizona (1212 meters) and to a lesser extent the Agua Fria National Monument

(CAFAUG) population (988 m) in central Arizona displayed ellipses expanded toward

the positive, MR characteristic, area of the PC1 axis. Although these populations mainly

displayed trait characteristics of the SD ecotype, it is evident that they have some

morpho-physiological trait characteristics found in the MR ecotype. Based exclusively on

the PC1 scores using an ANOVA and Tukey HSD test, I found significant differences

between the five SD and the three MR ecotype populations (Fig. S2.4). Therefore, the

TSZSAN and CAFAUG populations did not differ from the other 3 SD ecotype

populations. However, using a PERMANOVA and pairwise permutation MANOVAs on

all 27 traits simultaneously, I found the significant population differences (F = 4.07, df =

7, P > 0.001; Fig. S2.4). Specifically, the TSZSAN population significantly differed from

all other SD ecotype populations except for the CAFAUG population. Simultaneously,

the CAFAUG population only significantly differed from all MR populations and the

lowest elevation population of the SD ecotype.

RDA analysis of pooled traits with environmental predictors

RDA and PCA ordination techniques of all 27 traits showed general similar trait

patterns in their respective biplot and triplot (Fig. 2.7 and 2.9). Forward selection of

environmental predictors (provenance latitude, longitude, mean annual precipitation,

MAT transfer distance) revealed that MAT transfer distance, MAP (mean annual

precipitation) and elevation were the only three variables that significantly explain trait

variation in *P. fremontii*. However, elevation had to be dropped from the analysis because

it displays high collinearity with MAT transfer distance. Ecotype grouping which also showed to explain trait variation was included in the analysis as a categorical genetic predictor.

RDA Axis 1 described 30.6% of the variation in all 27 traits (compared to 32.3% in the PCA). This axis displayed highly significant relationships with MAT transfer distance and both ecotypes. RDA analysis found that the amount of variance explained by these predictor variables (i.e., constrained variances) was 32% while the unconstrained variance (i.e., the amount of variance remaining in the response variables) was 68%. Although Axis 2 described only 2.4% of the variation (compared to 10.9% in the PCA) and was not significant, it was correlated with MAP (environmental predictor), hydraulic efficiency traits (D_{pv}, F_{sl}, F_{pl}), whole canopy traits (LAI, Al, A_s:A_l, H) and wood trait D_{stem} (Fig. 2.9).

Discussion

My results demonstrated that local adaptation of *P. fremontii* populations over its geographical distribution comprises many different traits that are coordinated across multiple scales from epidermal and vascular tissue to individual organ and whole-plant architecture. These findings support my economic spectrum similarity hypothesis, and more broadly adaptive syndrome theory, postulating that many traits are expressed within an ecotype to best survive their specific environment (Rueda et al. 2018). The coordination of traits indicates that *P. fremontii* is comprised of genotypes that are highly specialized to cope with local environmental conditions and have resulted in the evolution of ecotypes at regional levels that each have a suite of adaptive traits (an

40

adaptive syndrome) that make each best adapted to its ecoregion. Simultaneously, I found finer differences in trait coordination at the population level that reflect gradual adaptation strategies at local environmental conditions. Thus, results underscore the potential importance of using assisted migration as a possible solution to restoration of *Populus* species conducted under rapidly shifting climate conditions.

Adaptive syndrome trait correlations within the MR ecotype

Late bud burst and early budset of the high latitude/elevation MR ecotype revealed an adaptive trade-off between avoiding freezing temperatures and maximizing growth (Cooper et al. 2019; Evans et al. 2016; Fischer et al. 2017; Friedman et al. 2011; Grady et al. 2015). My results paralleled previous research using all 16 populations in the same mid-elevation common garden as the one used in the present study (Cooper et al. 2019). However, Cooper et al. (2019) also repeatedly measured phenology in two additional replicated gardens that represent the two extreme edges of *P. fremontii's* climatic distribution to estimate phenological plasticity. Interestingly, the warm-adapted SD ecotype trees displayed greater phenological plasticity than the cold-adapted MR ecotype trees, reflecting the extent to which exposure to freezing temperatures acts as an agent of selection in cold-adapted genotypes (Cooper et al. 2019; Hultine et al. 2020). On the other hand, phenological characteristics, i.e., earlier budburst, later budset) displayed by SD ecotype trees may have resulted from the combined effects of infrequent exposure to freezing temperatures, longer optimal growing seasons and extreme mid-summer temperatures in the Sonoran Desert that limits net carbon gain.

Previous investigations have found that plants with thicker stems and larger leaves are frequently accompanied by less frequent branching with wider branching

angles (Cornelissen 1999; Corner 1949; Trueba et al. 2016; Wright and Westoby 2002).

Accordingly, I found larger leaves and canopies areas to be characteristic traits of the MR

ecotype (Table. 3). The larger A_c in the MR ecotype trees may reflect selection to

maximize sun exposure and limit self-shading. Additionally, the MR trees had leaves

with petioles that were more elliptical (i.e., flattened) compared to the SD ecotype. Past

investigations on *P. fremontii* have identified the flattened non-rigid petioles oriented

perpendicular to the blade to be responsible for the characteristic fluttering of leaves

under breezy conditions (Niklas 1991; Roden and Pearcy 1993). Other previous studies

have concluded that leaf fluttering maximizes carbon gain homogenizing light

distribution throughout the multi-layered canopy (Sprugel 1989). Thus, in trees with

larger A_{il}, A_c, A_l, and shorter growing season lengths, the characteristic petiole flattened-

leaf flutter combined with broader branching canopies might increase the number of

leaves operating in near optimal light-quenching conditions by reducing leaf shading

throughout the day. The genetic basis of these architectural traits is also consistent with

other cottonwood studies showing that the fractal architecture of different tree genotypes

is genetically based and heritable (Bailey et al. 2004), which affects sink-source

relationships and herbivores such as aphids (Compson et al. 2011).

In accordance with my hypothesis, MR ecotype trees exhibited a suite of

conservative hydraulic traits that together represent an adaptive syndrome resulting in

higher survival to freezing temperatures (Chave et al. 2009; Körner 2003; Sperry and

Sullivan 1992). Susceptibility to freeze-thaw-induced xylem cavitation increases with

vessel size because air bubbles are more easily released from the dissolution of gas

during thawing in larger diameter vessels (Mayr and Sperry 2010; Sperry and Sullivan

1992). Consequently, the Hd_s was significantly lower in MR stems, reflecting the presence of smaller diameter vessels relative to SD stems. Similarly, Hd_s has been correlated with sapwood area-specific hydraulic conductivity (Hajek et al. 2014; Kolb and Sperry 1999). The reduced hydraulic efficiency in many of the wood xylem traits may explain why compared with SD trees, the MR ecotype leaves displayed lower mean D_{stom} and G_{smax} values, reflecting an upper bound on water delivery from woody tissues to the canopy.

On the other hand, the MR trees displayed higher values for traits that are characteristic for high tissue structural integrity and frost protection, including D_{stem} and F_b. Although D_{stem} is correlated with a reduced hydraulic conductivity (Reich 2014), it has been correlated with greater mechanical support against xylem implosion by negative pressure (cavitation resistance) caused by low xylem water potentials (Hacke et al. 2001) and wood mechanical strength (Chave et al. 2009; Niklas and Spatz 2010, 2012). Bark in broadleaved species has been found to be a better thermal insulator than conifer bark (Pásztory and Ronyecz 2013) while stem shrinkage associated with freeze–thaw cycles has been correlated with the thickness of the bark (Zweifel and Häsler 2000; Améglio et al. 2001). Consequently, in angiosperms around the world, outer bark thickness has been found to increase in environments with temperature seasonality (Rosell 2016). Bark thickness has also been associated with the protection of phloem and other living tissues from freezing temperatures (Améglio et al. 2001; Arco Molina et al. 2016; Charrier et al. 2017).

Adaptive syndrome trait correlations within the SD ecotype

As I hypothesized, the SD ecotype featured a coordinated suite of functional traits (i.e., a different adaptive syndrome) that prioritize greater water transport efficiency to reduce foliar thermal load via enhanced evaporative cooling. Thus, the SD ecotype displayed smaller leaves with a potentially reduced exposure to short-wave radiation from sunlight. Likewise, the thinner leaves with higher SLA likely have a lower thermal capacitance – or heat storage over time – than similar sized leaves with a lower SLA. Additionally, SD ecotype leaves displayed a relatively high D_{stom} and low S_{stom} arrangement, which allows the leaf to rapidly adjust stomatal conductance to changes in air temperatures and humidity (Hetherington and Woodward 2003).

Because leaves with smaller S_{stom} display smaller cross-sectional area of the guard cells and reduced pore depths, these leaves can achieve a greater stomatal conductance (g_s) per unit area occupied by stomata (Franks and Farquhar 2007). Accordingly, I found that based on their stomatal morphological characteristics, SD trees exhibited a larger theoretical G_{smax} than the MR ecotype. Many Sonoran Desert ecotype trees are exposed to mid-summer temperatures that approach or even exceed 50 °C. These extreme temperatures can simultaneously damage the electron transport capacity of Photosystem II and increase photorespiration (Allakhverdiev et al. 2008; Hultine et al. 2020; O'Sullivan et al. 2017). Therefore, warm-adapted trees likely prioritize maintaining midday leaf conductance to evaporatively cool the canopy (Fauset et al. 2018; Hultine et al. 2019, 2020; Michaletz et al. 2015). The combination of these leaf morpho-physiological features allows SD trees to achieve higher levels of transpirational cooling of their leaves while reducing heat gain from incident light radiation (Hultine et al. 2019,

2020). For example, another recent study using genotypes from the same common garden as the present study reported that the SD ecotype trees displayed 35% higher midday leaf transpiration rates and 4 °C lower leaf temperature than the MR ecotype trees (Hultine et al. 2019).

Repeated measures of A_{il} and SLA indicated SD trees continuously displayed smaller and thinner leaves as an additional possible adaptation to summer extreme temperatures during the growing season (Table S1). The reduced leaf size, relative to the MR leaves, suggest that the SD trees displayed more rapid turnover rates of leaves with cheaper construction costs over the growing season. This might be due to the high cost of maintaining leaves relative to their return in carbon during the hottest part of the summer. Extreme high temperatures negatively affect the carbon balance of leaves by simultaneously reducing photosynthesis and increasing respiration (Haworth et al. 2018; Sharkey 2005).

Greater investment in the construction of larger leaves and larger petioles in MR leaves was associated with having a greater theoretical K_p. However, the higher K_p was offset by the larger leaf area and thus K_l was uniform across the two ecotypes. Additionally, I found a significant positive relationship between positive MAT transfer distance or elevation and the ratio between K_l (supply) and G_{smax} (demand) at the population level. These results imply that SD ecotype trees possess a set of leaf morphological traits that allow larger and faster utilization of water for transpiration, but at the risk of greater leaf water demand relative to supply via the petiole. Measurements of leaf Ψ_{md} appeared to reflect a greater hydraulic risk strategy and weaker stomatal control over plant water potential in SD ecotype trees (Table S1). Specifically, mean Ψ_{md}

measured over the growing season regularly fell below -1.88 MPa; the xylem pressure at which hydraulic failure has been previously reported to occur in *P. fremontii* (Choat et al. 2012; Leffler et al. 2000; Li et al. 2008) (Table S1). Given these results, it appears that SD ecotype trees take on a risky trade-off strategy between maximizing delivery to the canopy at the expense of increasing vulnerability to cavitation which may limit these trees to river reaches with predictable and abundant groundwater availability during the entire growing season.

Alternatively, the risky water use strategy in SD trees may have been partially mitigated by maintaining a substantially higher A_s:A_l relative to the MR ecotype trees. Given that SD trees have most likely been selected to maximize canopy thermal regulation via evaporative cooling, it was not surprising that at the whole tree level, water supply (i.e., A_s) relative to demand (i.e., A_l) was high relative to MR trees. Seasonal increases in A_s:A_l has been reported to be a strategy in other species to increase water supply to canopies during summer drought or under high temperature (Carter and White 2009; Eamus et al. 2000; O'Grady et al. 2009). Similarly, a previous investigation in *P. fremontii* observed that A_s:A_l was correlated with groundwater availability (Gazal et al. 2006). Accordingly, SD trees exhibited higher A_s:A_l coupled with a greater F_{sl} and Hd_s that reflects the greater hydraulic efficiency to meet the higher water demand for leaf evaporative cooling (Drake et al. 2018; Gleason et al. 2012; Sterck et al. 2008; Zaehle 2005).

Trait contrasts among populations

Differences in functional traits in *P. fremontii* at the population level resembled differences between the two ecotypes. However, I detected finer variations in phenotypic

46

characteristics across the climatic gradient in which the eight populations were sourced from. This was particularly true among the SD ecotype populations. Specifically, middle elevation TSZSAN population which displayed slight intermediate trait characteristics between the two ecotypes. Due to the geographical and environmental characteristics of its source site (southernmost latitude and middle range climate), this population seems to display trait characteristic that reflect climatic adaptation to its intermediate local environmental conditions.

Thus, while displaying SD ecotype characteristics in most LES and WES spectra traits, TSZSAN population exhibited intermediate D_{stom}, Al, and H between the two ecotypes (Table S2, S4, S5). Additionally, $A_s{:}A_l$ in this population was more characteristic of the MR ecotype even though it is the southernmost geographically located of population of the SD ecotype. Consequently, multivariate analyses clustered this population with the MR ecotype populations in the architecture trait spectrum and as its own intermediate group in the WES and the pooled all traits PCA (Fig. S2.2, S2.3 and S2.4). Although the 95% confidence intervals representing the TSZSAN populations overlapped the other four SD ecotype populations, its horizontal range (PC1) exhibited a clear tendency toward the positive, MR ecotype side of the PC1 (Fig. 2.8).

Conclusions

Climate change implications

Drought – inter-drought cycles and extreme temperature swings will likely become amplified throughout most of the planet over the next several decades as a consequence of climate change (Garfin et al. 2013; Williams et al. 2020). Results from

the present study underscore how extreme events will likely lead to widespread maladaptation and reduced fitness in *Populus* species in response to climate change. For example, the SD ecotype displayed greater capacity to supply water to their canopies to avoid thermal stress but potentially at the expense of being more susceptible to hydraulic disfunction caused by maintaining lower minimum water potentials, having a higher theoretical maximum stomatal conductance, and having a larger mean hydraulic diameter in woody stems. Thus, increases in drought frequency can be expected to reduce the habitat niche of SD genotypes to locations where soil water availability remains stable independent of drought, such as along the margins of perennially-flowing streams (Hultine et al. 2019). The MR ecotype, on the other hand, displayed a set of morphological traits designed to increase sunlight exposure and maximize safety from freeze-thaw cavitation, but as a consequence may be unable to cool their canopies when exposed to episodic heatwaves that are likely to increase in frequency and intensity. What remains an open question is whether trait expression is plastic enough to overcome rapid changes in environmental conditions. As the size of the SD ecotype ellipses of the leaf, architecture, and pooled traits PCAs showed, the SD ecotype exhibited greater trait variability, perhaps a reflection of greater trait plasticity or higher genetic diversity among genotypes relative to the MR ecotype.

The combination of multiple functional trait spectra demonstrates adaptive syndromes for different ecoregions and present a powerful way to enhance our mechanistic understanding of local adaptation within species. As regional mean annual temperature, drought severity and heat wave occurrence increase over the next several decades, this research improves our understanding of the possible effect that these

changes will have on *P. fremontii* and other widely distributed *Populus* species across their geographical ranges. These results, therefore, improve our capacity to match genotypes with traits that may yield greater resistance to changing environmental conditions of a given location, and therefore the detection of genotypes best suited for possible repopulation efforts along a species' historical geographical distribution.

Acknowledgements

Tables

Table 2.1. Climatic variables of the eight provenances and their corresponding two ecotypes studied at the Agua Fria National Monument common garden. Climatic characteristics include mean annual temperature (MAT), mean warmest monthly temperature (MWMT), and mean coldest monthly temperature (MCMT). Transfer distances for MAT (MAT of the garden minus MAT of the provenance), MWMT, and MCMT. The population CAFAUG is located near the common garden and thus has a transfer distance of zero.

Population	Elevation (m)	Latitude	Longitude	MAT (°C)	MWMT (°C)	MCMT (°C)	MAT (°C) Transfer	MWMT (°C) Transfer	MCMT (°C) Transfer
MR Ecotype									
KKHOPI	1940	35.8115	-110.18038	10.7	23.0	-1.3	6.7	5.7	9.1
JLAJAK	1521	34.9613	-110.38956	12.3	25.3	-0.7	5.1	3.4	8.5
CLFLCR	1301	35.6088	-111.31369	14.1	27.2	0.8	3.3	1.5	7.0
SD Ecotype									
TSZSAN	1212	31.4382	-110.76260	16.9	26.2	8	0.5	2.5	-0.2
CAFAUG	988	34.2338	-111.04478	17.4	28.7	7.8	0	0	0
NRVNEW	666	33.9540	-112.13526	19.9	31.4	10.0	-2.5	-2.7	-2.2
LBWBIL	161	34.2761	-114.05856	22.3	34.6	10.9	-4.9	-5.9	-3.1
CCRCOL	72	33.3621	-114.69856	22.6	33.9	12.2	-5.2	-5.2	-4.4

Table 2.2. Hypothesized correlations between the set of functional traits studied in this research and the two ecotypes (Sonoran Desert ecotype and the Mogollon Rim ecotype) present in the Agua Fria National Monument common garden.

	Acronym	Unit	SD Ecotype	MR Ecotype
Phenology				
Spring Budburst	BB	Day of the Year	Early	Late
Fall Budset	BS	Day of the Year	Late	Early
Leaf Traits				
Individual Leaf Area	A_{il}	cm^2	Small	Large
Specific Leaf Area	SLA	$cm^2\,g^{-1}$	High	Low
Stomatal Density	D_{stom}	#Stomata mm^{-2}	High	Low
Stomatal Size	S_{stom}	μm^2	Small	Large
Theoretical Maximum Stomatal Conductance	G_{smax}	$mmol\ m^{-2}\,s^{-1}$	High	Low
Petiole Area	A_p	mm^2	Small	Large
Petiole Flatness	L_{pf}	$mm^2\,mm^{-2}$	Low	High
Petiole Lumen Area	A_{pl}	μm^2	Large	Small
Petiole Hydraulic Mean Diameter	Hd_p	μm	Large	Small
Petiole Lumen Fraction	F_{pl}	$\mu m^2\,\mu m^{-2}$	Large	Small
Petiole Vessel Density	D_{pv}	# vessel mm^{-2}	High	Low
Petiole Theoretical Hydraulic Conductivity	K_p	$mg\ m\ Mpa^{-1}\,s^{-1}$	High	Low
Leaf Theoretical Hydraulic Conductivity	K_l	$mg\ m^{-1}\ Mpa^{-1}\,s^{-1}$	High	Low
Architecture Traits				
Whole-Tree Leaf Area	A_l	m^2	Small	Large
Tree Height	H	m	Tall	Short
Canopy Area	A_c	m^2	Small	Large
Sapwood to Leaf Area	$A_s{:}A_l$	$cm^2\,cm^{-2}$	Large	Small
Leaf Area Index	LAI	$m^2\,m^{-2}$	High	Low
Wood Traits				
Specific Stem Density	D_{stem}	$g\ cm^{-3}$	Low	High
Bark %	F_b	%	Low	High
Stem Lumen Area	A_{sl}	μm^2	Large	Small
Stem Hydraulic Mean Diameter	Hd_s	μm	Large	Small
Stem Lumen Fraction	F_{sl}	$\mu m^2\,\mu m^{-2}$	Large	Small
Stem Vessel Density	D_{sv}	# vessel mm^{-2}	High	Low
Pre-Dawn Water Potential	Ψ_{pd}	Mpa	Same	Same
Mid-Day Water Potential	Ψ_{md}	MPa	Low	High

Table 2.3. Results of Mean ± standard error (n = 48 to 80) comparison of *Populus fremontii* traits at ecotypes level (Arizona Sonoran Desert (SD) and the Mogollon Rim (MR) in the Agua Fria National Monument common garden. Abbreviations for each Parameter are shown in Table 2.2

	t-value	df	SD Ecotype	MR Ecotype
Phenology				
BB	**-15.65*****	78	65 ± 11	111 ± 14
BS	**8.63*****	78	297 ± 6	284 ± 7
Leaf Spectrum				
A_{il}	**8.98*****	78	18 ± 5.25	30 ± 6.81
SLA	**-8.42*****	78	121 ± 11.9	99 ± 9.64
D_{stom}	**12.81*****	77.6	430 ± 73	258 ± 47
S_{stom}	**14.22*****	78	250 ± 34	394 ± 58
G_{smax}	**9.24*****	77.1	1.25 ± 0.18	0.93 ± 0.12
A_p	**-4.64*****	46	1.04 ± 0.48	1.69 ± 0.43
L_{pf}	**-3.25****	46	1.39 ± 0.23	1.59 ± 0.16
A_{pl}	-0.84	45.9	91.85 ± 32	98.14 ± 20
Hd_p	-1.43	38.5	23.4 ± 3.1	24.7 ± 2.9
F_{pl}	0.09	46	0.06 ± 0.02	0.05 ± 0.02
D_{pv}	1.09	46	677 ± 354	575 ± 232
K_p	**-4.81*****	46	7e-07±4e-07	1e-06±4e-07
K_l	-0.62	46	3e-04±1e-04	3e-04±9e-05
Architecture Spectrum				
A_l	**-2.26***	62	7.52 ± 2.63	9.03 ± 2.55
H	**2.34***	78	3.08 ± 0.49	2.84 ± 0.36
A_c	**4.02*****	46.8	2.16 ± 0.56	2.82 ± 0.78
$A_s{:}A_l$	**10.9*****	43.5	3.56 ± 0.55	2.58 ± 0.10
LAI	0.68	59.3	3.61 ± 1.73	3.36 ± 1.27
Wood Spectrum				
D_{stem}	**-4.06*****	46	0.41 ± 0.03	0.44 ± 0.03
F_b	**-5.91*****	46	0.29 ± 0.06	0.39 ± 0.06
A_{sl}	1.88.	46	779 ± 192	679 ± 153
Hd_s	**2.28***	46	40.4 ± 4	37.6 ± 4
F_{sl}	**2.66***	46	0.23 ± 0.04	0.20 ± 0.05
D_{sv}	0.24	46	318 ± 78.2	313 ±85.1
Ψ_{pd}	-0.56	46	-0.46 ± 0.04	-0.45 ± 0.08
Ψ_{md}	**-4.82*****	46	-1.58 ± 0.14	-1.38 ± 0.13

† Signif. codes: *** 0.001 ** 0.01 * 0.05 . 0.1

Figures
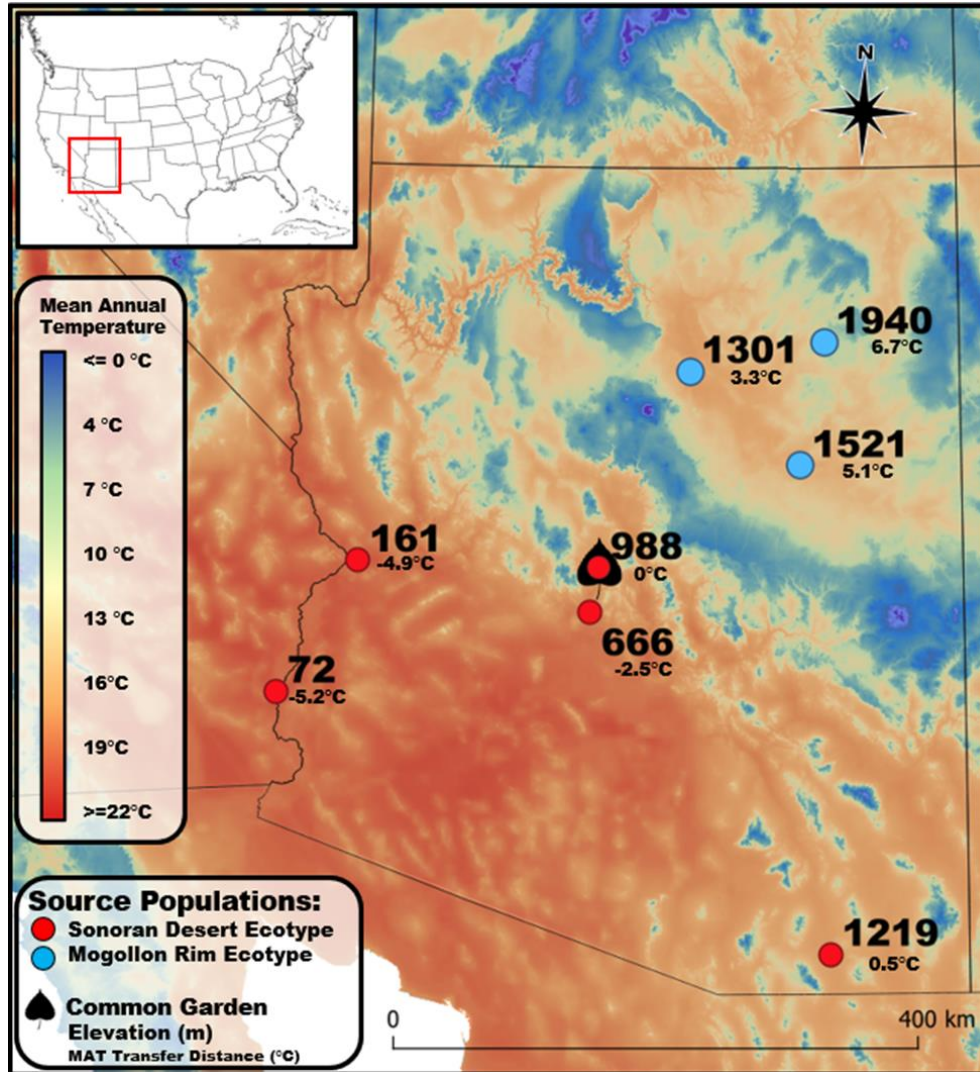
Figure 2.1. Location of 8 source population sites of *Populus fremontii* and the Agua Fria common garden locations (Fremont cottonwood leaf icon). Light blue points denote populations coming from the Mogollon Rim ecotype while the pink points indicate populations coming from the Sonoran Desert ecotype ([Fick, S.E. and R.J. Hijmans, 2017. Worldclim 2: New 1-km spatial resolution climate surfaces for global land areas. International Journal of Climatology. (http://worldclim.org/version2)]. QGIS Development Team (2020). QGIS Geographic Information System. Open-Source Geospatial Foundation Project. http://qgis.osgeo.org".

Spring Budburst

Fall Budset

Julian Day
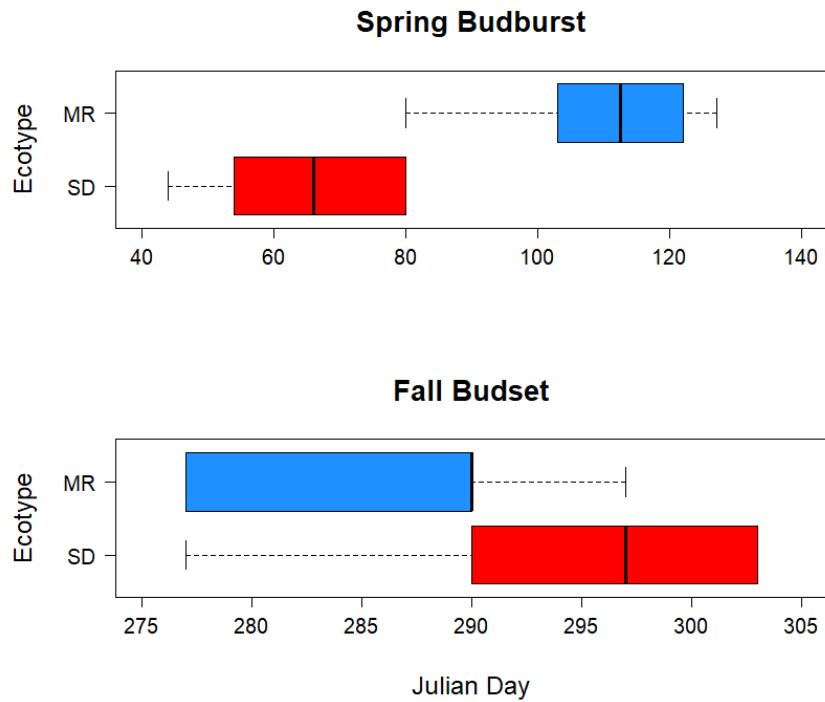
Figure 2.2. Box and whisker plots showing the median, 25th and 75th percentiles (boxes) and the 10th and 90th percentiles (error bars) of a) spring budburst and b) fall budset of the Sonoran Desert and Mogollon Rim ecotypes. Ecotype phenology was measured at the beginning and end of the 2017 growing season (Budburst: $t = -15.65$, $df = 78$, $P < 0.001$; Budset: $t = 5.02$, $df = 78$, $P < 0.001$).
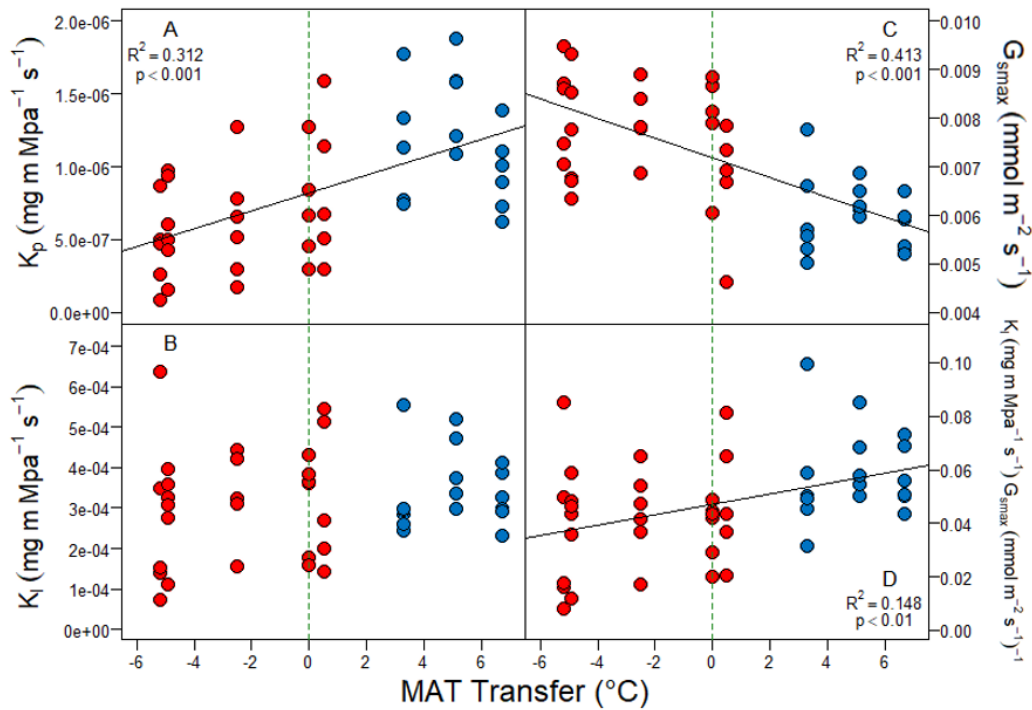
Figure 2.3. Relationship between petiole theoretical hydraulic conductivity (K_p; mg m-1 MPa–1 s–1), leaf area normalized theoretical hydraulic conductivity of the petiole (K_l; mg m-1 s-1 MPa-1), leaf theoretical stomatal conductance (G_{smax} mmol m-2 s-1), the ratio between K_l and G_{smax} and source population mean annual temperature MAT transfer in the Sonoran Desert ecotype (red, n=30) and Mogollon Rim ecotype (blue, n = 18). Vertical dotted lines indicate the mean annual temperature (MAT °C) of the garden.
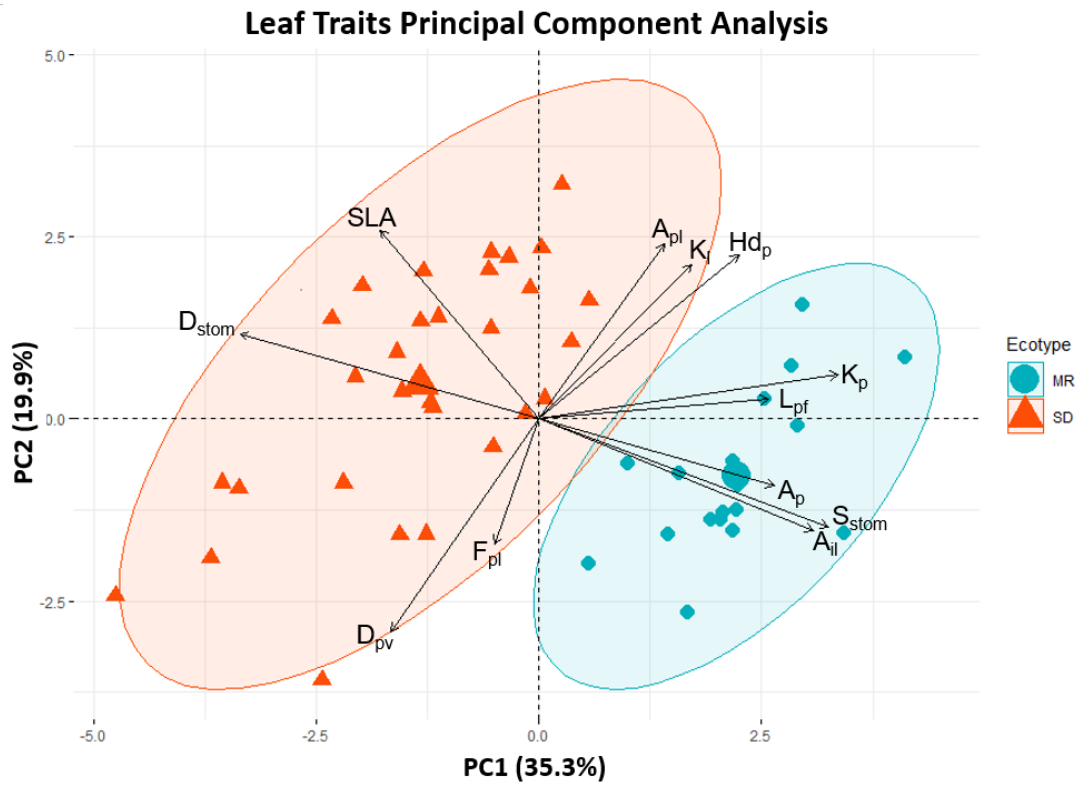
Figure 2.4. Principal component analysis (PCA) summarizing leaf trait spectrum variables at genotype level related with the 2 ecotypes, Sonoran Desert (SD) and the Mogollon Rim (MR). Plot of PC1 (37.1% of total variation) and PC2 (18.6% variation) showing 95% confidence ellipses of ecotype means.
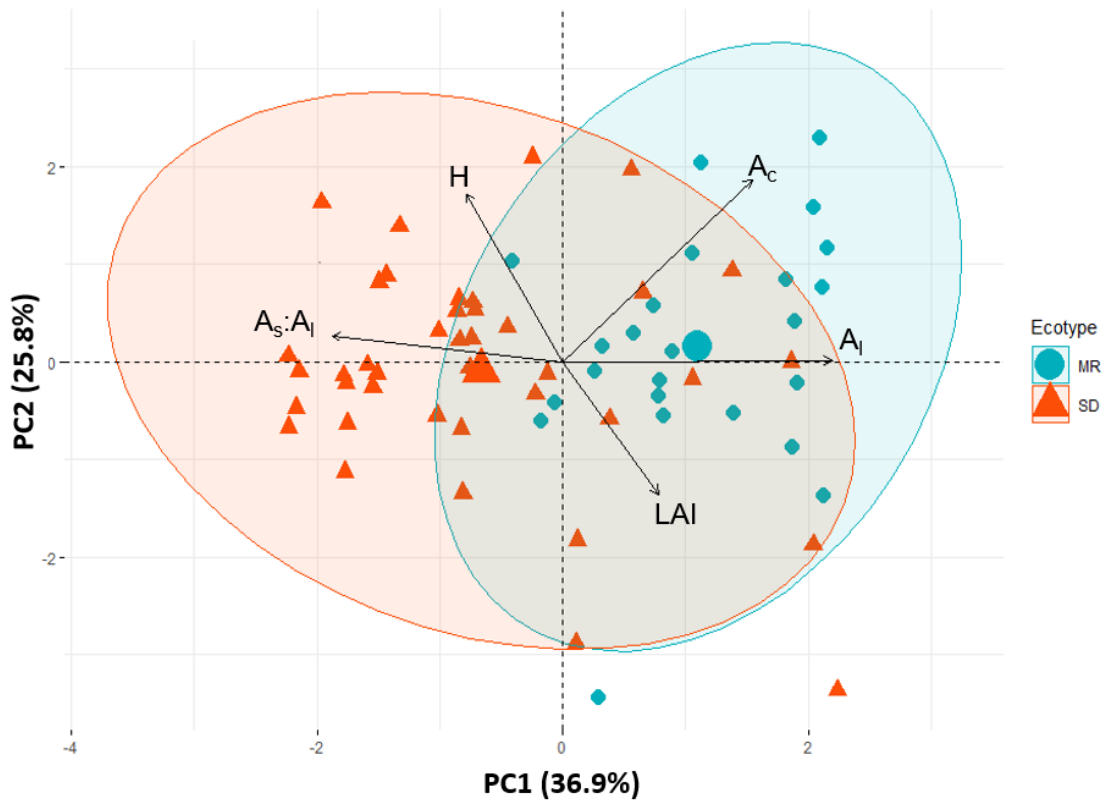
Figure 2.5. Principal component analysis (PCA) summarizing the whole-plant architecture traits spectrum variables at genotype level related with the 2 ecotypes, Sonoran Desert (SD) and the Mogollon Rim (MR). Plot of PC1 (45.2% of total variation) and PC2 (30.8% variation) showing 95% confidence ellipses of ecotype means.
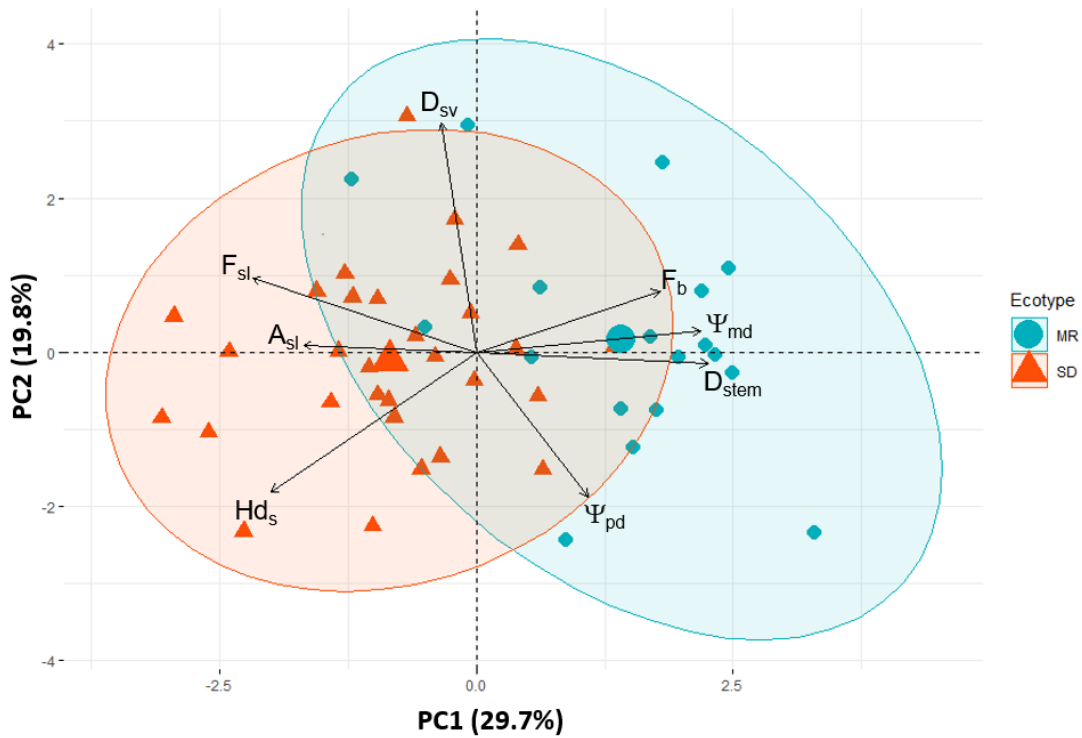
Figure 2.6. Principal component analysis (PCA) summarizing wood traits spectrum variables at genotype level related with the 2 ecotypes, Sonoran Desert (SD) and the Mogollon Rim (MR). Plot of PC1 (29.7% of total variation) and PC2 (19.8% variation) showing 95% confidence ellipses of ecotype means.
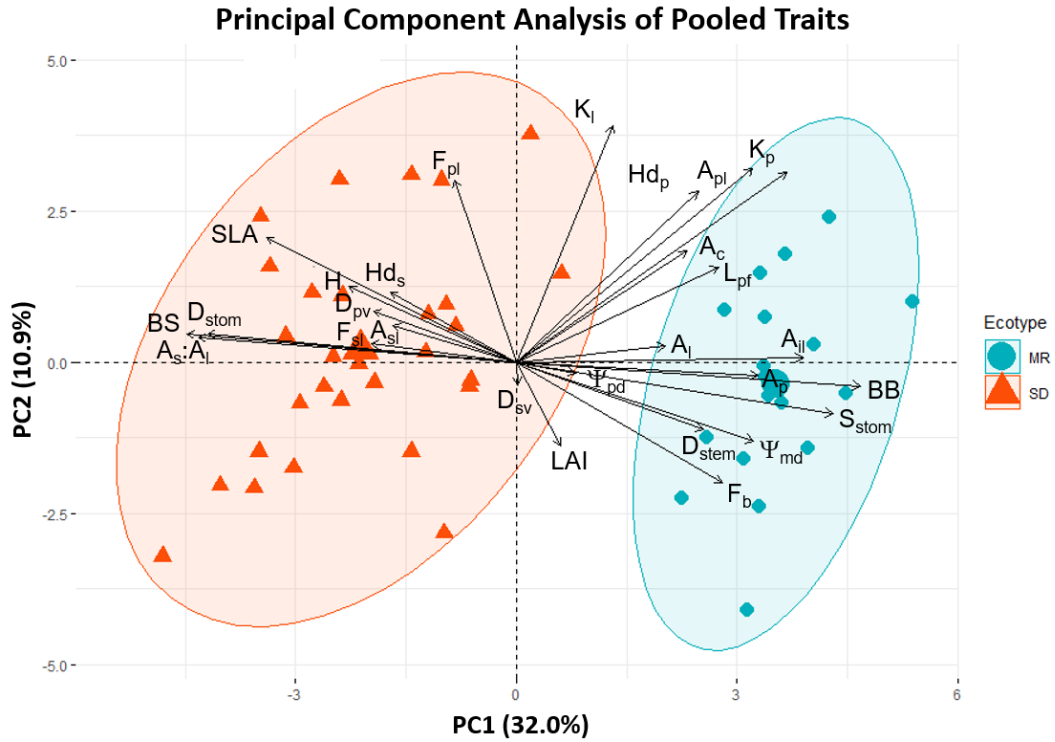
Figure 2.7. Principal component analysis (PCA) summarizing all 27 traits variables at genotype level related with the 2 ecotypes, Arizona Sonoran Desert (SD) and the Mogollon Rim (MR). Plot of PC1 (32% of total variation) and PC2 (10.9% variation) showing 95% confidence ellipses of ecotype means.
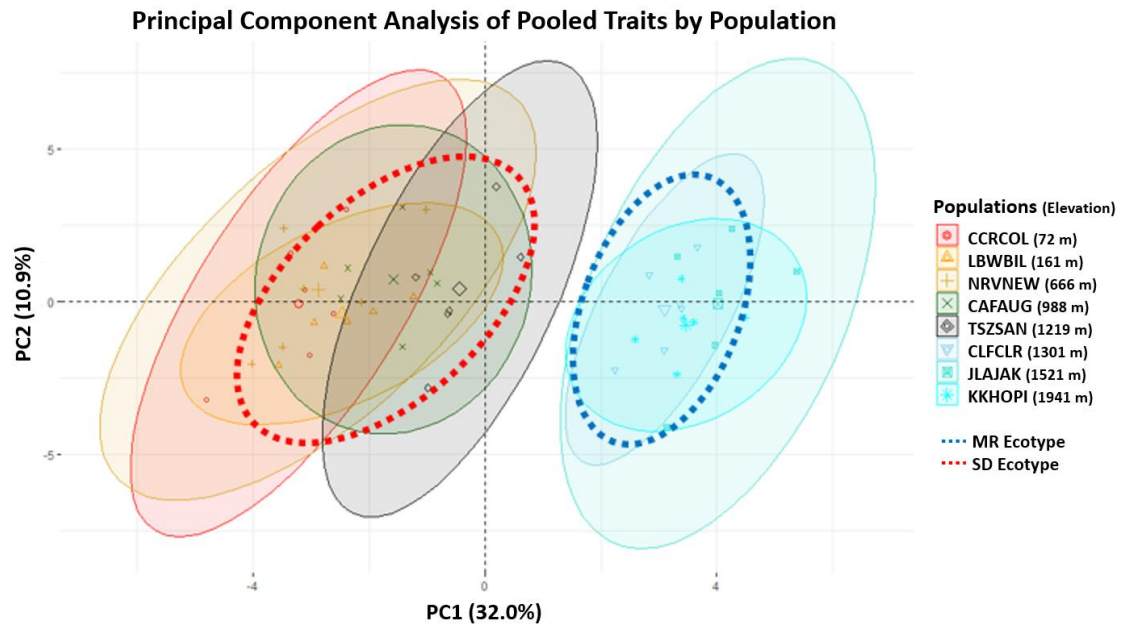
Figure 2.8. Principal component analysis (PCA) summarizing all 27 traits variables at genotype level related with 8 populations that collectively represent the entire elevational range of the species. Plot of PC1 (32% of total variation) and PC2 (10.9% variation) showing 95% confidence ellipses of population means.

Figure 2.9. Redundancy analysis triplot with explanatory variables (Transfer.MAT = transfer mean annual temperature, MAP = population mean annual precipitation and the two ecotypes) and all 27 traits as response variables. Individual genotypes (n = 48) are marked as red dots. The relationship between the explanatory variables (blue vectors) and response variables (red vectors) can be interpreted by the alignment of the vectors.

References

Ackerly D, Knight C, Weiss S, Barton K, Starmer K (2002) Leaf size, specific leaf area and microhabitat distribution of chaparral woody plants: Contrasting patterns in species level and community level analyses. Oecologia 130(3), 449–457. https://doi.org/10.1007/s004420100805

Allakhverdiev SI, Kreslavski VD, Klimov VV, Los DA, Carpentier R, Mohanty P (2008) Heat stress: An overview of molecular responses in photosynthesis. Photosynthesis Research 98(1–3), 541–550. https://doi.org/10.1007/s11120-008-9331-0

Améglio T, Cochard H, Ewers FW (2001) Stem diameter variations and cold hardiness in walnut trees. Journal of Experimental Botany *52*(364), 2135–2142. https://doi.org/10.1093/jexbot/52.364.2135

Anderson MJ (2001) A new method for non-parametric multivariate analysis of variance. Austral Ecology *26*(1), 32–46. https://doi.org/10.1046/j.1442-9993.2001.01070.x

Ansley R.J, Mirik M, Surber BW, Park SC (2012) Canopy Area and Aboveground Mass of Individual Redberry Juniper (*Juniperus pinchotii*) Trees. Rangeland Ecology & Management 65, 189–195. https://doi.org/10.2307/41495360

Arco Molina JG, Hadad MA, Patón Domínguez D, Roig FA (2016) Tree age and bark thickness as traits linked to frost ring probability on *Araucaria araucana* trees in norther Patagonia. Dendrochronologia 37, 116–125. https://doi.org/10.1016/j.dendro.2016.01.003

Bailey JK, Bangert RK, Schweitzer JA, Trotter RT, Shuster SM, Whitham TG (2004) Fractal geometry is heritable in trees. Evolution 58(9), 2100–2102. https://doi.org/10.1111/j.0014-3820.2004.tb00493.x

Barbour MA, Rodriguez-Cabal MA, Wu ET, Julkunen-Tiitto R, Ritland CE, Miscampbell AE, Jules ES, Crutsinger GM (2015) Multiple plant traits shape the genetic basis of herbivore community assembly. Functional Ecology 29(8), 995–1006. https://doi.org/10.1111/1365-2435.12409

Bates D, Mächler M, Bolker B, Walker S (2015) Fitting linear mixed-effects models using lme4. Journal of Statistical Software 67(1). https://doi.org/10.18637/jss.v067.i011

Blasini DE, Koepke DF, Grady KC, Allan GJ, Gehring CA, Whitham TG, Cushman SA, Hultine KR (2020) Data from: Adaptive trait syndromes along multiple economic spectra define cold and warm adapted ecotypes in a widely distributed foundation tree species. Dryad Digital Repository. https://doi.org/10.5061/dryad.gf1vhhmn9

Borcard D, Gillet F, Legendre P (2011) Numerical ecology with R. Springer. https://doi.org/10.1007/978-1-4419-7976-6

Buesa RJ, Peshkov MV (2009) Histology without xylene. Annals of Diagnostic Pathology 13(4), 246–256. https://doi.org/10.1016/j.anndiagpath.2008.12.005

Carter JL, White DA (2009) Plasticity in the Huber value contributes to homeostasis in leaf water relations of a mallee Eucalypt with variation to groundwater depth. Tree Physiology 29(11), 1407–1418. https://doi.org/10.1093/treephys/tpp076

Chapin FS, Matson PA, Vitousek PM (2011) Principles of terrestrial ecosystem ecology. Springer. https://doi.org/10.1007/978-1-4419-9504-9

Charrier G, Nolf M, Leitinger G, Charra-Vaskou K, Losso A, Tappeiner U, Améglio T, Mayr S (2017) Monitoring of freezing dynamics in trees: A simple phase shift causes complexity. Plant Physiology 173(4), 2196–2207. https://doi.org/10.1104/pp.16.0181

Chave J, Coomes D, Jansen S, Lewis SL, Swenson NG, Zanne AE (2009) Towards a worldwide wood economics spectrum. Ecology Letters 12(4), 351–366. https://doi.org/10.1111/j.1461-0248.2009.01285.x

Choat B, Jansen S, Brodribb TJ, Cochard H, Delzon S, Bhaskar R, Bucci SJ, Feild TS, Gleason SM, Hacke UG, Jacobsen AL, Lens F, Maherali H, Martínez-Vilalta J, Mayr S, Mencuccini M, Mitchell PJ, Nardini A, Pittermann J, … Zanne AE (2012) Global convergence in the vulnerability of forests to drought. Nature 491(7426), 752–755. https://doi.org/10.1038/nature11688

Clausen J, Keck DD, Hiesey WM (1940) Experimental studies on the nature of species. Effect of varied environments on western North American plants. Carnegie Institution of Washington Publication. https://doi.org/10.1086/280930

Cochard H, Forestier S, Améglio T (2001) A new validation of the Scholander pressure chamber technique based on stem diameter variations. Journal of Experimental Botany *52*(359), 1361–1365. https://doi.org/10.1093/jexbot/52.359.1361

Compson ZG, Larson KC, Zinkgraf MS, Whitham TG (2011) A genetic basis for the manipulation of sink–source relationships by the galling aphid *Pemphigus batae*. Oecologia 167(3), 711–721. https://doi.org/10.1007/s00442-011-2033-x

Cooper HF, Grady KC, Cowan JA, Best RJ, Allan GJ, Whitham TG (2019) Genotypic variation in phenological plasticity: Reciprocal common gardens reveal adaptive responses to warmer springs but not to fall frost. Global Change Biology 25(1), 187–200. https://doi.org/10.1111/gcb.14494

Cornelissen JHC (1999) A triangular relationship between leaf size and seed size among woody species: Allometry, ontogeny, ecology and taxonomy. Oecologia 118(2), 248–255. https://doi.org/10.1007/s004420050725

Cornelissen JHC, Lavorel S, Garnier E, Díaz S, Buchmann N, Gurvich DE, Reich PB, Steege HT, Morgan HD, Heijden MG, Pausas JG, Poorter H (2003) Handbook of protocols for standardised and easy measurement of plant functional traits worldwide. Australian Journal of Botany 51(4), 335–380. https://doi.org/10.1071/BT02124

Corner EJH (1949) The Durian theory or the origin of the modern tree. Annals of Botany 13(4), 367–414. https://doi.org/10.1093/oxfordjournals.aob.a083225

Cushman SA, Max T, Meneses N, Evans LM, Ferrier S, Honchak B, Whitham TG, Allan GJ (2014) Landscape genetic connectivity in a riparian foundation tree is jointly driven by climatic gradients and river networks. Ecological Applications 24, 1000–1014. https://doi.org/10.1890/13-1612.1

de Villemereuil P, Schielzeth H, Nakagawa S, Morrissey M (2016) General methods for evolutionary quantitative genetic inference from generalized mixed models. Genetics 204(3), 1281–1294. https://doi.org/10.1534/genetics.115.186536

Denny EG, Gerst KL, Miller-Rushing AJ, Tierney GL, Crimmins TM, Enquist CAF, Guertin P, Rosemartin AH, Schwartz MD, Thomas KA, Weltzin JF (2014) Standardized phenology monitoring methods to track plant and animal activity for science and resource management applications. International Journal of Biometeorology 58(4), 591–601. https://doi.org/10.1007/s00484-014-0789-5\

Drake JE, Tjoelker MG, Vårhammar A, Medlyn BE, Reich PB, Leigh A, Pfautsch S, Blackman CJ, López R, Aspinwall MJ, Crous KY, Duursma RA, Kumarathunge D, De Kauwe MG, Jiang M, Nicotra AB, Tissue DT, Choat B, Atkin OK, Barton CVM (2018) Trees tolerate an extreme heatwave via sustained transpirational cooling and increased leaf thermal tolerance. Global Change Biology 24(6), 2390–2402. https://doi.org/10.1111/gcb.14037

Eamus D, O'Grady AP, Hutley L (2000) Dry season conditions determine wet season water use in the wet-tropical savannas of northern Australia. Tree Physiology 20(18), 1219–1226. https://doi.org/10.1093/treephys/20.18.1219

Eckenwalder JE (1996). Systematics and evolution of *Populus*. I. In Stettler RF, Bradshaw HD, Heilman PE, Hinckley TM (Eds), Biology of *Populus* and its implications for management and conservation: 7–32. NRC Research Press.

Eguchi N, Morii N, Ueda T, Funada R, Takagi K, Hiura T, Sasa K, Koike T (2008) Changes in petiole hydraulic properties and leaf water flow in birch and oak saplings in a CO2-enriched atmosphere. Tree Physiology 28(2), 287–295. https://doi.org/10.1093/treephys/28.2.287

Eilmann B, Zweifel R, Buchmann N, Graf Pannatier E, Rigling A (2011) Drought alters timing, quantity, and quality of wood formation in Scots pine. Journal of Experimental Botany 62(8), 2763–2771. https://doi.org/10.1093/jxb/erq443

Evans LM, Kaluthota S, Pearce DW, Allan GJ, Floate K, Rood SB, Whitham TG (2016) Bud phenology and growth are subject to divergent selection across a latitudinal gradient in *Populus angustifolia* and impact adaptation across the distributional range and associated arthropods. Ecology and Evolution 6(13), 4565–4581. https://doi.org/10.1002/ece3.2222

Fauset S, Freitas HC, Galbraith DR, Sullivan MJP, Aidar MPM, Joly CA, Phillips OL, Vieira SA, Gloor MU (2018) Differences in leaf thermoregulation and water use strategies between three co-occurring Atlantic forest tree species: Leaf energy balance of Atlantic forest trees. Plant, Cell and Environment 41(7), 1618–1631. https://doi.org/10.1111/pce.13208

Fischer DG, Wimp GM, Hersch-Green E, Bangert RK, LeRoy CJ, Bailey JK, Schweitzer JA, Dirks C, Hart SC, Allan GJ, Whitham TG (2017) Tree genetics strongly affect forest productivity, but intraspecific diversity–productivity relationships do not. Functional Ecology 31(2), 520–529. https://doi.org/10.1111/1365-2435.12733

Franks PJ, Farquhar GD (2007) The mechanical diversity of stomata and its significance in gas-exchange control. Plant Physiology 143(1), 78–87. https://doi.org/10.1104/pp.106.089367

Franks PJ, Farquhar GD (2001) The effect of exogenous abscisic acid on stomatal development, stomatal mechanics, and leaf gas exchange in *Tradescantia virginiana*. Plant Physiology 125(2), 935–942. https://doi.org/10.1104/pp.125.2.935

Freschet GT, Cornelissen JHC, van Logtestijn RSP, Aerts R (2010) Evidence of the 'plant economics spectrum' in a subarctic flora. Journal of Ecology 98(2), 362–373. https://doi.org/10.1111/j.1365-2745.2009.01615.x

Friedman JM, Roelle JE, Cade BS (2011) Genetic and environmental influences on leaf phenology and cold hardiness of native and introduced riparian trees. International Journal of Biometeorology 55(6), 775–787. https://doi.org/10.1007/s00484-011-0494-6

Garfin G, Jardine A, Merideth R, Black M, LeRoy S (2013) Assessment of Climate Change in the Southwest United States. National Climate Assessment Regional Technical Input Report Series Assessment 531. https://doi.org/10.5822/978-1-61091-484-0

Gärtner H, Lucchinetti S, Schweingruber FH (2014) New perspectives for wood anatomical analysis in dendrosciences: The GSL1-microtome. Dendrochronologia 32(1), 47–51. https://doi.org/10.1016/j.dendro.2013.07.002

Gazal RM, Scott RL, Goodrich DC, Williams DG (2006) Controls on transpiration in a \ semiarid riparian cottonwood forest. Agricultural and Forest Meteorology 137(1–2), 56–67. https://doi.org/10.1016/j.agrformet.2006.03.002

Germino MJ, Moser AM, Sands AR (2019) Adaptive variation, including local adaptation, requires decades to become evident in common gardens. Ecological Applications 29(2), 1–7. https://doi.org/10.1002/eap.1842

Gleason SM, Butler DW, Ziemińska K, Waryszak P, Westoby M (2012) Stem xylem conductivity is key to plant water balance across Australian angiosperm species: Plant stem hydraulic traits. Functional Ecology 26(2), 343–352. https://doi.org/10.1111/j.1365-2435.2012.01962.x

Grady KC, Ferrier SM, Kolb TE, Hart SC, Allan GJ, Whitham TG (2011) Genetic variation in productivity of foundation riparian species at the edge of their distribution: Implications for restoration and assisted migration in a warming climate. Global Change Biology 17(12), 3724–3735. https://doi.org/10.1111/j.1365-2486.2011.02524.x

Grady KC, Kolb TE, Ikeda DH, Whitham TG (2015) A bridge too far: Cold and pathogen constraints to assisted migration of riparian forests: Assisted migration in riparian restoration. Restoration Ecology 23(6), 811–820. https://doi.org/10.1111/rec.12245

Grady KC, Laughlin DC, Ferrier SM, Kolb TE, Hart SC, Allan GJ, Whitham TG (2013) Conservative leaf economic traits correlate with fast growth of genotypes of a foundation riparian species near the thermal maximum extent of its geographic range. Functional Ecology 27, 427–438. https://doi.org/10.1111/1365-2435.12060

Grossman GD, Nickerson DM, Freeman MC (1991) Principal component analyses of assemblage structure data: Utility of tests based on eigenvalues. Ecology 72(1), 341–347. https://doi.org/10.2307/1938927

Hacke UG, Sperry JS, Pittermann J (2000) Drought experience and cavitation resistance in six shrubs from the Great Basin, Utah. Basic and Applied Ecology 1(1), 31–41. https://doi.org/10.1078/1439-1791-00006

Hacke UG, Sperry JS, Pockman WT, Davis SD, McCulloh KA (2001) Trends in wood density and structure are linked to prevention of xylem implosion by negative pressure. Oecologia 126(4), 457–461. https://doi.org/10.1007/s004420100628

Hajek P, Leuschner C, Hertel D, Delzon S, Schuldt B (2014) Tradeoffs between xylem hydraulic properties, wood anatomy and yield in *Populus*. Tree Physiology 34(7), 744–756. https://doi.org/10.1093/treephys/tpu048

Haworth M, Belcher CM, Killi D, Dewhirst RA, Materassi A, Raschi A, Centritto M (2018) Impaired photosynthesis and increased leaf construction costs may induce floral stress during episodes of global warming over macroevolutionary timescales. Scientific Reports 8(1), 6206. https://doi.org/10.1038/s41598-018-24459-z

Hetherington AM, Woodward FI (2003) The role of stomata in sensing and driving environmental change. Nature 424(6951), 901–908. https://doi.org/10.1038/nature01843

Hilu KW, Randall JL (1984) Convenient method for studying grass leaf epidermis. Taxon 33(3), 413. https://doi.org/10.2307/1220980

Hultine KR, Allan GJ, Blasini D, Bothwell HM, Cadmus A, Cooper HF, Doughty CE, Gehring CA, Gitlin AR, Grady KC, Hull JB, Keith AR, Koepke DF, Markovchick L, Corbin Parker JM, Sankey TT, Whitham TG (2020). Adaptive capacity in the foundation tree species *Populus fremontii*: Implications for resilience to climate change and non-native species invasion in the American Southwest. Conservation Physiology 8(1). https://doi.org/10.1093/conphys/coaa061

Hultine KR, Burtch KG, Ehleringer JR (2013) Gender specific patterns of carbon uptake and water use in a dominant riparian tree species exposed to a warming climate. Global Change Biology 19(11), 3390–3405. https://doi.org/10.1111/gcb.12230

Hultine KR, Bush SE (2011). Ecohydrological consequences of non-native riparian vegetation in the southwestern United States: A review from an ecophysiological perspective: Non-native species impacts on riparian ecohydrology. Water Resources Research 47(7). https://doi.org/10.1029/2010WR010317

Hultine KR, Bush SE, Ehleringer JR (2010) Ecophysiology of riparian cottonwood and willow before, during, and after two years of soil water removal. Ecological Applications 20(2), 347–361. https://doi.org/10.1890/09-0492.1

Hultine KR, Froend R, Blasini D, Bush SE, Karlinski M, Koepke DF (2019) Hydraulic traits that buffer deep-rooted plants from changes in hydrology and climate. Hydrological Processes 34(2), 209–222. https://doi.org/10.1002/hyp.13587

Ikeda DH, Bothwell HM, Lau MK, O'Neill GA, Grady KC, Whitham TG (2014) A genetics-based Universal Community Transfer Function for predicting the impacts of climate change on future communities. Functional Ecology 28(1), 65–74. https://doi.org/10.1111/1365-2435.12151

Ikeda DH, Max TL, Allan GJ, Lau MK, Shuster SM, Whitham TG (2017) Genetically informed ecological niche models improve climate change predictions. Global Change Biology 23, 164–176. https://doi.org/10.1111/gcb.13470

Jackson DA (1993) Stopping rules in principal components analysis: A comparison of heuristical and statistical approaches. Ecology 74(8), 2204–2214. https://doi.org/10.2307/1939574

Jones DA, O'Hara KL, Battles JJ, Gersonde RF (2015) Leaf area prediction using three alternative sampling methods for seven Sierra Nevada conifer species. Forests 6(8), 2631–2654. https://doi.org/10.3390/f6082631

Jones HG (2014). Plants and microclimate: A quantitative approach to environmental plant physiology (3rd ed.). Cambridge University Press. https://doi.org/10.1017/CBO9780511845727

Joshua Leffler A, England LE, Naito J (2000) Vulnerability of Fremont cottonwood (*Populus fremontii* Wats.) individuals to xylem cavitation. Western North American Naturalist 60(2), 204–210. https://scholarsarchive.byu.edu/wnan/vol60/iss2/10

Kassambara A, Mundt F (2017) factoextra: Extract and visualize the results of multivariate data analyses. R package version 1.0.5. https://CRAN.Rproject.org/package=factoextra

Kawecki TJ, Ebert D (2004) Conceptual issues in local adaptation. Ecology Letters 7(12), 1225–1241. https://doi.org/10.1111/j.1461-0248.2004.00684.x

Kenefic LS, Seymour RS (1999). Leaf area prediction models for *Tsuga canadensis* in Maine. Canadian Journal of Forest Research 29(10), 1574–1582. https://doi.org/10.1139/x99-134

Kleyer M, Minden V (2015) Why functional ecology should consider all plant organs: An allocation-based perspective. Basic and Applied Ecology 16(1), 1–9. https://doi.org/10.1016/j.baae.2014.11.002

Kolb KJ, Sperry JS (1999) Differences in drought adaptation between subspecies of sagebrush (*Artemisia tridentata*). Ecology 80(7), 2373–2384. https://doi.org/10.2307/176917

Körner C (2003) Alpine plant life: Functional plant ecology of high mountain ecosystems (2nd ed.). Springer. https://doi-org.ezproxy1.lib.asu.edu/10.1007/978-3-642-18970-8

Kuznetsova A, Brockhoff PB, Christensen RHB (2017). LmerTest package: Tests in linear mixed effects models. Journal of Statistical Software 82(13). https://doi.org/10.18637/jss.v082.i13

Lambers H, Chapin FS, Pons TL (2008) Plant Physiological Ecology. Springer New York, NY. https://doi.org/10.1007/978-0-387-78341-3

Lambers H, Chapin FS, Pons TL (1998) Photosynthesis, respiration, and long-distance transport. Plant Physiological Ecology 10–153. https://doi.org/10.1007/978-1-4757-2855-2_2

Lambers H, Poorter H (1992) Inherent variation in growth rate between higher plants: A search for physiological causes and ecological consequences. Advances in Ecological Research 23, 187–261. https://doi.org/10.1016/S0065-2504(08)60148-8

Lauri P (2019) Corner's rules as a framework for plant morphology, architecture and functioning – Issues and steps forward. New Phytologist 221(4), 1679–1684. https://doi.org/10.1111/nph.15503

Lê S, Josse J, Husson F (2008) FactoMineR: An R package for multivariate analysis. Journal of Statistical Software 25, 1–18. https://doi.org/10.18637/jss.v025.i01

Li Y, Sperry JS, Taneda H, Bush SE, Hacke UG (2008) Evaluation of centrifugal methods for measuring xylem cavitation in conifers, diffuse- and ring-porous angiosperms. New Phytologist 177(2), 558–568. https://doi.org/10.1111/j.1469-8137.2007.02272.x

Lindtke D, González-Martínez SC, Macaya-Sanz D, Lexer C (2013). Admixture mapping of quantitative traits in *Populus* hybrid zones: Power and limitations. Heredity 111(6), 474–485. https://doi.org/10.1038/hdy.2013.69

Mayr S, Schmid P, Laur J, Rosner S, Charra-Vaskou K, Dämon B, Hacke UG (2014) Uptake of water via branches helps timberline conifers refill embolized xylem in late winter. Plant Physiology 164(4), 1731–1740. https://doi.org/10.1104/pp.114.236646

Mayr S, Sperry JS (2010) Freeze-thaw-induced embolism in *Pinus contorta*: Centrifuge experiments validate the 'thaw-expansion hypothesis' but conflict with ultrasonic emission data. New Phytologist 185(4), 1016–1024. https://doi.org/10.1111/j.1469-8137.2009.03133.x

Merritt DM, Leroy Poff N (2010) Shifting dominance of riparian *Populus* and *Tamarix* along gradients of flow alteration in western North American rivers. Ecological Applications 20(1), 135–152. https://doi.org/10.1890/08-2251.1

Messier J, Lechowicz MJ, McGill BJ, Violle C, Enquist BJ (2017) Interspecific integration of trait dimensions at local scales: The plant phenotype as an integrated network. Journal of Ecology 105(6), 1775–1790. https://doi.org/10.1111/1365-2745.12755

Michaletz ST, Weiser MD, Zhou J, Kaspari M, Helliker BR, Enquist BJ (2015) Plant thermoregulation: Energetics, trait-environment interactions, and carbon economics. Trends in Ecology & Evolution 30(12), 714–724. https://doi.org/10.1016/j.tree.2015.09.006

Mooney HA, Billings WD (1961) Comparative physiological ecology of arctic and alpine populations of *Oxyria digyna*. Ecological Monographs 31(1), 1–29. https://doi.org/10.2307/1950744

Niklas KJ (1991) Flexural stiffness allometries of angiosperm and fern petioles and rachises: Evidence for biomechanical convergence. Evolution 45(3), 734. https://doi.org/10.2307/2409924

Niklas KJ, Spatz HC (2012) Mechanical properties of wood disproportionately increase with increasing density. American Journal of Botany 99(1), 169–170. https://doi.org/10.3732/ajb.1100567

Niklas KJ, Spatz HC (2010) Worldwide correlations of mechanical properties and green wood density. American Journal of Botany 97(10), 1587–1594. https://doi.org/10.3732/ajb.1000150

Nobel PS (2009) Physicochemical and environmental plant physiology (4th ed.). Elsevier/Academic Press. https://doi.org/10.1016/B978-0-12-374143-1.X0001-4

O'Grady AP, Cook PG, Eamus D, Duguid A, Wischusen JDH, Fass T, Worldege D (2009) Convergence of tree water use within an arid-zone woodland. Oecologia 160(4), 643–655. https://doi.org/10.1007/s00442-009-1332-y

O'Neill GA, Hamann A, Wang T (2008) Accounting for population variation improves estimates of the impact of climate change on species growth and distribution. Journal of Applied Ecology 45(4), 1040–1049. https://doi.org/10.1111/j.1365-2664.2008.01472.x

O'Sullivan OS, Heskel MA, Reich PB, Tjoelker MG, Weerasinghe LK, Penillard A, Zhu L, Egerton JJG, Bloomfield KJ, Creek D, Bahar NHA, Griffin KL, Hurry V, Meir P, Turnbull MH, Atkin OK (2017) Thermal limits of leaf metabolism across biomes. Global Change Biology 23(1), 209–223. https://doi.org/10.1111/gcb.13477

Pásztory Z, Ronyecz I (2013) The thermal insulation capacity of tree bark. Acta Silvatica et Lignaria Hungarica 9(1), 111–117. https://doi.org/10.2478/aslh-2013-0009

Peres-Neto PR, Jackson DA, Somers KM (2005) How many principal components? Stopping rules for determining the number of non-trivial axes revisited. Computational Statistics and Data Analysis 49(4), 974–997. https://doi.org/10.1016/j.csda.2004.06.015

Preibisch S, Saalfeld S, Tomancak P (2009) Globally optimal stitching of tiled 3D microscopic image acquisitions. Bioinformatics 25(11), 1463–1465. https://doi.org/10.1093/bioinformatics/btp184

Preston KA, Cornwell WK, DeNoyer JL (2006) Wood density and vessel traits as distinct correlates of ecological strategy in 51 California coast range angiosperms. New Phytologist 170(4), 807–818. https://doi.org/10.1111/j.1469-8137.2006.01712.x

R Core Team (2019) R: A language and environment for statistical computing. R Foundation Statistical Computing. https://www.r-project.org/

Ravikumar S, Surekha R, Thavarajah R (2014) Mounting media: An overview. J NTR University of Health Sciences 3(5), 1. https://doi.org/10.4103/2277-8632.128479

Reich PB (2014) The world-wide 'fast–slow' plant economics spectrum: A traits manifesto. Journal of Ecology, 102(2), 275–301. https://doi.org/10.1111/1365-2745.12211

Reich PB, Wright IJ, Cavender-Bares J, Craine JM, Oleksyn J, Westoby M, Walters MB (2003) The evolution of plant functional variation: Traits, spectra, and strategies. International Journal of Plant Sciences 164(S3), S143–S164. https://doi.org/10.1086/374368

Roden JS, Pearcy RW (1993) Effect of leaf flutter on the light environment of poplars. Oecologia 93(2), 201–207. https://doi.org/10.1007/BF00317672

Rosas T, Mencuccini M, Barba J, Cochard H, Saura-Mas S, Martínez-Vilalta J (2019) Adjustments and coordination of hydraulic, leaf and stem traits along a water availability gradient. New Phytologist 223(2), 632–646. https://doi.org/10.1111/nph.15684

Rosell JA (2016) Bark thickness across the angiosperms: More than just fire. New Phytologist 211(1), 90–102. https://doi.org/10.1111/nph.13889

Rueda M, Godoy O, Hawkins BA (2018) Trait syndromes among North American trees are evolutionarily conserved and show adaptive value over broad geographic scales. Ecography 41(3), 540–550. https://doi.org/10.1111/ecog.03008

Sack L, Cowan PD, Jaikumar N, Holbrook NM (2003) The 'hydrology' of leaves: Co-ordination of structure and function in temperate woody species. Plant, Cell and Environment 26(8), 1343–1356. https://doi.org/10.1046/j.0016-8025.2003.01058.x

Sack L, Frole K (2006) Leaf structural diversity is related to hydraulic capacity in tropical rain forest trees. Ecology 87(2), 483–491. https://doi.org/10.1890/05-0710

Scholander PF, Bradstreet ED, Hemmingsen EA, Hammel HT (1965) Sap pressure in vascular plants: Negative hydrostatic pressure can be measured in plants. Science 148(3668), 339–346. https://doi.org/10.1126/science.148.3668.339

Scholz A, Klepsch M, Karimi Z, Jansen S (2013) How to quantify conduits in wood? Frontiers in Plant Science 4, 1–11. https://doi.org/10.3389/fpls.2013.00056

Sharkey TD (2005) Effects of moderate heat stress on photosynthesis: Importance of thylakoid reactions, rubisco deactivation, reactive oxygen species, and thermotolerance provided by isoprene. Plant, Cell and Environment 28(3), 269–277. https://doi.org/10.1111/j.1365-3040.2005.01324.x

Smith DM, Allen SJ (1996) Measurement of sap flow in plant stems. Journal of Experimental Botany 47(305), 1833–1844. https://doi.org/10.1093/jxb/47.12.1833

Sokal RR, Rohlf FJ (1995) Biometry: The principles and practice of statistics in biological research (3rd ed.). W.H. Freeman and Co., New York. https://doi.org/10.2307/2412280

Sperry JS, Saliendra NZ (1994) Intra- and inter-plant variation in xylem cavitation in *Betula occidentalis*. Plant, Cell and Environment 17(11), 1233–1241. https://doi.org/10.1111/j.1365-3040.1994.tb02021.x

Sperry JS, Sullivan JEM (1992) Xylem embolism in response to freeze-thaw cycles and water stress in ring-porous, diffuse-porous, and conifer species. Plant Physiology 100(2), 605–613. https://doi.org/10.1104/pp.100.2.605

Sprugel DG (1989) The relationship of ever greenness, crown architecture, and leaf size. The American Naturalist 133(4), 465–479. https://doi.org/10.1086/284930

Sridharan G, Shankar AA (2012) Toluidine blue: A review of its chemistry and clinical utility. Journal of Oral and Maxillofacial Pathology 16(2), 251–255. https://doi.org/10.4103/0973-029X.99081

Sterck FJ, Zweifel R, Sass-Klaassen U, Chowdhury Q (2008) Persisting soil drought reduces leaf specific conductivity in Scots pine (*Pinus sylvestris*) and pubescent oak (*Quercus pubescens*). Tree Physiology 28(4), 529–536. https://doi.org/10.1093/treephys/28.4.529

Stromberg JC (1993) Frémont cottonwood-Goodding willow riparian forests: A review of their ecology, threats, and recovery potential. Journal of the Arizona Nevada Academy of Sciences 26(3), 97–110.

Trueba S, Isnard S, Barthélémy D, Olson ME (2016) Trait coordination, mechanical behaviour and growth form plasticity of *Amborella trichopoda* under variation in canopy openness. AoB PLANTS 8, https://doi.org/10.1093/aobpla/plw068

Tyree ME, Zimmermann MH (2002) Xylem Structure and the ascent of sap (2nd edn.). Springer Verlag. https://www.science.org/doi/10.1126/science.222.4623.500.b

Valladares F, Skillman JB, Pearcy RW (2002) Convergence in light capture efficiencies among tropical forest understory plants with contrasting crown architectures: A case of morphological compensation. American Journal of Botany 89(8), 1275–1284. https://doi.org/10.3732/ajb.89.8.1275

Wang T, Hamann A, Spittlehouse DL, Murdock TQ (2012) ClimateWNA-high-resolution spatial climate data for western North America. Journal of Applied Meteorology and Climatology 51(1), 16–29. https://doi.org/10.1175/JAMC-D-11-043.1

Williams AP, Cook ER, Smerdon JE, Cook BI, Abatzoglou JT, Bolles K, Baek SH, Badger AM, Livneh B (2020) Large contribution from anthropogenic warming to an emerging North American megadrought. Science 368(6488), 314–318. https://doi.org/10.1126/science.aaz9600

Whitham TG, DiFazio SP, Scheitzer JA, Shuster SM, Allan GJ, Bailey JK, Woolbright SA (2008) Extending genomics to natural communities and ecosystems. Science 320, 492–495. https://doi.org/10.1126/science.1153918

Worrall JJ, Egeland L, Eager T, Mask RA, Johnson EW, Kemp PA, Sheppard WD (2008) Rapid mortality of *Populus tremuloides* in southwestern Colorado, USA. Forest Ecology and Management 255(3), 686–696. https://doi.org/10.1016/j.foreco.2007.09.071

Worrall JJ, Rehfeldt GE, Hamann A, Hogg EH, Marchetti SB, Michaelin M. Gray LK (2013) Recent declines of *Populus tremuloides* in North America linked to climate. Forest Ecology and Management 299, 35–51. https://doi.org/10.1016/j.foreco.2012.12.033

Wright IJ, Reich PB, Westoby M, Ackerly DD, Baruch Z, Bongers F, Cavender-Bares J, Chapin T, Cornelissen JHC, Diemer M, Flexas J, Garnier E, Groom PK, Gulias J, Hikosaka K, Lamont BB, Lee T, Lee W, Lusk C, … Villar R (2004) The worldwide leaf economics spectrum. Nature 428(6985), 821–827. https://doi.org/10.1038/nature02403

Wright IJ, Westoby M (2002) Leaves at low versus high rainfall: Coordination of structure, lifespan and physiology. New Phytologist 155(3), 403–416. https://doi.org/10.1046/j.1469-8137.2002.00479.x

Zaehle S (2005) Effect of height on tree hydraulic conductance incompletely compensated by xylem tapering. Functional Ecology 19(2), 359–364. https://doi.org/10.1111/j.0269-8463.2005.00953.x

Zhou H, Chen Y, Zhu C, Li Z, Fang G, Li Y, Fu A (2020) Climate change may accelerate the decline of desert riparian forest in the lower Tarim River, northwestern China: Evidence from tree-rings of *Populus euphratica*. Ecological Indicators 111. https://doi.org/10.1016/j.ecolind.2019.105997

Zweifel R, Häsler R (2000) Frost-induced reversible shrinkage of bark of mature subalpine conifers. Agricultural and Forest Meteorology 102(4), 213–222. https://doi.org/10.1016/S0168-1923(00)00135-0

3. TRADEOFFS BETWEEN LEAF COOLING AND HYDRAULIC SAFETY IN A

DOMINANT ARID LAND RIPARIAN TREE SPECIES

Abstract

Leaf carbon gain optimization in hot environments requires balancing leaf thermoregulation with avoiding excessive water loss via transpiration and hydraulic failure. The tradeoffs between leaf thermoregulation and transpirational water loss can determine the ecological consequences of heat waves that are increasing in frequency and intensity. I evaluated leaf thermoregulation strategies in warm (>40 °C maximum summer temperature) and cool-adapted (<40 °C maximum summer temperature) genotypes of the foundation tree species, *Populus fremontii* using a common garden near the mid-elevational point of its distribution. I measured leaf temperatures and assessed three modes of leaf thermoregulation: leaf morphology, midday canopy stomatal conductance and stomatal sensitivity to vapor pressure deficit. Data were used to parameterize a leaf energy balance model to estimate contrasts in midday leaf temperature in warm- and cool-adapted genotypes. Warm-adapted genotypes had 39% smaller leaves and 38% higher midday stomatal conductance, reflecting a 3.8 °C cooler mean leaf temperature than cool adapted genotypes. Leaf temperatures modeled over the warmest months were on average 1.1 °C cooler in warm- relative to cool-adapted genotypes. Results show that plants adapted to warm environments are predisposed to tightly regulate leaf temperatures during heat waves, potentially at an increased risk of hydraulic failure.

Introduction

Leaf energy budgets are governed in part by the absorbance of incoming solar radiation and exchange of latent and sensible heat energy (Lambers et al. 2008; Michaletz et al. 2015; Fauset et al. 2018). Leaf size, and conductance to water vapor alter leaf temperature by governing thickness of leaf boundary layers and how much heat loss occurs through sensible and latent heat flux per unit surface area (Michaletz et al. 2016; Leigh et al. 2017; Dong et al. 2017). Environmental conditions within plant canopies such as sunlight, air temperature, humidity, and wind speed influence leaf radiant heating and heat transfer between leaves and the surrounding microclimate (Jones 2014; Gutschick 2016; Michaletz et al. 2016).

Leaf carbon budgets are tightly coupled to leaf energy budgets because increases in leaf temperature (T_{leaf}) (see Table 3.1 for definitions and abbreviations) above an optimal temperature reduces photosynthetic rates while increasing rates of respiration (Teskey et al. 2015). Likewise, leaf temperature affects the solubility of CO_2 in the liquid phase, kinetics of Rubisco, electron transport efficiency, and mesophyll conductance (Cen and Sage 2005, Yamori et al. 2006, Lambers et al. 2008). In particular, high leaf temperatures increase rates of photorespiration and subsequently negatively affect net photosynthesis (Berry and Bjorkman 1980, Atkin et al. 2006; Wahid et al. 2007; Lambers et al. 2008). Exposure to extreme heat waves can also damage photosynthetic processes as high temperatures disrupt cell membranes and metabolism (Hazel 1995). Therefore, traits that facilitate the maintenance of leaf temperatures close to the optima for photosynthesis should be highly favored by selection (Helliker and Richter 2008; Michaletz et al. 2015, 2016; Slot and Winter 2016).

Leaves exhibiting morpho-physiological traits that modify thermal fluxes can display substantial differences between T_{leaf} and air temperature (T_{air}) (Michaletz et al. 2015, 2016; Leigh et al. 2017; Blasini et al. 2020). Leaf size, shape, orientation, reflectance, and stomatal density can all modify T_{leaf} relative to T_{air} (Beerling et al. 2001; Michaletz et al. 2015; Leigh et al. 2017; O'Sullivan et al. 2017; Wright et al. 2017). For example, under hot air temperature and high irradiance conditions, larger leaves are particularly susceptible to experience damaging leaf temperatures because they form thicker boundary layers that slow sensible and latent heat loss (Farquhar and Sharkey 1982; Martin et al. 1999; Lambers et al. 2008; Wright et al. 2017). Consequently, larger leaves (i.e., large surface area) tend to display larger leaf-to-air temperature differences than smaller leaves (Leigh et al. 2017; Wright et al. 2017). On the other hand, because the high latent heat vaporization of water, stomatal regulation and subsequent leaf evaporative cooling caused by transpiration is arguably the most effective mechanism for regulating leaf temperature in extreme hot environments (Upchurch and Mahan 1988; Radin et al. 1994; Hetherington and Woodward 2003; Curtis et al. 2012; Drake et al. 2018). Recent evidence suggests that some plant taxa adapted to extreme hot environments display an alternative water-use strategy that prioritizes leaf evaporative cooling over immediate returns on water loss in the form of carbon acquisition (Urban et al. 2017; Aparecido et al. 2020). However, an inevitable tradeoff with maintaining high transpiration rates in hot and dry conditions runs the risk of operating with leaf water potentials at or near the turgor loss point and hydraulic failure. Thus, fine-tuning stomatal regulation of leaf water potential to balance midday leaf cooling with hydraulic failure avoidance may be a critically important trait in heat-adapted plants.

Here, I examine stomatal regulation of leaf water potential relative to midday leaf cooling in *Populus fremontii*, *Sarg.* (Fremont cottonwood), an obligate riparian phreatophytic tree species that inhabits arid regions in the southwest United States and northern Mexico. This species is an ideal candidate for studying genotypic variation in traits related to leaf thermoregulation because it is found across extreme broad elevational (0 to 2000 m.a.s.l) and climate gradients that encompass subfreezing to extreme hot temperatures (>40 ℃). Recent common garden experiments have found that *P. fremontii* displays large intraspecific variation in productivity (Grady et al. 2011), phenology (Cooper et al. 2019), and functional trait coordination (Blasini *et al.* 2020) in relation to the mean annual temperature (MAT) transfer distance, defined as the MAT of the source population location subtracted from the common garden location. Previous studies have identified three *P. fremontii* ecotypes with boundaries that largely reflect distinct geographic regions. These include the relatively warm Sonoran Desert region, the relatively cool Colorado Plateau region of Utah and northern Arizona, and the California Central Valley region with a climate that is intermediate between the other two regions (Ikeda et al. 2017). Previous studies have identified genotypes sourced from populations adapted to cooler temperatures in the Colorado Plateau region that display a distinct combination of shorter growing seasons (i.e., later leaf flush and earlier fall senescence) with more conservative trait expression, while warm-adapted genotypes from the Sonoran Desert region exhibit longer growing seasons with more acquisitive trait expression at multi-organ levels (Cooper et al. 2019; Blasini et al. 2020). Here I define genotypes from populations with higher mean maximum summer temperatures than the common garden location as a warm-adapted ecotype, and a cold-adapted ecotype as

79

genotypes from populations at or below mean maximum summer temperatures in relation to the common garden location.

Climate projections predict that the North American region in which *P. fremontii* occurs will become warmer and more arid over the remainder of the century (Breshears et al. 2013; Garfin et al. 2013; Seager et al. 2014). During the first decade of the 21st century, the region experienced higher daily average temperatures and more recurrent heat waves than in the previous 100 years (Garfin et al. 2013). As a consequence of episodic drought and heatwaves, many *P. fremontii* gallery forests have experienced recent mortality surges across its range (Whitham et al. 2020).

I examined the overarching hypothesis that genotypes from the warm-adapted ecotype prioritize leaf cooling over hydraulic safety compared to genotypes from the cool-adapted ecotype. To test this hypothesis, I measured leaf temperature, leaf morphology and sap-flux-scaled canopy transpiration I and stomatal conductance (G_s) in *P. fremontii* genotypes sourced from seven populations representing the warm- and cool-adapted ecotypes and growing together in a common garden located near the mid-point of the species climate distribution (Cooper et al. 2019; Hultine et al. 2019). I evaluated three primary modes of canopy thermal regulation, involving adjustment in: 1. maximum midday stomatal conductance, 2. stomatal sensitivity to leaf to air vapor pressure deficit (VPD), and 3. leaf morphology including specific leaf area, leaf size and stomatal size and density. The field data were used to parameterize a leaf energy balance model to predict how leaf morphology and stomatal conductance influence leaf temperature over a wide range of thermal conditions. This allowed us to test four inter-related sub-hypotheses: 1. Genotypes sourced from the warm-adapted ecotype maintain cooler

midday canopies under well-watered conditions than genotypes sourced from the cool-adapted ecotype in mid-summer. 2. Genotypes sourced from the warm-adapted ecotype produce smaller leaves with higher specific leaf areas and higher maximum theoretical stomatal conductance (G_{smax}) based on stomatal density and size than genotypes sourced from the cool-adapted ecotype. 3. Genotypes sourced from the warm-adapted ecotype maintains higher midday stomatal conductance and lower stomatal sensitivity to VPD than the genotypes sourced from the cool-adapted ecotype to facilitate leaf cooling. 4. As a consequence of having higher maximum G_s and lower stomatal sensitivity to VPD, genotypes sourced from the warm-adapted ecotype operate with a lower mid-day leaf water potential (Ψ_{md}) over the summer than genotypes sourced from the cool-adapted ecotype. Results from this investigation are expected to help identify genotypes that are likely to best cope with increases in temperature and episodic heat waves that are predicted for the southwestern US, and more broadly provide new insights into local adaptation to extreme thermal stress and subsequent tradeoffs associated with leaf thermal regulation in dominant woody taxa.

Methods

Study site

An experimental common garden was established in October 2014 with 16 *Populus fremontii* populations (~4,100 propagated cuttings) that collectively represent the climatic and elevational range of the species (Cooper et al. 2019; Hultine et al. 2019). The garden was located within the Agua Fria National Monument in central Arizona (34° 15' 34.42" N; 112° 03' 29.39" W; elevation 988 m) (Fig. 3.1) and was established on a

1.2 Ha portion of former cropland next to the ephemerally flowing Agua Fria River.

During the winter of 2013 – 2014, cuttings were collected from 16 populations which

collectively represent the entire climatic range of the Sonoran Desert ecoregion (Ikeda et

al. 2017). A total of 12 genotypes per population, were collected at each of the 16 source

sites. Genotypes were collected at least 20 meters apart to avoid using clones within each

population. The individual cuttings were treated with root hormone and potted in the

Northern Arizona University greenhouse for 4 months. In the garden, 0.3 m tall saplings

were planted 2 m apart from each other in a randomized block design with a total of four

replicated blocks, each with 16 populations comprising 64 trees each. A drip irrigation

system was used to water each tree with approximately 20 L, two to three times per week

during the growing season.

From the original 16 populations established in the garden, I studied 7 populations

with a total of 56 genotypes (n = 8 genotypes per population) representing the broadest

possible range in mean annual temperature of the source populations, from 10.7 to 22.6

°C, and an elevation gradient from 72 to 1,940 m (Fig. 3.1). Apart from the local Agua

Fria National Monument population, I had an even representation of 6 populations

sourced from 3 sites with higher and lower mean maximum summer temperatures than

the common garden location. The three populations from the lower Sonoran Desert were

defined as warm-adapted ecotype because the extreme mean maximum summer

temperatures (>40 °C) they experience at their source sites is above that of the common

garden location (Fig. 3.2). Populations from higher elevation provenances in the Sonoran

Desert and Colorado Plateau came from sources with similar or lower mean maximum

summer temperatures than the common garden location and therefore were categorized as

cool adapted genotypes (Fig. 3.2). Consequently, I studied intraspecific differences in leaf thermoregulation in relation with mean annual temperature (MAT) and mean maximum summer temperatures (MMST) transfer distances (Table 3.2), defined as the MAT and MMST of the source population location subtracted from the MAT and MMST of the common garden location (Grady et al. 2011).

Meteorological data

A micrometeorological station installed at the garden measured relative humidity, air temperature, photosynthetically active radiation (Q, μmol m^{-2} s^{-1}), and wind speed continuously every 30 seconds and stored as 30 minutes means from May 30 (day 151) to Oct 23 (day 296) of 2017 with a Campbell CR10X-2M data logger (Campbell Scientific, Logan, UT, USA). Air temperature and relative humidity were measured with a shielded Vaisala HMP 60 AC temperature/humidity probe (Vaisala, Woburn, MA, USA) placed 3 m above the ground surface. Photosynthetic active radiation was measured with an Apogee SQ-110-SS sun calibration quantum Sensor (Apogee Instruments, Logan, UT, USA). I used air temperature and relative humidity to calculate air vapor pressure deficit (VPD, kPa) using both half-hourly and daily averages.

Morphological traits:

Stomatal anatomy

In 2016, I randomly collected fully expanded leaves from mid-height and south-facing canopy of each genotype (n=56) to determine stomatal density, length, width and area. I followed the nail polish impression method (Hilu and Randall 1984) to obtain four impressions per leaf, two impressions in both the abaxial and adaxial sides of the leaves (n = 560 impressions). An Olympus CX41 light microscope (Olympus Corp., Center

Valley, PA, USA) was used to observe and obtain images from the impressions with a Moticam Pro 282A camera (Motic Instruments, Richmond, BC, Canada). Stomatal density (D_{stom}) was calculated as the number of stomata in eighty 0.59 mm^2 digital images at 10× magnification. Stomatal size (S_{stom}) (length × width) was observed on 800 stomata from digital images at 40× magnification (n = 100 per population) using an open-source imaging program, ImageJ (https://imagej.nih.gov/ij/). I calculated maximum theoretical stomatal conductance to water vapor (G_{smax}, mmol m^{-2} s^{-1}) following Franks and Farquhar (2001):

$$G_{smax} = \frac{d_w \cdot D_{stom} \cdot a_{max}}{v\left(l + \frac{\pi}{2}\sqrt{\frac{a_{max}}{\pi}}\right)} \tag{1}$$

where d_w is the diffusivity of water in air (2.43×10^{-5} m^2/s), v is the molar volume of air (0.024 m^3/mol; Jones 2014), D_{stom} is the stomatal density, a_{max} is the maximum area of the open stomatal pore, approximated as $\pi(p/2)^2$, where p is stomatal pore length (µm), assumed to be stomatal length divided by two (Franks and Farquhar, 2007)

Leaf traits

Specific leaf area (SLA, cm^2 g^{-1}) was calculated as the one-sided area of a fresh leaf, divided by its oven-dry mass (Wright and Westoby 2002). SLA was measured in June, July, and September 2017. A subset of 12–20 fully expanded leaves from the mid and south facing section of the canopy were collected per tree and scanned with a high-resolution computer scanner, one-sided leaf area was measured with ImageJ. The scanned leaves were then oven-dried for 72 hours at 75 °C and weighed to calculate SLA. Individual leaf area (A_{il}, cm^2) was derived from the average individual leaf area from these measurements (Ackerly et al. 2002).

Whole tree allometry

In July 2017, I used allometric relationships between whole-tree stem diameter and leaf area through a branch summation approach to estimate whole-tree canopy leaf area (A_l) and sapwood area (A_s). The diameter of all leaf-bearing branches from the main stem in each of the 56 trees were measured with a digital caliper. To calculate whole canopy leaf area, a subset of the collected leaves per genotype was scanned with a high-resolution computer scanner, and one-sided leaf area was measured with Image J. Then, I generated a regression of branch diameter to leaf area from a subset of branches per genotype. Scanned leaves were oven-dried for 72 hours at 75 °C within each subset of branches, and then multiplied their weight by SLA to determine total leaf area of the branch. (see section 2.3.2). Whole-tree height (H), canopy diameters (4–8 measurements per genotype) and their respective canopy areas were measured five times in the 2017 growing season with a telescoping measuring pole. Canopy area (A_c) was determined using the ellipse equation, πab, where a is the mean radius of longest canopy axis and b is the radius of two perpendicular canopy axes (Ansley et al. 2012).

Sap-flux-scaled canopy transpiration and stomatal conductance

I installed heat dissipation sensors (Granier 1987) that measured stem sap flux density (J_s, g H2O m-2 sapwood s-1) on all 56 genotypes from June 2nd (day 153) to Octobe[r] 2nd (day 275) 2017. Each sensor consisted of a pair of 20 mm long, 2 mm diameter stainless steel probes inserted approximately 15 cm apart along the axis of the hydro-active xylem. The sap flux density was calculated from the differences in temperature between the heated and unheated reference probes. Sap flux density, J_s (g cm^{-2} s^{-1}), was calculated as

$$J_s = qk^p \tag{2}$$

For diffuse porous tree species (*e.g., Populus fremontii*), q is the prefactor coefficient

(0.0119), p is the scaling exponent (1.23), and k is related to the temperature difference

between the two probes (Granier 1987; Bush et al. 2010):

$$k = \frac{\Delta T_0}{\Delta T} - 1 \tag{3}$$

Where ΔT is the difference in temperature between the heated and unheated probes and

ΔT_0 is the temperature difference during hydrostatic conditions (data provided in

repository). I assumed that hydrostatic conditions only occurred during evening when

VPD was at or near zero. Thus, in some cases a single value for ΔT_0 was used to

calculate k over several days.

I calculated canopy transpiration (E, g m^{-2} s^{-1}) using the total sap flux density and

sapwood area to leaf area ratio (A_s:A_l) according to:

$$E = J_s \cdot \frac{A_s}{A_l} \tag{4}$$

From the sap flux measurements, I also calculated canopy conductance (G_c, mmol

m^{-2} s^{-1}) using a simplified version of the Penman–Monteith equation (Campbell and

Norman 1998; Hultine et al. 2013; Monteith and Unsworth 2013):

$$G_c = \frac{y \cdot \lambda}{\rho \cdot c_p \cdot VPD} \cdot \frac{J_s \cdot A_s}{A_l} \tag{5}$$

where A_s is conducting sapwood area (m^2), A_l is the total leaf area (m^2), y is the

psychrometric constant (kPa K^{-1}), λ is the latent heat of vaporization (J kg^{-1}), ρ is the

density of moist air (kg m^{-3}), and c_p is the specific heat of air at constant pressure (J kg^{-1}

K^{-1}).

A_s was obtained by estimating the internal bark diameter and the depth of hydro-active xylem. Because of the young age of the trees (2.5 years), and because *Populus* trees tend to have large active sapwood depths with uniform sap velocities (Lambs and Muller 2002), I assumed the active sapwood included the entire cross-sectional area beneath the bark. Leaf area index (LAI), the projected leaf area per unit of ground area (Watson 1947; Bréda 2003; Chapin et al. 2011), provides a way to estimate the physical boundaries between the whole-tree canopy and the surrounding atmosphere (Bréda 2003). Therefore, whole tree leaf area (A_l) and canopy area (A_c) were used to calculate intraspecific differences in LAI and therefore canopy boundary layer resistances, where LAI is given by:

$$LAI = \frac{A_l}{A_c} \tag{6}$$

Canopy stomatal conductance (G_s) was extracted from measurements of G_c by evaluating leaf boundary layer conductance (G_{bl}; mmol m^{-2}s^{-1}), which can be small enough in broadleaf plants to decouple plant canopies from atmospheric conditions. I therefore calculated G_{bl} according to Jones, 2014) to compare with calculated values of G_s (shown below):

$$G_{bl} = 306.7 \cdot \sqrt{\frac{\mu_c}{d_l}} \tag{7}$$

Where (d_l) is the mean leaf characteristic dimension calculated for each genotype (d_l = 0.72 · leaf width) and (u_c) is the mean canopy wind speed (Campbell and Norman 1998; Jones 2014). Mean μ_c (m s^{-1}) was estimated from wind speed (μ) measured at 3 m above

the ground level and by multiplying canopy frictional velocity (μ_v) to μ. μ_v was

calculated following Campbell and Norman (1998) as:

$$\mu_v = \frac{\mu \cdot 0.4}{\ln\frac{z-d}{z_m}} \tag{8}$$

Where z is the genotype canopy height (m), d is the zero-plane displacement (m), z_m is

the roughness length (m), and 0.4 is the von Karman constant. I used population specific

values of G_c and G_{bl} to estimate canopy stomatal conductance:

$$G_s = \frac{1}{\frac{1}{G_c} - \frac{1}{G_{bl}}} \tag{9}$$

I calculated a dimensionless decoupling coefficient (Ω) (Martin 1989; Hultine et

al. 2013) to evaluate the sensitivity of transpiration to changes in boundary layer

conductance.

$$\Omega = \frac{\varepsilon + 2 + \frac{G_r}{G_{bl}}}{\varepsilon + 2 + \frac{G_{bl+G_r}}{G_s} + \frac{G_r}{G_{bl}}} \tag{10}$$

Where ε is the change of latent heat to the change in sensible heat of saturated air and G_r

is the long-wave radiative transfer conductance. Ω is expected to reach its upper limit

(1.0) as the influence of stomatal resistance over transpiration decline.

Leaf water potentials

From June to September 2017, leaf water potentials (Ψ) were measured every

month at predawn (Ψ_{pd}, 0300 – 0500 h local time) and midday (Ψ_{md}; 1100 – 1300 h) on

each genotype that was instrumented with sap flux probes using the Scholander pressure

chamber (PMS Instruments, Corvallis, OR; Scholander et al. 1965; Turner 1988). To take

these measurements, a single shoot tip from each of the 56 genotypes was cut with a

sharp razor blade at mid-height and south-facing canopy. Differences between Ψ_{pd} and Ψ_{md} ($\Delta\Psi$) were calculated for each genotype, population, and ecotype over each measurement period, to provide an index of the transpiration-induced changes in water potential gradients from the roots to the leaves.

Leaf temperature

I measured leaf temperature on 17 warm- and 24 cool-adapted genotypes (total n = 41) instrumented with the sap flux probes in the common garden between 13:00 and 15:00 h of August [2]8th (day 240) and Septembe[r] 1st (day 244) of 2017. I evaluated leaf temperature on three to four separate leaves in each individual genotype using a thermal imaging camera ThermaCam (Flir One, Flir Systems, Wilsonville, OR USA). This handheld device integrates a thermal and visual sensor of 80×60 and 1440×1080 pixels, respectively, to a smartphone, with a typical accuracy range of $\pm$ 3 °C or $\pm$ 5% (https://www.flir.com/products/flir-one-gen-3/). Leaf temperatures were taken 30 cm away from a full expanded leaf at three to four different locations in the canopy. Only leaves located in the middle (1.5 to 2.0 m) and sun-lit areas of each tree canopies were used to measure leaf temperature. This resulted in a total of 81 and 92 leaf temperature measurements for day 240 and day 244 respectively (total n = 173 measurements, 99 measurements for cool adapted genotype and 74 for warm adapted genotypes on both days).

Statistical analysis and leaf energy balance modeling

All statistical analyses were conducted in R version 4.0.2 (R Development Core Team 2011). Prior to analyzing the data, I examined whether each variable met the assumptions of normality and homogeneity of variance, using a Shapiro and Barlett test.

Analysis of trait variation between cool- and warm-adapted ecotypes

Morphological trait comparisons between cool- and warm-adapted ecotypes, including all measurements of leaf morphology, leaf area to sapwood area ratios, and mean daily sap-flux-scaled canopy fluxes were conducted using a standard student's t-test.

Because riparian tree species are found exclusively in places with abundant water available, stomatal conductance and whole-tree water use in this species are intrinsically influenced by atmospheric characteristics like irradiance, atmospheric CO_2 concentrations and atmospheric vapor pressure deficit (Landsberg et al. 2017). Specifically, increases in VPD have been found to correlate with decreases in stomatal conductance while the stomatal sensitivity to changes in VPD has been described to be proportional to the stomatal conductance at low VPD levels (<1 kPa). This sensitivity of stomatal conductance to changes in VPD can be estimated from (Domec et al. 2009; Hultine et al. 2013; Oren et al. 1999):

$$G_s = G_{sref} - m \cdot (ln\,VPD) \tag{11}$$

where G_{sref} is the value of G_s at VPD = 1 kPa in a log-linear relationship and m (the slope of the regression fit) describes the sensitivity of G_s to changes in VPD (i.e., ln VPD). I also calculated stomatal sensitivity standardized by G_{sref}^- (S) according to Oren et al (1999) as -m G_{sref}^{-1}. Regression analyses was used to investigate the relationships between G_s and G_s:G_{Sref} of the cool- and warm-adapted ecotypes to log(VPD) during the hottest time of the day (11:00 to 19:00). Comparisons in mean G_s and G_s:G_{Sref} between ecotypes in response to log(VPD) and the interaction ecotype*log(VPD) were analyzed using analysis of covariance (ANCOVA).

Differences in Ψ_{pd}, Ψ_{md} and $\Delta\Psi$ between cool- and warm-adapted genotypes were analyzed by individual mixed-effects repeated measures ANOVA (type III with Satterthwa'te's method) using the 'lmer' R package (Bates et al. 2015; Kuznetsova et al. 2017). In this test, individual traits were represented as response variables while the group (cool and warm-adapted ecotypes) and month were treated as categorical fixed effects with two and three levels, respectively. Individual genotype nested within ecotypes was incorporated as a random effect.

Leaf energy budget model parameterization

A leaf energy balance model was executed in R (R Core Team, 2018) through the 'tealeaves' package (Muir 2019). The model calculates leaf temperature from a suite of leaf traits, environmental parameters, and physical constants. Leaf traits included leaf size, stomatal ratio (stomata density adaxial: stomatal density abaxial), and mean canopy stomatal conductance during the hottest time of the day (11:00 to 19:00) from June 2nd (day 153) to October 2nd (day 275) 2017 were included in the model. The environmental parameters used in the model included air temperature, relative humidity, and wind speed collected at the common garden during the hottest time of the day from June 2nd (day 153) to October 2nd (day 275) 2017. Other environmental parameters included in the model were atmospheric pressure at 998 meter above sea level (90.0 kPa), reflectance for shortwave irradiance (albedo) (0.2, unitless), and incident short-wave (solar) radiation flux density (1000 W/m^2) (Muir 2019, Okajima et al. 2012).

Sensitivity analysis was performed on three and two environmental and morphophysiological variables, respectively, to determine their overall effect on leaf temperature resulted from the leaf energy balance model. These variables were air

temperature, relative humidity, wind speed (environmental) and stomatal conductance and leaf size (morphophysiological). I used the 'konfound' package in R to run the sensitivity analysis (Frank et al. 2013) to determine the influence that environmental variables (relative humidity, wind speed and air temperature) and morphophysiological traits (leaf size and stomatal conductance) have on the modeled leaf temperatures in *P. fremontii*.

Analysis of trait variation among populations

I performed a principal component analysis (PCA) to analyze the relationship between seven morphophysiological traits (A_{il}, A_s:A_l, D_{stom}, G_s, Ψ_{md}, SLA and S_{stom}) and ΔT at the population level using the 'factoextra' and 'FactoMineR' packages (Kassambara and Mundt, 2017; Lê et al. 2008). I determined the number of meaningful PCA axes using the Kaiser criterion and the Broken Stick Model in the 'vegan' and 'biodiversity' R package. Trait representation in the principal component biplot was based on the magnitude of the correlation between each trait and the principal component. Thus, traits in this biplot were represented as vectors with a length and direction indicating the strength and trend of a given tr'it's relationship among other traits. Specific location of the vector in the biplot indicates the positive or negative impact that a trait has on each of the two components x-axis, first component (PC1) and y-axis, second component (PC2). To analyze the relationship between the seven populations and the traits distribution in the PCA biplot, I constructed seven 95% confidence ellipses based on the PCA scores of each population. Subsequently, I performed ANOVA Tu'ey's HSD tests to assess significant differences in PC axes scores at the population level.

Results

Leaf traits and leaf temperature

As hypothesized, under well-watered conditions, the warm-adapted ecotype displayed cooler midday leaf temperatures than cool-adapted ecotype during the hottest time of the day (13:00 to 15:00). Average leaf temperature in the warm-adapted ecotype was 2.80 °C below the common garden ambient temperature while cool-adapted ecotypes exhibited a mean leaf temperature of 0.98 °C above air temperature (t = 3.84, df = 50, P < 0.001) (Fig. 3.3a, Table 3.2). Warm-adapted ecotype displayed 39% smaller leaves (t = 4.15, df = 68, P < 0.001) (Fig. 3.3b) with 35% greater stomatal densities (t =-5.95, df = 67.39, P < 0.001) (Fig. 3.3c) and 13% higher specific leaf area (t = 2.85, df = 40, P < 0.01, Table 3.3) than the cool-adapted ecotype. The warm-adapted ecotype exhibited slightly greater (8%) maximum theoretical stomatal conductance (G_{smax}) than the cool-adapted ecotype (Table 3.3).

Sap-flux-scaled canopy transpiration and stomatal conductance

Mean J_s measured over the growing season was largely similar between warm-versus cool-adapted ecotypes until about mid-August (~ Day 230) after which J_s was on average 12% higher in the warm-adapted ecotype. Mean J_s varied dramatically over the course of the growing season from less than 5 g m^{-2} s^{-1} to over 60 g m^{-2} s^{-1} depending on vapor pressure deficit (Fig. S3.1) and photosynthetic active radiation (Q, data not shown). The warm-adapted ecotype displayed a 36% greater A_s:A_l than the cool-adapted ecotype (t = 9.92, df = 54, P < 0.001) (Fig. 3.3d, Table 3.2). As a consequence, the warm-adapted ecotype exhibited 42.2% higher mean afternoon sap-flux-scaled canopy transpiration rates (t = -7.49, df = 199.2, P < 0.001) over the course of the growing season, with

contrasts between ecotypes becoming particularly large starting in mid-August around Day 230 (Fig. 3.4a).

Similarly, the warm-adapted ecotype exhibited 38.8% higher canopy conductance (G_c) than the cool-adapted ecotype (Table 3.3). I found that cool and warm-adapted ecotypes displayed their lowest canopy stomatal conductance values of the season (2.57 and 3.03 mmol m^{-2} s^{-1}, respectively) on June 19 (Day 170), the day with the second highest recorded afternoon VPD (7.33 kPa) during the season (Fig. 3.4b). On the other hand, both cool and warm-adapted ecotypes displayed their greatest G_c values (50.5 and 69.5 mmol m^{-2} s^{-1}, respectively) on the day with the lowest VPD (1.35 kPa) recorded in the season (Day 205, July 24) (Fig. 3.4b).

Canopies of both warm- and cool-adapted ecotypes were well coupled to the atmosphere such that the mean canopy decoupling coefficient was never higher than 0.05 for either group (Table 3.4). Therefore, cool- and warm-adapted ecotypes displayed G_s values that mirrored G_c. The warm-adapted ecotype exhibited 37.8% higher whole-season G_s (20.4 mmol m^{-2} s^{-1}) than the cool-adapted ecotype (14.8 mmol m^{-2} s^{-1}) (Table 3.4). Log-scale VPD explained 53% (F = 136.7, P < 0.0001) and 62% (F = 198.4, P < 0.0001) of the variation in mean daytime G_s of warm- and cool-adapted ecotypes, respectively (Fig. 3.5a). Analysis of covariance revealed that across both ecotypes, G_s was highly correlated with VPD (F = 294.9, P < 0.0001). Increases in VPD resulted in decreases in G_s (Fig. 3.4 and 3.5a). However, the relationship between G_s and VPD differed between warm- and cool-adapted ecotypes (F = 46.9, P < 0.0001). The interaction between VPD and ecotypes was significant (F = 9.40, P < 0.01), suggesting 94ifferfferences in G_s between cool and warm-adapted ecotypes were dependent on VPD.

Differences in G_s between these two ecotypes substantially decrease at higher VPD (Fig. 3.5a).

There was a strong correlation between G_s :G_{sref} and VPD in both warm- (R^2 = 0.53, F = 2222 , P < 0.0001) and cool-adapted (R^2 = 0.58, F = 2733 , P < 0.0001) ecotypes (Fig. 3.5b). At the reference value of VPD = 1 kPa, reference G_s (i.e., G_{sref}) was 59% higher in the warm-adapted ecotype relative to the cool-adapted ecotype (66.3 mmol m^{-2} s^{-1} versus 41.7 mmol m^{-2} s^{-1}, Fig. 3.5a). However, the slope (m) that relates G_s with VPD was also 62% higher in warm-adapted ecotype than cool-adapted ecotype (-71.1 mmol m^{-2} s^{-1} versus 46.5 mmol m^{-2} s^{-1}, Fig. 3.5a). Thus, stomatal sensitivity (S) to VPD was nearly equal between cool- (1.10 ± 0.020) and warm-adapted ecotypes (1.12 ± 0.029) (Fig. 3.5b).

Leaf water potentials

Pre-dawn water potentials (Ψ_{pd}) ranged from -0.30 MPa to -0.70 MPa throughout the growing season, indicating the trees were relatively well-watered, with the exception of occasional brief periods between irrigation events. I did not find significant differences in Ψ_{pd} between warm- and cool-adapted ecotypes (Fig. 3.6a). However, the warm-adapted ecotype operated with lower mid-day leaf water potentials (Ψ_{min}) than the cool-adapted ecotype throughout the summer (F = 11.63, df = 1, P < 0.01, Fig. 3.6b, Table S3.1), supporting hypothesis 4. Differences were most pronounced later in the growing season paralleling increased differences in canopy E between groups (i.e., Fig. 3.4a). Specifically, differences in Ψ_{min} between cool- and warm-adapted ecotypes were less than 0.1 MPa on day 157 and 180, but increased to 0.23 MPa (t = 3.15, df = 40, P < 0.01) and 0.33 MPa (t = 3.36, df = 40, P < 0.01) on day 208 and 236, respectively, with mean

Ψ_{min} in the warm-adapted ecotype falling below -2.0 MPa on day 236 (Fig. 3.6b). As a consequence of progressive differences in Ψ_{min}, differences in $\Delta\Psi$ between ecotypes also increased over the growing season (Fig. 3.6c).

Leaf energy balance model

Leaf temperature derived from the 'tealeaves' leaf energy balance model predicted leaves from the cool-adapted ecotype to be consistently hotter than the warm-adapted ecotype under identical air temperature scenarios (Fig. 3.7). The average of all modeled leaf temperatures was 1.09 °C hotter in the cool-adapted ecotype than the warm-adapted ecotype. Differences in leaf temperature between ecotypes were largely independent of air temperature, reflecting the similarity in stomatal sensitivity to VPD between ecotypes (Fig. 3.5b). Sensitivity analysis showed that of the five variables explored (air temperature, relative humidity, wind speed, stomatal conductance, and leaf size), air temperature had the greatest effect on modeled leaf temperatures (Fig. S3.2a). However, when air temperature held at a fixed value, leaf temperature was constrained primarily by canopy stomatal conductance (Fig. S3.2b).

Relationship between morpho-physiological traits and ΔT at the population level

According to the Kaiser criterion and the Broken-Stick Model (Borcard et al. 2011), only the first principal component significantly explained the variance of the seven morpho-physiological traits and ΔT. This principal component (PC1) accounted for 56.7% of the variance and showed a significant positive relationship with A_{il}, ΔT, Ψ_{md}, and S_{stom} while showing a negative significant correlation with $A_s:A_l$, D_{stom}, G_s, and SLA. ANOVA and Tu'ey's HSD tests on population-level PC1 scores detected four significant different groups among the seven populations included in this study (Fig. 3.8, S3.3).

Specifically, the two highest elevation populations with the most positive MAT and MMST transfer distances formed their own group (group "a"), while the third highest elevation population (elevation 1219 m) was its own group ("b"). Interestingly, group "c" was made up of three populations, the two lowest elevation populations with the most negative MAT and MMST transfer distances and the local population of the garden (elevation, 988 m). The last group "d" was formed by the third lowest elevation population (elevation, 666 m) and the lowest elevation population which was also found in group "c".

Discussion

I examined the overarching hypothesis that warm-adapted genotypes of the foundation tree species *Populus fremontii* prioritize leaf cooling over hydraulic safety compared to cool-adapted genotypes. Using an experimental common garden. I assessed whether warm adapted genotypes maintained cooler mid-summer leaf temperatures than cool-adapted genotypes and whether cooler leaf temperatures were correlated with a higher mean midday stomatal conductance, smaller leaf size or both. Mid-summer, mid-afternoon leaf temperatures of genotypes sourced from the warm-adapted ecotype were on average 3.8 °C cooler than genotypes from the cool-adapted ecotype, supporting my first sub-hypothesis. Contrasts in leaf temperatures between these two ecotypes corresponded with contrasts in leaf morphological traits including leaf size, specific leaf area and stomatal density, supporting my second sub-hypothesis. Genotypes of the warm-adapted ecotype also expressed a higher mean stomatal canopy conductance and associated transpiration rates, although stomatal sensitivity to VPD (S) was similar

between the two ecotypes, thus partially supporting my third sub-hypothesis. Finally, the higher stomatal conductance in warm-adapted ecotype was coupled with lower mid-day leaf water potentials (Ψ_{md}) compared to the cool-adapted ecotype, supporting my fourth sub-hypothesis. Taken together, these results indicate that the warm-adapted ecotype maintains cooler mid-summer leaf temperatures that may be critical for maintaining leaf carbon budgets and avoiding leaf thermal damage under a warming climate in the southwestern US. However, increased leaf thermal regulation in the warm-adapted ecotype appears to correspond with enhanced hydraulic "risk taking" that could result in greater susceptibility to water deficits that are also predicted to increase in frequency and intensity in the southwest in the near future.

Significance of leaf temperature

Genotypes on the warm edge of *P. fremontii's* distribution experience some of the most extreme summer heat waves in North America. Cooler leaf temperatures exhibited by genotypes sourced from the warm-adapted ecotype likely reflect extreme selection pressures to cope with chronic thermal stress that may be induced by air temperatures that often approach 50 °C. To optimize canopy thermal regulation, the warm-adapted ecotype displayed a suite of morpho-physiological traits and hydraulic strategies that simultaneously reduce leaf radiative load gain while increasing evaporative cooling. The combination of adaptive traits in the warm-adaptive ecotype is expected to reduce leaf photorespiration and maintenance respiration rates (Lloyd and Farquhar 2008; O'Sullivan et al. 2013; Slot et al. 2016), while avoiding irreversible damage to chloroplasts and subsequently electron transport capacity of photosystem II (Osmond and Björkman 1972; Kozaki and Takeba 1996). The critical temperatures that affect photosystem II activity

are generally species-specific or related to previous high temperature exposure (Knight and Ackerly 2003' O'Sullivan et al. 2017; Teskey et al. 2015; Yordanov 1992). However, high temperature exposure has consistently been correlated with loss of chloroplast thermostability and decline of photosynthesis II (PSII) quantum yield (Berry and Bjorkman 1980; Hüve et al. 2011). Similarly, thylakoid membranes increase their fluidity, leakiness, and partial dissociation of light-harvesting complexes of photosystem II at extreme hot temperatures (Armond et al. 1980; Briantais et al. 1996; Hüve et al. 2011), underscoring the importance of leaf thermal regulation in hot environments.

Similar to field data collected from leaf thermal imagery, the 'tealeaves' leaf energy balance model predicted cooler leaf temperatures in the warm-adapted ecotype relative to the cool-adapted ecotype, under the same environmental conditions. However, the leaf energy balance model yielded a much smaller difference of 1.1 °C instead of the 3.8 °C found in my leaf thermal measurements. This difference could be explained by the fact that stomatal sensitivity to VPD was similar between ecotypes. According to the model, T_{leaf} was strongly governed by G_s (Fig. S3.2b), and at relatively low VPD (i.e., VPD < 3 kPa), mean G_s of the warm-adapted ecotype was 55% to 60% higher than the cool-adapted ecotype (Fig. 3.5a). However, under warmer and drier conditions, G_s between ecotypes converged reflecting their similar sensitivities to VPD (Fig. 3.5b). Therefore, differences in mid-summer, afternoon leaf temperatures detected by the model were largely a function of the cool-adapted ecotype having a larger mean leaf size than the warm-adapted ecotype (Fig. 3.3b), and not differences in evaporative cooling. Nevertheless, given the 36% higher mean $A_s:A_l$ (Fig. 3.3d), and the equal to or higher mean J_s of the warm-adapted ecotype relative to the cool-adapted ecotype (Fig. S3.1), it is

99

highly plausible that afternoon leaf evaporative cooling was significantly more pronounced in the warm-versus cool adapted ecotypes.

Minor changes in leaf temperature can have a significant impact of leaf carbon budgets because both mitochondrial respiration and photorespiration increase exponentially with tissue temperature'(O'Sullivan et al. 2017; Slot et al. 2016). For example, Q_{10} values (a proportional change in respiration with a 10 °C increase in temperature) in the tissues of species in the genus *Populus* have been reported between 1.28 and 5.89 (Griffin et al. 2001; Gielen et al. 2003). Thus, a leaf temperature increases of just 1 °C in these species would result in a 12.8% to 58.9% increase in leaf respiration, although short-term (i.e., hours to days) thermal acclimation to warmer temperature could reduce plant Q_{10} values (Tjoelker et al. 2001; Atkin and Tjoelker, 2003). Likewise, photorespiration rates in C3 plants can increase substantially at leaf temperatures above 25 °C, with a corresponding decrease in leaf carboxylation rates that can substantially reduce photosynthesis (Busch et al. 2013). Although the effect of higher temperatures on leaf photorespiration can vary by a species' optimum growth temperature (Cavanagh and Kubien 2014; Galmes et al. 2016), photorespiration increases are generally related to the effect of high temperature on Rubisco specificity and the differences in solubility between CO_2 and O_2 (von Caemmerer and Quick 2000).

Hydraulic "risk taking" as an adaptive strategy to maintain cooler canopies

Intuitively, plants that maintain a relatively high stomatal conductance despite high atmospheric demand (e.g., high VPD) run the risk of steep declines in leaf turgor, xylem conductance or both, even when the rhizosphere remains moist (Grossiord et al. 2020; Brodribb et al. 2017; Sperry et al. 2002). In the present study, Ψ_{md} was 0.3 MPa

lower in the warm- relative to cool-adapted ecotypes by the end of the warm-season, corresponding with increased differences in G_s between ecotypes. For drought intolerant species such as *P. fremontii*, small contrasts in Ψ_{md} may reflect important contrasts in plant water status between warm- and cool-adapted ecotypes. In fact, by late summer, mean Ψ_{md} in the warm-adapted ecotype fell below the xylem pressure (-1.88 MPa) at which near complete hydraulic failure occurs in *P. fremontii* – defined as the water potential that leads to 88% loss of xylem conductivity (Ψ_{88}: Choat et al. 2012). Conversely, mean Ψ_{md} in the cool-adapted ecotype never fell below -1.76; a level that is slightly above the reported threshold for hydraulic failure in *P. fremontii*. Whether contrasts in Ψ_{md} reflect differences in Ψ_{88} or other plant xylem traits among ecotypes is an open question. A similar study conducted at the same common garden as the present study reported that *P. fremontii* genotypes belonging to the relatively warm Sonoran Desert ecoregion had lower wood densities and xylem vessels with higher hydraulic mean diameters than genotypes sourced from the cooler Mogollon Rim ecoregion (Blasini *et al*. 2020): traits that could portend greater risk of hydraulic failure in the Sonoran Desert genotypes. In the present study, the warm-adapted ecotype had higher stomatal densities and a higher mean theoretical maximum stomatal conductance compared to the cool-adapted ecotype. Taken together, the lower Ψ_{md} values indicate that the warm-adapted ecotype may be adapted to operate with lower hydraulic safety margins to maintain cooler leaves. That in turn, may limit the hydrological niche of the warm-adapted ecotype to locations with high perennial soil moisture availability (Hultine et al. 2019).

Not surprisingly given their lower Ψ_{md} values, the reference midday G_s (i.e., G_{sref}) was almost 60% higher in the warm- versus cool-adapted ecotype. However, contrasts between ecotypes were not driven by differences in J_s, per se, but from the warm-adapted ecotype having a near 40% higher A_s:A_l. Leaf area to sapwood area ratios (the inverse of A_s:A_l) strongly decrease with aridity in angiosperm tree taxa (Gleason et al. 2013; Togashi et al. 2015). A relatively high A_s:A_l can buffer plants from steep gradients in xylem water potential by maximizing the supply of water to individual leaves relative to demand that in turn, can maximize leaf evaporative cooling under well-watered conditions. On the other hand, mean stomatal sensitivity to VPD was similar between ecotypes indicating that stomatal responses to atmospheric demand or dryness is a fixed trait among *P. fremontii* populations given similar exposure to soil water conditions.

4.3 Adaptive trait syndromes at the population level

A primary advantage of common gardens in ecological studies is that they provide opportunities for potential evaluation of the coordination among traits – i.e., adaptive trait syndromes – and resource fluxes within and among plants (Freschet et al. 2010; Reich 2014). For example, a previous study conducted on *P. fremontii* at the same common garden as the present study revealed that traits were not only coordinated across multiple organs and scales, but also identified two clearly defined adaptive trait syndromes (Blasini et al. 2020). Genotypes belonging to the relatively high-elevation Mogollon Rim ecoregion expressed a suite of conservative traits including spring leaf flush, leaf economic traits and wood economic traits relative to genotypes belonging to the relative low-elevation Sonoran Desert ecoregion (Blasini et al. 2020). Importantly, all five source populations that comprised the Sonoran Desert ecoregion shared similar mean trait values

with one another, while all three populations that comprised the Mogollon Rim ecoregion also shared similar mean trait values with one another. These results indicate that all populations studied from the Sonoran Desert ecoregion shared a similar "acquisitive" adaptive trait syndrome that appeared to arise from selection to avoid leaf thermal damage (Blasini et al. 2020). Similarly, all populations from the Mogollon Rim ecoregion shared a similar "conservative" adaptive trait syndrome that appeared to arise from selection to avoid frost damage (Blasini et al. 2020).

In the present study, I defined a warm-adapted population as one where mean maximum summer temperature rose above 40 °C. Indeed, results detected clear trait contrasts between the three warm-adapted populations, and the three coolest populations (Fig. 3.8) that mirrored contrasts previously reported between the Sonoran Desert and Mogollon Rim ecoregions (Blasini et al. 2020). However, in contrast to my overarching hypothesis, genotypes from the mid-elevation population expressed traits that more closely paralleled genotypes sourced from the three warmest populations than the three cooler populations (Fig. 3.8). One possible explanation is that selection pressures to cope with leaf thermal stress are expressed in genotypes from locations with lower mean maximum temperatures than 40 °C. Alternatively, the mean trait expression of the mid-elevation population may reflect a certain "home field advantage" over genotypes from other locations given the 0 °C transfer distance to the location of the common garden. Nevertheless, the clear adaptive trait syndromes identified here show that locally adapted *P. fremontii* populations may become maladapted under rapidly changing climate conditions across its geographical distribution.

Conclusions

   The resiliency of groundwater dependent forest ecosystems to environmental change depends largely on resiliency of phreatophytic vegetation such as *P. fremontii* to alterations in groundwater availability coupled with rising temperatures. The dynamics of fluvial hydrology and groundwater availability undoubtedly act as strong agents of selection in *P. fremontii* in terms of hydraulic architecture, xylem anatomy and stomatal regulation (Blasini et al. 2020; Hultine et al. 2010, 2020). *Populus fremontii* like other groundwater dependent taxa in the southwestern US occur in locations where groundwater is shallow enough for roots to maintain contact for most of the year. Shallow groundwater, therefore, allows *P. fremontii* trees to maximize productivity and resource uptake over hydraulic safety. However, hydraulic "risk taking" may be amplified in *P. fremontii* ecotypes occurring on the warm edge of its distribution in order to cope with growing season temperatures that often approach 50 °C. In the present study, warm-adapted ecotypes, including those sourced along the extreme warm-edge of *P. fremontii's* distribution, displayed a higher maximum stomatal conductance and lower mid-day leaf water potentials that corresponded with lower daytime leaf temperatures than ecotypes sourced from relatively cool locations. There is a growing body of evidence that some warm-adapted species forego hydraulic safety in order to optimize leaf temperature via transpirational cooling when exposed to hot conditions (Aparecido et al. 2020; Drake et al. 2018; Slot et al. 2016). Prioritizing leaf cooling over hydraulic safety would presumably limit the hydraulic niche of warm-adapted *P. fremontii* ecotypes to locations where groundwater is not only shallow but is largely absent of daily or seasonal fluctuations that can temporarily decouple roots from the capillary fringe.

Whether *P. fremontii* populations along the warm edge of its distribution can balance hydraulic safety margins with thermal safety margins in the face of rapidly increasing aridity is an open question. Future investigations will need to couple physiology and genetics techniques to determine to what extent *P. fremontii* could overcome future extreme climatic conditions in the southwestern US.

Acknowledgements

Tables

Table 3.1. List of abbreviations with common units

Abbreviation	Definition	Units
Meteorological variables		
VPD	Vapor pressure deficit	kPa
U	Open air wind speed	m s^{-1}
u$_c$	Canopy wind speed	m s^{-1}
u$_v$	Canopy frictional velocity	m s^{-1}
D	Zero plane displacement	m
z$_m$	Roughness length	m
d$_l$	Characteristic leaf dimension	m
Fluxes and conductance		
J$_s$	Sap flux density	g m^{-2} s^{-1}
G$_c$	Canopy conductance	mmol m^{-2} s^{-1} kPa
G$_s$	Canopy stomatal conductance	mmol m^{-2} s^{-1} kPa
G$_{bl}$	Boundary layer conductance	mmol m^{-2} s^{-1} kPa
G$_r$	Long-wave radiative transfer conductance	mmol m^{-2} s^{-1} kPa
γ	Psychrometric constant	kPa K^{-1}
λ	Latent heat of vaporization	J kg^{-1}
ρ	Density of moist air	kg m^{-3}
C$_p$	Specific heat of air	J kg^{-1} K^{-1}
e	Change in latent per change in sensible heat	Dimensionless
Ω	Canopy decoupling coefficient	Dimensionless
E	Whole-tree transpiration rate	g m^{-2} s^{-1}
G$_{smax}$	Theoretical maximum stomatal conductance	mmol m^{-2} s^{-1}
T$_{air}$	Air temperature	°C
Tl$_{leaf}$	Leaf temperature	°C
ΔT	Leaf-to-air temperature differences	°C
Plant measurements and allometry		
A$_{il}$	Individual Leaf Area	cm^2
A$_l$	Leaf area	m^2
A$_s$	Sapwood area	cm^2
H	Tree height	m
SLA	Specific Leaf Area	cm^2 g
D$_{stom}$	Stomatal Density	#Stomata mm^2
S$_{stom}$	Stomatal Size	μm^2

Table 3.2. Climatic variables of the seven provenances at the Agua Fria National Monument common garden. Climatic characteristics include mean annual temperature (MAT) and mean maximum summer temperature (MMST). Transfer distances for MAT (MAT of the garden minus MAT of the provenance) and MMST. The population CAF is located near the common garden and thus has a transfer distance of zero. Results of mean ± standard error (n = 56) comparison of whole-tree stem diameters and heights in a common garden in central Arizona.

Provenance Elevation (m)	Latitude	Longitude	MAT (°C)	MMST (°C)	MAT (°C) Transfer	MMST (°C) Transfer	Stem Diameter (cm)	Whole-tree height H (m)
1940	35.8115	-110.18038	10.7	29.9	6.7	5.2	28.15±2.82	3.15 ±0.51
1521	34.9613	-110.38956	12.3	33.6	5.1	1.5	12.78±1.07	2.44±0.98
1212	31.4382	-110.76260	16.9	34.7	0.5	0.4	27.92±2.42	2.25±0.40
988	34.2338	-111.04478	17.4	35.1	0.0	0.0	11.25±0.86	2.25±0.40
666	33.9540	-112.13526	19.9	38.0	-2.5	-2.9	26.59±3.95	2.42±0.68
161	34.2761	-114.05856	22.3	41.2	-4.9	-6.1	21.81±2.82	1.83±0.36
72	33.3621	-114.69856	22.6	39.9	-5.2	-4.8	32.50±4.04	2.03±0.66

Table 3.3. Results of mean ± standard error and percent difference (n = 56) comparison of *Populus fremontii* functional traits between warm- and cool-adapted genotypes in a common garden in central Arizona.

Trait	Cool	Warm	Percent Difference
Leaf Size (mm^2)	24.16(±1.27)	17.27(±0.97)	40%
Specific Leaf Area (cm^2 g)	107.18(±3.43)	121.26(±3.41)	13%
Stomatal Density (Stomata mm^{-2})	194.61(±9.11)	263.54(±7.12)	35%
Sapwood to Leaf Area (cm m^{-1})	0.029(±7.4e-04)	0.039(±6.7e-04)	36%
Transpiration (g m^{-2} s^{-1})	0.47(±0.01)	0.67(±0.02)	42.2%
Canopy Conductance (mmol m^{-2} s^{-1})	14.4(±0.70)	20.0(±1.09)	38.8%
Canopy Stomatal Conductance (mmol m^{-2} s^{-1})	14.8(±1.16)	20.4(±1.64)	37.8%
Leaf Temperatu–e - Air Temperature (°C)	0.98 (± 0.72)	-2.80 (± 0.70)	3.8 °C
Maximum theoretical stomatal conductance (mmol m^{-2} s^{-1})	1.12(± 0.18)	1.21(± 0.24)	8%

Table 3.4. Results of mean ± standard error (n = 56) comparison of afternoon canopy stomatal conductance, afternoon stomatal conductance, and decoupling coefficient between warm- and cool-adapted ecotypes in a common garden in central Arizona.

Ecotypes	Gc (mmol m^{-2} s^{-1})	Gs (mmol m^{-2} s^{-1})	Decoupling Coefficient
WARM	20.0 (±1.55)	20.4 (±1.64)	0.047 (±0.002)
COOL	14.4 (±1.10)	14.8 (±1.16)	0.048 (±0.003)
Population (m)	Gc	Gs	Decoupling Coefficient
72	20.0 (±1.20)	20.6 (±1.25)	0.052 (±0.005)
161	14.2 (±4.43)	14.4 (±1.79)	0.034 (±0.004)
666	25.3 (±7.93)	26.1 (±3.38)	0.055 (±0.007)
988	16.4 (±3.00)	17.0 (±3.25)	0.047 (±0.008)
1212	12.7 (±3.49)	12.9 (±3.59)	0.064 (±0.004)
1521	10.3 (±1.12)	10.6 (±.50)	0.037 (±0.002)
1940	18.1 (±5.65)	18.6 (±2.51)	0.044 (±0.006)

Figures
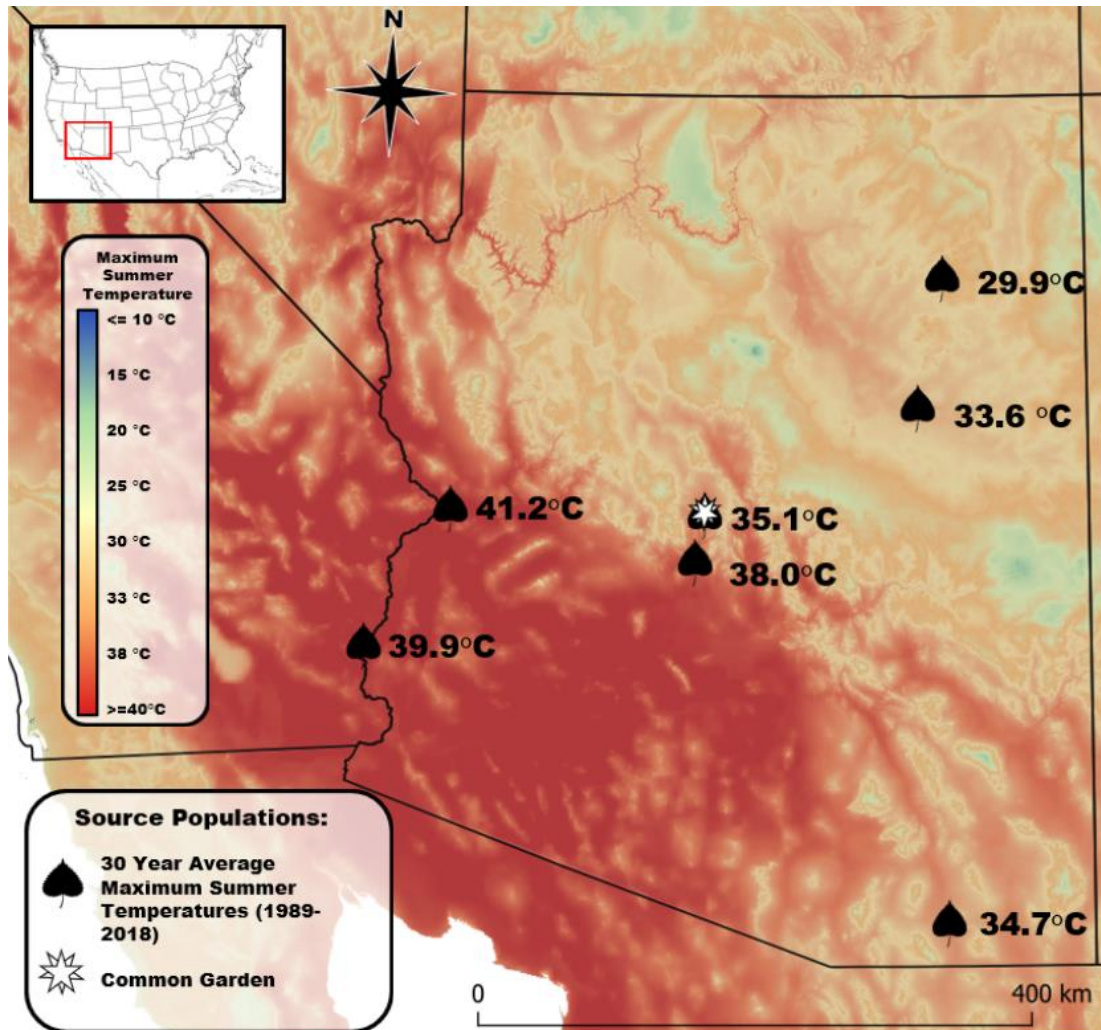
Figure 3.1. Location of the Agua Fria common garden (white star) and seven population sites of *Populus fremontii* (Fremont cottonwood leaf icon) with their 30-year maximum summer temperatures (Fick and Hijmans, 2017. Worldclim 2: New 1-km spatial resolution climate surfaces for global land areas. International Journal of Climatology, http://worldclim.org/version2). QGIS Development Team (2021). QGIS Geographic Information System. Open-Source Geospatial Foundation Project. http://qgis.osgeo.org

111

30 Year (1989-2018) Maximum Summer Temperatures (ºC)

Figure 3.2. Box and whisker plots showing the median, 25th and 75th percentiles (boxes) and the [1]0th and [9]0th percentiles (error bars) of 30-year (1989-2018) maximum annual average summer temperatures grouped by the seven population sites of *Populus fremontii*. PRISM data (http://prism.oregonstate.edu). Red boxes represent populations adapted to mean maximum summer temperatures of >40 °C (warm-adapted ecotypes) and gray boxes represent populations adapted to mean maximum summer temperatures of <40 °C (cool-adapted ecotypes). Dotted red line represents 40 °C maximum average summer temperatures.

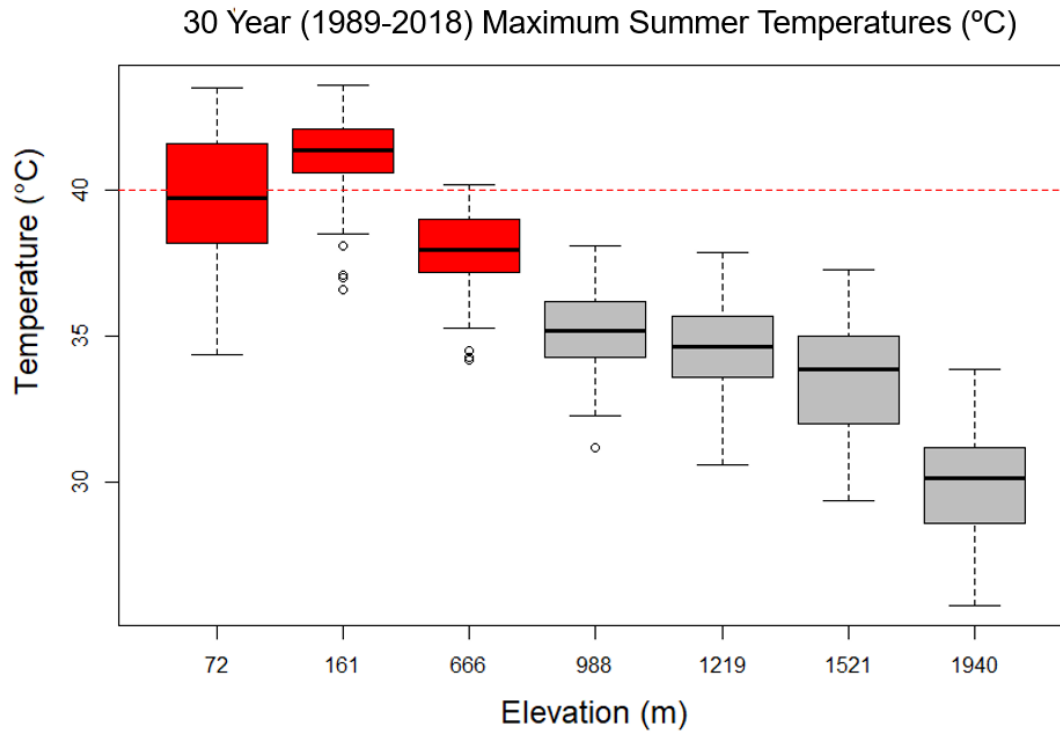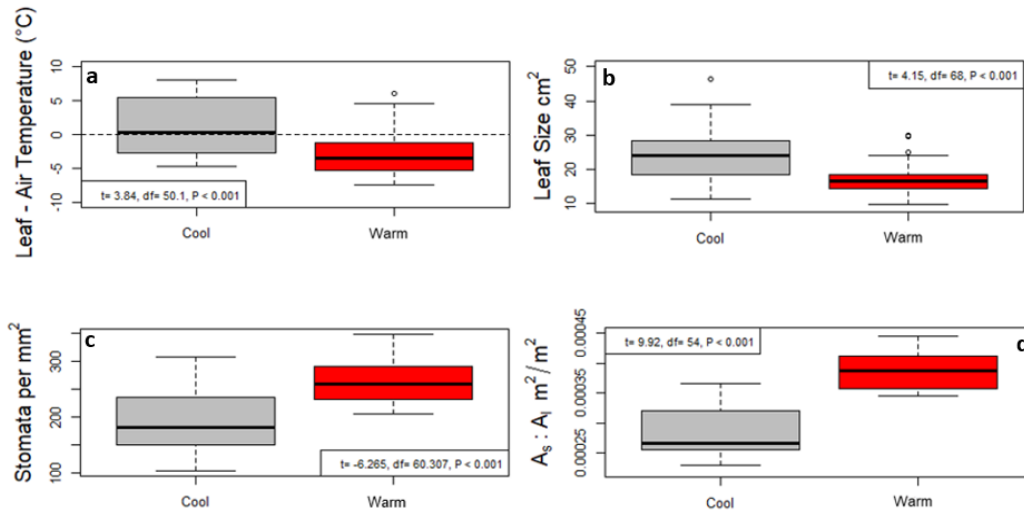**Figure 3.3.** Multi-panel box and whisker plots showing the median, [2]5th and 75th percentiles (boxes) and the [1]0th and [9]0th percentiles (error bars) of difference between the air and leaf temperatures (a) leaf size (b), stomatal density (c), sapwood to leaf area ratio (d) of *Populus fremontii* genotypes occurring in a common garden in central Arizona. Internal legends indicate the t-value (t), degree of freedom (df) and p-value (p) of the relationship between cool and warm- adapted ecotypes. Warm-adapted genotypes (ecotype) were sourced from cuttings of mature *P. fremontii* trees occurring along the species warmest edge of its thermal distribution (n=24 genotypes). Cool-adapted genotypes (ecotype) was sourced from cuttings of mature *P. fremontii* trees occurring along the species colder edge of its thermal distribution (n = 32 genotypes).

113
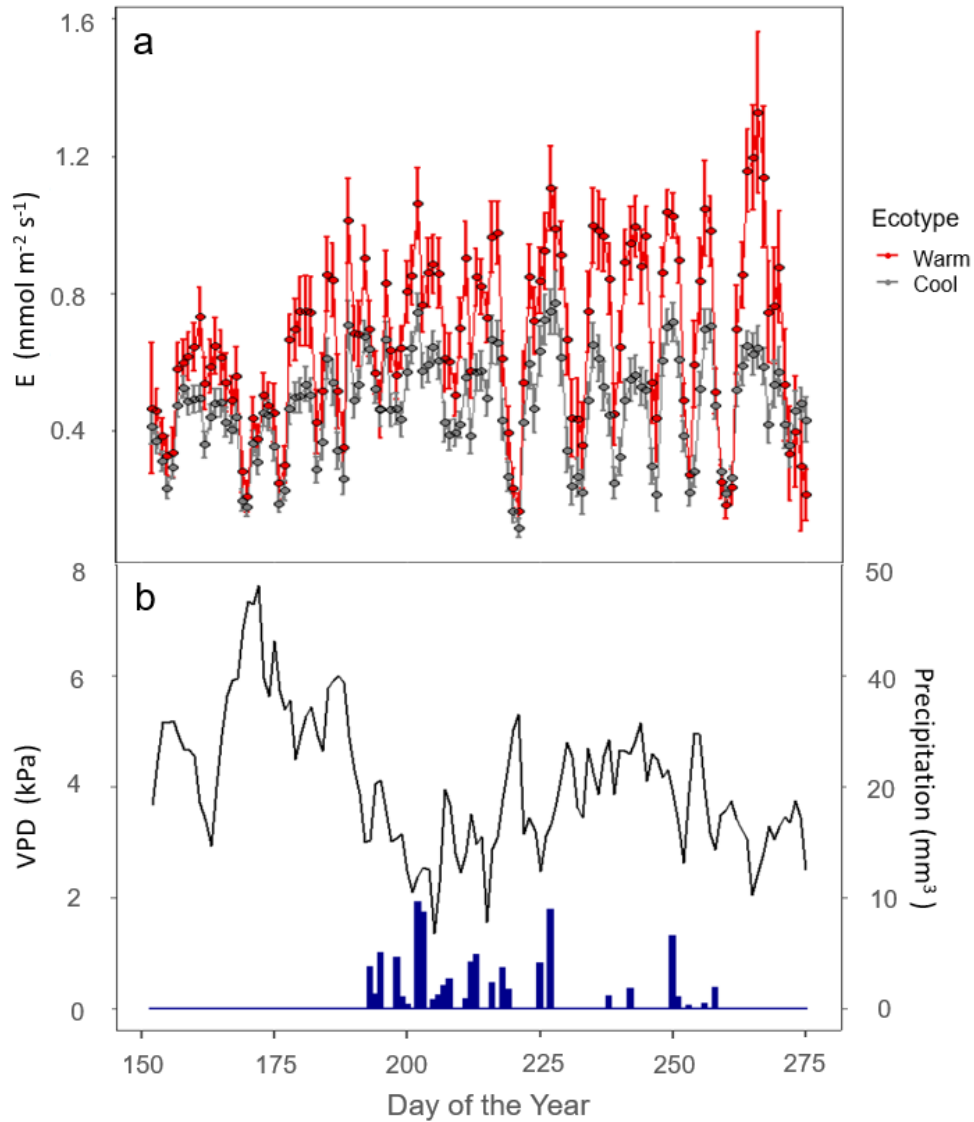
Figure 3.4. (a) Mean daily sap-flux scaled E measured between the hours of 1100 to 1900 from day of year 158 (June 7th) to day of year 275 (October 2nd) of the 2017 growing season on 24 warm- adapted genotypes and 32 cool adapted genotypes occurring in a common garden in central Arizona. Error bars represent the standard errors of the mean. Warm-adapted genotypes (ecotype) were sourced from cuttings of mature *P. fremontii* trees occurring along the species warmest edge of its thermal distribution (n = 24 genotypes). Cool-adapted genotypes (ecotype) was sourced from cuttings of mature *P. fremontii* trees occurring along the species colder edge of its thermal distribution (n = 32 genotypes). (b) Mean daytime vapor pressure deficit (vpd) values calculated from measurements of local air temperature and relative humidity and precipitation values of the area of the garden obtained at PRISM data (http://prism.oregonstate.edu).

114
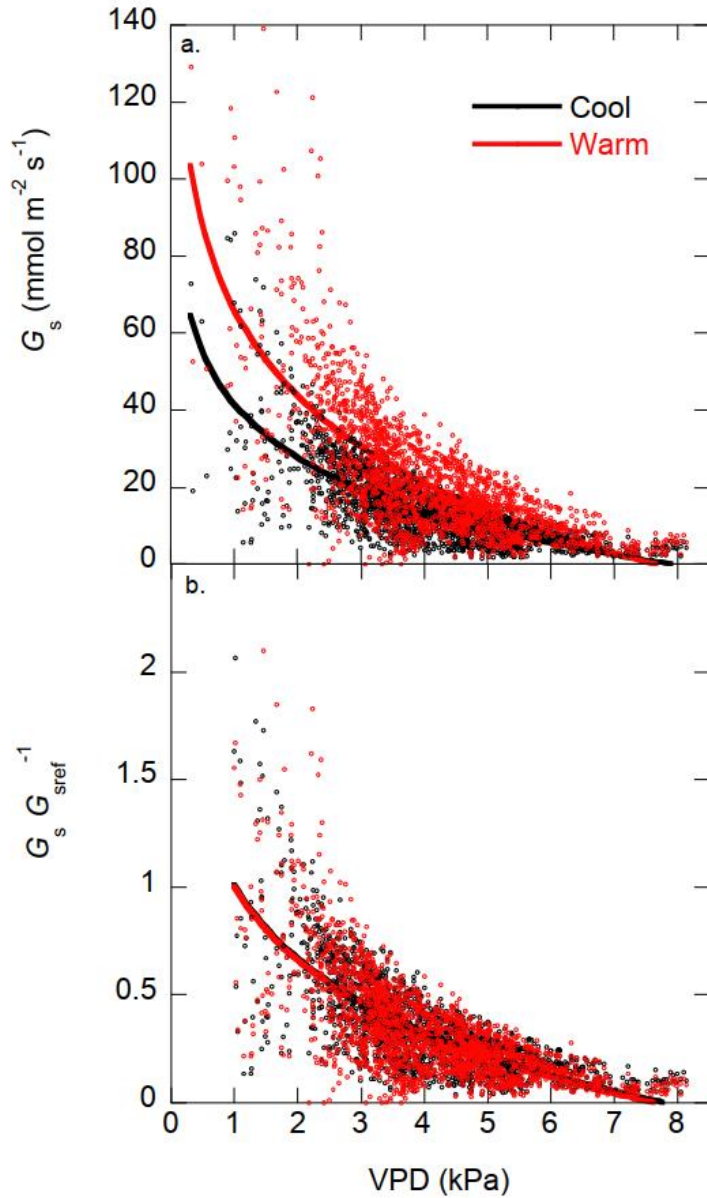
Figure 3.5. a. Relationship between mean daily canopy stomatal conductance per unit leaf area (G_s) and mean daytime vapor pressure deficit (vpd) in warm- and cool-adapted *Populus fremontii* ecotypes at an experimental common garden in central Arizona. Data were collected from day of year 158 (June 7th) to day of year 275 (October 2nd) of the 2017 growing season. b. stomatal conductance of warm- and cool-adapted ecotypes, normalized by a reference G_s (G_{sref}), defined at vpd = 1 kPa for data from day of year 158 to day of year 275 of the 2017 growing season.
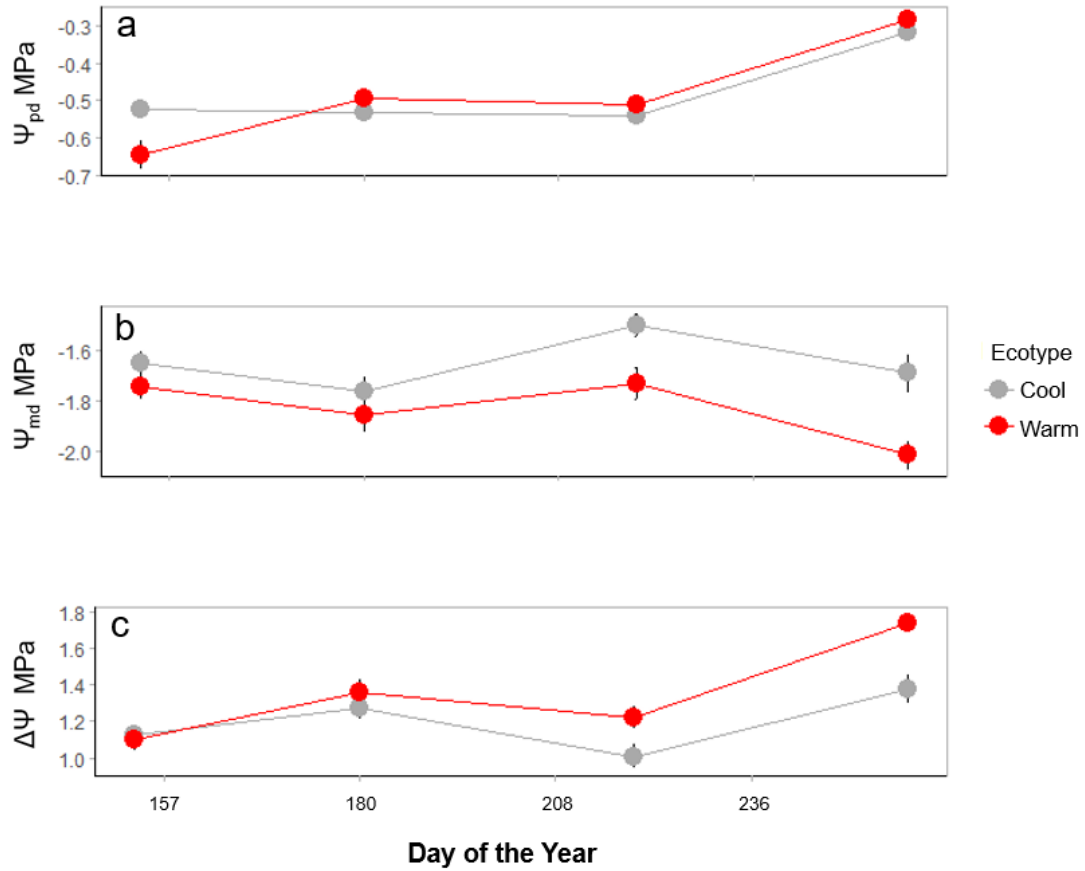
Figure 3.6. Mean predawn Ψ_{pd} (a), mid-day Ψ_{md} (b) and the difference between pre-dawn Ψ_{pd} and mid-day Ψ_{md} ($\Delta\Psi$) (c) measured during four periods of the 2017 growing season on 24 warm-adapted genotypes and 32 cool-adapted *Populus fremontii* genotypes in a common garden located in central Arizona. Error bars represent the standard errors of the mean.
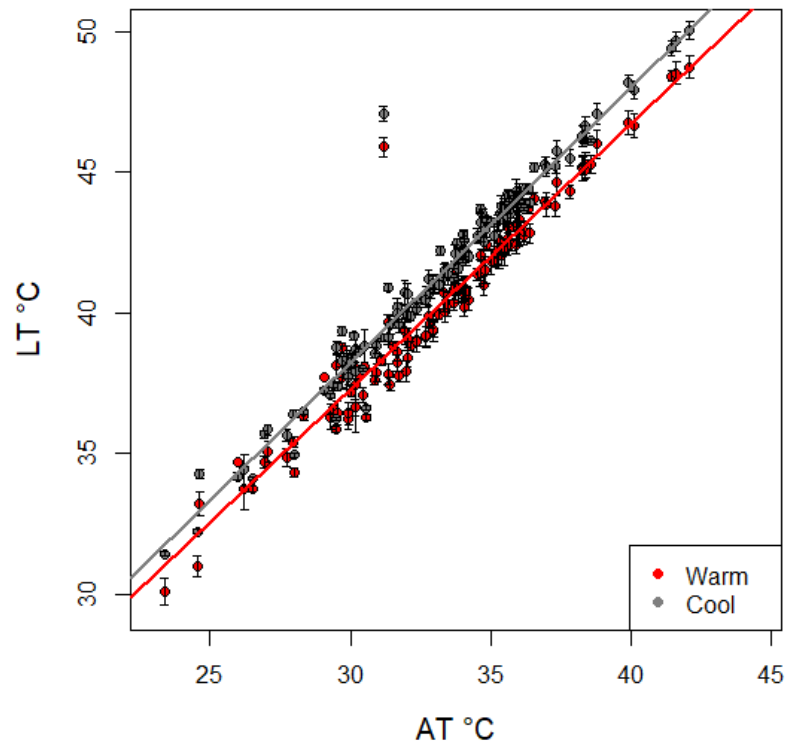
Figure 3.7. Relationship between energy balance estimations of leaf temperature and air temperature of warm- and cool-adapted *Populus fremontii* ecotypes. Estimates were modeled from measurements of leaf morphology, stomatal conductance, air temperature, relative humidity and wind speed (see Figure S3).
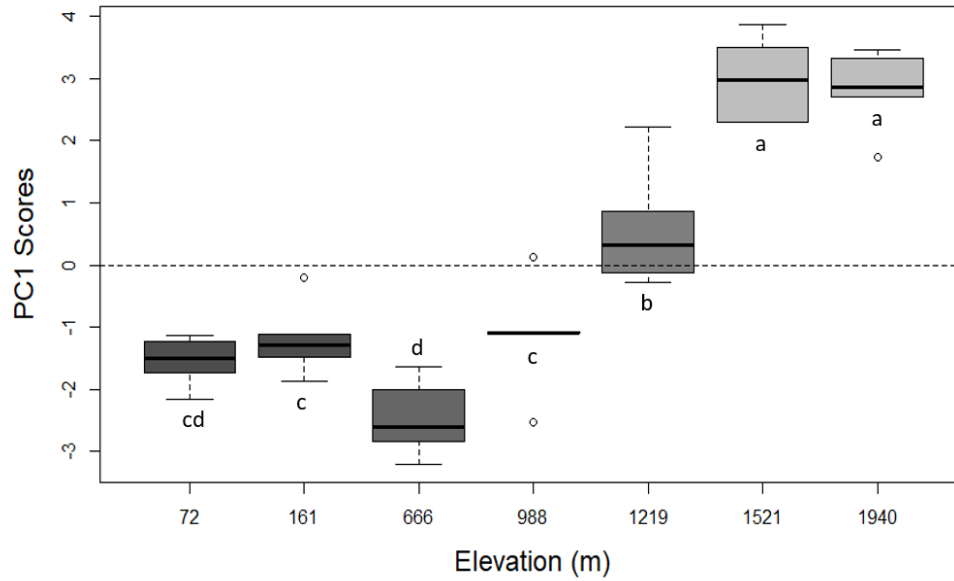
Figure 3.8. Relationship among the elevation of the seven source populations with principal component 1 loadings from a PCA using seven morpho-physiological traits and leaf-to-air temperature differences at the genotype that collectively represent the entire elevational range of *Populus fremontii*. Vertical bars represent standard errors (i.e., variation of genotypes within populations). Populations with different lowercase letters next to the data box and whisker indicate significant pairwise differences in PC1 scores using Tukey's HSD test.

References

Ackerly D, Knight C, Weiss S, Barton K, Starmer K (2002) Leaf size, specific leaf area and microhabitat distribution of chaparral woody plants: contrasting patterns in species level and community level analyses. Oecologia 130, 449–457. https://doi.org/10.1007/s004420100805

Ansley R.J, Mirik M, Surber BW, Park SC (2012) Canopy Area and Aboveground Mass of Individual Redberry Juniper (*Juniperus pinchotii*) Trees. Rangeland Ecology & Management 65, 189–195. https://doi.org/10.2307/41495360

Aparecido LMT, Woo S, Suazo C, Hultine KR, Blonder B (2020) High water use in desert plants exposed to extreme heat. Ecology Letters 23, 1189–1200. https://doi.org/10.1111/ele.13516

Atkin OK, Bloomfield KJ, Reich PB, Tjoelker MG, Asner GP, Bonal D, … Zaragoza-Castells J (2015) Global variability in leaf respiration in relation to climate, plant functional types and leaf traits. New Phytologist 206, 614–636. https://doi.org/10.1111/nph.13253

Akin OK, Tjoelker MG (2003) Thermal acclimation and the dynamic response of plant respiration to temperature. Trends Plant Sci. 8, 343–351. https://doi.org/10.1016/S1360-1385(03)00136-5

Atkin OK, Scheurwate RI, Pons TL (2006) High thermal acclimation potential of both photosynthesis and respiration in two lowland *Plantago* species in contrast to an alpine congeneric. Global Change Biology 12, 500-515. https://doi.org/10.1111/j.1365-2486.2006.01114.x

Armond UA, Bjorkman O, Staehelin LA (1980) Dissociation of supramolecular complexes in chloroplast membranes a manifestation of heat damage to the photosynthetic apparatus. Biochimica et Biophysica Acta 601, 433-442. https://doi.org/10.1016/0005-2736(80)90547-7

Bates D, Mächler M, Bolker B, Walker S (2015) Fitting linear mixed-effects models using lme4. Journal of Statistical Software 67(1), 1-48. https://doi.org/10.18637/jss.v067.i011

Beerling DJ, Osborne CP, Chaloner WG (2001) Evolution of leaf-form in land plants linked to atmospheric CO2 decline in the Late Palaeozoic era. Nature 410, 352–354. https://doi.org/10.1038/35066546

Berry J, Bjorkman O (1980) Photosynthetic Response and Adaptation to Temperature in Higher Plants. Annual Review of Plant Physiology 31, 491–543. https://doi.org/10.1146/annurev.pp.31.060180.002423

Blasini DE, Koepke DF, Grady KC, Allan GJ, Gehring CA, Whitham TG, … Hultine KR (2020) Adaptive trait syndromes along multiple economic spectra define cold and warm adapted ecotypes in a widely distributed foundation tree species. Journal of Ecology 109, 1298–1318. https://doi.org/10.1111/1365-2745.13557

Bréda NJJ (2003) Ground-based measurements of leaf area index: A review of methods, instruments and current controversies. Journal of Experimental Botany 54, 2403–2417. https://doi.org/10.1093/jxb/erg263

Breshears DD, Adams HD, Eamus D, McDowell NG, Law DJ, Will RE, … Zou CB (2013) The critical amplifying role of increasing atmospheric moisture demand on tree mortality and associated regional die-off. Frontiers in Plant Science 4, 264. https://doi.org/10.3389/fpls.2013.00266

Briantais JM, Dacosta J, Goulas Y (1996) Heat stress induces in leaves an increase of the minimum level of chlorophyll fluorescence, F_o: A time-resolved analysis. Photosynthesis Research 48, 189–196. https://doi.org/10.1007/BF00041008

Brodribb TJ, McAdam SAM, Carins Murphy MR (2017) Xylem and stomata, coordinated through time and space. Plant, Cell and Environment 40, 872– 880. ht tps://doi.org/10.1111/pce.12817

Borcard D, Gillet F, Legendre P (2011) Numerical ecology with R. Springer. https://doi.org/10.1007/978-1-4419-7976-6.

Bush SE, Hultine KR, Sperry JS, Ehleringer JR, Phillips N (2010) Calibration of thermal dissipation sap flow probes for ring- and diffuse-porous trees. Tree Physiology 30, 1545–1554. https://doi.org/10.1093/treephys/tpq096

Busch FA, Sage TL, Cousins AB, Sage RF (2013) C3 plants enhance rates of photosynthesis by reassimilating photo respired and respired CO_2. Plant, Cell and Environment 36, 200-212. https://doi.org/10.1111/j.1365-3040.2012.02567.x

Campbell G, Norman J (1998) An Introduction to Environmental Biophysics, 2nd ed. Springer-Verlag New York, New York. https://doi.org/10.1007/978-1-4612-1626-1

Cavanagh AP, Kubien DS (2014) Can phenotypic plasticity in Rubisco performance contribute to photosynthetic acclimation? Photosynthesis Research 119, 203-214. https://doi.org/10.1007/s11120-013-9816-3

Cen YP, Sage RF (2005) The Regulation of Rubisco Activity in Response to Variation in Temperature and Atmospheric CO_2 Partial Pressure in Sweet Potato. Plant Physiology 139, 979–990. https://doi.org/10.1104/pp.105.066233

Chapin FS, Matson PA, Vitousek PM (2011) Principles of terrestrial ecosystem ecology. Springer. https://doi.org/10.1007/978-1-4419-9504-9

Choat B, Jansen S, Brodribb TJ, Cochard H, Delzon S, Bhaskar R, Bucci SIild TS, Gleason SM, Hacke UG, Jacobsen AL, Lens F, Maherali H, Martínez-Vilalta J, Mayr S, Mencuccini M, Mitchell PJ, Nardini A, Pittermann J, … Zanne AE (2012) Global convergence in the vulnerability of forests to drought. Nature 491(7426), 752–755. https://doi.org/10.1038/nature11688

Cooper HF, Grady KC, Cowan JA, Best RJ, Allan GJ, Whitham TG (2019) Genotypic variation in phenological plasticity: Reciprocal common gardens reveal adaptive responses to warmer springs but not to fall frost. Global Change Biology 25, 187–200. https://doi.org/10.1111/gcb.14494

Curtis EM, Leigh A, Rayburg S (2012) Relationships among leaf traits of Australian arid zone plants: alternative modes of thermal protection. Australian Journal of Botany 60, 471–483. https://doi.org/10.1071/BT11284

Domec JC, Noormets A, King JS, Sun G, McNulty SG, Gavazzi MJ, Boggs JL, Treasure EA (2009) Decoupling the influence of leaf and root hydraulic conductances on stomatal conductance and its sensitivity to vapour pressure deficit as a soil dries in a drained loblolly pine plantation. Plant Cell and Environment 32, 980–991. https://doi.org/10.1111/j.1365–3040.2009.01981.x

Dong N, Prentice IC, Harrison SP, Song QH, Zhang YP (2017) Biophysical homoeostasis of leaf temperature: A neglected process for vegetation and land-surface modelling. Global Ecology and Biogeography 26, 998–1007. https://doi.org/10.1111/geb.12614

Drake JE, Tjoelker MG, Vårhammar A, Medlyn BE, Reich PB, Leigh A, Pfautsch S, Blackman CJ, López R, Aspinwall MJ, Crous KY, Duursma RA, Kumarathunge D, De Kauwe MG, Jiang M, Nicotra AB, Tissue DT, Choat B, Atkin OK, Barton CVM (2018) Trees tolerate an extreme heatwave via sustained transpirational cooling and increased leaf thermal tolerance. Global Change Biology 24(6), 2390–2402. https://doi.org/10.1111/gcb.14037

Farquhar GD, Sharkey TD (1982) Stomatal conductance and photosynthesis. Annual Review of Plant Physiology 33, 317–345. https://doi.org/10.1146/annurev.pp.33.060182.001533

Fauset S, Freitas HC, Galbraith DR, Sullivan MJP, Aidar MPM, Joly C.A, … Gloor MU (2018) Differences in leaf thermoregulation and water use strategies between three co-occurring Atlantic forest tree species: Leaf energy balance of Atlantic forest trees. Plant, Cell and Environment 41, 1618–1631. https://doi.org/10.1111/pce.13208

Frank KA, Maroulis SJ, Duong MQ, Kelcey BM (2013) What Would It Take to Change an Inference? Using Rubin's Causal Model to Interpret the Robustness of Causal Inferences. Educational Evaluation and Policy Analysis 35(4),437-460. https://doi.org/10.3102/0162373713493129

Franks PJ, Farquhar GD (2007) The mechanical diversity of stomata and its significance in gas-exchange control. Plant Physiology 143(1), 78–87. https://doi.org/10.1104/pp.106.089367

Franks PJ, Farquhar GD (2001) The effect of exogenous abscisic acid on stomatal development, stomatal mechanics, and leaf gas exchange in *Tradescantia virginiana*. Plant Physiology 125(2), 935–942. https://doi.org/10.1104/pp.125.2.935

Freschet GT, Cornelissen JHC, van Logtestijn RSP, Aerts R (2010) Evidence of the 'plant economics spectrum' in a subarctic flora. Journal of Ecology 98(2), 362–373. https://doi.org/10.1111/j.1365-2745. 2009.01615.x

Galmés J, Hermida-Carrera C, Laanisto L, Niinemets Ü (2016) A compendium of temperature responses of Rubisco kinetic traits: variability among and within photosynthetic groups and impacts on photosynthesis modeling. J Exp Bot 67, 5067–5091. https://doi.org/10.1093/jxb/erw267

Garfin G, Jardine A, Merideth R, Black M, LeRoy S (Eds.) (2013) Assessment of Climate Change in the Southwest United States. Natl Clim Assess Reg Tech Input Rep Ser Assess 531. https://doi.org/10.5822/978-1-61091-484-0

Gielen B, Liberloo M, Bogaert J, Calfapietra C, DeAngelis P, Miglietta F, Scarascia-Mugnozza G, Ceulemans R (2003) Three years of free-air CO2 enrichment (POPFACE) only slightly affect profiles of light and leaf characteristics in closed canopies of *Populus*. Global Change Biology 9, 1022–1037. https://doi.org/10.1046/j.1365-2486.2003.00644.x

Gleason SM, Butler DW, Waryszak P (2013) Shifts in leaf and stem hydraulic traits across aridity gradients in eastern Australia. International Journal of Plant Sciences 174, 1292–130. https://doi.org/10.1086/673239

Grady KC, Ferrier SM, Kolb TE, Hart SC, Allan GJ, Whitham TG (2011) Genetic variation in productivity of foundation riparian species at the edge of their distribution: implications for restoration and assisted migration in a warming climate. Global Change Biology 17, 3724–3735. https://doi.org/10.1111/j.1365-2486.2011.02524.x

Granier A (1987) Evaluation of transpiration in a Douglas-fir stand by means of sap flow measurements. Tree Physiology 4, 309–320. https://doi.org/10.1093/treephys/3.4.309

Griffin KL, Tissue DT, Turnbull MH, Schuster W, Whitehead D (2001) Leaf dark respiration as a function of canopy position in Nothofagus fusca trees grown at ambient and elevated CO_2 partial pressures for five years. Functional Ecology 15, 497– 505. https://doi.org/10.1046/j.0269-8463.2001.00539.x

Grossiord C, Buckley TN, Cernusak LA, Novick KA, Poulter B, Siegwolf RTW, Sperry JS, McDowell NG (2020) Plant responses to rising vapor pressure deficit. New Phytol 226, 1550-1566. https://doi.org/10.1111/nph.16485

Gutschick VP 2016 Leaf energy balance: basics and modeling from leaves to canopies. Dordrecht: Springer Netherlands, 23–58. https://doi.org/10.1007/978-94-017-7291-4_2

Hazel JR (1995) Thermal Adaptation in Biological Membranes: Is Homeoviscous Adaptation the Explanation? Annual Review of Physiology 57, 19–42. https://doi.org/10.1146/annurev.ph.57.030195.000315

Helliker BR, Richter SL (2008) Subtropical to boreal convergence of tree-leaf temperatures. Nature 454, 511–514. https://doi.org/10.1038/nature07031

Hetherington AM, Woodward FI (2003) The role of stomata in sensing and driving environmental change. Nature 424, 901–908. https://doi.org/10.1038/nature01843

Hilu KW, Randall JL (1984) Convenient method for studying grass leaf epidermis. Taxon, 33(3), 413. https://doi.org/10.2307/1220980

Hultine KR, Allan GJ, Blasini D, Bothwell HM, Cadmus A, Cooper HF, … Whitham TG (2020) Adaptive capacity in the foundation tree species *Populus fremontii*: implications for resilience to climate change and non-native species invasion in the American Southwest. Conservation Physiology 8(1), coaa061. https://doi.org/10.1093/conphys/coaa061

Hultine KR, Burtch KG, Ehleringer JR (2013) Gender specific patterns of carbon uptake and water use in a dominant riparian tree species exposed to a warming climate. Global Change Biology 19, 3390–3405. https://doi.org/10.1111/gcb.12230

Hultine KR, Froend R, Blasini D, Bush SE, Karlinski M, Koepke DF (2019) Hydraulic traits that buffer deep-rooted plants from changes in hydrology and climate. Hydrological Processes 34(2), 209–222. https://doi.org/10.1002/hyp.13587

Hüve K, Bichelea I, Ivanovab H, Keerbergb O, Parnik T, Rasulova B, Tobias M, Niinemets U (2011) Temperature responses of dark respiration in relation to leaf sugar concentration. Physiologia Plantarum 144(4), 320–34. https://doi.org/10.1111/j.1399-3054.2011.01562.x

Ikeda DH, Max TL, Allan GJ, Lau MK, Shuster SM, Whitham TG (2017) Genetically informed ecological niche models improve climate change predictions. Global Change Biology 23, 164–176. https://doi.org/10.1111/gcb.13470

Jones HG (2014) Plants and Microclimate: A Quantitative Approach to Environmental Plant Physiᵒˡogy, 3rd ed. Cambridge University Press, Cambridge.

Kassambara A, Mundt F (2017) factoextra: Extract and visualize the results of multivariate data analyses. R package version 1.0.5. https://CRAN.Rproject.org/package=factoextra.

Knight CA, Ackerly DD (2003) Evolution and plasticity of photosynthetic thermal tolerance, specific leaf area and leaf size: congeneric species from desert and coastal environments. New Phytologist 160, 337–347. https://doi.org/10.1046/j.1469-8137.2003.00880.x

Kozaki A, Takeba G (1996) Photorespiration protects C3 plants from photooxidation. Nature. 384(6609), 557–560. https://doi.org/10.1038/384557a0

Kuznetsova A, Brockhoff PB, Christensen RHB (2017) lmerTest package: Tests in linear mixed effects models. Journal of Statistical Software, 82(13), 1–26. https://doi.org/10.18637/jss.v082.i13

Lambers H, Chapin FS, Pons TL (2008) Plant Physiological Ecology. Springer New York, NY. https://doi.org/10.1007/978-0-387-78341-3

Lambs L, Muller E (2002) Sap flow and water transfer in the Garonne River riparian woodland, France: First results on poplar and willow. Annals of Forest Science 59, 301–305. https://doi.org/10.1051/forest:2002026

Landsberg J, Waring R, Ryan M (2017) Water relations in tree physiology: where to from here? Tree Physiology 37(1), 18–32, https://doi.org/10.1093/treephys/tpw102

Lê S, Josse J, Husson F (2008) FactoMineR: An R package for multivariate analysis. Journal of Statistical Software 25, 1–18. https://doi.org/10.18637/jss.v025.i01

Leigh A, Sevanto S, Close JD, Nicotra AB (2017) The influence of leaf size and shape on leaf thermal dynamics: does theory hold up under natural conditions? Plant, Cell and Environment 40, 237–248. https://doi.org/10.1111/pce.12857

Lloyd J, Farquhar GD (2008) Effects of rising temperatures and [CO_2] on the physiology of tropical forest trees. Phil. Trans. R. Soc. B. 363, 1811–1817. https://doi.org/10.1098/rstb.2007.0032

Martin P (1989) The significance of radiative coupling between vegetation and the atmosphere. Agricultural and Forest Meteorology 49, 45–53. https://doi.org/10.1016/0168-1923(89)90061-0

Martin TA, Hinckley TM, Meinzer FC, Sprugel DG (1999) Boundary layer conductance, leaf temperature and transpiration of *Abies amabilis* branches. Tree Physiology 19, 435–443. https://doi.org/10.1093/treephys/19.7.435

Michaletz ST, Weiser MD, McDowell NG, Zhou J, Kaspari M, Helliker BR, Enquist BJ (2016) The energetic and carbon economic origins of leaf thermoregulation. Nature Plants 2, 16129. https://doi.org/10.1038/nplants.2016.129

Michaletz ST, Weiser MD, Zhou J, Kaspari M, Helliker BR, Enquist BJ (2015) Plant Thermoregulation: Energetics, Trait-Environment Interactions, and Carbon Economics. Trends in Ecology and Evolution 30, 714–724. https://doi.org/10.1016/j.tree.2015.09.006

Monteith J, Unsworth M (2013) Principles of Environmental Physics, Fourth Edition: Plants, Animals, and the Atmosphere. Elsevier, 400.

Muir CD (2019) Tealeaves: an R package for modelling leaf temperature using energy budgets. AoB Plants 11, 1–10. https://doi.org/10.1093/aobpla/plz054

Oren R, Sperry JS, Katul G, Pataki DE, Ewers BE, Phillips N, Schafer KVR (1999) Survey and synthesis of intra- and interspecific variation in stomatal sensitivity to vapour pressure deficit. Plant, Cell and Environment 22, 1515–1526. https://doi.org/10.1046/j.1365-3040.1999.00513.x

Okajima Y Taneda H Noguchi K Terashima I (2012) Optimum leaf size predicted by a novel leaf energy balance model incorporating dependencies of photosynthesis on light and temperature. Ecological Research 27, 333–346. https://doi.org/10.1007/s11284-011-0905-5

Osmond CB, Björkman O (1972) Simultaneous measurements of oxygen effects on net photosynthesis and glycolate metabolism in C3 and C4 species of *Atriplex*. Carnegie Inst Wash 71, 141'148.

O'Sullivan OS, Heskel MA, Reich PB, Tjoelker MG, Weerasinghe LK, Penillard A, Zhu L, Egerton JJG, Bloomfield KJ, Creek D, Bahar NHA, Griffin KL, Hurry V, Meir P, Turnbull MH, Atkin OK (2017) Thermal limits of leaf metabolism across biomes. Global Change Biology 23(1), 209–223. https://doi.org/10.1111/gcb.13477

O'Sullivan OS, Weerasinghe KK, Evans JR, Egerton JJ, Tjoelker MG, Atkin OK (2013) High-resolution temperature responses of leaf respiration in snow gum (*Eucalyptus pauciflora*) reveal high-temperature limits to respiratory function. Plant Cell and Environment 36, 1268–1284. https://doi.org/10.1111/pce.12057

Radin JW, Lu Z, Percy RG, Zeiger E (1994) Genetic variability for stomatal conductance in Pima cotton and its relation to improvements of heat adaptation. Proceedings of the National Academy of Sciences 91, 7217–7221. https://doi.org/10.1073/pnas.91.15.7217

Reich PB (2014) The world-wide 'fast–slow' plant economics spectrum: A traits manifesto. Journal of Ecology, 102(2), 275–301. https://doi.org/10.1111/1365-2745.12211

Scholander PF, Bradstreet ED, Hemmingsen EA, Hammel HT (1965) Sap pressure in vascular plants: Negative hydrostatic pressure can be measured in plants. Science 148(3668), 339–346. https://doi.org/10.1126/science.148.3668.339

Seager R, Goddard L, Nakamura J, Henderson N, Lee DE (2014) Dynamical Causes of the 2010/11 Texas–Northern Mexico Drought. Journal of Hydrometeorology 15, 39–68. https://doi.org/10.1175/JHM-D-13-024.1

Slot M, Winter K (2016) The effects of rising temperature on the ecophysiology of tropical forest trees. In: Santiago LS, Goldstein G (eds.)Tropical tree physiology. Switzerland: Springer International Publishing, 385–412. https://doi.org/10.1007/978-3-319-27422-5_18

Sperry JS, Hacke UG, Oren R, and Comstock JP (2002) Water deficits and hydraulic limits to leaf water supply. Plant, Cell and Environment 25, 251-263. https://doi.org/10.1046/j.0016-8025.2001.00799.x

Teskey R, Wertin T, Bauweraerts I, Ameye M, Mcguire MA, Steppe K (2015) Responses of tree species to heat waves and extreme heat events: Tree response to extreme heat. Plant, Cell and Environment 38, 1699–1712. https://doi.org/10.1111/pce.12417

Tjoelker M, Olesksyn J, Reich P (2001) Modelling respiration of vegetation: Evidence \
for a general temperature-dependent Q10. Global Change Biology,7(2), 223–230.
https://doi.org/10.1046/j.1365-2486.2001.00397.x.

Togashi HF, Prentice IC, Evans BJ, Forrester DI, Drake P, Feikema P, Brooksbank K,
Eamus D, Taylor D (2015) Morphological and moisture availability controls of
the leaf area-to-sapwood area ratio: analysis of measurements on Australian trees.
Ecology and Evolution, 5(6), 1263–1270. https://doi.org/10.1002/ece3.1344

Turner NC (1988) Measurement of plant water status by the pressure chamber technique.
Irrig Sci 9(4), 289-308. https://doi.org/10.1007/BF00296704

Upchurch DR, Mahan JR (1988) Maintenance of constant leaf temperature by plants—II.
Experimental observations in cotton. Environmental and Experimental Botany 28,
359–366. https://doi.org/10.1016/0098-8472(88)90060-3

Urban J, Ingwers M, McGuire MA, Teskey RO (2017) Stomatal conductance increases
with rising temperature. Plant Signaling & Behavior 12, 1–3.
https://doi.org/10.1080/15592324.2017.1356534

von Caemmerer S, Quick WP (2000) Rubisco: physiology in vivo. In: Leegood RC,
Sharkey TD, von Caemmerer S, eds. Photosynthesis: physiology and metabolism.
Dordrecht: Kluwer Academic Publishers, 85–113.

Wahid A, Gelani S, Ashraf M, Foolad MR (2007) Heat tolerance in plants: an overview.
Environ. Exp. Bot. 61, 199–223. https://doi.org/10.1016/j.envexpbot.2007.05.011

Watson D.J. (1947). Comparative Physiological Studies on the Growth of Field Crops.
Annals of Botany 11(41), 41–76. http://www.jstor.org/stable/42907002

Whitham TG, Gehring CA, Bothwell HM, Cooper HF, Hull JB, Allan GJ, Grady KC,
Markovchick L, Shuster SM, Parker J, Cadmus AE, Ikeda DH, Bangert RK,
Hultine KR, Blasini DE (2020). Using the Southwest Experimental Garden Array
to enhance riparian restoration in response to global change: identifying and
deploying genotypes and populations for current and future environments. In
Riparian Research and Management: Past, Present, Future, Vol. 2, ed. SW
Carothers, RR Johnson, DM Finch, KJ Kingsley, RH Hamre, pp. 63–79. Gen.
Tech. Rep. RMRS-GTR-411. Fort Collins, CO: U.S. Dep. Agric. For. Serv.
Rocky Mt. Res. Stn.

Wright I, Dong N, Maire V, Prentice C, Westoby M, Diaz S, … Wilf P (2017) Global
Climatic Drivers of Leaf Size. *Plant Ecology* 357(6354), 917–920.
https://doi.org/10.1126/science.aal4760

Wright IJ, Westoby M (2002) Leaves at low versus high rainfall: Coordination of structure, lifespan and physiology. New Phytologist 155(3), 403–416. https://doi.org/10.1046/j.1469-8137.2002.00479.x

Yamori W, Suzuki K, Noguchi K, Nakai M, Terashima I (2006) Effects of Rubisco kinetics and Rubisco activation state on the temperature dependence of the photosynthetic rate in spinach leaves from contrasting growth temperatures. Plant, Cell and Environment 29, 1659–1670. https://doi.org/10.1111/j.1365-3040.2006.01550.x

Yordanov I (1992) Response of photosynthetic apparatus to temperature stress and molecular mechanisms of its adaptations. Photosynthetica. 26(4), 517-531.

4. RADIAL GROWTH DECREASES WITH ENHANCED HEAT STRESS WHILE CANOPY STOMATAL CONDUCTANCE, INFERRED FROM δ^{13}C AND δ^{18}O OF TREE-RING CELLULOSE, DOES NOT IN A WARM-DESERT RIPARIAN TREE SPECIES (*POPULUS FREMONTII*)

Abstract

Global climate change and its effect on local environmental conditions are expected to have a profound impact on the performance and survivorship of local-adapted tree species worldwide. Riparian trees species in arid lands can be especially vulnerable to be adversely affected by climate change. Tree-ring isotopic variations have been commonly used to study physiological responses of trees to changes in environmental conditions across multiple ecosystems. Thus, understanding how tree growth and physiology simultaneously respond to environmental changes will be critical to estimate climate change may impact a foundational tree species, *Populus fremontii*. I studied radial growth patterns, δ^{13}C in tree-ring holocellulose, and δ^{18}O in tree-ring α-cellulose in 38 eight-year-old *P. fremontii* genotypes occurring in a flood-irrigated common garden located at the hot edge of this species' thermal distribution. I hypothesized that (1) genotypes sourced from locations with the highest mean annual maximum temperature (MAMT) transfer distance (defined as the MAMT of the common garden subtracted from the MAMT of the genotypic source location),would exhibit the lowest mean annual increment growth (MAIG), and (2) δ^{13}C and δ^{18}O would increase with transfer distance, reflecting a lower mean annual canopy stomatal conductance at a higher transfer distance. It was found that MAIG decreased 20% with increasing provenances' MAMT. Conversely, MAIG was not directly correlated with either tree-ring δ^{13}C or δ^{18}O,

indicating that mean annual radial growth was not well coupled to mean annual canopy stomatal conductance. Results indicate that climate warming will reduce tree productivity regardless of impacts on canopy gas exchange.

Introduction

Tree species display a high degree of climate adaptation from the cellular level to whole organs (Howe et al. 2003; Savolainen et al. 2007; Aitken et al. 2008). However, because of the multiple effects of climate change on environmental conditions worldwide, tree populations adapted to local environmental conditions will likely become maladapted to their future native environments, increasing forest mortality, and decreasing forest carbon sequestration (Allen et al. 2010; Whitham et al. 2020). Tree-rings record the effect of climate change on plant performance over extended period of times (Gessler et al. 2014). For instance, the width of individual growth rings can reveal how changing environmental conditions influenced tree growth and mortality (Schweingruber 1997; Briffa et al. 2002; Gessler et al. 2009; Cailleret et al. 2017). Additionally, stable isotopes in tree-rings have been widely used to study tree physiological responses to local environmental conditions and reconstructing local and regional climate variables (McCarroll and Loader 2004; Roden and Siegwolf 2012; Johnstone et al. 2013). This technique is based on the isotopic composition changes that carbon, hydrogen and oxygen molecules undergo once they are fixed as cellulose in trees' annual rings (McCarroll and Loader 2004). This change in isotopic composition from the environment to internal plant structures is influenced by the tree's physiological responses to changes in environmental conditions (Francey and Farquhar 1982; Waterhouse et al, 2000; Roden 2005).

Plant carbon isotopic variations in holocellulose is a function of fractionation against ^{13}C as CO_2 diffuses through the stomata, and fractionation against ^{13}C by

RuBisCO during carbon fixation (McCarroll and Loader 2004; Roden 2005).

Specifically, compared to the isotopic composition of atmospheric CO_2, ^{13}C inside the leaves is initially reduced because the lighter carbon isotope, ^{12}C, diffuses through stomata at higher rates than the heavier ^{13}C molecules (Francey and Farquhar 1982; Ehleringer and Cerling 1995). The heavier ^{13}C experiences a second and much larger fractionation (~29‰) in C3 plants due to the preference of the primary photosynthetic enzyme RuBisCO to carboxylate ^{12}C (Farquhar et al. (1982, 1989); Francey and Farquhar 1982). In C3 plants, the isotopic composition, $\delta^{13}C$, of the photosynthate approximates:

$$\delta^{13}C_p = \delta^{13}C_a - a - (b - a)\ c_i/c_a \tag{1}$$

Where $\delta^{13}C_p$ is the fractional difference between $^{13}C/^{12}C$ in air surrounding the leaf while c_i and c_a are the CO_2 concentrations in the leaf intercellular spaces and atmosphere, respectively. The constant a represents the first fractionation of $^{13}CO_2$ in air (4.4‰) and b represents the second fractionation by Rubisco (29‰) (Farquhar et al. (1982, 1989); Francey and Farquhar 1982).

Therefore, the final carbon isotopic composition of tree-rings records the balance between the supply of CO_2 via stomata and the demand for CO_2 by RuBisCO (McCarroll and Loader 2004). Under hot and dry conditions, a reduction of stomatal conductance would be expected to limit water loss. This lower stomatal conductance would reduce the supply of CO_2 to the leaf, decreasing c_i/c_a and increasing $\delta^{13}C_p$ (Farquhar et al. 1989). Thus, stomatal conductance-derived isotopic signals are stronger in water limiting conditions while under optimal moisture conditions the photosynthetic rate-derived isotopic imprint is amplified (McCarroll and Loader 2004). Consequently, carbon isotope

composition will be strongly correlated with stomatal conductance in arid and semi-arid regions (Warren et al. 2001; Leavitt et al. 2011).

The original isotopic signature of oxygen fixed by trees comes from the isotopic composition of water taken up by the roots. Temperature is considered one of the main controlling factors of $\delta^{18}O$ composition of source water because its influence in the isotopic ratio of precipitation and soil moisture (Helliker and Richter 2008; McCarroll and Loader 2004; Siegwolf et al. 2022). However, the final oxygen isotopic composition in tree ring α-holocellulose is more likely to be influenced by biochemical processes that take place during tissue formation (McCarroll and Loader 2004, Gessler et al. 2014). For instance, evaporative $\delta^{18}O$ enrichment occurs when the heavier isotope, ^{18}O, diffuses out of the leaves at a slower rate than the lighter, ^{16}O, when water is transpired from the leaf surface (Farquhar and Lloyd 1993). Even though this enrichment can be regulated by the amount of ^{18}O present in the atmosphere (Roden and Ehleringer 2000), transpiration rates have been found to persistently increase the ratio of heavier isotope ^{18}O relative to ^{16}O in leaf water (McCarroll and Loader 2004). Additionally, it has been found that leaf to air vapour pressure deficit, controlled by air humidity, leaf morphology and boundary layer characteristics, display a strong influence on evaporative enrichment in the leaf (Buhay et al. 1996; McCarroll and Loader 2004). Thus, $\delta^{18}O$ enriched isotopic signal is integrated in the leaves original photosynthetic products (Roden and Ehleringer 2000).

Although biochemical fractionation of sucrose and the exchange of oxygen between leaf and xylem water during ring formation can modify the isotopic signature of enriched leaf water $\delta^{18}O$, a mechanistic model was developed that quantifies the biochemical oxygen fractionation during tree-ring cellulose formation (Roden and

Ehleringer 2000; Gessler et al. 2014; Szejner et al. 2016). This model is based on two principles, first, that oxygen in CO_2 is completely exchanged with water before fixation, yielding a 27‰ enrichment of $\delta^{18}O$ in the leaf cellulose as a product of the carbonyl–water interaction during biosynthesis (Sternberg et al. 1984), and second, that the amount of oxygen exchange with xylem water during the sucrose-cellulose conversion is constant irrespective of species or environmental conditions (Yakir and DeNiro 1990; Roden et al. 2000; Siegwolf et al. 2022). Thus, oxygen tree-ring cellulose isotopic composition is commonly used to reconstruct long-term relative humidity, mean annual temperature, VPD and tree transpiration rates, which is regulated by stomatal conductance (Barbour et al. 2000; Roden and Ehleringer 2000; McCarroll and Loader 2004; Szejner et al. 2016).

In this investigation, I used radial growth, $\delta^{13}C$ in tree-ring holocellulose and $\delta^{18}O$ in tree-ring α-cellulose to evaluate the inter-annual physiological responses of obligate riparian phreatophytic tree species, *Populus fremontii*, to long-term exposure to extreme hot temperatures. Through its geographic range, *P. fremontii* populations are exposed to climatic extremes that ranges between subfreezing and extreme hot temperatures. This extreme variation in climatic adaptation at the population level explains the great degree of interspecific variation in productivity (Grady et al. 2011, 2013), phenology (Cooper et al. 2022), functional trait coordination (Blasini et al. 2020), and stomatal conductance and leaf thermoregulation (Blasini et al. 2022) in relation to mean maximum summer temperature (MMST). Because of the projected impact that climate change will have on water and plant carbon interactions in the arid Southwest (Garfin et al. 2013), it is crucial to understand the possible long-term effect that warmer temperatures will have on this species' growth and overall physiological performance at an intraspecific level. The

current pace of climate change in this region has the potential to exacerbate maladaptation of locally adapted tree populations by the middle of this century (Wang et al. 2009).

Thus, I used a common garden located at the hot edge of this species thermal distribution to measure radial growth, $\delta^{13}C$ in tree-ring holocellulose and $\delta^{18}O$ in tree-ring α-cellulose in 14 *Populus fremontii* populations sourced across an elevation gradient spanning from 49 to 1268 m. elevation. In this flood-irrigated garden, this investigation simultaneously assessed the long-term effect that extreme temperatures and VPD have on stomatal conductance and growth rates at an intraspecific level. While intraspecific inter-annual growth and the relationship between radial growth and plant water status were assessed with $\delta^{13}C$ measurements in tree-ring holocellulose, $\delta^{18}O$ in tree-ring α-cellulose was used to estimate population-specific physiological adjustments in stomatal conductance. Riparian tree species are restricted to places with reliable water availability. Therefore, in the case of these species, atmospheric conditions such as VPD, and irradiance are the main factors influencing stomatal conductance and whole-tree water use (Kannenberg et al. 2021; Kannenberg et al. 2022). Thus, increases in temperature and VPD have been found to correlate with significant reductions in stomatal conductance and consequently photosynthetic and growth rates across a broad selection of plants species (Lambers et al.2008).

In this garden, Grady et al. (2011, 2013) found populations sourced from places with similar mean annual maximum air temperature (MAMT) to that of the garden displayed higher growth rates than populations adapted to cooler temperatures during their seedling stage. Therefore, in this present investigation, it is hypothesized that (1)

135

populations adapted to similar extreme thermal conditions such as those experienced in

the common garden continue to display higher growth rates than populations from cooler

temperatures. (2) populations from warmer provenances will exhibit lower abundances of

$\delta^{13}C$ and $\delta^{18}O$ which will be indicative of higher stomatal conductance and transpiration.

(3) interannual measurements of growth and tree-ring $\delta^{13}C$ and $\delta^{18}O$ across all genotypes

should reflect the annual variations in MAMT and VPD. Results from this study help

elucidate potential climate change-related reductions in tree productivity and gas

exchange in *P. fremontii*.

Methods

Study site

The experimental common garden is located at the Palo Verde Ecological Reserve

(PVER; Fig. 4.1). The garden was established in March 2007 on what was prior part of

the Palo Verde dam construction floodplain of the lower Colorado River (approximately

5 km from Blythe, California N 33.71391, W-114.49600, elevation 87 m). This

floodplain was used to grow cotton (*Gossypium hirsutum*) and alfalfa (*Medicago sativa*)

before the establishment of the garden. Soils at the garden were composed chiefly of

coarse-loamy, mixed, super active, calcareous, hyperthermic Typic Torrifluvents (USDA

NRCS, 2010).

This common garden consisted of propagated plantings from 16 provenances of

P. fremontii encompassing the geographic range of what was previously defined as the

Sonoran Desert ecotype of *P. fremontii* (Ikeda et al. 2017). All cuttings were collected

randomly from within 10 m of rivers in Arizona and California (Fig. 4.1). To avoid using

clones within each population, initial identification of genotypes was based on spatial discreteness and all cuttings were collected randomly from trees at least 10 m apart. Cuttings were grown in Tinus root-trainers filled with sterilized soil media (equal parts of peat moss, perlite, and vermiculite) in the Northern Arizona University greenhouse (Flagstaff, Arizona) at ambient air temperature to maintain bud dormancy. Soils were radiantly heated to 22 °C to promote root initiation and development. In March 2007, all cuttings were transplanted randomly across 66 blocks ($16 \times 9 \times 16$ rows at 2 m spacing per block). Until 2017, the garden was flood irrigated every two weeks during the summer with approximately 300 L m^{-2} (c. 1 acre-foot) of reclaimed water from the city of Blythe (K. Grady, personal communication, 2017).

Population climate

From the original 16 populations established in the garden, I studied 14 populations with a total of 38 genotypes (1-3 genotypes per population). The mean annual maximum daily temperature (MAMT) of the source locations of the 14 populations included in this investigation ranged from 24.39 to 30.94 °C which approximates 50% of the total MAMT temperature range of *P. fremontii* (Fig. 4.1). The elevation of the provenance sites ranged from 58 to 1277 meters above sea-level, mean annual temperature (MAT) ranged from 16.08 to 21.97 °C, and mean annual precipitation (MAP) from 9.4 to 45.97 cm (Table 4.1). For this study, I focused on population mean annual maximum air temperature (MAMT) transfer distance (MAMT of the common garden minus MAMT of the population source site), as this was found to have a strong correlation with above-ground net primary productivity (ANPP; Grady et al. 2011). Provenance climatic data were compiled for years 1987–2002 from weather stations

137

affiliated with the Western Regional Climate Center (WRCC, 2010) located within a 10 km radius and 80 m of election from provenance. For the two provenance sites (elevation 616 and 1277 m) that did not have weather stations affiliated with the Western Regional Climate Center and the PVER common garden site, I used modeled climate estimates from PRISM data. Copyright © <2022>, PRISM Climate Group, Oregon State University, http://prism.oregonstate.edu.

Field sampling

A 12 mm diameter increment borer was used in the spring of 2015 to collect cores from 38 trees samples representing 14 populations at the PVER common garden near Blythe, CA. Because the amount of material recovered from 12 mm diameter increment borers exceed the adequate quantities of wood needed for stable isotope analyses, one individual sample per tree was collected. Individual cores were held in clamps to discern ring boundaries and ring width. To enhance boundary distinction, cores were resurfaced at slight angles. Crossdating, the assignment of dates to rings, length measurements and subsequent individual tree-rings excision from the cores was respectively done with a dissecting microscope, a high Precision film micrometer ruler and a scalpel at the Desert Botanical Garden in Phoenix, Arizona.

From each of the 38 cores, the four most recent years of growth (2011-2014) were excised and collected to conduct the isotopic analysis (152 tree-rings). Protocols from Sternberg (1989), Leavitt and Danzer (1993), and Leuenberger et al. (1998) were followed to extract holocellulose and α-cellulose from individual tree-rings at the Southern Oregon University Stable Isotope Facility (SOUSIF). Accordingly, year-specific tree-ring portions of each tree were ground in a mill to 20 mesh (0.84 mm), then,

the ground tissues were placed in extraction permeable bags produced from a polymer

fabric. Waxes, oils and resins were extracted in a soxhlet apparatus, and the samples were

boiled to remove hydrophilic compounds, and bleached to remove inorganic salts and

low molecular weight polysaccharides (including gums and starches). Further extraction

to α-cellulose included the removal of holocellulose by extra soaking in NaOH solution

and then in acetic acid. To homogenize α-cellulose samples, fibers were separated using a

Hielscher UP200S ultrasonic probe for sonicating the material in 1 mL of chilled

deionized water with 30 s of ultrasound (Laumer et al. 2009).

The ratios of $^{13}C/^{12}C$ were obtained from the CO_2 resulted from the combustion of

0.3 mg of α -cellulose loaded into tin capsules in an elemental analyzer (Elementar vario

PYRO cube) coupled to an IsoPrime 100 isotope ratio mass spectrometer. From the 38

original cores (152 ring samples), only 36 cores (144 rings) provided successful $\delta\,^{13}C$

measurements. Typical overall precision was ±0.07‰ for $\delta\,^{13}C$ values. For $\delta^{18}O$

measurements, 0.3 mg samples of α-cellulose were loaded into silver capsules and

converted to CO by pyrolysis (Saurer et al. 1998) in a hot (1400 °C) alumina glassy

carbon reactor (Thermo-Finnigan TC/EA) and separated from other gases in a 0.6-m

molecular sieve 5A gas chromatography (GC) column connected to a IsoPrime 100

isotope ratio mass spectrometer. Only 34 original cores (136 rings) of the 38 original

cores (152 ring samples) provided successful $\delta^{18}O$ measurements. Typical overall

precision was ±0.20‰ for $d^{18}O$ values. Isotopic values were expressed in the delta (δ)

notation relative to the ^{13}C composition of Vienna Peedee Belemnite Standard and ^{18}O of

Vienna SMOW (Szejner et al. 2016). The mass spectrometers used in this investigation

were located at the Southern Oregon University Stable Isotope Facility (SOUSIF).

Growth Measurements

In 2015, diameter at breast height (DBH) were measured for each of the trees cored with a diameter field tape. DBH measurements were converted to basal area (BA) of the current year following the formula for the area of a circle. Lengths of each of the four outer-most tree-rings in each tree core were subtracted from its corresponding DBH to determine previous four years DBH and BA. The differences between each of the four outer-most trees-rings were used to calculate the mean annual growth (MAG, cm/year) between 2011 and 2014. The difference between the BA derived from the subtraction of the measured DBH and the four outer-most trees-rings were used to calculate and mean annual increment growth (MAIG, cm^2/year)

Statistics

R version 4.0.2 was used (R Core Team, 2020) to run all statistical analyses in this study. Assumptions of normality and homogeneity of variance were tested with Shapiro and Barlett test prior analyzing the data. Not normal and heteroscedastic data were normalized by log10, square root or box-cox transformations. Genotype growth and isotopic data were analyzed using simple linear regressions with MAMT transfer distance as the predictor and growth, δ^{13}C and δ^{18}O as response variables. Additionally, I used multiple linear regressions to assess the simultaneous effect of MAMT transfer distance, δ^{13}C and δ^{18}O on MAIG. I also used the Akaike information criterion (AIC) and analysis of variance (ANOVA) test to find the association of predictors (MAMT transfer distance, δ^{13}C and δ^{18}O) with stronger influence on MAIG.

To explore the multivariate relationships between growth, δ^{13}C and δ^{18}O, I used 'FactoMineR' package (Kassambara and Mundt 2017; Lê et al. 2008) to conduct a

principal component analysis (PCA) with these variables. Significant PCA axes were determined using the Broken Stick Model in the 'vegan' and 'biodiversity' R package (Oksanen et al. 2019; Kindt and Coe 2005). Then, I used a single regression analysis to evaluate the relationships between the significant principal components resulted from the PCA and MAMT transfer distance.

To identify how the climate in the garden could have influenced the variation in tree-ring MAIG, $\delta^{13}C$, and $\delta^{18}O$, I calculated Pearson's correlation coefficients (r) between the interannual differences in MAIG, $\delta^{13}C$, and $\delta^{18}O$ and annual meteorological data in the garden (mean annual maximum temperature and vapor pressure deficit). To corroborate the correlations between climate variables of the garden, MAIG, $\delta^{13}C$ and $\delta^{18}O$, I used multiple regression analyses.

I conducted three individual mixed-effects repeated measures ANOVA (type III with Satterthwaite's method) using the 'lmer' R package (Bates et al. 2015; Kuznetsova et al. 2017) to determine the effect that different years might have on each of the variables studied in this investigation (MAIG, $\delta^{13}C$, and $\delta^{18}O$). Thus, these analyses were used to indirectly analyze temporal changes in MAIG, $\delta^{13}C$, and $\delta^{18}O$ as a function of inter-annual changes in mean annual maximum temperature and vapor pressure deficit in the garden. In these analyses, MAIG, $\delta^{13}C$, and $\delta^{18}O$ were treated as the response variable in each analysis while source populations and years were treated as categorical fixed effects with fourteen and four levels, respectively. Individual genotype was incorporated as a random effect.

Results

Growth (MAIG)

Consistent with my hypothesis, populations with lower MAMT transfer distances displayed higher radial growth. I found a significant relationship between population tree-ring-derived mean annual growth (MAG) and MAMT transfer distances ($F_{1,36} = 10.37$, $r^2 = 0.20$, $P < 0.01$; Fig. 4.2a). Similarly, source population MAMT were significantly correlated to basal area-derived mean annual increase growth (MAIG) ($F_{1,36} = 17.99$, $r^2 = 0.31$, $P < 0.001$; Fig. 4.2b). These two results suggest that intraspecific differences in growth rates in the common garden were influenced by the differences in source temperature of populations' source sites (Table 4.1).

Tree ring isotopes

Although MAIG displayed significant relationships with MAMT transfer distances, I did not find the same significant relationships between tree ring isotopes composition and MAMT transfer distances. In particular, the relationship between $\delta^{13}C$ and population MAMT transfer distance was not significant ($F_{1,36} = 0.20$, $r^2 = -0.02$, $P > 0.05$; Fig. 4.3a). Similarly, I did not find a significant relationship between $\delta^{18}O$ and MAMT transfer distance ($F_{1,34} = 0.58$, $r^2 = -0.01$, $P > 0.05$; Fig. 4.3b). Additionally, the relationship between $\delta^{13}C$ and $\delta^{18}O$ was not significant ($F_{1,34} = 0.71$, $r^2 = -0.01$, $P > 0.05$; Fig. 4.4).

Relationship between growth, tree ring isotopes and MAMT transfer distance

Area at breast height-derived mean annual increase growth (MAIG) did not show a significant correlation with either $\delta^{13}C$ ($F_{1,36} = 2.23$, $r^2 = 0.03$, $P > 0.05$; Fig. 4.5a) or $\delta^{18}O$ ($F_{1,34} = 0.51$, $r^2 = -0.01$, $P > 0.05$; Fig. 4.5b). Multiple linear models were built with

growth (MAIG) as response variable and different combinations of MAMT transfer distance, $\delta^{13}C$, and $\delta^{18}O$ as predictor variables to examine the impact of these three factors on MAIG. After comparing all linear model combinations with the Akaike information criterion (AIC) and an analysis of variance (ANOVA), it was found that the two models with the lowest AIC scores were significantly different from the other four models (Table 4.2). Thus, MAMT transfer distance and $\delta^{13}C$ displayed the lowest AIC score ($F_{2,33} = 11.71$, $r^2 = 0.38$, $P < 0.001$, AIC = 441.18, Table 4.2) followed by MAMT transfer distance, $\delta^{13}C$, and $\delta^{18}O$ ($F_{3,32} = 7.80$, $r^2 = 0.37$, $P < 0.001$, AIC = 442.73, Table 4.2). Interestingly, these two models displayed lower AIC values than each of the single regression models between MAIG and MAMT transfer distance, $\delta^{13}C$, and $\delta^{18}O$ (Table 4.2).

A principal component analysis (PCA) was used to further explore the relationships between MAIG, $\delta^{13}C$ and $\delta^{18}O$. According to the Broken-Stick Model (Borcard et al. 2011), only the first principal component (PC1) accounting for 42% of the variance significantly explained the variance between MAIG, $\delta^{13}C$ and $\delta^{18}O$. The *dimdesc()* function of the 'FactoMineR' package identified that both MAIG and $\delta^{13}C$ displayed significant relationships with PC1 (Fig. 4.6). MAIG and $\delta^{13}C$ exhibited different directions regarding PC1 which describes an enrichment of ^{13}C in genotypes with lower MAIG values.

Relationship between interannual radial growth, $\delta^{13}C$ and $\delta^{18}O$ isotopes and PVER garden climatic conditions, mean annual maximum temperature (MAMT_PVER) and vapor pressure deficit (VPD_PVER)

Mixed-effects repeated measures ANOVA found a significant effect of year ($F_{3,72}$ =154.37, P < 0.001), MAMT transfer distance ($F_{13,24}$ =2.74, P < 0.05) and the interaction between year and MAMT transfer distance ($F_{39,72}$ = 3.28, P < 0.001) on MAIG. Post hoc comparisons using the Tukey test revealed that MAIG was significantly greater in 2013 than in 2011 (Fig. 4.7a). Tree-ring δ^{13}C exhibited a significant relationship with year only ($F_{3,72}$ =16.36, P < 0.001). The first two years of this study, 2011 and 2012, exhibited more negative δ^{13}C values than 2013 and 2014 ($F_{3,48}$ =6.93, P < 0.001, Fig. 4.7b). Year also displayed a significant relationship with tree-ring δ^{18}O values ($F_{3,69}$ =8.94, P < 0.001). In this case, I found that 2011 and 2014 showed higher (less negative) δ^{18}O values than 2012 and 2013 ($F_{3,48}$ =7.18, P < 0.001, Fig. 4.7c).

Correlation coefficients showed there was a significant positive correlation between interannual differences in MAIG and δ^{13}C (r = 0.323, P < 0.001) (Table 4.3). Also, interannual changes in tree-ring δ^{18}O exhibited significant negative correlations with both MAMT$_{PVER}$ (r = -0.304, P < 0.001) and VPD$_{PVER}$ (r = -0.169, P < 0.05) (Table 4.3, S4.1) between 2011 and 2014. These significant correlations were corroborated using 2 single regression analyses with MAIG and δ^{18}O as the response variables and MAMT transfer distance, δ^{13}C, and MAMT$_{PVER}$ as predictor variables (Table 4.4). Because of the high collinearity between MAMT$_{PVER}$ and VPD$_{PVER}$ values, I only used MAMT$_{PVER}$ in each multiple regression model. MAIG did not display any significant relationships with the climatic variable of the garden. However, like the correlation analysis, δ^{18}O showed a significant relationship with MAMT$_{PVER}$ ($F_{2,141}$ = 4.438, r^2 = 0.01, P < 0.01, Table 4.4).

Discussion

In this investigation, I studied radial growth and tree-ring $\delta^{13}C$ and $\delta^{18}O$ to assess interannual physiological responses of 14 *P. fremontii* populations to extreme temperatures in a common garden located at the warm edge of this species geographic distribution. As expected in my first hypothesis, in this investigation it was found that genotypes adapted to environments with similar temperatures as the common garden display higher growth rates than populations with larger MAMT transfer distances. Contrary to my second hypothesis, I did not find significant correlations between provenance's MAMT transfer distance and tree-ring isotopic measurements ($\delta^{13}C$ and $\delta^{18}O$). However, by combining Pearson's correlation and multivariate analysis, I detected significant relationships between MAIG, tree-ring $\delta^{13}C$, and MAMT transfer distance. Lastly, my third hypothesis predicted that annual climatic variations in the garden, MAMT$_{PVER}$ and VPD$_{PVER}$, would have a significant influence on MAIG, tree-ring $\delta^{13}C$ and $\delta^{18}O$ in all the genotypes present in this study. Although I did not find a significant influence of these climatic variables on MAIG and tree-ring $\delta^{13}C$, this study found a significant negative relationship between tree-ring $\delta^{18}O$ and MAMT$_{PVER}$ and VPD$_{PVER}$.

Radial growth and transfer distance

Growth is one of the most important physiological indicators of environment stress on plants. Corroborating previous results from Grady et al. (2011, 2013), this investigation found that genotypes with the lowest MAMT transfer distances from the PVER garden exhibited higher radial growth than genotypes from cooler provenances. Because of the high diversity of climates found in its geographic range, *P. fremontii* has been the object of multiple common garden-based investigations that have confirmed its

high degree of adaptive specialization to local temperatures at the population level (Blasini et al. 2020, 2022, Cooper et al. 2019, 2022, Hultine et al. 2020, Sankey et al. 2020; Whitham et al. 2020). It is likely that genotypes adapted to cooler temperatures exhibited reductions in growth because of their potential maladaptation to the extreme higher temperatures of the PVER garden. Blasini et al. (2022) found significant differences in *P. freemontii* stomatal conductance and leaf temperature between warm- and cool-adapted populations in a mid-elevation common garden experiment. Thus, it is possible that leaf temperatures in genotypes with higher MAMT transfer distances from this extreme hot common garden reached levels beyond their optimum temperature for photosynthesis. By not properly thermoregulating their leaves in this garden, these genotypes might have experienced significant increases of photorespiration, reduction in net photosynthesis rates and lower subsequent tree growth (Brienen et al. 2015, Yang et al. 2022).

In this garden, Grady et al. (2011, 2013) found populations sourced from places with similar extreme temperatures to that of the garden displayed higher growth rates than populations adapted to cooler temperatures during their seedling stage. Further evidence of the influence of climate adaptation on *P. fremontii* growth can be found on the results from Cooper et al. (2022) where diameter at root crown and whole-tree height measurements were taken in three reciprocal common gardens at low (hot), mid (mild), and upper (cool) elevational points of the species distribution. It was found that the genotypes displaying the greatest growth in each garden were the ones with the smallest temperature transfer distances between their source sites and their respective common gardens. Differences in phenology can offer another potential mechanism

behind the difference in growth rates in this study. In previous similar studies with

P.fremontii, it has been found that colder (high latitude) adapted populations have shorter

growing seasons than warm (lower latitude) adapted populations (Blasini et al. 2020;

Cooper et al. 2022). Although I did not find a significant relationship between latitude of

source populations and MAIG, this could have been caused by the highly uniform

latitudinal representation of the species' distribution in this study.

Tree-ring $\delta^{13}C$ and $\delta^{18}O$

Under well-watered conditions, it was expected that variation in tree ring $\delta^{13}C$

would provide evidence for local adaptation to temperature reflecting higher stomatal

conductance values in warm-adapted genotypes. However, contrary to my hypothesis,

tree-ring $\delta^{13}C$ did not show a significant relationship with MAMT transfer distance. It

was expected that high temperature and high VPD would induce stomatal closure to

reduce water loss in genotypes with higher MAMT transfer distances, resulting in higher

$\delta^{13}C$ abundance in tree ring cellulose in these genotypes. A potential explanation for lack

of a significant relationship between tree-ring $\delta^{13}C$ and MAMT distance could be related

to intraspecific differences in hydraulic architecture (e.g., ratio between whole-tree

sapwood to leaf area or Huber values).

In previous investigations, *P. fremontii* populations sourced from hotter

provenances displayed larger Huber values than populations sourced from cooler

provenances (Blasini et al. 2020, 2022). Additionally, unlike populations from cooler

provenances, hot-adapted populations exhibit leaf turnover during the hottest time of the

summer (Blasini *et al*. unpublished data). These intra-seasonal adjustments of whole-tree

leaf area can result in larger seasonal variation in Huber values. By reducing their whole-

tree leaf areas relative to their sapwood areas, trees can reduce canopy conductance without reducing stomatal conductance per unit leaf area (Carter et al. 2009; MacInnis-Ng et al. 2004; Zeppel and Eamus 2008). If so, patterns of tree-ring $\delta^{13}C$ and $\delta^{18}O$ could decouple from patterns of inter-annual growth.

Other explanations might be found in the fact that tree-ring $\delta^{13}C$ can deviate from expected values derived from leaf-scale models in several ways. For example, it has been reported that in deciduous trees like *P. fremontii*, tree-ring $\delta^{13}C$ values could be altered through the remobilization of stored non-structural carbohydrates (NSCs) during periods of high demand, generally during the spring (Helle and Schleser 2004). In such cases, fractionation processes, independent from photosynthetic gas exchange could influence tissue $\delta^{13}C$ (Gottlicher et al. 2006, Gessler et al. 2009; Gessler et al. 2014). Other studies have investigated the potential effects of refixation of CO_2 by phosphoenolpyruvate carboxylase (Cernusak et al. 2009), mesophyll conductance (Seibt et al. 2008), soil nutrient status (Voelker et al. 2014) and respiratory isotope fractionation (Werner et al. 2011) on tree-ring $\delta^{13}C$ values with mixed results.

Similar to my expectations for $\delta^{13}C$ abundance, I predicted that cool-adapted genotypes would have higher $\delta^{18}O$ abundance as a consequence of reduced stomatal conductance yielding lower leaf water turnover rates and greater subsequent leaf evaporative enrichment compared to warm-adapted genotypes. However, like the $\delta^{13}C$ results, I did not find meaningful differences between genotypes in tree-ring $\delta^{18}O$ or a significant trend with MAMT transfer distance. It is known that source water enrichment, leaf water evaporative fractionation, and the exchange of sugars with water during the transport processes are the main processes controlling tree-ring $\delta^{18}O$ (Gessler et al. 2014;

148

McCarroll and Loader 2004; Yang et al. 2022). Because the source water in the garden is the same across all trees, it was very plausible to expect that any difference in $\delta^{18}O$ would be primarily derived from differences in leaf water evaporative enrichment.

Unlike the results of tree-ring $\delta^{13}C$ where I could identify pronounced differences in variability among populations, I found a very uniform range in $\delta^{18}O$ values across all populations. It has been suspected that oxygen existing in organic compounds and in water can be exchanged during phloem loading and transport (Gessler et al. 2014; Offermann et al. 2011). Consequently, it can be suspected that the isotopic signal generated from the evaporative fractionation in the leaves could have been lost during these processes. It is known that depending on physiological processes linked to storage and remobilization during the mixing of soluble carbohydrates and starch, there might be additional exchanges of oxygen with water (Gessler et al. 2013, Offermann et al. 2011). Thus, oxygen isotope fractionation resulting of leaf water evaporative enrichment and stomatal conductance might be modified once the sugars are mobilized to the phloem.

I was expecting to be able to use *Populus fremontii* tree ring $\delta^{13}C$ and $\delta^{18}O$ data in a mechanistic model that gives insight into the relationship between stomatal conductance and photosynthetic capacity based on these two measurements (Scheidegger et al. 2000, Weigt et al. 2017, Yang et al. 2022). In this model, it is proposed that the information on evaporative enrichment contained in the $\delta^{18}O$ of organic matter can be used to distinguish the possible causes of changes in c_i as derived from $\delta^{13}C$ (Scheidegger et al. 2000). However, I did not find a significant relationship between $\delta^{13}C$ and $\delta^{18}O$ that could meaningfully explain potential intraspecific differences between stomatal

conductance and photosynthetic capacity. Thus, the use of this mechanistic model with the results obtained in this investigation was not justified.

Relationship between radial growth and isotope tree-ring $\delta^{13}C$ and $\delta^{18}O$

In this study, $\delta^{13}C$ or $\delta^{18}O$ did not vary significantly with MAIG. This could suggest that the relationships between carbon allocation, gas exchange and annual stem growth in *P. fremontii* are not directly correlated. Although changes in interannual MAIG most likely correlate with growth conditions, trees can assimilate carbohydrates that might not be invested into growth. Therefore, stomatal conductance and photosynthesis could not always be assumed to correlate with growth.

By analyzing the relationships between MAMT transfer distance, $\delta^{13}C$, $\delta^{18}O$, and MAIG with a linear regression and principal component analysis, I could detect a negative relationship between $\delta^{13}C$ enrichment and MAMT transfer distance. Additional support for these results were obtained by comparing the interannual measurements of all genotypes in this study. Interannual measurements of MAIG showed a strong positive correlation with $\delta^{13}C$. These results suggest that in years with increases in MAIG, tree-ring $\delta^{13}C$ values were less negative (decrease in $\delta^{13}C$). The opposite trend, more negative $\delta^{13}C$ with reduced MAIG, would suggest a potential relationship between gas exchange and carbon allocation to annual stem growth. This positive trend between MAIG and less negative $\delta^{13}C$ values indirectly aligns with my second hypothesis because populations from warmer provenances, displaying greater MAIG, were expected to exhibit lower $\delta^{13}C$, indicating higher stomatal conductance. My results parallel other recent common garden investigations on *P. fremontii* that have found that (1) this species possesses a high degree of coordination across multiple trait spectra to adapt to local climate

150

constraints on photosynthetic gas exchange, growth and survival (Blasini et al. 2020) and (2) warm-adapted populations display greater rates of whole-tree stomatal conductance and transpiration (Blasini et al. 2022) as an adaptive strategy to maintain cooler canopies in extreme hot environments.

Interannual local garden climate effect on MAIG, $\delta^{13}C$, and $\delta^{18}O$

Interannual measurements of MAIG and $\delta^{13}C$ did not display any significant correlation with either PVER garden climatic conditions, mean annual maximum temperature ($MAMT_{PVER}$) and vapor pressure deficit (VPD_{PVER}). However, these climatic variables exhibited a significant influence on interannual tree-ring $\delta^{18}O$ values in most of the populations included in this investigation. It is known that variation in tree-ring $\delta^{18}O$ can be influenced by isotopic values of source water, leaf water evaporative enrichment, and the exchange of xylem water and phloem sugars during wood synthesis processes (McCarroll and Loader 2004, Gessler et al. 2014, Yang et al. 2022).

Because the same water source was used to irrigate this common garden, it can be assumed that the isotopic values of this source water did not play a significant role in the interannual changes in tree-ring $\delta^{18}O$. In the case of leaf water evaporative enrichment, I know that to reduce water loss, plants close their stomata during periods of high temperature and vapor pressure deficit. Reduction of stomatal conductance leads to a lower mix between the unenriched water from the xylem and ^{18}O-enriched water at the leaf evaporative sites (Farquhar and Lloyd 1993; Guerrieri et al. 2017). Therefore, it is very likely that the influence of the garden climate on stomatal conductance was the reason for those interannual changes in tree-ring $\delta^{18}O$ values. Although previous research on *P. fremontii* have found large intraspecific differences in transpiration and stomatal

151

conductance rates across this species' elevational gradient (Blasini et al. 2022), in this study I did not find clear intraspecific differentiation in the way MAMT$_{PVER}$ or VPD$_{PVER}$ influenced interannual changes in tree-ring $\delta^{18}O$. However, as specified earlier, this lack of differentiation could be explained by the intraspecific differences in hydraulic architecture traits (e.g., Sapwood to leaf area) or the remobilization of previous year's stored NSCs during periods of high demand.

It is important to recognize that this study was based on data from only four years and with samples taken from 38 individuals. This offered some limitations regarding the overall conclusions of my results. However, this investigation lays the groundwork for future studies involving single species studies with tree-ring isotopes in a common garden setting. Given the high variability found in certain populations, it would have been advisable to increase the sample size per populations in this type of studies.

Conclusions

By disentangling the potential effect that warmer temperatures have on radial growth, $\delta^{13}C$ and $\delta^{18}O$ in tree-ring cellulose in warm-desert riparian tree species (*Populus fremontii*), this study provides an overview of the challenges related to the utilization of dendroisotopic techniques in a common garden to understand intraspecific differences of tree carbon and water use strategies under climate change. It was found that under extreme hot temperatures, populations adapted to greater mean maximum annual temperatures display greater radial growth than populations adapted to cooler mean annual maximum temperatures. Although a direct relationship between growth and $\delta^{13}C$ was not detected, climate variables including mean maximum annual temperatures of the

source populations and mean maximum annual temperature of the common garden influenced the relationship between radial growth and $\delta^{13}C$. These results suggest that the relationship between tree productivity and $\delta^{13}C$ might be subjected to multiple environmental, physiological, and genetic factors. Likewise, $\delta^{18}O$ did not provide meaningful information about intraspecific differences in physiological adjustments in stomatal conductance to the extreme temperature of the garden. However, $\delta^{18}O$ did exhibit significant relationships with local garden climatic variables such as MAMT and VPD. Consequently, this study highlights the extent that thermal stress can reduce tree growth, and presumably fitness in populations that are locally adapted to a narrow range of climate conditions. Also, this study exposed the limitations related to the utilization of stable isotopes in tree-rings to identify intraspecific differences regarding the physiological responses to the environmental conditions of a common garden.

Acknowledgements

Tables

Table 4.1. Summary of the climatic conditions of the provenance locations selected throughout Arizona and California that were collected for study in the common garden at Palo Verde Ecological Reserve (indicated with *).

Elevation (m)	Transfer MAMT (°c)	Transfer MAT (°c)	Tmax (°c)	Tmin (°c)	Tmean (°c)	PPT (cm)
58	0.22	0.03	30.72	13.22	21.97	10.13
82	0.00	0.00	30.94	13.06	22.00	9.40
82*	0.00	0.00	30.94	13.06	22.00	9.40
393	0.61	0.47	30.33	12.72	21.53	22.91
570	3.44	3.22	27.50	10.06	18.78	19.81
616	3.14	2.40	27.80	8.20	19.60	39.62
625	1.78	3.25	29.17	8.33	18.75	30.99
671	3.72	2.83	27.22	11.11	19.17	42.88
710	2.06	2.22	28.89	10.67	19.78	31.50
738	4.67	3.47	26.28	10.78	18.53	50.29
1061	4.06	3.36	26.89	10.39	18.64	34.29
1149	6.56	5.72	24.39	8.17	16.28	41.40
1161	4.67	5.92	26.28	5.89	16.08	45.47
1277	5.24	5.50	25.70	9.20	16.50	45.97

Table 4.2. Results from the multiple regression analysis to assess the relationship between MAMT transfer distance, $\delta^{13}C$, $\delta^{18}O$ and MAIG in a common garden at the warmest edge of *P.fremontii* climate range.

	Dependent variable: MAIG					
	(MAIG~MAMT)	(MAIG~$\delta^{13}C$)	(MAIG~$\delta^{18}O$)	(MAIG~MAMT+$\delta^{13}C$)	(MAIG~MAMT+$\delta^{18}O$)	(MAIG~MAMT+$\delta^{13}C$+$\delta^{18}O$)
MAMT	-39.402***			-40.466***	-38.987***	-39.745***
	(9.480)			(9.052)	(9.688)	(9.203)
$\delta^{13}C$		47.536		53.960**		56.232**
		(32.012)		(25.684)		(26.160)
$\delta^{18}O$			-24.537		-9.570	-17.637
			(34.368)		(28.813)	(27.608)
Constant	333.756***	1,555.100*	936.685	1,839.989**	608.032	2,408.906**
	(30.724)	(892.192)	(989.160)	(717.527)	(826.379)	(1,147.729)
Observations	36	36	36	36	36	36
R^2	0.337	0.061	0.015	0.415	0.339	0.422
Adjusted R^2	0.317	0.033	-0.014	0.380	0.299	0.368
Residual Std. Error	108.726 (df = 34)	129.388 (df = 34)	132.528 (df = 34)	103.646 (df = 33)	110.177 (df = 33)	104.589 (df = 32)
F Statistic	17.274*** (df = 1; 34)	2.205 (df = 1; 34)	0.510 (df = 1; 34)	11.711*** (df = 2; 33)	8.466*** (df = 2; 33)	7.803*** (df = 3; 32)
AIC	443.701	456.229	457.955	441.182*	445.581	442.726*

Note:*p**p***p<0.01

Table 4.3. Pearson's correlation coefficients between four years (2011-2014) tree ring measurements of MAIG, $\delta^{13}C$ and $\delta^{18}O$ and their respective annual environmental parameters in the garden: mean annual maximum temperature ($MAMT_{PVER}$) and mean annual vapor pressure deficit (VPD_{PVER}).

	MAIG	$\delta^{13}C$	$\delta^{18}O$	$MAMT_{PVER}$	VPD_{PVER}
MAIG	1	**0.323*****	0.014	0.147	0.141
$\delta^{13}C$	**0.323*****	1	-0.022	0.147	0.112
$\delta^{18}O$	0.014	-0.022	1	**-0.231****	**-0.169***
$MAMT_{PVER}$	0.147	0.147	**-0.231****	1	**0.948*****
VPD_{PVER}	0.141	0.112	**-0.169***	**0.948*****	1

Pearson coefficients are reported and (*), (**) and (***) indicate $p < 0.05$, $p < 0.01$ and $p < 0.001$, respectively

Table 4.4. Results from simple regression analyses that assess the relationship between and among tree-ring MAIG, δ^{13}C, δ^{18}O and MAMT transfer distance and the climatic interannual conditions in the garden. Climate conditions included mean annual maximum temperature in the PVER garden (MAMT$_{PVER}$) and vapor pressure deficit (VPD$_{PVER}$). Because of the high collinearity between MAMT$_{PVER}$ and VPD$_{PVER}$ values, I only reported the MAMT$_{PVER}$ in this table. Only the adjusted R^2 and the coefficient, β, were reported when t-test showed β values were significantly different from zero.

Model	Adjusted R^2	Significant Parameter	Estimate (β)	Standard Error	t-value	p
MAIG ~ MAMT + δ^{13}C + δ^{18}O + MAMT$_{PVER}$	0.39	**MAMT ***** δ^{13}**C ***** MAMT$_{PVER.}$ (0.07)	-222.688	1797.738	-0.124	***
δ^{18}O ~ MAMT + δ^{13}C + MAMT$_{PVER}$	0.03	**MAMT$_{PVER}$ ****	50.569	8.511	5.942	*

(*), (**) and (***) indicate $p < 0.05$, $p < 0.01$ and $p < 0.001$, respectively
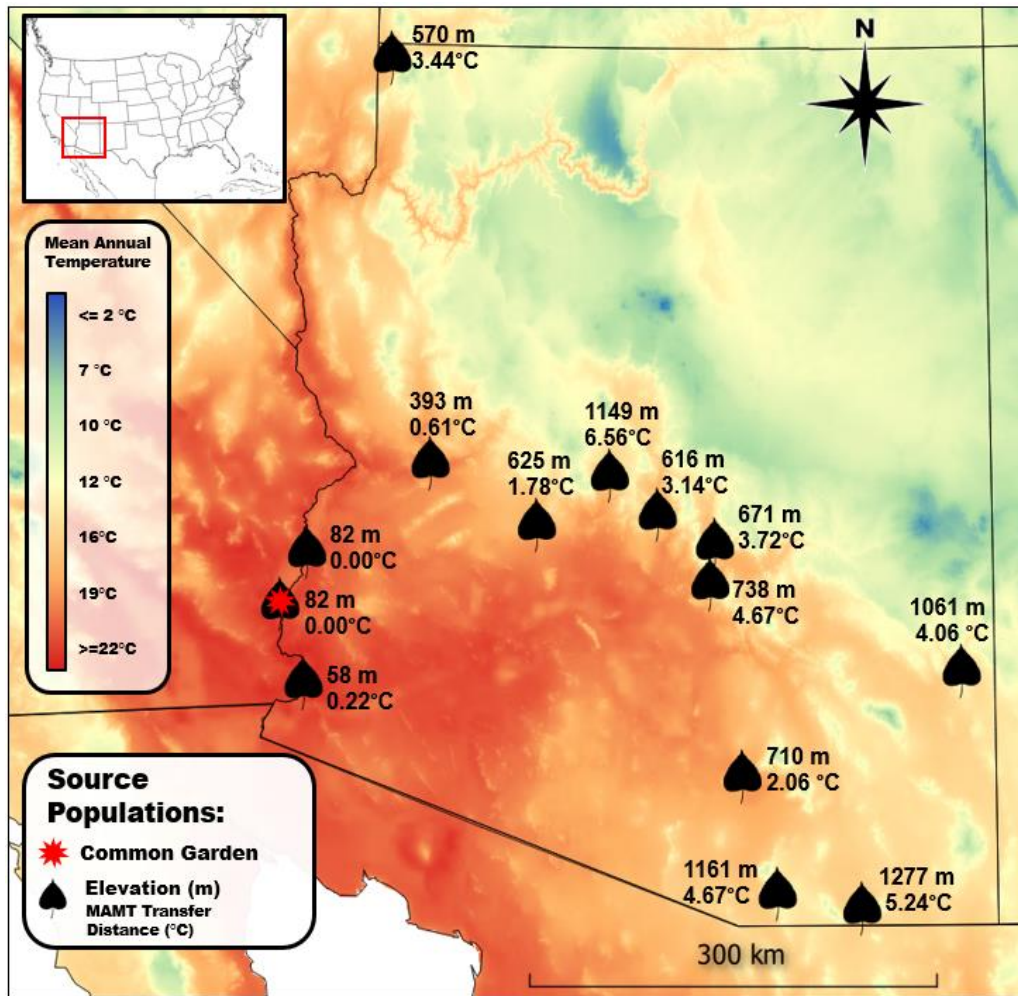
Figures

Figure 4.1. Location of the Palo Verde Ecological Restoration (PVER) common garden (red star) and 14 population sites of *Populus fremontii* (Fremont cottonwood leaf icon) with their elevations and population mean annual maximum air temperature (MAMT) transfer distance (mean annual maximum air temperature (MAMT) of common garden minus MAMT of population source sites). Map developed on QGIS Geographic Information System. Open-Source Geospatial Foundation Project. http://qgis.osgeo.org
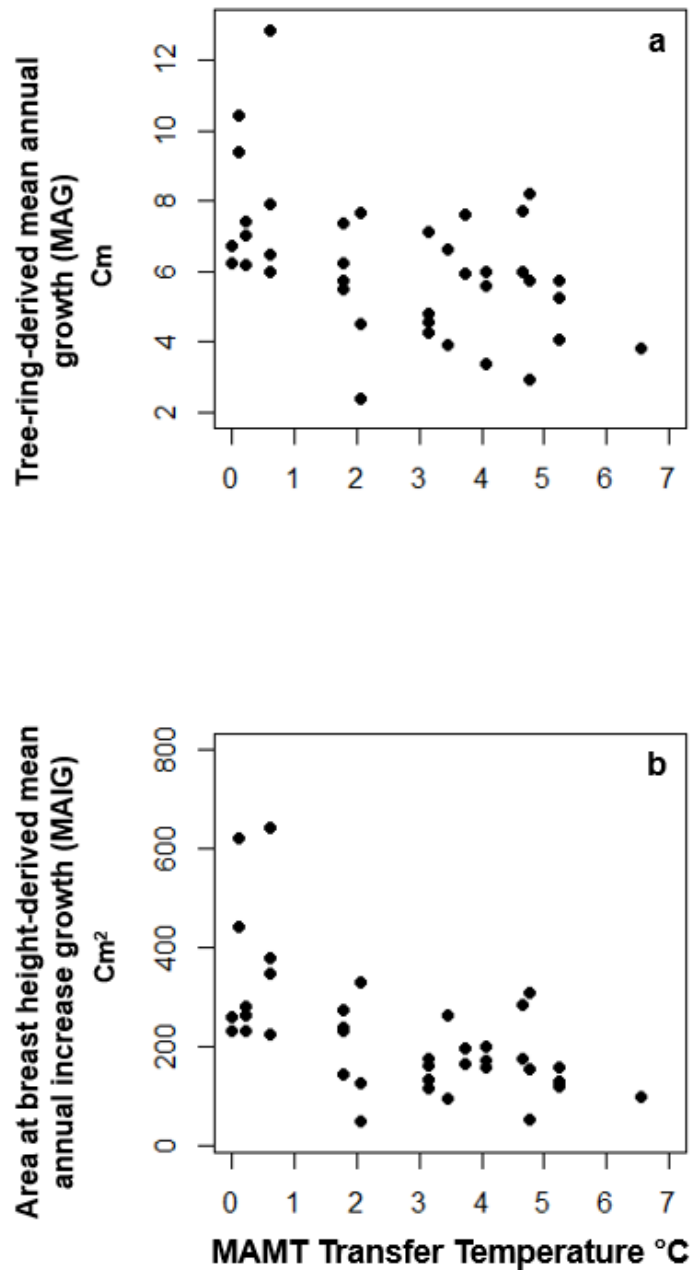
159

Figure 4.2. Relationship between (a) tree-ring-derived mean annual growth (MAG) and (b) area at breast height-derived mean annual increase growth (MAIG) with population mean annual maximum air temperature (MAMT) transfer distance (mean annual maximum air temperature (MAMT) of common garden minus MAMT of population source sites) measured on 38 genotypes planted in a common garden located at the hottest edge of this *P. fremontii* thermal distribution (Palo Verde Ecological Reserve in Blythe, California).
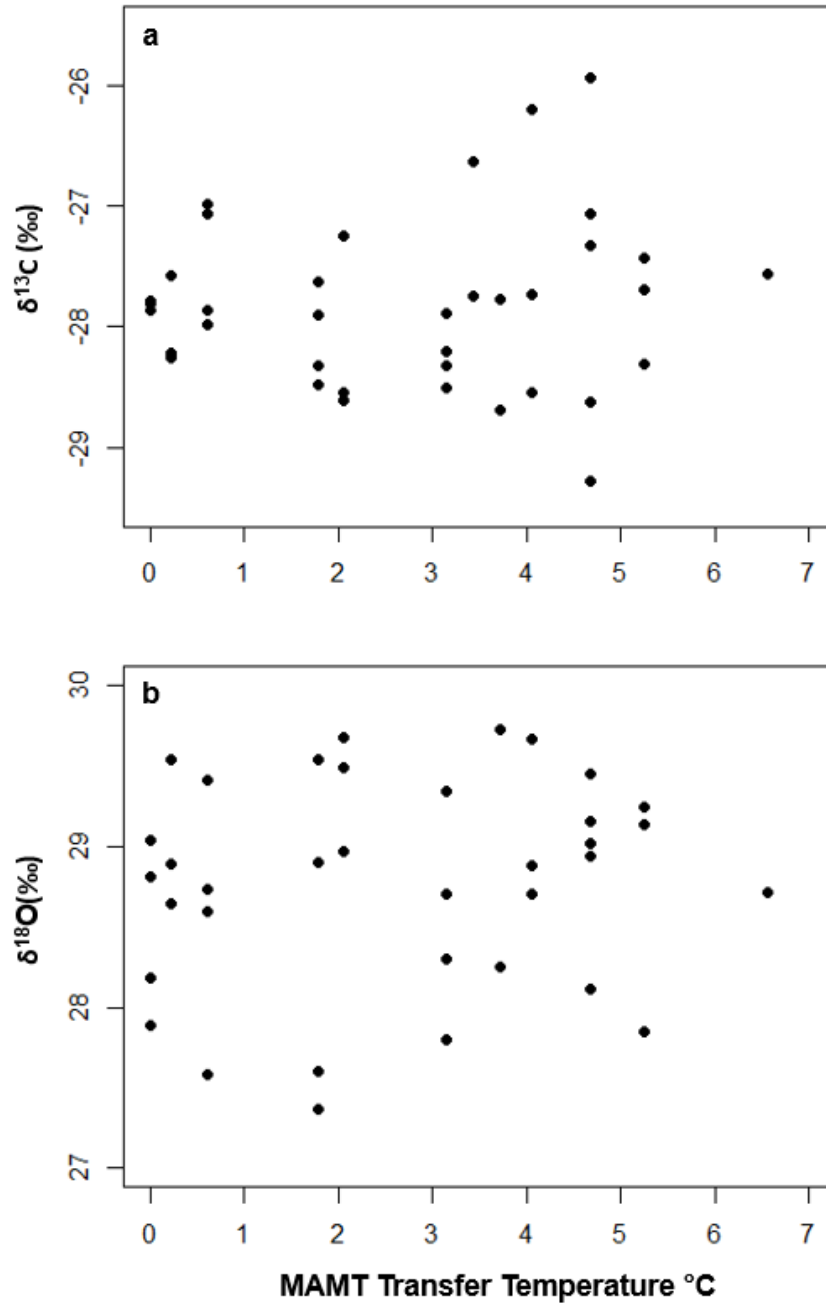
160

Figure 4.3. Relationship between (a) $\delta^{13}C$ and (b) $\delta^{18}O$ versus population mean annual maximum air temperature (MAMT) transfer distance (mean annual maximum air temperature (MAMT) of common garden minus MAMT of population source sites) measured on 36 ($\delta^{13}C$) and 34 ($\delta^{18}O$) genotypes from 14 ($\delta^{13}C$) and 13 ($\delta^{18}O$) populations planted in a common garden located at the hottest edge of this species thermal distribution (Palo Verde Ecological Reserve in Blythe, California).
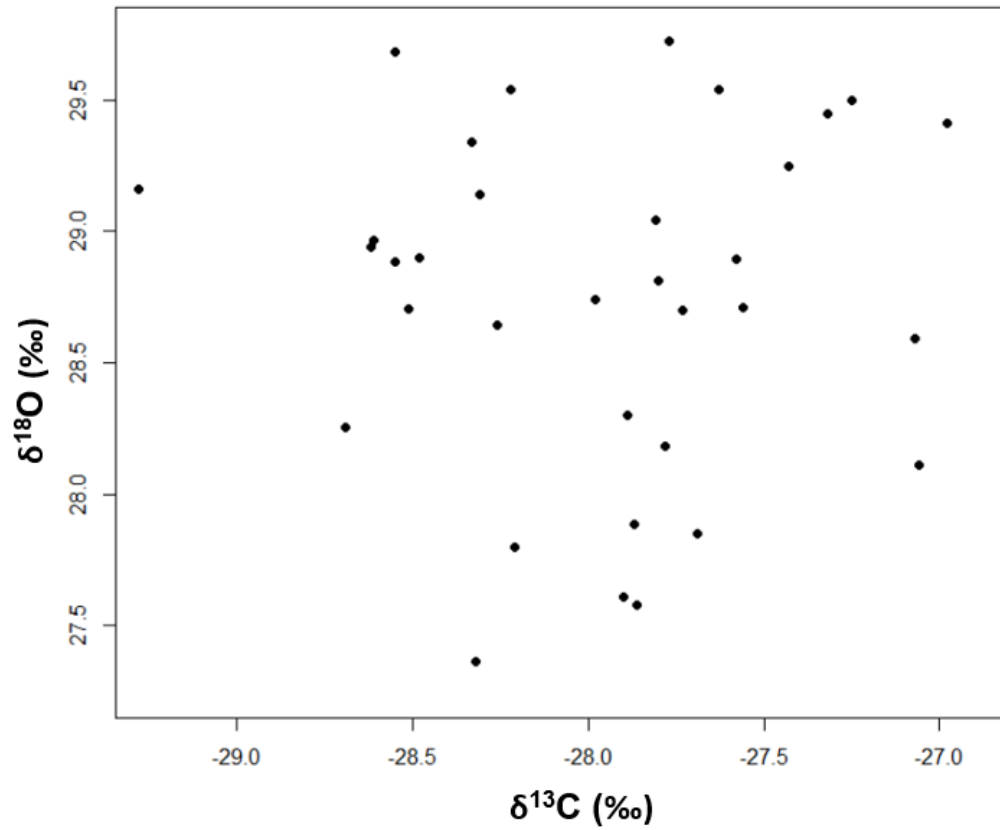
Figure 4.4. Relationship between $\delta^{13}C$ and $\delta^{18}O$ measured on 34 genotypes from 13 populations planted in a common garden located at the hottest edge of this species thermal distribution (Palo Verde Ecological Reserve in Blythe, California).
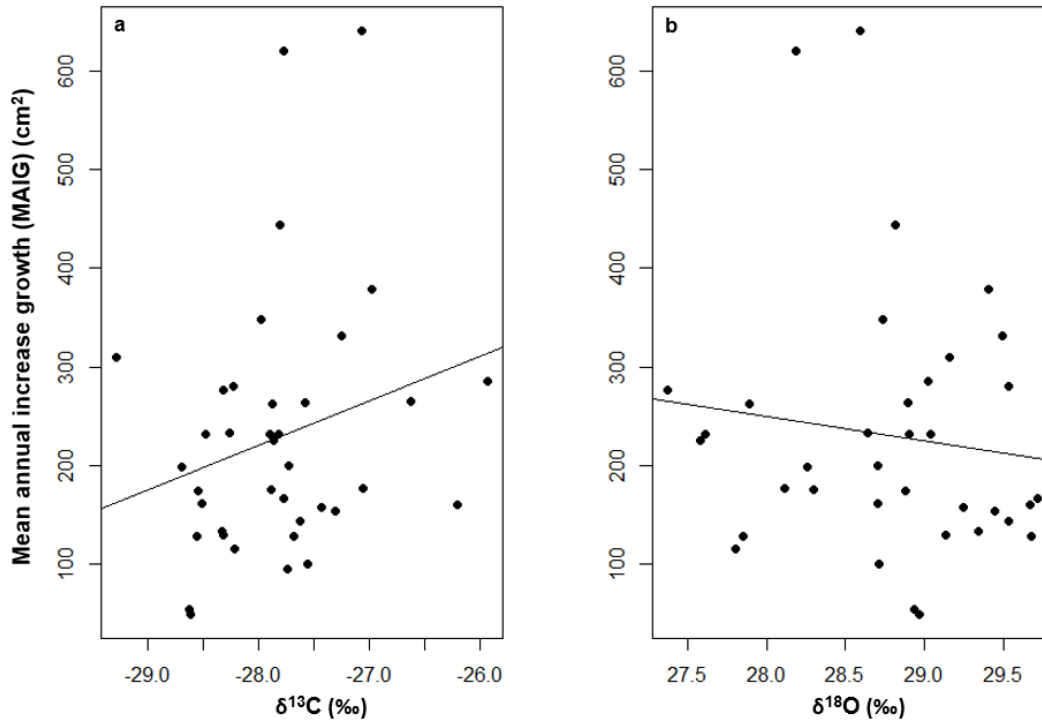
Figure 4.5. Relationship between area at breast height-derived mean annual increase growth (MAIG) with (a) $\delta^{13}C$ and (b) $\delta^{18}O$ measured on 36 ($\delta^{13}C$) and 34 ($\delta^{18}O$) genotypes from 14 ($\delta^{13}C$) and 13 ($\delta^{18}O$) populations planted in a common garden located at the hottest edge of this species thermal distribution (Palo Verde Ecological Reserve in Blythe, California).

Figure 4.6. Principal component analysis (PCA), axes (PC1 and PC2), summarizing the relationships between area at breast height-derived mean annual increase growth (MAIG), $\delta^{13}C$ and $\delta^{18}O$ measured on 36 genotypes from 13 populations planted in a common garden located at the hottest edge of this species thermal distribution (Palo Verde Ecological Reserve in Blythe, California).

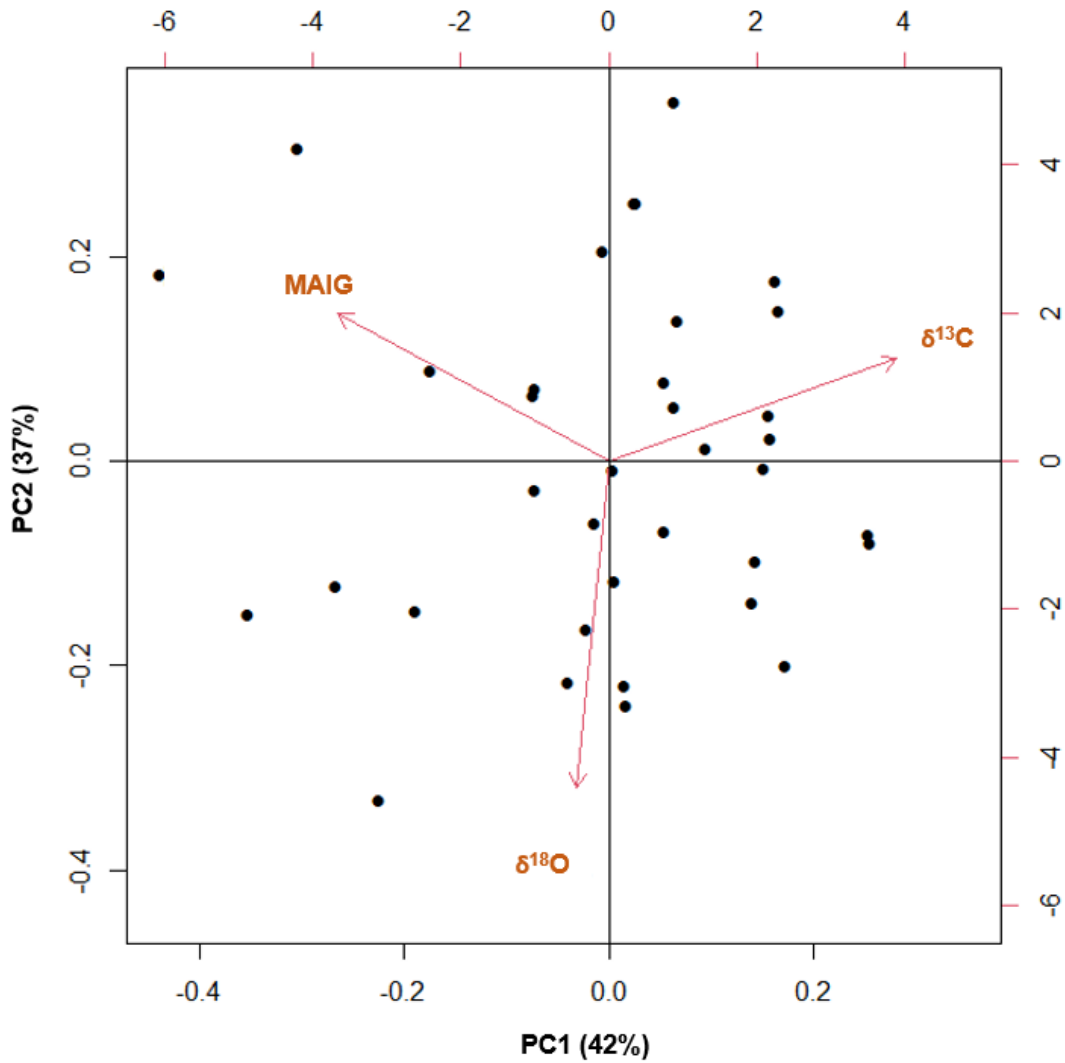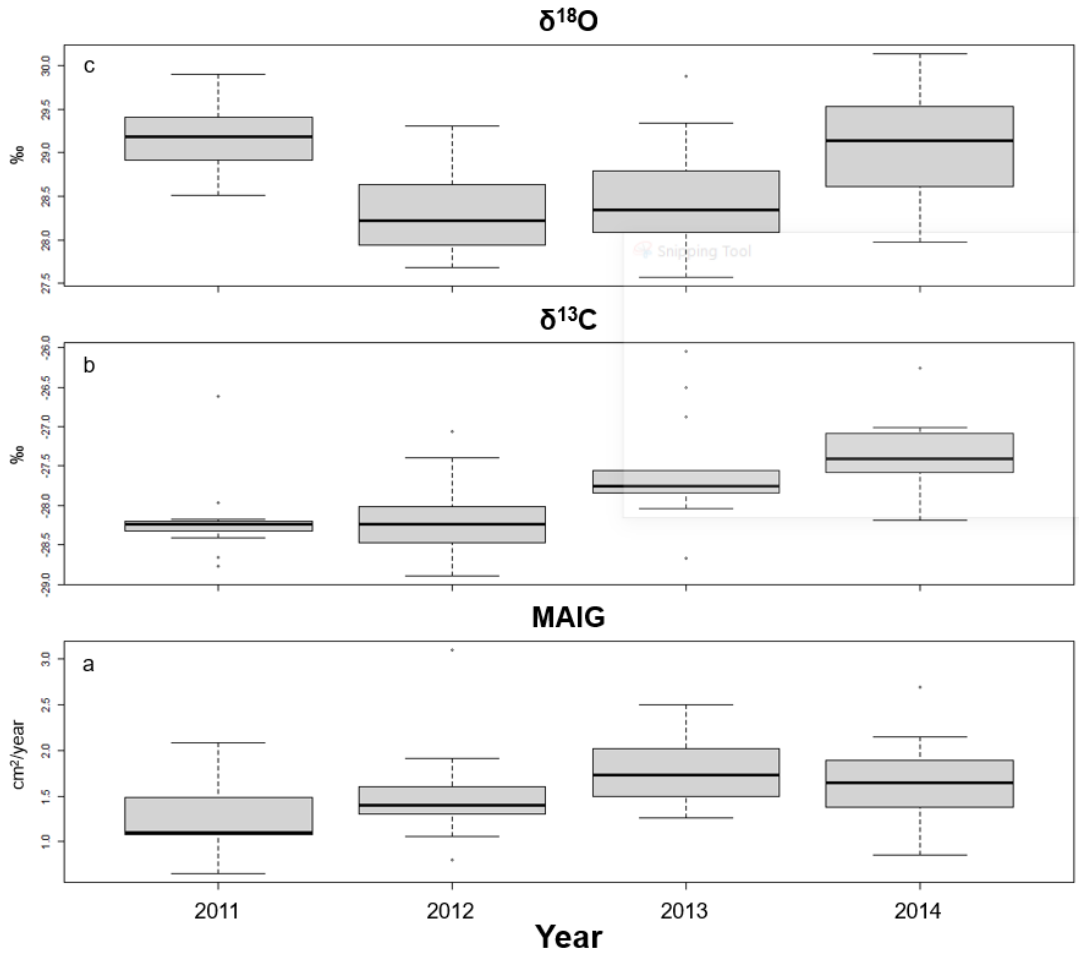**Figure 4.7.** Box and whisker plots showing the median, 25th and 75th percentiles (boxes) and the 10th and 90th percentiles (error bars) of tree-ring (a) mean annual increased growth (MAIG), (b) $\delta^{13}C$ and (c) $\delta^{18}O$ grouped by year (2011–2014).

References

Aitken SN, Yeaman S, Holliday JA, Wang T, Curtis-McLane S (2008) Adaptation, migration or extirpation: climate change outcomes for tree populations. Evol Appl. 1(1):95–111. https://doi.org/10.1111/j.1752-4571.2007.00013.x

Allen CD, Macalady AK, Chenchouni H, Bachelet D, McDowell N, Vennetier M, Kitzberger T, Rigling A, Breshears DV, Hogg EH, Gonzalez P, Fensham R, Zhang Z, Castro J, Demidova N, Lim JH, Allard G, Running SW, Semerci A, Cobb N (2010) A global overview of drought and heat-induced tree mortality reveals emerging climate change risks for forests. Forest Ecology and Management 259(4): 660–684. https://doi.org/10.1016/j.foreco.2009.09.001

Anchukaitis KJ, Evans MN, Wheelwright NT, Schrag DP (2008) Stable isotope chronology and climate signal calibration in neo-tropical montane cloud forest trees. J Geophys Res 113:03030. https://doi.org/10.1029/2007JG000613

Barbour MM (2007) Stable oxygen isotope composition of plant tissue: a review. Global Biogeochem Cycles 34:83–94. https://doi.org/10.1071/FP06228

Barbour MM, Schurr U, Henry BK (2000) Variation in the oxygen isotope ratio of phloem sap sucrose from castor bean. Evidence in support of the Péclet effect. Plant Physiology 123:671–680. https://doi.org/10.1104/pp.123.2.671

Bates D, Mächler M, Bolker B, Walker S (2015) Fitting linear mixed-effects models using lme4. Journal of Statistical Software, 67(1). https://doi.org/10.18637/jss.v067.i011

Blasini DE, Koepke DF, Bush SE, Allan GJ, Gehring CA, Whitham TG, Hultine KR (2022)Tradeoffs between leaf cooling and hydraulic safety in a dominant arid land riparian tree species. Plant, Cell and Environment 1–18. https://doi.org/10.1111/pce.14292

Blasini DE, Koepke DF, Grady KC, Allan GJ, Gehring CA, Whitham TG, Hultine KR. (2020) Adaptive trait syndromes along multiple economic spectra define cold and warm adapted ecotypes in a widely distributed foundation tree species. Journal of Ecology 109:1298–1318. https://doi.org/10.1111/1365-2745.13557

Borcard D, Gillet F, Legendre P (2011) Numerical ecology with R. Springer. https://doi.org/10.1007/978-1-4419-7976-6

Brandes E, Wenninger J, Koeniger P, Schindler D, Rennenberg H, Leibundgut C, Mayer H, Gessler A (2007) Assessing environmental and physiological controls over water relations in a Scots pine (*Pinus sylvestris L.*) stand through analyses of stable isotope composition of water and organic matter. Plant Cell Environ 30:113–127. https://doi.org/10.1111/j.1365-3040.2006.01609.x

Brienen RJ, Phillips OL, Feldpausch TR, Gloor E, Baker TR (2015) Long-term decline of the Amazon carbon sink. Nature 519: 344–348. https://doi.org/10.1038/nature14283

Briffa KR, Osborn TJ, Schweingruber FH, Jones PD, Shiyatov SG, Vaganov EA (2002) Tree-ring width and density data around the Northern Hemisphere: Part 1, local and regional climate signals. The Holocene 12, 737–757. https://doi.org/10.1191/0959683602hl587rp

Buhay WM, Edwards TWD, Aravena R (1996) Evaluating kinetic fractionation factors for ecologic and palaeoclimatic reconstructions from oxygen and hydrogen isotope ratios in plant water and cellulose. Geochimica et Cosmochimica Acta 60, 2209–2218. https://doi.org/10.1016/0016-7037(96)00073-7

Cailleret M, Jansen S, Robert EMR, Desoto L, Aakala T, Antos JA, Beikircher B, Bigler C, Bugmann H, Caccianiga M, Čada V, Camarero JJ, Cherubini P, Cochard H, Coyea MR, Čufar K, Das AJ, Davi H, Delzon S, Dorman M, Gea-Izquierdo G, Gillner S, Haavik LJ, Hartmann H, Hereş AM, Hultine KR, Janda P, Kane JM, Kharuk VI, Kitzberger T, Klein T, Kramer K, Lens F, Levanic T, Linares Calderon JC, Lloret F, Lobo-Do-Vale R, Lombardi F, López Rodríguez R, Mäkinen H, Mayr S, Mészáros I, Metsaranta JM, Minunno F, Oberhuber W, Papadopoulos A, Peltoniemi M, Petritan AM, Rohner B, Sangüesa-Barreda G, Sarris D, Smith JM, Stan AB, Sterck F, Stojanović DB, Suarez ML, Svoboda M, Tognetti R, Torres-Ruiz JM, Trotsiuk V, Villalba R, Vodde F, Westwood AR, Wyckoff PH, Zafirov N, Martínez-Vilalta, J (2017) A synthesis of radial growth patterns preceding tree mortality. Global Change Biology 23: 1675–1690. https://doi.org/10.1111/gcb.13535

Carter JL, White DA (2009) Plasticity in the Huber value contributes to homeostasis in leaf water relations of a mallee Eucalypt with variation to groundwater depth, Tree Physiology, 29 (11): 1407–1418. https://doi-org.ezproxy1.lib.asu.edu/10.1093/treephys/tpp076

Cernusak LA, Tcherkez G, Keitel C, Cornwell WK, Louis D, Santiago E, Knohl FA, Barbour AM, Williams DG, Reich PB, Ellsworth DS, Dawson TE, Griffiths HG, Farquhar GD, Wright IJ (2009) Why are non-photosynthetic tissues generally C-13 enriched compared with leaves in C-3 plants? Review and synthesis of current hypotheses. Functional Plant Biology 36:199–213. https://doi.org/10.1071/FP08216

Chapin FS, Matson PA, Vitousek PM (2011) Principles of terrestrial ecosystem ecology. Springer. https://doi.org/10.1007/978-1-4419-9504-9

Cooper HF, Best RJ, Andrews LV, Corbin JPM, Garthwaite I, Grady KC, Gehring CA, Hultine KR, Whitham TG, Allan GJ (2022) Evidence of climate-driven selection on tree traits and trait plasticity across the climatic range of a riparian foundation species. Molecular Ecology, 00, 1–17. https://doi.org/10.1111/mec.16645

Cooper HF, Grady KC, Cowan JA, Best RJ, Allan GJ, Whitham T (2019) Genotypic variation in phenological plasticity: Reciprocal common gardens reveal adaptive responses to warmer springs but not to fall frost. Global Change Biology 25(1): 187–200. https://doi.org/10.1111/gcb.14494

Dawson TE, Ehleringer JR (1993) Isotopic enrichment of water in the woody tissues of plants implications for plant water source, water uptake, and other studies which use the stable isotopic composition of cellulose. Geochim Cosmochim Acta 57:3487–3492. https://doi.org/10.1016/0016-7037(93)90554-A

Ehleringer JR, Cerling TE (1995) Atmospheric CO2 and the ratio of intercellular to ambient CO_2 concentrations in plants. Tree Physiol 15:105–11. https://doi.org/110.1093/treephys/15.2.105

Farquhar GD, Ehleringer JR, Hubick KT (1989) Carbon Isotope Discrimination and Photosynthesis. Annual Review of Plant Physiology and Plant Molecular Biology 40:1, 503–537. https://doi.org/10.1146/annurev.pp.40.060189.002443

Farquhar GD, Lloyd J (1993) Carbon and oxygen isotope effects in the exchange of carbon dioxide between terrestrial plants and the atmosphere. Stable Isot Plant Carbon-water Relations 47–70. https://doi.org/10.1016/B978-0-08-091801-3.50011-8

Farquhar GD, O'Leary MH, Berry JA (1982) On the relationship between carbon isotope discrimination and the inter-cellular carbon-dioxide concentration in leaves. Aust J Plant Physiol 9:121–137. https://doi.org/10.1071/PP9820121

Francey RJ, Farquhar GD (1982) An explanation of 13C/12C variations in tree rings. Nature 297:28–31. https://doi.org/10.1038/297028a0

Garfin G, Jardine A, Merideth R, Black M, LeRoy S (Eds.) (2013) Assessment of Climate Change in the Southwest United States. Natl Clim Assess Reg Tech Input Rep Ser Assess 531. https://doi.org/10.5822/978-1-61091-484-0

Gessler A, Brandes E, Buchmann N, Helle G, Rennenberg H, Barnard RL (2009) Tracing carbon and oxygen isotope signals from newly assimilated sugars in the leaves to the tree-ring archive. Plant Cell and Environment 32(7):780-95. https://doi.org/10.1111/j.1365-3040.2009.01957.x

Gessler A, Brandes E, Keitel C, Boda S, Kayler Z, Granier A, Barbour M, Farquhar GD, Treydte K (2013) The oxygen isotope enrichment of leaf-exported assimilates— does it always reflect lamina leaf water enrichment? New Phytol 200:144–157. https://doi.org/10.1111/nph.12359

Gessler A, Ferrio JP, Hommel R, Hommel R, Treydte K, Werner RA, Monson RK (2014) Stable isotopes in tree rings: Towards a mechanistic understanding of isotope fractionation and mixing processes from the leaves to the wood. Tree Physiol 34:796–818. https://doi.org/10.1093/treephys/tpu040

Glenn EP, Nagler PL (2005) Comparative ecophysiology of *Tamarix ramosissima* and native trees in western US riparian zones. J Arid Environ 61: 419–46. https://doi.org/10.1016/j.jaridenv.2004.09.025

Gottlicher S, Knohl A, Wanek W, Buchmann N, Richter A (2006) Short term changes in carbon isotope composition of soluble carbohydrates and starch: from canopy leaves to the root system. Rapid Commun Mass Spectrom 20:653–660. https://doi.org/10.1002/rcm.2352

Grady KC, Ferrier SM, Kolb TE, Hart S, Allan G, Whitham T (2011) Genetic variation in productivity of foundation riparian species at the edge of their distribution: Implications for restoration and assisted migration in a warming climate. Global Change Biology 17(12):3724-3735. https://doi.org/10.1111/j.1365-2486.2011.02524.x

Grady KC, Laughlin DC, Ferrier SM, Kolb TE, Hart S, Allan G, Whitham T (2013) Conservative leaf economic traits correlate with fast growth of genotypes of a foundation riparian species near the thermal maximum extent of its geographic range. Functional Ecology 27:428–438. https://doi.org/10.1111/1365-2435.12060

Guerrieri R, Jennings K, Belmecheri S, Asbjornsen H, Ollinger S (2017) Evaluating climate signal recorded in tree-ring $\delta^{13}C$ and $\delta^{18}O$ values from bulk wood and α-cellulose for six species across four sites in the northeastern US. Rapid Commun Mass Spectrom. 2017:31;2081-2091. https://doi.org/10.1002/rcm.7995

Helle G, Schleser GH (2004) Beyond CO2-fixation by Rubisco – an interpretation of 13C/12C variations in tree rings from novel intra-seasonal studies on broad-leaf trees. Plant, Cell and Environment 27, 367–380. https://doi.org/10.1111/j.0016-8025.2003.01159.x

Helliker BR, Richter SL (2008) Subtropical to boreal convergence of tree-leaf temperatures. Nature 454, 511–514. https://doi.org/10.1038/nature07031

Horton JL, Kolb TE, Hart SC (2001) Responses of riparian vegetation to interannual variation in groundwater depth in a semi-arid river basin. Plant, Cell and Environment 24:293–304. https://doi.org/10.1046/j.1365-3040.2001.00681.x

Howe GT, Aitken SN, Neale DB, Jermstad KD, Wheeler NC, Chen TH (2003) From genotype to phenotype: unraveling the complexities of cold adaptation in forest trees. Can. J. Bot. 81: 1247–1266. https://doi.org/10.1139/b03-141

Hultine KR, Allan GJ, Blasini DE, Bothwell HM, Cadmus A, Cooper HF, Doughty CE, Gehring CA, Gitlin AR, Grady KC, Keith AR, Koepke DF, Markovchick L, Corbin Parker JM, Sankey TT, Whitham TG (2020) Adaptive capacity in the foundation tree species *Populus fremontii:* implications for resilience to climate change and non-native species invasion in the American Southwest. Conservation Physiology 8(1), coaa061. https://doiorg.ezproxy1.lib.asu.edu/10.1093/conphys/coaa061

Hultine KR, Bush SE, Ehleringer JR (2010) Ecophysiology of riparian cottonwood and willow before, during, and after two years of soil water removal. Ecological Applications, 20: 347–361. https://doi.org/10.1890/09-0492.1

Ikeda DH, Max TL, Allan GJ, Lau MK, Shuster SM, Whitham TG (2017) Genetically informed ecological niche models improve climate change predictions. Global Change Biology, 23, 164–176. https://doi.org/10.1111/gcb.13470

IPCC. 2007. Climate Change 2007: Impacts, Adaptation and Vulnerability. Contribution of Working Group II to the Fourth Assessment Report of the Intergovernmental Panel on Climate Change. Cambridge University Press, Cambridge, UK.

Johnstone JA, Roden JS, Dawson TE (2013) Oxygen and carbon stable isotopes in coast redwood tree rings respond to spring and summer climate signals, J. Geophys. Res. Biogeosci., 118, 1438–1450. https://doi.org/10.1002/jgrg.20111

Kannenberg SA, Driscoll AW, Szejner P, Anderegg WR, Ehleringer JR (2021) Rapid increases in shrubland and forest intrinsic water-use efficiency during an ongoing megadrought. of Proc. Natl. Acad. Sci. U.S.A. 118:52. https://doi.org/10.1073/pnas.2118052118

Kannenberg SA, Guo JS, Novick KA, Anderegg WRL, Feng X, Kennedy D, Konings AG, Martínez-Vilalta J, Matheny AM (2022) Opportunities challenges and pitfalls in characterizing plant water-use strategies. Functional Ecology, 36, 24–37. https://doi.org/10.1111/1365-2435.13945

Kassambara A and Mundt F (2017) factoextra: Extract and visualize the results of multivariate data analyses. R package version 1.0.5. https://CRAN.Rproject.org/package=factoextra

Keith AR, Bailey JK, Lau MK, Whitham TG (2017) Genetics-based interactions of foundation species affect community diversity, stability, and network structure. Proc Royal Soc B. 284(1854): 20162703. https://doi.org/10.1098/rspb.2016.2703

Kindt R, Coe R (2005) Tree Diversity Analysis. A Manual and Software for Common Statistical Methods for Ecological and Biodiversity Studies. Nairobi: World Agroforestry Centre (ICRAF). http://dx.doi.org/10.13140/RG.2.1.1993.7684

Kuznetsova A, Brockhoff PB, Christensen RHB (2017) lmerTest package: Tests in linear mixed effects models. Journal of Statistical Software, 82(13), 1–26. https://doi.org/10.18637/jss.v082.i13

Lambers H, Chapin FS, Pons TL (2008) Plant Physiological Ecology. Springer New York, NY. https://doi.org/10.1007/978-0-387-78341-3

Lamit LJ, Holeski LM, Flores-Rentería L, Whitham TG, Gehring CA (2016) Tree genotype influences ectomycorrhizal fungal community structure: ecological and evolutionary implications. Fung Ecol 24:124–134. https://doi.org/10.1016/j.funeco.2016.05.013

Landsberg J, Waring R, Ryan M (2017) Water relations in tree physiology: where to from here? Tree Physiology 37(1):18–32. https://doi.org/10.1093/treephys/tpw102

Laumer W, Andreu L, Helle G, Schleser GH, Wieloch T, Wissel H (2009) A novel approach for the homogenization of cellulose to use micro-amounts for stable isotope analyses. Rapid Commun Mass Spectrom 23(13):1934–40. https://doi.org/10.1002/rcm.4105

Leavitt SW, Danzer SR (1993) Methods for batch processing small wood samples to holocellulose for stable-carbon isotope analysis. Anal Chem 65(1):87–89. https://doi.org/10.1021/ac00049a017

Leavitt SW, Woodhouse CA, Castro CL, Wright WE, Meko Dm, Touchan R, Griffin D, Ciancarelli B (2011) The North American monsoon in the U.S. Southwest: Potential for investigation with tree-ring carbon isotopes. Quat Int 235:101–107. https://doi.org/10.1016/j.quaint.2010.05.006

Leuenberger M, Borella S, Stocker T, Saurer M, Siegwolf R, Schweingruber F, Matyssek R (1998) Stable isotopes in tree-rings as climate and stress indicators. Final Report NRP 31, VDF, ETH Zurich. https://doi.org/10.1016/j.quascirev.2003.06.017

Lê S, Josse J, Husson F (2008) FactoMineR: An R package for multivariate analysis. Journal of Statistical Software, 25, 1–18. https://doi.org/10.18637/jss.v025.i01

Lite SJ, Stromberg JC (2005) Surface water and ground-water thresholds for maintaining *Populus–Salix* forests, San Pedro River, Arizona. Biological Conservation 125:153–167. https://doi.org/10.1016/j.biocon.2005.01.020

Lloyd J, Farquhar GD (2008) Effects of rising temperatures and [CO_2] on the physiology of tropical forest trees. Philos Trans R Soc B Biol Sci 363:1811–1817. https://doi.org/10.1098/rstb.2007.0032

MacInnis-Ng C, McClenahan K, Eamus D (2004) Convergence in hydraulic architecture, water relations and primary productivity amongst habitats and across seasons in Sydney. Functional Plant Biology 31, 429–439. https://doi.org/10.1071/FP03194

McCarroll D, Loader NJ (2004) Stable isotopes in tree rings. Quat Sci Rev 23:771–801. https://doi.org/10.1016/j.quascirev.2003.06.017

Offermann C, Ferrio JP, Holst J, Grote R, Siegwolf R, Kayler Z, Gessler A (2011) The long way down-are carbon and oxygen isotope signals in the tree ring uncoupled from canopy physiological processes? Tree Physiology 31: 1088–1102. https://doi.org/10.1093/treephys/tpr093

Oksanen J, Blanchet G, Friendly M, Kindt R, Legendre P, McGlinn D, Minchin P, O'Hara R, Simpson G, Solymos, Henry H, Szoecs E and Wagner H (2019) vegan: Community Ecology Package. R package version 2.5-6. https://CRAN.R-project.org/package=vegan

Poff B, Koestner KA, Neary DG, Henderson V (2011) Threats to Riparian Ecosystems in Western North America: An Analysis of Existing Literature. Journal of the American Water Resources Association (JAWRA) 47(6):1241–1254. https://doi.org/10.1111/j.1752-1688.2011.00571.x

Potts DL, Williams DG (2004) Response of tree ring holocellulose delta C-13 to moisture availability in *Populus fremontii* at perennial and intermittent stream reaches. West North Am Nat 64:27–37. http://www.jstor.org/stable/41717338

PRISM Climate Group (2010) Oregon State University. http://www.prismclimate.org

QGIS Development Team (2021) QGIS geographic information system. Open-Source Geospatial Foundation Project. http://qgis.osgeo.org

R Core Team (2020). R: A language and environment for statistical computing. R Foundation Statistical Computing. Retrieved from https://www.r-project.org/

Roden JS (2005) Carbon and oxygen isotope ratios of tree ring cellulose along a precipitation transect in Oregon, United States. J Geophys Res 110:1–11. https://doi.org/10.1029/2005JG000033

Roden JS, Ehleringer JR (2000) Hydrogen and oxygen isotope ratios of tree ring cellulose for field-grown riparian trees. Oecologia 123:481–489. https://doi.org/10.1007/s004420000349

Roden JS, Lin G, Ehleringer JR (2000) A mechanistic model for interpretation of hydrogen and oxygen isotope ratios in tree-ring cellulose - Evidence and implications for the use of isotopic signals transduced by plants. Geochimica et Cosmochimica Acta 64(1). https://doi.org/10.1016/S0016-7037(99)00195-7

Roden JS, Siegwolf R (2012) Is the dual-isotope conceptual model fully operational? Tree Physiology, 32(10):1179–1182. https://doi.org/10.1093/treephys/tps099

Rood SB, Braatne JH, Hughes FMR (2003) Ecophysiology of riparian cottonwoods: streamflow dependency, water relations and restoration. Tree Physiology 23: 1113–1124. https://doi.org/10.1093/treephys/23.16.1113

Sankey T, Hultine K, Blasini D, Koepke D, Bransky N, Grady K, Cooper H, Gehring C, Allan G (2021) UAV thermal image detects genetic trait differences among populations and genotypes of Fremont cottonwood (*Populus fremontii, Salicaceae*). Remote Sensing in Ecology and Conservation 7(4). https://doi.org/10.1002/rse2.185

Saurer M, Robertson I, Siegwolf R, Leuenberger M (1998) Oxygen Isotope Analysis of Cellulose: An Interlaboratory Comparison. Anal Chem 70:2074–2080. https://doi.org/10.1021/ac971022f

Savolainen O, Pyhäjärvi T, Knürr T (2007) Gene flow and local adaptation in trees. Annu. Rev. Ecol. Evol. System 595–619. https://doi.org/10.1146/annurev.ecolsys. 38. 091206.095646

Scheidegger Y, Saurer M, Bahn M, Siegwolf R (2000) Linking stable oxygen and carbon isotopes with stomatal conductance and photosynthetic capacity: a conceptual model. Oecologia 125:350–357. https://doi.org/10.1007/s004420000466

Schweitzer JA, Bailey JK, Fischer DG, LeRoy CJ, Lonsdorf EV, Whitham TG, Hart SC (2008) Plant-soil-microorganism interactions: heritable relationship between plant genotype and associated soil microorganisms. Ecology 89: 773–781. http://www.jstor.org/stable/27651599

Schweingruber FH (1997) Tree-rings and environment: Dendroecology. Berne, Stuttgart, Vienna: Paul Haupt Publisher. https://doi.org/10.1111/j.1469-8137.1998.149-8.x

Seibt U, Rajabi A, Griffiths H, Berry JA (2008) Carbon isotopes and water use \ efficiency: Sense and sensitivity. Oecologia 155:441–454. https://doi.org/10.1007/s00442-007-0932-7

Siegwolf RTW, Brooks JR, Roden J, Saurer M (2022) Stable Isotopes in Tree Rings. Inferring Physiological, Climatic and Environmental Responses. Springer. 879. https://doi.org/10.1007/978-3-030-92698-4

Sternberg L (1989) Oxygen and hydrogen isotope ratios in plant cellulose: mechanisms and applications. In: Rundel PW, Ehleringer JR, Nagy KA (eds) Stable isotopes in ecological research. Springer, New York. https://doi.org/10.1002/9780470015902.a0021231.pub2

Sternberg L, Deniro MJ, Keeley JE (1984) Hydrogen, oxygen, and carbon isotope ratios of cellulose from submerged aquatic crassulacean Acid metabolism and non-crassulacean Acid metabolism plants. Plant Physiology 76(1):68-70. https://doi.org/10.1104/pp.76.1.68

Szejner P, Wright W, Babst F, Belmecheri S, Trouet V, Leavitt S, Ehleringer J, Monson R (2016) Latitudinal gradients in tree ring stable carbon and oxygen isotopes reveal differential climate influences of the North American Monsoon System. Journal of Geophysical Research: Biogeosciences 121:1978-1991. https://doi.org/10.1002/2016JG003460

Voelker SL, Meinzer FC, Lachenbruch B, Renée Brooks J, Guyette RP (2014) Drivers of radial growth and carbon isotope discrimination of bur oak (*Quercus macrocarpa Michx*.) across continental gradients in precipitation, vapour pressure deficit and irradiance. Plant, Cell and Environment 37, 766–779. https://doi.org/10.1111/pce.12196

Wang SY, Gillies RR, Jin J, Hipps LE (2009) Recent rainfall cycle in the Intermountain Region as a quadrature amplitude modulation from the Pacific decadal oscillation. Geophys Res   Lett 36:1–6. https://doi.org/10.1029/2008GL036329

Warren CR, McGrath JF, Adams MA (2001) Water availability and carbon isotope discrimination in conifers. Oecologia 127:476–486. https://doi.org/10.1007/s004420000609

Waterhouse J., Barker AC, Carter AHC (2000) Stable Carbon Isotopes in Scots Pine Tree Rings Preserve a Record of Flow of the River Ob. Geophysical Research Letters 21:3529–3532. https://doi.org/10.1029/2000GL006106

Weigt RB, Streit K, Saurer M, Siegwolf RTW (2017) The influence of increasing temperature and CO_2 concentration on recent growth of old-growth larch: contrasting responses at leaf and stem processes derived from tree-ring width and stable isotopes. Tree Physiology 38: 706–720. https://doi.org/10.1093/treephys/tpx148

Werner RA, Buchmann N, Siegwolf RTW, Kornexl BE, Gessler A (2011) Metabolic fluxes, carbon isotope fractionation and respiration—lessons to be learned from plant biochemistry. New Phytol 191:10–15. https://doi.org/10.1111/j.1469-8137.2011.03741.x

Western Regional Climate Center (WRCC). (2010) http://www.wrcc.dri.edu

Whitham TG, DiFazio SP, Schweitzer JA, Shuster SM, Allan GJ, Bailey JK, Woolbright SA (2008) Extending genomics to natural communities and ecosystems. Science 320: 492–495. https://doi.org/10.1126/science.1153918

Whitham TG, Gehring CA, Bothwell HM, Cooper HF, Hull JB, Allan GJ, Grady KC, Markovchick L, Shuster SM, Parker J, Cadmus AE, Ikeda DH, Bangert RK, Hultine KR, Blasini DE (2020). Using the Southwest Experimental Garden Array to enhance riparian restoration in response to global change: identifying and deploying genotypes and populations for current and future environments. In Riparian Research and Management: Past, Present, Future, Vol. 2, ed. SW Carothers, RR Johnson, DM Finch, KJ Kingsley, RH Hamre, pp. 63–79. Gen. Tech. Rep. RMRS-GTR-411. Fort Collins, CO: U.S. Dep. Agric. For. Serv. Rocky Mt. Res. Stn

Yakir D, DeNiro MJ (1990) Oxygen and Hydrogen Isotope Fractionation during Cellulose Metabolism in *Lemna gibba* L. Plant Physiol 93:325–332. https://doi.org/10.1104/pp.93.1.325

Yang R, Zhao F, Fan Z, Panthi S, Fu P, Bräuning A, Grießinger J, Li Z (2022) Long-term growth trends of *Abies delavayi* and its physiological responses to a warming climate in the Cangshan Mountains, southwestern China. Forest Ecology and Management 505. https://doi.org/10.1016/j.foreco.2021.119943

Zeppel M, Eamus D (2008) Coordination of leaf area, sapwood area and canopy conductance lead to species convergence of tree water use in a remnant evergreen woodland. Aust. J. Bot. 56:97–108. https://doi.org/10.1071/BT07091

5. DISSERTATION SUMMARY

The investigations presented in this dissertation greatly improve our understanding of the morpho-physiological mechanisms responsible for adaptation to local climate conditions in the foundation species *Populus fremontii* throughout its geographical range. The results of these studies simultaneously offer a more complete picture of the impact that climate change will have on this species' survival while identifying the different set of functional traits expressed in genotypes that could be used in future restoration efforts.

The use of the Agua Fria National Monument common garden allowed the elimination of the environmental variations that exist among these provenances that collectively represent a significant portion of the entire elevational and climatic range of the species. In the second chapter of this dissertation, I used an experimental common garden located in the mid-point of the species' elevational and climatic distribution to complete the most extensive morpho-physiological functional trait study on this *P. fremontii* to date. I found that throughout its climatic range, this species exhibits highly specialized coordinated set of traits that explain local climatic adaptation across multiple scales from epidermal tissue to individual organ and whole-plant level. Specifically, I could identify two distinct ecotypes each with its own suite of adaptive traits (adaptive trait syndrome) reflecting adaptation to two extremely different regional environmental conditions. While the Mogollon rim ecotype exhibited trait coordination reflecting adaptation to survive freezing temperatures, the lower Sonoran Desert ecotype displayed a set of traits that enhance foliar thermal protection through greater water transport efficiency. Additionally, this study detected finer variations in trait coordination revealing

more localized set of adaptation strategies to the local climatic conditions found at the populations level. Through this study, it was demonstrated the relevancy of the use of multiple functional trait spectra in single species studies to increase our understanding of the mechanisms behind local adaptation. These findings are key for improved estimates of how increases in regional mean annual temperatures will affect this species across its geographic range and what types of traits and consequently what genotypes will have greater resilience to the effect of climate change. Accordingly, these findings can provide crucial information to establish general guidelines determining the selection of genotypes to be included in future restoration efforts in the region.

By conducting a leaf thermoregulation study in the same common garden and with the same populations used in my second chapter, I could find further evidence of the high level of climate-driven adaptation that *P. fremontii* exhibits through its entire climatic range. Specifically, in this third chapter I found that genotypes sourced from places where maximum summer temperatures exceed 40 °C display significant cooler leaves temperatures (3.8 °C) than genotypes sourced from provenances with cooler temperatures. In this study, it was revealed that the combination of several morphological traits, higher stomatal canopy conductance, and lower mid-day water potential were positively correlated with cooler leaf temperatures. These results suggest that genotypes adapted to extreme temperatures rely on a suite of morpho-physiological and hydraulic strategies that provide canopy thermal regulation via the combined effect of transpirational cooling and the reduction of leaf radiative load gains. This strategy could result in greater susceptibility of these genotypes to experience hydraulic failure if extreme thermal events are coupled with drier conditions. Because the Southwest United

States is becoming increasingly hotter and drier as a direct effect of global climate change (Garfin *et al.* 2013, USGCR 2017), this investigation describes the potential mechanisms in which hotter air temperature and drier condition could lead to episodic mortality events in *P. freemontii* genotypes found at the hottest edge of its climatic distribution. Thus, this study reveals the future hydraulic niche limitations that this species will face in places in the lower Sonoran Desert where water might become absent during the hotter times of the year.

Through a multi-year study of tree growth and physiological responses estimated from tree-ring isotope measurements in a common garden located at the hot edge of *P. fremontii's* thermal distribution, I identified the potential negative effects that long-term exposure to extreme hot temperatures can have on growth in genotypes sourced from provenances with cooler mean annual maximum temperature (MAMT) than the garden. The reduction in growth in these genotypes could have been caused by the combined effect of high photorespiration levels and low net photosynthetic rates caused by high leaf temperatures. Genotypes sourced from cooler provenances experienced temperature increases comparable to the expected regional changes in the Southwest United States. Therefore, this investigation simultaneously improves our understanding of how climate change might affect above ground net primary productivity in *P. fremontii* while identifying which genotypes might be better fit to grow in future warmer conditions.

To expand on the work presented in this dissertation, I recommended establishing long-term morpho-physiological studies replicating and expanding the work presented in this dissertation. In this way, we could have a more complete picture of the cumulative effect that climate change will have on this species at population level. Particularly, long-

term morpho-physiological studies using genotypes through their different developmental stages, from seedling to mature trees, would be a powerful tool to have a more comprehensive picture of the effect that climate change can have on this species. Also, it would be recommended to study additional morpho-physiological traits that could further increase our understanding of how extreme temperature and drought could affect *P. fremontii* through its climatic range. For instance, because of the high sensibility of light harvesting complexes of photosystem II to thermal stress (Yamada et al. 1996; Weng et al. 2005), measurements of chlorophyll a fluorescence could be used to estimate leaf thermal tolerance among different *P. fremontii* populations. Also, hydraulic functional traits like the stem xylem vulnerability to cavitation or the leaf turgor loss point which indicates the capacity of a plant to keep cell turgor pressure under water stress (Zhu et al. 2018) could greatly improve our understanding of the intraspecific differences in drought tolerance in *P. fremontii*. Finally, to have a more realistic picture of the combined effect that extreme temperatures and drought will have on this *P. fremontii*, it would be recommended to expose genotypes sourced from provenance representing the entire climatic range of the species to experimental climate warming using whole-tree chambers where air temperature, CO_2 and VPD can be gradually modified. This type of study combined with gradual drought treatments would provide a much accurate view of the impact that climate change will have on this species' survival while shedding light on the potential physiological responses that this species might display to the combined stress caused by extreme temperatures and drier conditions.

REFERENCES

Ackerly D, Knight C, Weiss S, Barton K, Starmer K (2002) Leaf size, specific leaf area and microhabitat distribution of chaparral woody plants: Contrasting patterns in species level and community level analyses. Oecologia 130(3), 449–457. https://doi.org/10.1007/s004420100805

Aitken SN, Yeaman S, Holliday JA, Wang T, Curtis-McLane S (2008) Adaptation, migration or extirpation: climate change outcomes for tree populations. Evol Appl. 1(1):95–111. https://doi.org/10.1111/j.1752-4571.2007.00013.x

Adams HD, Guardiola-Claramonte M, Barron-Gafford GA, Villegas JC, Breshears DD, Zou CB, Troch PA, Huxman TE (2009) Temperature sensitivity of drought-induced tree mortality portends increased regional die-off under global-change-type drought. Proceedings of the National Academy of Sciences of the United States of America 106:7063–6. https://doi.org/10.1890/ES15-00203.1

Addington RN, Mitchell RJ, Oren R, Donovan LA (2004) Stomatal sensitivity to vapor pressure deficit and its relationship to hydraulic conductance in *Pinus palustris*. Tree Physiology 24:561–569. https://doi.org/10.1093/treephys/24.5.561

Allakhverdiev SI, Kreslavski VD, Klimov VV, Los DA, Carpentier R, Mohanty P (2008) Heat stress: An overview of molecular responses in photosynthesis. Photosynthesis Research 98(1–3), 541–550. https://doi.org/10.1007/s11120-008-9331-0

Allen CD, Breshears DD (1998) Drought-induced shift of a forest-woodland ecotone: rapid landscape response to climate variation. Proceedings of the National Academy of Science of the United States of America 95:14839–42. https://doi.org/10.1073/pnas.95.25.14839

Allen CD, Macalady AK, Chenchouni H, Bachelet D, McDowell N, Vennetier M, Kitzberger T, Rigling A, Breshears DV, Hogg EH, Gonzalez P, Fensham R, Zhang Z, Castro J, Demidova N, Lim JH, Allard G, Running SW, Semerci A, Cobb N (2010) A global overview of drought and heat-induced tree mortality reveals emerging climate change risks for forests. Forest Ecology and Management 259(4): 660–684. https://doi.org/10.1016/j.foreco.2009.09.001

Améglio T, Cochard H, Ewers FW (2001) Stem diameter variations and cold hardiness in walnut trees. Journal of Experimental Botany *52*(364), 2135–2142. https://doi.org/10.1093/jexbot/52.364.2135

Anchukaitis KJ, Evans MN, Wheelwright NT, Schrag DP (2008) Stable isotope chronology and climate signal calibration in neo-tropical montane cloud forest trees. J Geophys Res 113:03030. https://doi.org/10.1029/2007JG000613

Anderson MJ (2001) A new method for non-parametric multivariate analysis of variance. Austral Ecology *26*(1), 32–46. https://doi.org/10.1046/j.1442-9993.2001.01070.x

Ansley R.J, Mirik M, Surber BW, Park SC (2012) Canopy Area and Aboveground Mass of Individual Redberry Juniper (*Juniperus pinchotii*) Trees. Rangeland Ecology & Management 65, 189–195. https://doi.org/10.2307/41495360

Aparecido LMT, Woo S, Suazo C, Hultine KR, Blonder B (2020) High water use in desert plants exposed to extreme heat. Ecology Letters 23, 1189–1200. https://doi.org/10.1111/ele.13516

Atkin OK, Bloomfield KJ, Reich PB, Tjoelker MG, Asner GP, Bonal D, … Zaragoza-Castells J (2015) Global variability in leaf respiration in relation to climate, plant functional types and leaf traits. New Phytologist 206, 614–636. https://doi.org/10.1111/nph.13253

Atkin OK, Scheurwate RI, Pons TL (2006) High thermal acclimation potential of both photosynthesis and respiration in two lowland *Plantago* species in contrast to an alpine congeneric. Global Change Biology 12, 500-515. https://doi.org/10.1111/j.1365-2486.2006.01114.x

Akin OK, Tjoelker MG (2003) Thermal acclimation and the dynamic response of plant respiration to temperature. Trends Plant Sci. 8, 343–351. https://doi.org/10.1016/S1360-1385(03)00136-5

Archer SR, Predick KI (2008). Climate Change and Ecosystems of the Southwestern. United States Rangelands 30(3):23–28. https://doi.org/10.2111/1551-501X(2008)30[23:CCAEOT]2.0.CO;2

Arco Molina JG, Hadad MA, Patón Domínguez D, Roig FA (2016) Tree age and bark thickness as traits linked to frost ring probability on *Araucaria araucana* trees in northern Patagonia. Dendrochronologia 37, 116–125. https://doi.org/10.1016/j.dendro.2016.01.003

Armond UA, Bjorkman O, Staehelin LA (1980) Dissociation of supramolecular complexes in chloroplast membranes a manifestation of heat damage to the photosynthetic apparatus. Biochimica et Biophysica Acta 601, 433-442. https://doi.org/10.1016/0005-2736(80)90547-7

Bailey JK, Bangert RK, Schweitzer JA, Trotter RT, Shuster SM, Whitham TG (2004) Fractal geometry is heritable in trees. Evolution 58(9), 2100–2102. https://doi.org/10.1111/j.0014-3820.2004.tb00493.x

Barbour MA, Rodriguez-Cabal MA, Wu ET, Julkunen-Tiitto R, Ritland CE, Miscampbell AE, Jules ES, Crutsinger GM (2015) Multiple plant traits shape the genetic basis of herbivore community assembly. Functional Ecology 29(8), 995–1006. https://doi.org/10.1111/1365-2435.12409

Bates D, Mächler M, Bolker B, Walker S (2015) Fitting linear mixed-effects models using lme4. Journal of Statistical Software 67(1). https://doi.org/10.18637/jss.v067.i011

Blasini, DE, Koepke DF, Bush, SE, Allan GJ, Gehring CA, Whitham TG, Day T, Hultine KR (2022) Tradeoffs between leaf cooling and hydraulic safety in a dominant arid land riparian tree species. Plant, Cell and Environment 1–18. https://doi.org/10.1111/pce.14292

Blasini DE, Koepke DF, Grady KC, Allan GJ, Gehring CA, Whitham TG, Cushman SA, Hultine KR (2020) Adaptive trait syndromes along multiple economic spectra define cold and warm adapted ecotypes in a widely distributed foundation tree species. Journal of Ecology 1–21. https://doi.org/10.1111/1365-2745.13557

Borcard D, Gillet F, Legendre P (2011) Numerical ecology with R. Springer. https://doi.org/10.1007/978-1-4419-7976-6

Breshears DD, Adams HD, Eamus D, McDowell NG, Law DJ, Will RE, Williams AP, Zou CB (2013) The critical amplifying role of increasing atmospheric moisture demand on tree mortality and associated regional die-off. Frontiers in Plant Science 4, 266. https://doi.org/10.3389/fpls.2013.00266

Breshears DD, Myers OB, Meyer CW, Barnes FJ, Zou CB, Allen CD, McDowell NG, Pockman, WT (2009) Tree die-off in response to global change-type drought: mortality insights from a decade of plant water potential measurements. Frontiers in Ecology and the Environment 7, 185-189. https://esajournals.onlinelibrary.wiley.com/doi/abs/10.1890/080016

Buesa RJ, Peshkov MV (2009) Histology without xylene. Annals of Diagnostic Pathology 13(4), 246–256. https://doi.org/10.1016/j.anndiagpath.2008.12.005

Cailleret M, Jansen S, Robert EMR, Desoto L, Aakala T, Antos JA, Beikircher B, Bigler C, Bugmann H, Caccianiga M, Čada V, Camarero JJ, Cherubini P, Cochard H, Coyea MR, Čufar K, Das AJ, Davi H, Delzon S, Dorman M, Gea-Izquierdo G, Gillner S, Haavik LJ, Hartmann H, Hereş AM, Hultine KR, Janda P, Kane JM, Kharuk VI, Kitzberger T, Klein T, Kramer K, Lens F, Levanic T, Linares Calderon JC, Lloret F, Lobo-Do-Vale R, Lombardi F, López Rodríguez R, Mäkinen H, Mayr S, Mészáros I, Metsaranta JM, Minunno F, Oberhuber W, Papadopoulos A, Peltoniemi M, Petritan AM, Rohner B, Sangüesa-Barreda G, Sarris D, Smith JM, Stan AB, Sterck F, Stojanović DB, Suarez ML, Svoboda M, Tognetti R, Torres-Ruiz JM, Trotsiuk V, Villalba R, Vodde F, Westwood AR, Wyckoff PH, Zafirov N, Martínez-Vilalta, J (2017) A synthesis of radial growth patterns preceding tree mortality. Global Change Biology 23: 1675–1690. https://doi.org/10.1111/gcb.13535

Campbell G, Norman J (1998) An Introduction to Environmental Biophysics, 2nd ed. Springer-Verlag New York, New York. https://doi.org/10.1007/978-1-4612-1626-1

Carter JL, White DA (2009) Plasticity in the Huber value contributes to homeostasis in leaf water relations of a mallee Eucalypt with variation to groundwater depth. Tree Physiology 29(11), 1407–1418. https://doi.org/10.1093/treephys/tpp076

Cavanagh AP, Kubien DS (2014) Can phenotypic plasticity in Rubisco performance contribute to photosynthetic acclimation? Photosynthesis Research 119, 203-214. https://doi.org/10.1007/s11120-013-9816-3

Cen YP, Sage RF (2005) The Regulation of Rubisco Activity in Response to Variation in Temperature and Atmospheric CO_2 Partial Pressure in Sweet Potato. Plant Physiology 139, 979–990. https://doi.org/10.1104/pp.105.066233

Cernusak LA, Tcherkez G, Keitel C, Cornwell WK, Louis D, Santiago E, Knohl FA, Barbour AM, Williams DG, Reich PB, Ellsworth DS, Dawson TE, Griffiths HG, Farquhar GD, Wright IJ (2009) Why are non-photosynthetic tissues generally C-13 enriched compared with leaves in C-3 plants? Review and synthesis of current hypotheses. Functional Plant Biology 36:199–213. https://doi.org/10.1071/FP08216

Chapin FS, Autumn K, Pugnaire S (1993) Evolution of Suites of Traits in Response to Environmental Stress. The American Naturalist 142: S78-S92. https://doi.org/10.1086/285524

Chapin FS, Matson PA, Vitousek PM (2011) Principles of terrestrial ecosystem ecology. Springer. https://doi.org/10.1007/978-1-4419-9504-9

Charrier G, Nolf M, Leitinger G, Charra-Vaskou K, Losso A, Tappeiner U, Améglio T, Mayr S (2017) Monitoring of freezing dynamics in trees: A simple phase shift causes complexity. Plant Physiology 173(4), 2196–2207. https://doi.org/10.1104/pp.16.0181

Chave J, Coomes D, Jansen S, Lewis SL, Swenson NG, Zanne AE (2009) Towards a worldwide wood economics spectrum. Ecology Letters 12(4), 351–366. https://doi.org/10.1111/j.1461-0248.2009.01285.x

Choat B, Jansen S, Brodribb TJ, Cochard H, Delzon S, Bhaskar R, Bucci SJ, Feild TS, Gleason SM, Hacke UG, Jacobsen AL, Lens F, Maherali H, Martínez-Vilalta J, Mayr S, Mencuccini M, Mitchell PJ, Nardini A, Pittermann J, … Zanne AE (2012) Global convergence in the vulnerability of forests to drought. Nature 491(7426), 752–755. https://doi.org/10.1038/nature11688

Clausen J, Keck DD, Hiesey WM (1940) Experimental studies on the nature of species. Effect of varied environments on western North American plants. Carnegie Institution of Washington Publication. https://doi.org/10.1086/280930

Cochard H, Forestier S, Améglio T (2001) A new validation of the Scholander pressure chamber technique based on stem diameter variations. Journal of Experimental Botany *52*(359), 1361–1365. https://doi.org/10.1093/jexbot/52.359.1361

Compson ZG, Larson KC, Zinkgraf MS, Whitham TG (2011) A genetic basis for the manipulation of sink–source relationships by the galling aphid *Pemphigus batae*. Oecologia 167(3), 711–721. https://doi.org/10.1007/s00442-011-2033-x

Cooper HF, Best RJ, Andrews LV, Corbin JPM, Garthwaite I, Grady KC, Gehring CA, Hultine KR, Whitham TG, Allan GJ (2022) Evidence of climate-driven selection on tree traits and trait plasticity across the climatic range of a riparian foundation species. Molecular Ecology, 00, 1–17. https://doi.org/10.1111/mec.16645

Cooper HF, Grady KC, Cowan JA, Best RJ, Allan GJ, Whitham TG (2019) Genotypic variation in phenological plasticity: Reciprocal common gardens reveal adaptive responses to warmer springs but not to fall frost. Global Change Biology 25(1), 187–200. https://doi.org/10.1111/gcb.14494

Cornelissen JHC (1999) A triangular relationship between leaf size and seed size among woody species: Allometry, ontogeny, ecology and taxonomy. Oecologia 118(2), 248–255. https://doi.org/10.1007/s004420050725

Cornelissen JHC, Lavorel S, Garnier E, Díaz S, Buchmann N, Gurvich DE, Reich PB, Steege HT, Morgan HD, Heijden MG, Pausas JG, Poorter H (2003) Handbook of protocols for standardised and easy measurement of plant functional traits worldwide. Australian Journal of Botany 51(4), 335–380. https://doi.org/10.1071/BT02124

Corner EJH (1949) The Durian theory or the origin of the modern tree. Annals of Botany 13(4), 367–414. https://doi.org/10.1093/oxfordjournals.aob.a083225

Curtis EM, Leigh A, Rayburg S (2012) Relationships among leaf traits of Australian arid zone plants: alternative modes of thermal protection. Australian Journal of Botany 60, 471–483. https://doi.org/10.1071/BT11284

Cushman SA, Max T, Meneses N, Evans LM, Ferrier S, Honchak B, Whitham TG, Allan GJ (2014) Landscape genetic connectivity in a riparian foundation tree is jointly driven by climatic gradients and river networks. Ecological Applications 24, 1000–1014. https://doi.org/10.1890/13-1612.1

Dawson TE, Ehleringer JR (1993) Isotopic enrichment of water in the woody tissues of plants implications for plant water source, water uptake, and other studies which use the stable isotopic composition of cellulose. Geochim Cosmochim Acta 57:3487–3492. https://doi.org/10.1016/0016-7037(93)90554-A

de Villemereuil P, Schielzeth H, Nakagawa S, Morrissey M (2016) General methods for evolutionary quantitative genetic inference from generalized mixed models. Genetics 204(3), 1281–1294. https://doi.org/10.1534/genetics.115.186536

Denny EG, Gerst KL, Miller-Rushing AJ, Tierney GL, Crimmins TM, Enquist CAF, Guertin P, Rosemartin AH, Schwartz MD, Thomas KA, Weltzin JF (2014) Standardized phenology monitoring methods to track plant and animal activity for science and resource management applications. International Journal of Biometeorology 58(4), 591–601. https://doi.org/10.1007/s00484-014-0789-5\

Diaz S, Kattge K, Cornelissen JH, Wright IJ, Lavorel S, Dray S, Reu B, Kleyer M, Wirth C, Prentice IC, Garnier E, Bonisch G, Westoby M, Poorter H, Reich PB, Moles AT, Dickie J, Gillison AN, Zanne AE, Chave J, Wright SJ, Sheremet'ev SN, Jactel H, Baraloto C, Cerabolini B, Pierce S, Shipley B, Kirkup D, Casanoves F, Joswig JS, Gunther A, Falczuk V, Ruger N, Mahecha MD, Gorne LD (2016) The global spectrum of plant form and function. Nature 529, 167–171. https://doi.org/10.1038/nature16489

Diffenbaugh NS, Ashfaq M, Scherer M (2011) Transient regional climate change: Analysis of the summer climate response in a high-resolution, century-scale ensemble experiment over the continental United States. Journal of geophysical research 116, D24111. https://doi.org/10.1029/2011JD016458

Domec JC, Noormets A, King JS, Sun G, McNulty SG, Gavazzi MJ, Boggs JL, Treasure EA (2009) Decoupling the influence of leaf and root hydraulic conductances on stomatal conductance and its sensitivity to vapour pressure deficit as a soil dries in a drained loblolly pine plantation. Plant Cell and Environment 32, 980–991. https://doi.org/10.1111/j.1365–3040.2009.01981.x

Dong N, Prentice IC, Harrison SP, Song QH, Zhang YP (2017) Biophysical homoeostasis of leaf temperature: A neglected process for vegetation and land-surface modelling. Global Ecology and Biogeography 26, 998–1007. https://doi.org/10.1111/geb.12614

Drake JE, Tjoelker MG, Vårhammar A, Medlyn BE, Reich PB, Leigh A, Pfautsch S, Blackman CJ, López R, Aspinwall MJ, Crous KY, Duursma RA, Kumarathunge D, De Kauwe MG, Jiang M, Nicotra AB, Tissue DT, Choat B, Atkin OK, Barton CVM (2018) Trees tolerate an extreme heatwave via sustained transpirational cooling and increased leaf thermal tolerance. Global Change Biology 24(6), 2390–2402. https://doi.org/10.1111/gcb.14037

Eamus D, O'Grady AP, Hutley L (2000) Dry season conditions determine wet season water use in the wet-tropical savannas of northern Australia. Tree Physiology 20(18), 1219–1226. https://doi.org/10.1093/treephys/20.18.1219

Eckenwalder JE (1996). Systematics and evolution of *Populus*. I. In Stettler RF, Bradshaw HD, Heilman PE, Hinckley TM (Eds), Biology of *Populus* and its implications for management and conservation: 7–32. NRC Research Press.

Eguchi N, Morii N, Ueda T, Funada R, Takagi K, Hiura T, Sasa K, Koike T (2008) Changes in petiole hydraulic properties and leaf water flow in birch and oak saplings in a CO2-enriched atmosphere. Tree Physiology 28(2), 287–295. https://doi.org/10.1093/treephys/28.2.287

Ehleringer JR, Cerling TE (1995) Atmospheric CO2 and the ratio of intercellular to ambient CO_2 concentrations in plants. Tree Physiol 15:105–11. https://doi.org/110.1093/treephys/15.2.105

Eilmann B, Zweifel R, Buchmann N, Graf Pannatier E, Rigling A (2011) Drought alters timing, quantity, and quality of wood formation in Scots pine. Journal of Experimental Botany 62(8), 2763–2771. https://doi.org/10.1093/jxb/erq443

Evans LM, Kaluthota S, Pearce DW, Allan GJ, Floate K, Rood SB, Whitham TG (2016) Bud phenology and growth are subject to divergent selection across a latitudinal gradient in *Populus angustifolia* and impact adaptation across the distributional range and associated arthropods. Ecology and Evolution 6(13), 4565–4581. https://doi.org/10.1002/ece3.2222

Farquhar GD, Ehleringer JR, Hubick KT (1989) Carbon Isotope Discrimination and Photosynthesis. Annual Review of Plant Physiology and Plant Molecular Biology 40:1, 503–537. https://doi.org/10.1146/annurev.pp.40.060189.002443

Farquhar GD, Lloyd J (1993) Carbon and oxygen isotope effects in the exchange of carbon dioxide between terrestrial plants and the atmosphere. Stable Isot Plant Carbon-water Relations 47–70. https://doi.org/10.1016/B978-0-08-091801-3.50011-8

Farquhar GD, O'Leary MH, Berry JA (1982) On the relationship between carbon isotope discrimination and the inter-cellular carbon-dioxide concentration in leaves. Aust J Plant Physiol 9:121–137. https://doi.org/10.1071/PP9820121

Farquhar GD, Sharkey TD (1982) Stomatal conductance and photosynthesis. Annual Review of Plant Physiology 33, 317–345. https://doi.org/10.1146/annurev.pp.33.060182.001533

Fauset S, Freitas HC, Galbraith DR, Sullivan MJP, Aidar MPM, Joly C.A, … Gloor MU (2018) Differences in leaf thermoregulation and water use strategies between three co-occurring Atlantic forest tree species: Leaf energy balance of Atlantic forest trees. Plant, Cell and Environment 41, 1618–1631. https://doi.org/10.1111/pce.13208

Fischer DG, Wimp GM, Hersch-Green E, Bangert RK, LeRoy CJ, Bailey JK, Schweitzer JA, Dirks C, Hart SC, Allan GJ, Whitham TG (2017) Tree genetics strongly affect forest productivity, but intraspecific diversity–productivity relationships do not. Functional Ecology 31(2), 520–529. https://doi.org/10.1111/1365-2435.12733

Francey RJ, Farquhar GD (1982) An explanation of 13C/12C variations in tree rings. Nature 297:28–31. https://doi.org/10.1038/297028a0

Frank KA, Maroulis SJ, Duong MQ, Kelcey BM (2013) What Would It Take to Change an Inference? Using Rubin's Causal Model to Interpret the Robustness of Causal Inferences. Educational Evaluation and Policy Analysis 35(4),437-460. https://doi.org/10.3102/0162373713493129

Franks PJ, Farquhar GD (2007) The mechanical diversity of stomata and its significance in gas-exchange control. Plant Physiology 143(1), 78–87. https://doi.org/10.1104/pp.106.089367

Franks PJ, Farquhar GD (2001) The effect of exogenous abscisic acid on stomatal development, stomatal mechanics, and leaf gas exchange in *Tradescantia virginiana*. Plant Physiology 125(2), 935–942. https://doi.org/10.1104/pp.125.2.935

Franks SJ, Weber JJ, Aitken SN (2014) Evolutionary and plastic responses to climate change in terrestrial plant populations. Evolutionary Applications 7, 123–139. https://doi.org/10.1111/eva.12112

Freschet GT, Cornelissen JHC, van Logtestijn RSP, Aerts R (2010) Evidence of the 'plant economics spectrum' in a subarctic flora. Journal of Ecology 98(2), 362–373. https://doi.org/10.1111/j.1365-2745.2009.01615.x

Friedman JM, Roelle JE, Cade BS (2011) Genetic and environmental influences on leaf phenology and cold hardiness of native and introduced riparian trees. International Journal of Biometeorology 55(6), 775–787. https://doi.org/10.1007/s00484-011-0494-6

Galmés J, Hermida-Carrera C, Laanisto L, Niinemets Ü (2016) A compendium of temperature responses of Rubisco kinetic traits: variability among and within photosynthetic groups and impacts on photosynthesis modeling. J Exp Bot 67, 5067–5091. https://doi.org/10.1093/jxb/erw267

Garfin G, Jardine A, Merideth R, Black M, LeRoy S (Eds.) (2013) Assessment of Climate Change in the Southwest United States. Natl Clim Assess Reg Tech Input Rep Ser Assess 531. https://doi.org/10.5822/978-1-61091-484-0

Gärtner H, Lucchinetti S, Schweingruber FH (2014) New perspectives for wood anatomical analysis in dendrosciences: The GSL1-microtome. Dendrochronologia 32(1), 47–51. https://doi.org/10.1016/j.dendro.2013.07.002

Gazal RM, Scott RL, Goodrich DC, Williams DG (2006) Controls on transpiration in a semiarid riparian cottonwood forest. Agricultural and Forest Meteorology 137(1–2), 56–67. https://doi.org/10.1016/j.agrformet.2006.03.002

Germino MJ, Moser AM, Sands AR (2019) Adaptive variation, including local adaptation, requires decades to become evident in common gardens. Ecological Applications 29(2), 1–7. https://doi.org/10.1002/eap.1842

Gessler A, Brandes E, Buchmann N, Helle G, Rennenberg H, Barnard RL (2009) Tracing carbon and oxygen isotope signals from newly assimilated sugars in the leaves to the tree-ring archive. Plant Cell and Environment 32(7):780-95. https://doi.org/10.1111/j.1365-3040.2009.01957.x

Gessler A, Brandes E, Keitel C, Boda S, Kayler Z, Granier A, Barbour M, Farquhar GD, Treydte K (2013) The oxygen isotope enrichment of leaf-exported assimilates—does it always reflect lamina leaf water enrichment? New Phytol 200:144–157. https://doi.org/10.1111/nph.12359

Gessler A, Ferrio JP, Hommel R, Hommel R, Treydte K, Werner RA, Monson RK (2014) Stable isotopes in tree rings: Towards a mechanistic understanding of isotope fractionation and mixing processes from the leaves to the wood. Tree Physiol 34:796–818. https://doi.org/10.1093/treephys/tpu040

Gielen B, Liberloo M, Bogaert J, Calfapietra C, DeAngelis P, Miglietta F, Scarascia-Mugnozza G, Ceulemans R (2003) Three years of free-air CO2 enrichment (POPFACE) only slightly affect profiles of light and leaf characteristics in closed canopies of *Populus*. Global Change Biology 9, 1022–1037. https://doi.org/10.1046/j.1365-2486.2003.00644.x

Gitlin AR, Sthultz CM, Bowker MA, Stumpf S, Paxton KL, Kennedy K, Muñoz A, Bailey JK, Whitham TG (2006) Mortality gradients within and among dominant plant populations as barometers of ecosystem change during extreme drought. Conservation Biology 20, 1477–86. https://doi.org/10.1111/j.1523-1739.2006.00424.x

Gleason SM, Butler DW, Waryszak P (2013) Shifts in leaf and stem hydraulic traits across aridity gradients in eastern Australia. International Journal of Plant Sciences 174, 1292–130. https://doi.org/10.1086/673239

Gleason SM, Butler DW, Ziemińska K, Waryszak P, Westoby M (2012) Stem xylem conductivity is key to plant water balance across Australian angiosperm species: Plant stem hydraulic traits. Functional Ecology 26(2), 343–352. https://doi.org/10.1111/j.1365-2435.2012.01962.x

Glenn EP, Nagler PL (2005) Comparative ecophysiology of *Tamarix ramosissima* and native trees in western US riparian zones. J Arid Environ 61: 419–46. https://doi.org/10.1016/j.jaridenv.2004.09.025

Gottlicher S, Knohl A, Wanek W, Buchmann N, Richter A (2006) Short term changes in carbon isotope composition of soluble carbohydrates and starch: from canopy leaves to the root system. Rapid Commun Mass Spectrom 20:653–660. https://doi.org/10.1002/rcm.2352

Grady KC, Ferrier SM, Kolb TE, Hart S, Allan G, Whitham T (2011) Genetic variation in productivity of foundation riparian species at the edge of their distribution: Implications for restoration and assisted migration in a warming climate. Global Change Biology 17(12):3724-3735. https://doi.org/10.1111/j.1365-2486.2011.02524.x

Grady KC, Kolb TE, Ikeda DH, Whitham TG (2015) A bridge too far: Cold and pathogen constraints to assisted migration of riparian forests: Assisted migration in riparian restoration. Restoration Ecology 23(6), 811–820. https://doi.org/10.1111/rec.12245

Grady KC, Laughlin DC, Ferrier SM, Kolb TE, Hart S, Allan G, Whitham T (2013) Conservative leaf economic traits correlate with fast growth of genotypes of a foundation riparian species near the thermal maximum extent of its geographic range. Functional Ecology 27:428–438. https://doi.org/10.1111/1365-2435.12060

Granier A (1987) Evaluation of transpiration in a Douglas-fir stand by means of sap flow measurements. Tree Physiology 4, 309–320. https://doi.org/10.1093/treephys/3.4.309

Griffin KL, Tissue DT, Turnbull MH, Schuster W, Whitehead D (2001) Leaf dark respiration as a function of canopy position in Nothofagus fusca trees grown at ambient and elevated CO_2 partial pressures for five years. Functional Ecology 15, 497– 505. https://doi.org/10.1046/j.0269-8463.2001.00539.x

Grossiord C, Buckley TN, Cernusak LA, Novick KA, Poulter B, Siegwolf RTW, Sperry JS, McDowell NG (2020) Plant responses to rising vapor pressure deficit. New Phytol 226, 1550-1566. https://doi.org/10.1111/nph.16485

Grossman GD, Nickerson DM, Freeman MC (1991) Principal component analyses of assemblage structure data: Utility of tests based on eigenvalues. Ecology 72(1), 341–347. https://doi.org/10.2307/1938927

Guerrieri R, Jennings K, Belmecheri S, Asbjornsen H, Ollinger S (2017) Evaluating climate signal recorded in tree-ring $\delta^{13}C$ and $\delta^{18}O$ values from bulk wood and α-cellulose for six species across four sites in the northeastern US. Rapid Commun Mass Spectrom. 2017:31;2081-2091. https://doi.org/10.1002/rcm.7995

Gutschick VP 2016 Leaf energy balance: basics and modeling from leaves to canopies. Dordrecht: Springer Netherlands, 23–58. https://doi.org/10.1007/978-94-017-7291-4_2

Hacke UG, Sperry JS, Pittermann J (2000) Drought experience and cavitation resistance in six shrubs from the Great Basin, Utah. Basic and Applied Ecology 1(1), 31–41. https://doi.org/10.1078/1439-1791-00006

Hacke UG, Sperry JS, Pockman WT, Davis SD, McCulloh KA (2001) Trends in wood density and structure are linked to prevention of xylem implosion by negative pressure. Oecologia 126(4), 457–461. https://doi.org/10.1007/s004420100628

Hajek P, Leuschner C, Hertel D, Delzon S, Schuldt B (2014) Tradeoffs between xylem hydraulic properties, wood anatomy and yield in *Populus*. Tree Physiology 34(7), 744–756. https://doi.org/10.1093/treephys/tpu048

Haworth M, Belcher CM, Killi D, Dewhirst RA, Materassi A, Raschi A, Centritto M (2018) Impaired photosynthesis and increased leaf construction costs may induce floral stress during episodes of global warming over macroevolutionary timescales. Scientific Reports 8(1), 6206. https://doi.org/10.1038/s41598-018-24459-z

Hazel JR (1995) Thermal adaptation in biological membranes: is home viscous adaptation the explanation? Annual Review of Physiology 57, 19–42. https://doi.org/10.1146/annurev.ph.57.030195.000315

Helle G, Schleser GH (2004) Beyond CO2-fixation by Rubisco – an interpretation of 13C/12C variations in tree rings from novel intra-seasonal studies on broad-leaf trees. Plant, Cell and Environment 27, 367–380. https://doi.org/10.1111/j.0016-8025.2003.01159.x

Helliker BR, Richter SL (2008) Subtropical to boreal convergence of tree-leaf temperatures. Nature 454, 511–514. https://doi.org/10.1038/nature07031

Hetherington AM, Woodward FI (2003) The role of stomata in sensing and driving environmental change. Nature 424, 901–908. https://doi.org/10.1038/nature01843

Hilu KW, Randall JL (1984) Convenient method for studying grass leaf epidermis. Taxon, 33(3), 413. https://doi.org/10.2307/1220980

Horton R, Buck T, Waterson P (2001) Explaining intranet use with the technology acceptance model. J Inf Technol 16, 237–249. https://doi.org/10.1080/02683960110102407

Horton JL, Kolb TE, Hart SC (2001) Responses of riparian vegetation to interannual variation in groundwater depth in a semi-arid river basin. Plant, Cell and Environment 24:293–304. https://doi.org/10.1046/j.1365-3040.2001.00681.x

Howe GT, Aitken SN, Neale DB, Jermstad KD, Wheeler NC, Chen TH (2003) From genotype to phenotype: unraveling the complexities of cold adaptation in forest trees. Can. J. Bot. 81: 1247–1266. https://doi.org/10.1139/b03-141

Hultine KR, Allan GJ, Blasini DE, Bothwell HM, Cadmus A, Cooper HF, Doughty CE, Gehring CA, Gitlin AR, Grady KC, Keith AR, Koepke DF, Markovchick L, Corbin Parker JM, Sankey TT, Whitham TG (2020) Adaptive capacity in the foundation tree species *Populus fremontii:* implications for resilience to climate change and non-native species invasion in the American Southwest. Conservation Physiology 8(1), coaa061. https://doiorg.ezproxy1.lib.asu.edu/10.1093/conphys/coaa061

Hultine KR, Bush SE (2011). Ecohydrological consequences of non-native riparian vegetation in the southwestern United States: A review from an ecophysiological perspective: Non-native species impacts on riparian ecohydrology. Water Resources Research 47(7). https://doi.org/10.1029/2010WR010317

Hultine KR, Bush SE, Ehleringer JR (2010) Ecophysiology of riparian cottonwood and willow before, during, and after two years of soil water removal. Ecological Applications, 20: 347–361. https://doi.org/10.1890/09-0492.1

Hultine KR, Burtch KG, Ehleringer JR (2013) Gender specific patterns of carbon uptake and water use in a dominant riparian tree species exposed to a warming climate. Global Change Biology 19, 3390–3405. https://doi.org/10.1111/gcb.12230

Hultine KR, Froend R, Blasini D, Bush SE, Karlinski M, Koepke DF (2019) Hydraulic traits that buffer deep-rooted plants from changes in hydrology and climate. Hydrological Processes 34(2), 209–222. https://doi.org/10.1002/hyp.13587

Hüve K, Bichelea I, Ivanovab H, Keerbergb O, Parnik T, Rasulova B, Tobias M, Niinemets U (2011) Temperature responses of dark respiration in relation to leaf sugar concentration. Physiologia Plantarum 144(4), 320–34. https://doi.org/10.1111/j.1399-3054.2011.01562.x

Huxman TE, Winkler DE, Mooney KA (2022) A common garden super-experiment: An impossible dream to inspire possible synthesis. Journal of Ecology 110, 997–1004. https://doi.org/10.1111/1365-2745.13793

Ikeda DH, Bothwell HM, Lau MK, O'Neill GA, Grady KC, Whitham TG (2014) A genetics-based Universal Community Transfer Function for predicting the impacts of climate change on future communities. Functional Ecology 28(1), 65–74. https://doi.org/10.1111/1365-2435.12151

Ikeda DH, Max TL, Allan GJ, Lau MK, Shuster SM, Whitham TG (2017) Genetically informed ecological niche models improve climate change predictions. Global Change Biology 23, 164–176. https://doi.org/10.1111/gcb.13470

IPCC. 2007. Climate Change 2007: Impacts, Adaptation and Vulnerability. Contribution of Working Group II to the Fourth Assessment Report of the Intergovernmental Panel on Climate Change. Cambridge University Press, Cambridge, UK.

Jackson DA (1993) Stopping rules in principal components analysis: A comparison of heuristical and statistical approaches. Ecology 74(8), 2204–2214. https://doi.org/10.2307/1939574

Jones DA, O'Hara KL, Battles JJ, Gersonde RF (2015) Leaf area prediction using three alternative sampling methods for seven Sierra Nevada conifer species. Forests 6(8), 2631–2654. https://doi.org/10.3390/f6082631

Jones HG (2014). Plants and microclimate: A quantitative approach to environmental plant physiology (3rd ed.). Cambridge University Press. https://doi.org/10.1017/CBO9780511845727

Johnstone JA, Roden JS, Dawson TE (2013) Oxygen and carbon stable isotopes in coast redwood tree rings respond to spring and summer climate signals, J. Geophys. Res. Biogeosci., 118, 1438–1450. https://doi.org/10.1002/jgrg.20111

Joshua Leffler A, England LE, Naito J (2000) Vulnerability of Fremont cottonwood (*Populus fremontii* Wats.) individuals to xylem cavitation. Western North American Naturalist 60(2), 204–210. https://scholarsarchive.byu.edu/wnan/vol60/iss2/10

Kannenberg SA, Driscoll AW, Szejner P, Anderegg WR, Ehleringer JR (2021) Rapid increases in shrubland and forest intrinsic water-use efficiency during an ongoing megadrought. of Proc. Natl. Acad. Sci. U.S.A. 118:52. https://doi.org/10.1073/pnas.2118052118

Kannenberg SA, Guo JS, Novick KA, Anderegg WRL, Feng X, Kennedy D, Konings AG, Martínez-Vilalta J, Matheny AM (2022) Opportunities challenges and pitfalls in characterizing plant water-use strategies. Functional Ecology, 36, 24–37. https://doi.org/10.1111/1365-2435.13945

Kassambara A and Mundt F (2017) factoextra: Extract and visualize the results of multivariate data analyses. R package version 1.0.5. https://CRAN.Rproject.org/package=factoextra

Kawecki TJ, Ebert D (2004) Conceptual issues in local adaptation. Ecology Letters 7(12), 1225–1241. https://doi.org/10.1111/j.1461-0248.2004.00684.x

Keith AR, Bailey JK, Lau MK, Whitham TG (2017) Genetics-based interactions of foundation species affect community diversity, stability, and network structure. Proc Royal Soc B. 284(1854): 20162703. https://doi.org/10.1098/rspb.2016.2703

Kenefic LS, Seymour RS (1999). Leaf area prediction models for *Tsuga canadensis* in Maine. Canadian Journal of Forest Research 29(10), 1574–1582. https://doi.org/10.1139/x99-134

Kindt R, Coe R (2005) Tree Diversity Analysis. A Manual and Software for Common Statistical Methods for Ecological and Biodiversity Studies. Nairobi: World Agroforestry Centre (ICRAF). http://dx.doi.org/10.13140/RG.2.1.1993.7684

Kleyer M, Minden V (2015) Why functional ecology should consider all plant organs: An allocation-based perspective. Basic and Applied Ecology 16(1), 1–9. https://doi.org/10.1016/j.baae.2014.11.002

Knight CA, Ackerly DD (2003) Evolution and plasticity of photosynthetic thermal tolerance, specific leaf area and leaf size: congeneric species from desert and coastal environments. New Phytologist 160, 337–347. https://doi.org/10.1046/j.1469-8137.2003.00880.x

Kolb KJ, Sperry JS (1999) Differences in drought adaptation between subspecies of sagebrush (*Artemisia tridentata*). Ecology 80(7), 2373–2384. https://doi.org/10.2307/176917

Körner C (2003) Alpine plant life: Functional plant ecology of high mountain ecosystems (2nd ed.). Springer. https://doi-org.ezproxy1.lib.asu.edu/10.1007/978-3-642-18970-8

Kozaki A, Takeba G (1996) Photorespiration protects C3 plants from photooxidation. Nature. 384(6609), 557–560. https://doi.org/10.1038/384557a0

Kuznetsova A, Brockhoff PB, Christensen RHB (2017) lmerTest package: Tests in linear mixed effects models. Journal of Statistical Software, 82(13), 1–26. https://doi.org/10.18637/jss.v082.i13

Laforest-Lapointe I, Martínez-Vilalta J, Retana J (2014) Intraspecific variability in functional traits matters: case study of Scots pine. Oecologia 175(4):1337–48. https://doi.org/10.1007/s00442-014-2967-x

Lambers H, Chapin FS, Pons TL (2008) Plant Physiological Ecology. Springer New York, NY. https://doi.org/10.1007/978-0-387-78341-3

Lambers H, Chapin FS, Pons TL (1998) Photosynthesis, respiration, and long-distance transport. Plant Physiological Ecology 10–153. https://doi.org/10.1007/978-1-4757-2855-2_2

Lambers H, Poorter H (1992) Inherent variation in growth rate between higher plants: A search for physiological causes and ecological consequences. Advances in Ecological Research 23, 187–261. https://doi.org/10.1016/S0065-2504(08)60148-8

Lambs L, Muller E (2002) Sap flow and water transfer in the Garonne River riparian woodland, France: First results on poplar and willow. Annals of Forest Science 59, 301–305. https://doi.org/10.1051/forest:2002026

Lamit LJ, Holeski LM, Flores-Rentería L, Whitham TG, Gehring CA (2016) Tree genotype influences ectomycorrhizal fungal community structure: ecological and evolutionary implications. Fung Ecol 24:124–134. https://doi.org/10.1016/j.funeco.2016.05.013

Landsberg J, Waring R, Ryan M (2017) Water relations in tree physiology: where to from here? Tree Physiology 37(1):18–32. https://doi.org/10.1093/treephys/tpw102

Laumer W, Andreu L, Helle G, Schleser GH, Wieloch T, Wissel H (2009) A novel approach for the homogenization of cellulose to use micro-amounts for stable isotope analyses. Rapid Commun Mass Spectrom 23(13):1934–40. https://doi.org/10.1002/rcm.4105

Lauri P (2019) Corner's rules as a framework for plant morphology, architecture and functioning – Issues and steps forward. New Phytologist 221(4), 1679–1684. https://doi.org/10.1111/nph.15503

Lê S, Josse J, Husson F (2008) FactoMineR: An R package for multivariate analysis. Journal of Statistical Software 25, 1–18. https://doi.org/10.18637/jss.v025.i01

Leavitt SW, Danzer SR (1993) Methods for batch processing small wood samples to holocellulose for stable-carbon isotope analysis. Anal Chem 65(1):87–89. https://doi.org/10.1021/ac00049a017

Leavitt SW, Woodhouse CA, Castro CL, Wright WE, Meko Dm, Touchan R, Griffin D, Ciancarelli B (2011) The North American monsoon in the U.S. Southwest: Potential for investigation with tree-ring carbon isotopes. Quat Int 235:101–107. https://doi.org/10.1016/j.quaint.2010.05.006

Leigh A, Sevanto S, Close JD, Nicotra AB (2017) The influence of leaf size and shape on leaf thermal dynamics: does theory hold up under natural conditions? Plant, Cell and Environment 40, 237–248. https://doi.org/10.1111/pce.12857

Leuenberger M, Borella S, Stocker T, Saurer M, Siegwolf R, Schweingruber F, Matyssek R (1998) Stable isotopes in tree-rings as climate and stress indicators. Final Report NRP 31, VDF, ETH Zurich. https://doi.org/10.1016/j.quascirev.2003.06.017

Li Y, Sperry JS, Taneda H, Bush SE, Hacke UG (2008) Evaluation of centrifugal methods for measuring xylem cavitation in conifers, diffuse- and ring-porous angiosperms. New Phytologist 177(2), 558–568. https://doi.org/10.1111/j.1469-8137.2007.02272.x

Lindtke D, González-Martínez SC, Macaya-Sanz D, Lexer C (2013). Admixture mapping of quantitative traits in *Populus* hybrid zones: Power and limitations. Heredity 111(6), 474–485. https://doi.org/10.1038/hdy.2013.69

Lite SJ, Stromberg JC (2005) Surface water and ground-water thresholds for maintaining *Populus–Salix* forests, San Pedro River, Arizona. Biological Conservation 125:153–167. https://doi.org/10.1016/j.biocon.2005.01.020

Lloyd J, Farquhar GD (2008) Effects of rising temperatures and [CO_2] on the physiology of tropical forest trees. Philos Trans R Soc B Biol Sci 363:1811–1817. https://doi.org/10.1098/rstb.2007.0032

MacInnis-Ng C, McClenahan K, Eamus D (2004) Convergence in hydraulic architecture, water relations and primary productivity amongst habitats and across seasons in Sydney. Functional Plant Biology 31, 429–439. https://doi.org/10.1071/FP03194

Martin P (1989) The significance of radiative coupling between vegetation and the atmosphere. Agricultural and Forest Meteorology 49, 45–53. https://doi.org/10.1016/0168-1923(89)90061-0

Martin TA, Hinckley TM, Meinzer FC, Sprugel DG (1999) Boundary layer conductance, leaf temperature and transpiration of *Abies amabilis* branches. Tree Physiology 19, 435–443. https://doi.org/10.1093/treephys/19.7.435

Mayr S, Schmid P, Laur J, Rosner S, Charra-Vaskou K, Dämon B, Hacke UG (2014) Uptake of water via branches helps timberline conifers refill embolized xylem in late winter. Plant Physiology 164(4), 1731–1740. https://doi.org/10.1104/pp.114.236646

Mayr S, Sperry JS (2010) Freeze-thaw-induced embolism in *Pinus contorta*: Centrifuge experiments validate the 'thaw-expansion hypothesis' but conflict with ultrasonic emission data. New Phytologist 185(4), 1016–1024. https://doi.org/10.1111/j.1469-8137.2009.03133.x

McCarroll D, Loader NJ (2004) Stable isotopes in tree rings. Quat Sci Rev 23:771–801. https://doi.org/10.1016/j.quascirev.2003.06.017

McDowell NG, Allen C, Marshall L (2010) Growth, carbon isotope discrimination, and mortality across a ponderosa pine elevation transect. Global Change Biology 16, 399–415. https://doi.org/10.1111/j.1365-2486.2009.01994.x

McDowell NG, White S, Pockman WT (2008) Transpiration and stomatal conductance across a steep climate gradient in the southern Rocky Mountains. Ecohydrology 1, 193–204. https://doi.org/10.1002/eco.20

Meddens AJH, Hicke JA, Macalady AK, Buotte PC, Cowles TR, Allen CD (2014) Patterns and causes of observed piñon pine mortality in the southwestern United States. New Phycologist 206, 91–97. https://doi.org/10.1111/nph.13193

Merritt DM, Poff NL (2010) Shifting dominance of riparian *Populus* and *Tamarix* along gradients of flow alteration in western North American rivers. Ecol App 20, 135–152.https://doi.org/10.1890/08-2251.1

Messier J, Lechowicz MJ, McGill BJ, Violle C, Enquist BJ (2017) Interspecific integration of trait dimensions at local scales: The plant phenotype as an integrated network. Journal of Ecology 105(6), 1775–1790. https://doi.org/10.1111/1365-2745.12755

Michaletz ST, Weiser MD, McDowell NG, Zhou J, Kaspari M, Helliker BR, Enquist BJ (2016) The energetic and carbon economic origins of leaf thermoregulation. Nature Plants 2, 16129. https://doi.org/10.1038/nplants.2016.129

Michaletz ST, Weiser MD, McDowell NG, Zhou J, Kaspari M, Helliker BR, Enquist BJ (2015) Plant thermoregulation, energetics, trait-environment interactions, and carbon economics. Trends in Ecology & Evolution 30, 714–724. https://doi.org/10.1016/j.tree.2015.09.006

Monteith J, Unsworth M (2013) Principles of Environmental Physics, Fourth Edition: Plants, Animals, and the Atmosphere. Elsevier, 400.

Mooney HA, Billings WD (1961) Comparative physiological ecology of arctic and alpine populations of *Oxyria digyna*. Ecological Monographs 31(1), 1–29. https://doi.org/10.2307/1950744

Muir CD (2019) Tealeaves: an R package for modelling leaf temperature using energy budgets. AoB Plants 11, 1–10. https://doi.org/10.1093/aobpla/plz054

Niklas KJ (1991) Flexural stiffness allometries of angiosperm and fern petioles and rachises: Evidence for biomechanical convergence. Evolution 45(3), 734. https://doi.org/10.2307/2409924

Niklas KJ, Spatz HC (2012) Mechanical properties of wood disproportionately increase with increasing density. American Journal of Botany 99(1), 169–170. https://doi.org/10.3732/ajb.1100567

Niklas KJ, Spatz HC (2010) Worldwide correlations of mechanical properties and green wood density. American Journal of Botany 97(10), 1587–1594. https://doi.org/10.3732/ajb.1000150

Nobel PS (2009) Physicochemical and environmental plant physiology (4th ed.). Elsevier/Academic Press. https://doi.org/10.1016/B978-0-12-374143-1.X0001-4

Noss RF, Laroe ET III, Scott JM (1995) Endangered ecosystems of the United States: a preliminary assessment of loss and degradation. Restoration & Management Notes 14.

Offermann C, Ferrio JP, Holst J, Grote R, Siegwolf R, Kayler Z, Gessler A (2011) The long way down-are carbon and oxygen isotope signals in the tree ring uncoupled from canopy physiological processes? Tree Physiology 31: 1088–1102. https://doi.org/10.1093/treephys/tpr093

O'Grady AP, Cook PG, Eamus D, Duguid A, Wischusen JDH, Fass T, Worldege D (2009) Convergence of tree water use within an arid-zone woodland. Oecologia 160(4), 643–655. https://doi.org/10.1007/s00442-009-1332-y

Okajima Y Taneda H Noguchi K Terashima I (2012) Optimum leaf size predicted by a novel leaf energy balance model incorporating dependencies of photosynthesis on light and temperature. Ecological Research 27, 333–346. https://doi.org/10.1007/s11284-011-0905-5

Oksanen J, Blanchet G, Friendly M, Kindt R, Legendre P, McGlinn D, Minchin P, O'Hara R, Simpson G, Solymos, Henry H, Szoecs E and Wagner H (2019) vegan: Community Ecology Package. R package version 2.5-6. https://CRAN.R-project.org/package=vegan

O'Neill GA, Hamann A, Wang T (2008) Accounting for population variation improves estimates of the impact of climate change on species growth and distribution. Journal of Applied Ecology 45(4), 1040–1049. https://doi.org/10.1111/j.1365-2664.2008.01472.x

Oren R, Sperry JS, Katul G, Pataki DE, Ewers BE, Phillips N, Schafer KVR (1999) Survey and synthesis of intra- and interspecific variation in stomatal sensitivity to vapour pressure deficit. Plant, Cell and Environment 22, 1515–1526. https://doi.org/10.1046/j.1365-3040.1999.00513.x

Osmond CB, Björkman O (1972) Simultaneous measurements of oxygen effects on net photosynthesis and glycolate metabolism in C3 and C4 species of *Atriplex*. Carnegie Inst Wash 71, 141–148.

O'Sullivan OS, Heskel MA, Reich PB, Tjoelker MG, Weerasinghe LK, Penillard A, Zhu L, Egerton JJG, Bloomfield KJ, Creek D, Bahar NHA, Griffin KL, Hurry V, Meir P, Turnbull MH, Atkin OK (2017) Thermal limits of leaf metabolism across biomes. Global Change Biology 23(1), 209–223. https://doi.org/10.1111/gcb.13477

O'Sullivan OS, Weerasinghe KK, Evans JR, Egerton JJ, Tjoelker MG, Atkin OK (2013) High-resolution temperature responses of leaf respiration in snow gum (*Eucalyptus pauciflora*) reveal high-temperature limits to respiratory function. Plant Cell and Environment 36, 1268–1284. https://doi.org/10.1111/pce.12057

Pásztory Z, Ronyecz I (2013) The thermal insulation capacity of tree bark. Acta Silvatica et Lignaria Hungarica 9(1), 111–117. https://doi.org/10.2478/aslh-2013-0009

Peres-Neto PR, Jackson DA, Somers KM (2005) How many principal components? Stopping rules for determining the number of non-trivial axes revisited. Computational Statistics and Data Analysis 49(4), 974–997. https://doi.org/10.1016/j.csda.2004.06.015

Poff B, Koestner KA, Neary DG, Henderson V (2011) Threats to Riparian Ecosystems in Western North America: An Analysis of Existing Literature. Journal of the American Water Resources Association (JAWRA) 47(6):1241–1254. https://doi.org/10.1111/j.1752-1688.2011.00571.x

Potts DL, Williams DG (2004) Response of tree ring holocellulose delta C-13 to moisture availability in *Populus fremontii* at perennial and intermittent stream reaches. West North Am Nat 64:27–37. http://www.jstor.org/stable/41717338

Preibisch S, Saalfeld S, Tomancak P (2009) Globally optimal stitching of tiled 3D microscopic image acquisitions. Bioinformatics 25(11), 1463–1465. https://doi.org/10.1093/bioinformatics/btp184

Preston KA, Cornwell WK, DeNoyer JL (2006) Wood density and vessel traits as distinct correlates of ecological strategy in 51 California coast range angiosperms. New Phytologist 170(4), 807–818. https://doi.org/10.1111/j.1469-8137.2006.01712.x

PRISM Climate Group (2010) Oregon State University. http://www.prismclimate.org

QGIS Development Team (2021) QGIS geographic information system. Open-Source Geospatial Foundation Project. http://qgis.osgeo.org

R Core Team (2020). R: A language and environment for statistical computing. R Foundation Statistical Computing. Retrieved from https://www.r-project.org/

Radin JW, Lu Z, Percy RG, Zeiger E (1994) Genetic variability for stomatal conductance in Pima cotton and its relation to improvements of heat adaptation. Proceedings of the National Academy of Sciences 91, 7217–7221. https://doi.org/10.1073/pnas.91.15.7217

Ravikumar S, Surekha R, Thavarajah R (2014) Mounting media: An overview. J NTR University of Health Sciences 3(5), 1. https://doi.org/10.4103/2277-8632.128479

Reich PB (2014) The world-wide 'fast–slow' plant economics spectrum: A traits manifesto. Journal of Ecology, 102(2), 275–301. https://doi.org/10.1111/1365-2745.12211

Reich PB, Wright IJ, Cavender-Bares J, Craine JM, Oleksyn J, Westoby M, Walters MB (2003) The evolution of plant functional variation: Traits, spectra, and strategies. International Journal of Plant Sciences 164(S3), S143–S164. https://doi.org/10.1086/374368

Roden JS (2005) Carbon and oxygen isotope ratios of tree ring cellulose along a precipitation transect in Oregon, United States. J Geophys Res 110:1–11. https://doi.org/10.1029/2005JG000033

Roden JS, Ehleringer JR (2000) Hydrogen and oxygen isotope ratios of tree ring cellulose for field-grown riparian trees. Oecologia 123:481–489. https://doi.org/10.1007/s004420000349

Roden JS, Lin G, Ehleringer JR (2000) A mechanistic model for interpretation of hydrogen and oxygen isotope ratios in tree-ring cellulose - Evidence and implications for the use of isotopic signals transduced by plants. Geochimica et Cosmochimica Acta 64(1). https://doi.org/10.1016/S0016-7037(99)00195-7

Roden JS, Pearcy RW (1993) Effect of leaf flutter on the light environment of poplars. Oecologia 93(2), 201–207. https://doi.org/10.1007/BF00317672

Roden JS, Siegwolf R (2012) Is the dual-isotope conceptual model fully operational? Tree Physiology, 32(10):1179–1182. https://doi.org/10.1093/treephys/tps099

Rood SB, Braatne JH, Hughes FMR (2003) Ecophysiology of riparian cottonwoods: streamflow dependency, water relations and restoration. Tree Physiology 23: 1113–1124. https://doi.org/10.1093/treephys/23.16.1113

Rosas T, Mencuccini M, Barba J, Cochard H, Saura-Mas S, Martínez-Vilalta J (2019) Adjustments and coordination of hydraulic, leaf and stem traits along a water availability gradient. New Phytologist 223(2), 632–646. https://doi.org/10.1111/nph.15684

Rosell JA (2016) Bark thickness across the angiosperms: More than just fire. New Phytologist 211(1), 90–102. https://doi.org/10.1111/nph.13889

Rueda M, Godoy O, Hawkins BA (2018) Trait syndromes among North American trees are evolutionarily conserved and show adaptive value over broad geographic scales. Ecography 41(3), 540–550. https://doi.org/10.1111/ecog.03008

Sack L, Cowan PD, Jaikumar N, Holbrook NM (2003) The 'hydrology' of leaves: Coordination of structure and function in temperate woody species. Plant, Cell and Environment 26(8), 1343–1356. https://doi.org/10.1046/j.0016-8025.2003.01058.x

Sack L, Frole K (2006) Leaf structural diversity is related to hydraulic capacity in tropical rain forest trees. Ecology 87(2), 483–491. https://doi.org/10.1890/05-0710

Sankey T, Hultine K, Blasini D, Koepke D, Bransky N, Grady K, Cooper H, Gehring C, Allan G (2021) UAV thermal image detects genetic trait differences among populations and genotypes of Fremont cottonwood (*Populus fremontii, Salicaceae*). Remote Sensing in Ecology and Conservation 7(4). https://doi.org/10.1002/rse2.185

Sartori K, Vasseur F, Violle C, Baron E, Gerard M, Rowe R, Ayala-Garay O, Christophe A, Garcia de Jalón L, Masclef D, Harscouet E, del Rey Granado M, Chassagneux A, Kazakou E, Vile D (2019) Leaf economics and slow-fast adaptation across the geographic range of *Arabidopsis thaliana*. Sci Rep 9, 10758. https://doi.org/10.1038/s41598-019-46878-2

Saurer M, Robertson I, Siegwolf R, Leuenberger M (1998) Oxygen Isotope Analysis of Cellulose: An Interlaboratory Comparison. Anal Chem 70:2074–2080. https://doi.org/10.1021/ac971022f

Savolainen O, Pyhäjärvi T, Knürr T (2007) Gene flow and local adaptation in trees. Annu. Rev. Ecol. Evol. System 595–619. https://doi.org/10.1146/annurev.ecolsys. 38. 091206.095646

Scholander PF, Bradstreet ED, Hemmingsen EA, Hammel HT (1965) Sap pressure in vascular plants: Negative hydrostatic pressure can be measured in plants. Science 148(3668), 339–346. https://doi.org/10.1126/science.148.3668.339

Scholander PF, Hammel HT, Bradstreet ED, Hemmingsen EA (1965) Sap pressure in vascular plants. Science 148, 339-346. https://doi.org/10.1126/science.148.3668.339

Scholz A, Klepsch M, Karimi Z, Jansen S (2013) How to quantify conduits in wood? Frontiers in Plant Science 4, 1–11. https://doi.org/10.3389/fpls.2013.00056

Seager R, Goddard L, Nakamura J, Henderson N, Lee DE (2014) Dynamical Causes of the 2010/11 Texas–Northern Mexico Drought. Journal of Hydrometeorology 15, 39–68. https://doi.org/10.1175/JHM-D-13-024.1

Seager R, Hooks A, Williams AP, Cook B, Nakamura J, Henderson N (2015) Climatology, Variability, and Trends in the U.S. Vapor Pressure Deficit, an Important Fire-Related Meteorological Quantity, Journal of Applied Meteorology and Climatology 54(6), 1121–1141. https://journals.ametsoc.org/view/journals/apme/54/6/jamc-d-14-0321.1.xml

Seibt U, Rajabi A, Griffiths H, Berry JA (2008) Carbon isotopes and water use efficiency: Sense and sensitivity. Oecologia 155:441–454. https://doi.org/10.1007/s00442-007-0932-7

Sharkey TD (2005) Effects of moderate heat stress on photosynthesis: Importance of thylakoid reactions, rubisco deactivation, reactive oxygen species, and thermotolerance provided by isoprene. Plant, Cell and Environment 28(3), 269–277. https://doi.org/10.1111/j.1365-3040.2005.01324.x

Scheidegger Y, Saurer M, Bahn M, Siegwolf R (2000) Linking stable oxygen and carbon isotopes with stomatal conductance and photosynthetic capacity: a conceptual model. Oecologia 125:350–357. https://doi.org/10.1007/s004420000466

Schweitzer JA, Bailey JK, Fischer DG, LeRoy CJ, Lonsdorf EV, Whitham TG, Hart SC (2008) Plant-soil-microorganism interactions: heritable relationship between plant genotype and associated soil microorganisms. Ecology 89: 773–781. http://www.jstor.org/stable/27651599

Schweingruber FH (1997) Tree-rings and environment: Dendroecology. Berne, Stuttgart, Vienna: Paul Haupt Publisher. https://doi.org/10.1111/j.1469-8137.1998.149-8.x

Schwinning S, Lortie CJ, Esque TC, DeFalco LA (2022) What common-garden experiments tell us about climate responses in plants. Journal of Ecology 110, 986–996. https://doi.org/10.1111/1365-2745.13887

Siegwolf RTW, Brooks JR, Roden J, Saurer M (2022) Stable Isotopes in Tree Rings. Inferring Physiological, Climatic and Environmental Responses. Springer. 879. https://doi.org/10.1007/978-3-030-92698-4

Slot M, Winter K (2016) The effects of rising temperature on the ecophysiology of tropical forest trees. In: Santiago LS, Goldstein G (eds.)Tropical tree physiology. Switzerland: Springer International Publishing, 385–412. https://doi.org/10.1007/978-3-319-27422-5_18

Smith DM, Allen SJ (1996) Measurement of sap flow in plant stems. Journal of Experimental Botany 47(305), 1833–1844. https://doi.org/10.1093/jxb/47.12.1833

Sokal RR, Rohlf FJ (1995) Biometry: The principles and practice of statistics in biological research (3rd ed.). W.H. Freeman and Co., New York. https://doi.org/10.2307/2412280

Sperry JS, Hacke UG, Oren R, and Comstock JP (2002) Water deficits and hydraulic limits to leaf water supply. Plant, Cell and Environment 25, 251-263. https://doi.org/10.1046/j.0016-8025.2001.00799.x

Sperry JS, Saliendra NZ (1994) Intra- and inter-plant variation in xylem cavitation in *Betula occidentalis*. Plant, Cell and Environment 17(11), 1233–1241. https://doi.org/10.1111/j.1365-3040.1994.tb02021.x

Sperry JS, Sullivan JEM (1992) Xylem embolism in response to freeze-thaw cycles and water stress in ring-porous, diffuse-porous, and conifer species. Plant Physiology 100(2), 605–613. https://doi.org/10.1104/pp.100.2.605

Sprugel DG (1989) The relationship of ever greenness, crown architecture, and leaf size. The American Naturalist 133(4), 465–479. https://doi.org/10.1086/284930

Sridharan G, Shankar AA (2012) Toluidine blue: A review of its chemistry and clinical utility. Journal of Oral and Maxillofacial Pathology 16(2), 251–255. https://doi.org/10.4103/0973-029X.99081

Sterck FJ, Zweifel R, Sass-Klaassen U, Chowdhury Q (2008) Persisting soil drought reduces leaf specific conductivity in Scots pine (*Pinus sylvestris*) and pubescent oak (*Quercus pubescens*). Tree Physiology 28(4), 529–536. https://doi.org/10.1093/treephys/28.4.529

Sternberg L (1989) Oxygen and hydrogen isotope ratios in plant cellulose: mechanisms and applications. In: Rundel PW, Ehleringer JR, Nagy KA (eds) Stable isotopes in ecological research. Springer, New York. https://doi.org/10.1002/9780470015902.a0021231.pub2

Sternberg L, Deniro MJ, Keeley JE (1984) Hydrogen, oxygen, and carbon isotope ratios of cellulose from submerged aquatic crassulacean Acid metabolism and non-crassulacean Acid metabolism plants. Plant Physiology 76(1):68-70. https://doi.org/10.1104/pp.76.1.68

Stromberg JC (1993) Frémont cottonwood-Goodding willow riparian forests: A review of their ecology, threats, and recovery potential. Journal of the Arizona Nevada Academy of Sciences 26(3), 97–110.

Szejner P, Wright W, Babst F, Belmecheri S, Trouet V, Leavitt S, Ehleringer J, Monson R (2016) Latitudinal gradients in tree ring stable carbon and oxygen isotopes reveal differential climate influences of the North American Monsoon System. Journal of Geophysical Research: Biogeosciences 121:1978-1991. https://doi.org/10.1002/2016JG003460

Teskey R, Wertin T, Bauweraerts I, Ameye M, Mcguire MA, Steppe K (2015) Responses of tree species to heat waves and extreme heat events: Tree response to extreme heat. Plant, Cell and Environment 38, 1699–1712. https://doi.org/10.1111/pce.12417

Tjoelker M, Olesksyn J, Reich P (2001) Modelling respiration of vegetation: Evidence for a general temperature-dependent Q10. Global Change Biology,7(2), 223–230. https://doi.org/10.1046/j.1365-2486.2001.00397.x.

Togashi HF, Prentice IC, Evans BJ, Forrester DI, Drake P, Feikema P, Brooksbank K, Eamus D, Taylor D (2015) Morphological and moisture availability controls of the leaf area-to-sapwood area ratio: analysis of measurements on Australian trees. Ecology and Evolution, 5(6), 1263–1270. https://doi.org/10.1002/ece3.1344

Trueba S, Isnard S, Barthélémy D, Olson ME (2016) Trait coordination, mechanical behaviour and growth form plasticity of *Amborella trichopoda* under variation in canopy openness. AoB PLANTS 8, https://doi.org/10.1093/aobpla/plw068

Turner NC (1988) Measurement of plant water status by the pressure chamber technique. Irrig Sci 9(4), 289-308. https://doi.org/10.1007/BF00296704

Tyree ME, Zimmermann MH (2002) Xylem Structure and the ascent of sap (2nd edn.). Springer Verlag. https://www.science.org/doi/10.1126/science.222.4623.500.b

Upchurch DR, Mahan JR (1988) Maintenance of constant leaf temperature by plants—II. Experimental observations in cotton. Environmental and Experimental Botany 28, 359–366. https://doi.org/10.1016/0098-8472(88)90060-3

Urban J, Ingwers M, McGuire MA, Teskey RO (2017) Stomatal conductance increases with rising temperature. Plant Signaling & Behavior 12, 1–3. https://doi.org/10.1080/15592324.2017.1356534

USGCRP (2017) Climate Science Special Report: Fourth National Climate Assessment, Volume I [Wuebbles DJ, DW Fahey, KA Hibbard, DJ Dokken, BC Stewart TK. 134 Maycock (eds.)]. U.S. Global Change Research Program, Washington, DC, USA. https://doi.org/10.7930/J0J964J6

Valladares F, Skillman JB, Pearcy RW (2002) Convergence in light capture efficiencies among tropical forest understory plants with contrasting crown architectures: A case of morphological compensation. American Journal of Botany 89(8), 1275–1284. https://doi.org/10.3732/ajb.89.8.1275

Voelker SL, Meinzer FC, Lachenbruch B, Renée Brooks J, Guyette RP (2014) Drivers of radial growth and carbon isotope discrimination of bur oak (*Quercus macrocarpa Michx.*) across continental gradients in precipitation, vapour pressure deficit and irradiance. Plant, Cell and Environment 37, 766–779. https://doi.org/10.1111/pce.12196

von Caemmerer S, Quick WP (2000) Rubisco: physiology in vivo. In: Leegood RC, Sharkey TD, von Caemmerer S, eds. Photosynthesis: physiology and metabolism. Dordrecht: Kluwer Academic Publishers, 85–113.

Wahid A, Gelani S, Ashraf M, Foolad MR (2007) Heat tolerance in plants: an overview. Environ. Exp. Bot. 61, 199–223. https://doi.org/10.1016/j.envexpbot.2007.05.011

Walther GR, Post E, Convey P, Menzel A, Parmesan C, Beebee TJ, Fromentin JM, Hoegh-Guldberg O, Bairlein F (2002) Ecological responses to recent climate change. Nature 416(6879):389-95. https://doi.org/10.1038/416389a

Wang T, Hamann A, Spittlehouse DL, Murdock TQ (2012) ClimateWNA-high-resolution spatial climate data for western North America. Journal of Applied Meteorology and Climatology 51(1), 16–29. https://doi.org/10.1175/JAMC-D-11-043.1

Wang SY, Gillies RR, Jin J, Hipps LE (2009) Recent rainfall cycle in the Intermountain Region as a quadrature amplitude modulation from the Pacific decadal oscillation. Geophys Res Lett 36:1–6. https://doi.org/10.1029/2008GL036329

Warren CR, McGrath JF, Adams MA (2001) Water availability and carbon isotope discrimination in conifers. Oecologia 127:476–486. https://doi.org/10.1007/s004420000609

Waterhouse J., Barker AC, Carter AHC (2000) Stable Carbon Isotopes in Scots Pine Tree Rings Preserve a Record of Flow of the River Ob. Geophysical Research Letters 21:3529–3532. https://doi.org/10.1029/2000GL006106

Watson D.J. (1947). Comparative Physiological Studies on the Growth of Field Crops. Annals of Botany 11(41), 41–76. http://www.jstor.org/stable/42907002

Weigt RB, Streit K, Saurer M, Siegwolf RTW (2017) The influence of increasing temperature and CO_2 concentration on recent growth of old-growth larch: contrasting responses at leaf and stem processes derived from tree-ring width and stable isotopes. Tree Physiology 38: 706–720. https://doi.org/10.1093/treephys/tpx148

Weiss JL, Castro CL, Overpeck JT (2009) Distinguishing pronounced droughts in the southwestern United States: Seasonality and effects of warmer temperatures. Climate 22, 5918–5932. https://doi.org/10.1175/2009JCLI2905.1

Weng JH, Lai MF (2005) Estimating heat tolerance among plant species by two chlorophylls fluorescence parameters. Photosynthetica, 43(3), 439-444. https://doi.org/10.1007/s11099-005-0070-6

Werner RA, Buchmann N, Siegwolf RTW, Kornexl BE, Gessler A (2011) Metabolic fluxes, carbon isotope fractionation and respiration—lessons to be learned from plant biochemistry. New Phytol 191:10–15. https://doi.org/10.1111/j.1469-8137.2011.03741.x

Western Regional Climate Center (WRCC). (2010) http://www.wrcc.dri.edu

Whitham TG, DiFazio SP, Schweitzer JA, Shuster SM, Allan GJ, Bailey JK, Woolbright SA (2008) Extending genomics to natural communities and ecosystems. Science 320: 492–495. https://doi.org/10.1126/science.1153918

Whitham TG, Gehring CA, Bothwell HM, Cooper HF, Hull JB, Allan GJ, Grady KC, Markovchick L, Shuster SM, Parker J, Cadmus AE, Ikeda DH, Bangert RK, Hultine KR, Blasini DE (2020). Using the Southwest Experimental Garden Array to enhance riparian restoration in response to global change: identifying and deploying genotypes and populations for current and future environments. In Riparian Research and Management: Past, Present, Future, Vol. 2, ed. SW Carothers, RR Johnson, DM Finch, KJ Kingsley, RH Hamre, pp. 63–79. Gen. Tech. Rep. RMRS-GTR-411. Fort Collins, CO: U.S. Dep. Agric. For. Serv. Rocky Mt. Res. Stn

Williams AP, Allen CD, Macalady AK, Griffin D, Woodhouse CA, Meko DM, Swetnam TW, Rauscher SA, Seager R, Grissino-Mayer HD (2013) Temperature as a potent driver of regional forest drought stress and tree mortality. Nature Climate Change 3, 292-297. https://doi.org/10.1038/nclimate1693

Williams AP, Cook BI, Smerdon JE (2022) Rapid intensification of the emerging southwestern North American megadrought in 2020–2021. Nat. Clim. Chang. 12, 232–234. https://doi-org.ezproxy1.lib.asu.edu/10.1038/s41558-022-01290-z

Williams AP, Cook ER, Smerdon JE, Cook BI, Abatzoglou JT, Bolles K, Baek SH, Badger AM, Livneh B (2020) Large contribution from anthropogenic warming to an emerging North American megadrought. Science 368(6488), 314–318. https://doi.org/10.1126/science.aaz9600

Worrall JJ, Egeland L, Eager T, Mask RA, Johnson EW, Kemp PA, Sheppard WD (2008) Rapid mortality of *Populus tremuloides* in southwestern Colorado, USA. Forest Ecology and Management 255(3), 686–696. https://doi.org/10.1016/j.foreco.2007.09.071

Worrall JJ, Rehfeldt GE, Hamann A, Hogg EH, Marchetti SB, Michaelin M. Gray LK (2013) Recent declines of *Populus tremuloides* in North America linked to climate. Forest Ecology and Management 299, 35–51. https://doi.org/10.1016/j.foreco.2012.12.033

Wright I, Dong N, Maire V, Prentice C, Westoby M, Diaz S, … Wilf P (2017) Global Climatic Drivers of Leaf Size. *Plant Ecology* 357(6354), 917–920. https://doi.org/10.1126/science.aal4760

Wright IJ, Reich PB, Westoby M, Ackerly DD, Baruch Z, Bongers F, Cavender-Bares J, Chapin T, Cornelissen JHC, Diemer M, Flexas J, Garnier E, Groom PK, Gulias J, Hikosaka K, Lamont BB, Lee T, Lee W, Lusk C, … Villar R (2004) The worldwide leaf economics spectrum. Nature 428(6985), 821–827. https://doi.org/10.1038/nature02403

Wright IJ, Westoby M (2002) Leaves at low versus high rainfall: Coordination of structure, lifespan and physiology. New Phytologist 155(3), 403–416. https://doi.org/10.1046/j.1469-8137.2002.00479.x

Yakir D, DeNiro MJ (1990) Oxygen and Hydrogen Isotope Fractionation during Cellulose Metabolism in *Lemna gibba* L. Plant Physiol 93:325–332. https://doi.org/10.1104/pp.93.1.325

Yamada M, Hidaka T, Fukamachi H (1996) Heat tolerance in leaves of tropical fruit crops as measured by chlorophyll fluorescence. Sci. Hortic, 67, 39–48. https://doi.org/10.1016/S0304-4238(96)00931-4

Yamori W, Suzuki K, Noguchi K, Nakai M, Terashima I (2006) Effects of Rubisco kinetics and Rubisco activation state on the temperature dependence of the photosynthetic rate in spinach leaves from contrasting growth temperatures. Plant, Cell and Environment 29, 1659–1670. https://doi.org/10.1111/j.1365-3040.2006.01550.x

Yang R, Zhao F, Fan Z, Panthi S, Fu P, Bräuning A, Grießinger J, Li Z (2022) Long-term growth trends of *Abies delavayi* and its physiological responses to a warming climate in the Cangshan Mountains, southwestern China. Forest Ecology and Management 505. https://doi.org/10.1016/j.foreco.2021.119943

Yordanov I (1992) Response of photosynthetic apparatus to temperature stress and molecular mechanisms of its adaptations. Photosynthetica. 26(4), 517-531

Zaehle S (2005) Effect of height on tree hydraulic conductance incompletely compensated by xylem tapering. Functional Ecology 19(2), 359–364. https://doi.org/10.1111/j.0269-8463.2005.00953.x

Zeppel M, Eamus D (2008) Coordination of leaf area, sapwood area and canopy conductance lead to species convergence of tree water use in a remnant evergreen woodland. Aust. J. Bot. 56:97–108. https://doi.org/10.1071/BT07091

Zhou H, Chen Y, Zhu C, Li Z, Fang G, Li Y, Fu A (2020) Climate change may accelerate the decline of desert riparian forest in the lower Tarim River, northwestern China: Evidence from tree-rings of *Populus euphratica*. Ecological Indicators 111. https://doi.org/10.1016/j.ecolind.2019.105997

Zhu SD, Chen YJ, Ye Q, He PC, Liu H, Li RH, Fu PL, Jiang GF, Cao KF (2018) Leaf turgor loss point is correlated with drought tolerance and leaf carbon economics traits. Tree Physiol. 38(5):658–663. https://doi.org/10.1093/treephys/tpy013

Zweifel R, Häsler R (2000) Frost-induced reversible shrinkage of bark of mature subalpine conifers. Agricultural and Forest Meteorology 102(4), 213–222. https://doi.org/10.1016/S0168-1923(00)00135-0

APPENDIX A

SUPPLEMENTAL TABLES AND FIGURES FOR CHAPTER 2

Table S2.1. Repeated measures data of *Populus fremontii* trees occurring at an experimental common garden at the Agua Fria National Monument in 2017 growing season. Measurements include individual leaf area (A_{il}, m^2), specific leaf area (SLA, cm^2/g), three height (H, m^2), canopy area (A_c, m^2), pre-dawn water potential (Ψ_{pd}, MPa) and mid-day water potential (Ψ_{md}, MPa). Numbers in parentheses represent the SD of the means. F values from mixed-model repeated measures ANOVA of individual leaf area (A_{il}), specific leaf area (SLA), canopy area (A_c), tree height (H), pre-dawn water potential (Ψ_{pd}), and mid-day water potential (Ψ_{md}). A_{il} and SLA data were collected on June 7 (DOY 158), July 25 (DOY 206), September 11 (DOY 254). A_c, TH, Ψ_{pd} and Ψ_{md} data were collected on June 6 (DOY 157), June 29 (DOY 180), July 27 (DOY 208), August 24 (DOY 236) and October 2 (DOY 275) 2017.

Traits	DOY	SD	MR	Mixed-model RMA	F-values
A_{il}	158 (June 7)	15.6 (5.34)	23.3 (6.78)	Time	**126.4*****
	206 (July 25)	15.5 (5.36)	28.3 (8.39)	Ecotype	**80.6*****
	254 (September 11)	22.7 (7.17)	38.6 (9.48)	Time*Ecotype	**15.8*****
SLA	158 (June 7)	121.9 (13.5)	106.0 (10.0)	Time	**6.9****
	206 (July 25)	118.5 (18.6)	99.5 (15.9)	Ecotype	**70.9*****
	254 (September 11)	121.2 (17.4)	90.9 (13.0)	Time*Ecotype	**6.3****
H	157 (June 6)	2.68 (0.46)	2.31 (0.33)	Time	**380.8*****
	180 (June 29)	2.97 (0.58)	2.58 (0.38)	Ecotype	**7.5****
	208 (July 27)	3.09 (0.58)	2.77 (0.48)	Time*Ecotype	1.1
	236 (August 24)	3.57 (0.66)	3.29 (0.48)		
	275 (October 2)	3.74 (0.68)	3.44 (0.57)		
A_c	157 (June 6)	2.2 (0.6)	2.6 (0.8)	Time	**15.5*****
	180 (June 29)	2.1 (0.6)	3.0 (0.9)	Ecotype	**24.5*****
	208 (July 27)	2.3 (0.7)	3.3 (0.9)	Time*Ecotype	**10.9*****
	236 (August 24)	2.3 (0.8)	3.1 (0.9)		
Ψ_{pd}	157 (June 6)	-0.61 (0.14)	-0.45 (0.14)	Time	**30.6*****
	180 (June 29)	-0.50 (0.07)	-0.51 (0.15)	Ecotype	0.03
	208 (July 27)	-0.52(0.09)	-0.53 (0.12)	Time*Ecotype	**9.1*****
	236 (August 24)	-0.29 (0.07)	-0.39 (0.15)		
	275 (October 2)	-0.38 (0.05)	-0.42 (0.12)		
Ψ_{md}	157 (June 6)	-1.75 (0.21)	-1.57 (0.21)	Time	**112.7*****
	180 (June 29)	-1.86 (0.24)	-1.71 (0.38)	Ecotype	**23.6*****
	208 (July 27)	-1.66 (0.26)	-1.42 (0.19)	Time*Ecotype	1.7
	236 (August 24)	-1.95 (0.26)	-1.59 (0.32)		
	275 (October 2)	-0.68 (0.49)	-0.63 (0.30)		

Table S2.2. Results of mean ± standard deviation (n=80) of leaf traits of *Populus fremontii* at population (elevation) level in the Agua Fria National Monument common garden. A_{il} (individual leaf area, m^2), SLA (specific leaf area, cm^2 g^{-1}), D_{stom} (stomatal density, # stomata μm^{-2}), S_{stom} (stomatal size, μm^2), G_{smax} (theoretical maximum stomatal conductance, mmol m^{-2} s^{-1}).

Elevation (m)	A_{il} (m^2)	SLA (cm^2 g^{-1})	D_{stom} (#stom mm^{-2})	S_{stom} (μm^2)	G_{smax} (mmol m^{-2} s^{-1})
1940	32.7 ± 7[a]	92.2 ± 3[a]	146.2 ± 25[a]	396.a ± 65[a]	0.89 ± 0.12[a]
1521	26.2 ± 5[ab]	95.4 ± 5[a]	153.6 ± 17[a]	410.2 ± 33[a]	0.92 ± 0.07[ab]
1301	31.4 ± 7[a]	108.0 ± 11[ab]	156.2 ± 38[a]	374.9 ± 68[a]	0.98 ± 0.08[a]
1212	21.1 ± 5[bc]	118.6 ± 13[ab]	206.7 ± 27[ab]	289.3 ± 34[b]	1.10 ± 0.15[abc]
988	16.7 ± 5[c]	124.8 ± 13[b]	271.8 ± 37[c]	243.1 ± 34[b]	1.31 ± 0.17[cd]
666	15.5 ± 6[c]	115.1 ± 12[b]	279.0 ± 36[c]	234.7 ± 16[b]	1.35 ± 0.14[d]
161	16.0 ± 3[c]	121.8 ± 10[b]	255.7 ± 36[bc]	240.3 ± 22[b]	1.17 ± 0.16[bcd]
72	20.3 ± 6[bc]	122.0 ± 15[b]	255.7 ± 43[bc]	243.7 ± 29[b]	1.30 ± 0.19[cd]
CV	24.21	13.6	28.4	27.2	19.9
Population	***	***	***	***	***

Table S2.3. Results of mean ± standard deviation (n=48) of petiole traits. A_p (petiole area, mm^2), F_{pl} (petiole flatness, mm^2 mm^{-2}), A_{pl} (petiole lumen area, µm^2), Hd_p (petiole hydraulic mean diameter, µm), F_{pl} (petiole lumen fraction, µm^2/µm^2), D_{pv} (petiole vessel density, #/mm^2), K_p (Mean petiole theoretical hydraulic conductivity, mg m^{-1} Mpa^{-1} s^{-1}), K_l (Leaf area normalized theoretical hydraulic conductivity, mg m^{-1} s^{-1} MPa^{-1}). Different letters indicate significant differences between populations at $P \leq 0.05$ (One-way ANOVA; Tukey test). The coefficient of variation (CV) in each trait. The significance of Population (Elevation) is shown as NS, non-significant; * < 0.05, **P < 0.01; ***P < 0.001.

Elevation (m)	A_p (mm^2)	L_{pf} (mm^{2}mm^{-2})	A_{pl} (µm^2)	Hd_p (µm)	F_{pl} (µm^2 µm^{-2})	D_{pv} (# vessels mm^{-2})	K_p (mg m Mpa^{-1} d$_{-1}$)	K_l (mg m^{-1} Mpa^{-1} s^{-1})
1940	1.49 ± 0.61[ab]	1.60 ± 0.06	98.4 ± 15	23.1 ± 3.01	0.07 ± 0.028	735.5 ± 321	9.6e-07 ± 2.7e-07[abc]	3.2e10-04 ± 1.7e-04
1521	1.74 ± 0.34[ab]	1.55 ± 0.09	108.3 ± 27	26.1 ± 3.60	0.05 ± 0.014	473.7 ± 134	1.4e-06 ± 3.5e-07[a]	3.7e10-04 ± 1.1e-04
1301	1.83 ± 0.26[a]	1.64 ± 0.27	87.6 ± 10	24.7 ± 0.44	0.04 ± 0.004	515.2 ± 118	1.1e-06 ± 3.8e-07[ab]	3.2e10-04 ± 1.1e-04
1212	1.16 ± 0.48[ab]	1.33 ± 0.20	76.3 ± 6	23.6 ± 0.24	0.06 ± 0.013	835.9 ± 218	8.1e-07 ± 4.7e-07[abc]	3.5e10-04 ± 1.7e-04
988	1.12 ± 0.46[ab]	1.62 ± 0.17	82.5 ± 9	25.9 ± 0.86	0.04 ± 0.015	550.3 ± 168	7.3e-07 ± 3.4e-07[abc]	3.1e10-04 ± 1.1e-04
666	1.10 ± 063[ab]	1.34 ± 0.27	91.9 ± 21	21.7 ± 3.04	0.06 ± 0.026	708.4 ± 390	6.2e-07 ± 3.9e-07[bc]	3.5e10-04 ± 1.1e-04
161	0.95 ± .52[ab]	1.33 ± 0.15	100.3 ± 21	23.5 ± 2.45	0.05 ± 0.018	488.9 ± 221	5.9e-07 ± 3.2e-07[bc]	2.9e10-04 ± 9.9e-05
72	0.89 ± 0.43[b]	1.33 ± 0.23	108.1 ± 63	22.1 ± 5.17	0.06 ± 0.024	799.6 ± 579	4.7e-07 ± 2.8e-07[c]	2.8e10-04 ± 2.1e-04
CV	15.5	15.5	29.5	12.7	37.1	30.6	52.2	37.9
Population	***	**	NS	NS	NS	NS	***	NS

Table S2.4. Results of Mean ± standard density (n=48–80) of architecture traits of *Populus fremontii* at population (Elevation) level in the Agua Fria National Monument common garden A_l (whole-tree leaf area, m^2), H (tree height, m), A_c (canopy area, m^2), A_s:A_l (sapwood to leaf area, m^2/m^2), LAI (leaf area index, m^2/m^2). Different letters indicate significant differences between populations at $P \leq 0.05$ (One-way ANOVA; Tukey test). The coefficient of variation (CV) in each trait. The significance of Population (Elevation) is shown as NS, non-significant; **$P < 0.01$; ***$P < 0.001$.

Elevation (m)	A_l (m^2)	H (m)	A_c (m^2)	A_s:A_l ($m^2\ m^{-2}$)	LAI ($m^2\ m^{-2}$)
1940	10.7 ± 2.4[a]	2.80 ± 0.37[a]	3.15 ± 0.51[a]	2.67 ± 0.22[a]	3.58 ± 1.04
1521	7.6 ± 2.2[abc]	2.62 ± 0.28[a]	2.44 ± 0.98[abc]	2.55 ± 0.01[a]	3.36 ± 1.95
1301	8.6 ± 2.1[abc]	3.08 ± 0.30[ab]	2.86 ± 0.67[ab]	2.53 ± 0.14[a]	3.12 ± 0.52
1212	9.8 ± 2.3[ab]	2.69 ± 0.37[a]	2.25 ± 0.40[bc]	2.65 ± 0.18[a]	4.44 ± 1.42
988	6.9 ± 1.7[abc]	3.06 ± 0.31[ab]	2.25 ± 0.40[bc]	3.54 ± 0.07[b]	3.05 ± 0.67
666	6.7 ± 2.2[bc]	3.10 ± 0.43[ab]	2.42 ± 0.68[abc]	4.21 ± 0.21[c]	2.81 ± 0.85
161	5.6 ± 2.1[c]	3.46 ± 0.35[b]	1.83 ± 0.36[c]	3.52 ± 0.07[c]	3.19 ± 0.72
72	8.3 ± 2.8[abc]	3.07 ± 0.67[ab]	2.03 ± 0.66[bc]	3.90 ± 0.18[bc]	3.47 ± 0.96
CV	33.1	15.5	12.7	20.2	33.9
Population	**	***	***	***	**NS**

Table S2.5. Results of Mean ± standard density (n=48) of woods traits of *Populus fremontii* at population (Elevation) level in the Agua Fria National Monument common garden D_{stem} (specific stem density, g/cm^3), A_{sl} (stem lumen area, µm^2), Hd_s (stem hydraulic mean diameter, µm), F_{sl} (stem lumen fraction, µm^2), stem bark percentage (F_b, %), Ψ_{md} (mid-day water potentials, MPa), Ψ_{pd} (pre-dawn water potential, MPa). Different letters indicate significant differences between populations at P ≤ 0.05 (One-way ANOVA; Tukey test). The coefficient of variation (CV) in each trait. The significance of Population (Elevation) is shown as NS, non-significant; .< 0.1; **P < 0.01; ***P < 0.001.

| Elevation (m)	D_{stem} (g cm^{-3})	F_b (%)	A_{sl} (µm^2)	Hd_s (µm)	F_{sl} (µm^2 µm^{-2})	D_{sv} (#vessels mm^{-2})	Ψ_{md} (Mpa)	Ψ_{pd} (Mpa)
1940	0.43 ± 0.012[ab]	0.40 ± 0.060[a]	686 ± 134	38.1 ± 4.5	0.228 ± 0.077	345 ± 109	-0.48 ± 0.076	-1.33 ± 0.15[a]
1521	0.45 ± 0.006[a]	0.41 ± 0.063a	651 ± 174	37.3 ± 4.3	0.188 ± 0.022	311 ± 78	-0.40 ± 0.82	-1.38 ± 0.11[ab]
1301	0.43 ± 0.044[ab]	0.36 ± 0.036[a]	698 ± 172	37.4 ± 5.3	0.183 ± 0.040	281 ± 64	-0.44 ± 0.085	-1.43 ± 0.12[abc]
1212	0.39 ± 0.024[b]	0.28 ± 0.056[ab]	747 ± 202	39.8 ± 2.9	0.232 ± 0.041	326 ± 83	-0.43 ± 0.016	-1.51 ± 0.16[abc]
988	0.42 ± 0.031[ab]	0.22 ± 0.054[b]	697 ± 79	40.3 ± 2.8	0.229 ± 0.036	329 ± 42	-0.45 ± 0.031	-1.56 ± 0.11[abc]
666	0.40 ± 0.017[ab]	0.32 ± 0.062[ab]	831 ± 211	40.5 ± 4.3	0.248 ± 0.030	333 ± 117	-0.48 ± 0.037	-1.65 ± 0.10[c]
161	0.41 ± 0.043[ab]	0.29 ± 0.021[ab]	674 ± 164	38.4 ± 5.3	0.221 ± 0.045	344 ± 71	-0.45 ± 0.057	-1.52 ± 0.16[abc]
72	0.40 ± 0.020[ab]	0.31 ± 0.037[ab]	942 ± 193	43.1 ± 3.6	0.238 ± 0.025	261 ± 54	-0.44 ± 0.056	-1.64 ± 0.13[bc]
CV	7.72	22.95	24.7	11.0	20.5	25.32	13.5	11.1
Population	*	**	*	.	NS	NS	NS	***
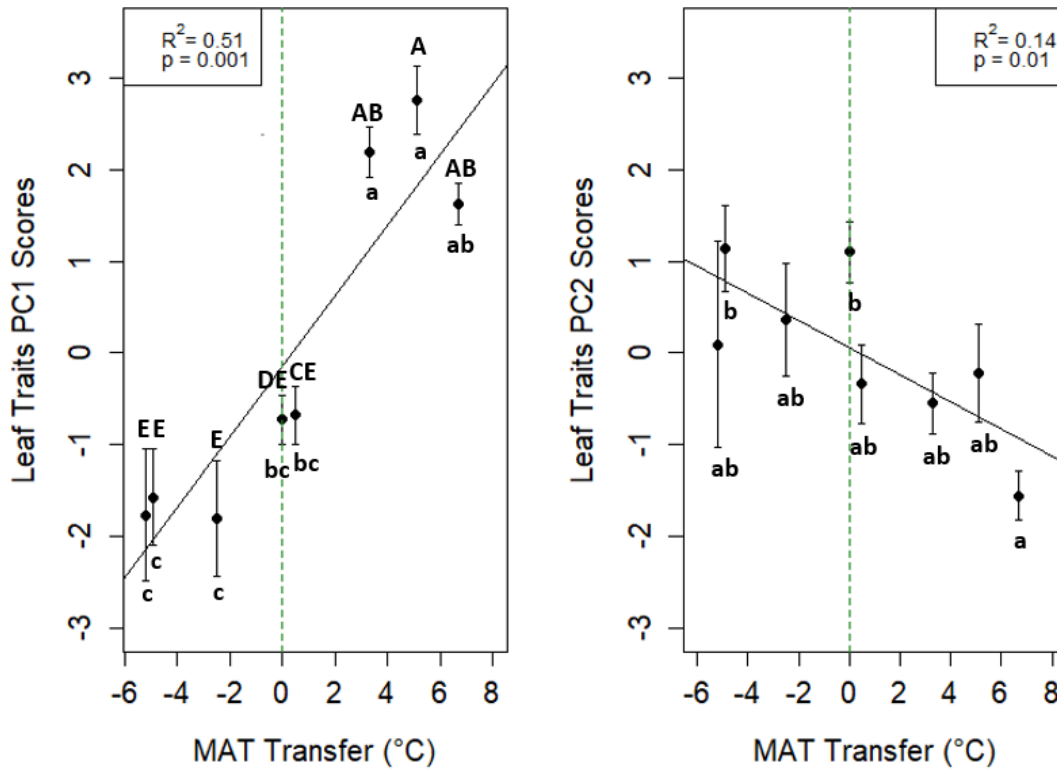
Figure S2.1. Relationship of the eight source populations mean annual temperature transfer with principal component 1 and 2 loadings of the within leaf traits spectrum PCA. Vertical bars represent standard errors (i.e., variation of genotypes within populations) and vertical dotted lines indicate the mean annual temperature (MAT °C) of the garden. Populations with different lowercase letters next to the data points indicate significant pairwise differences in PC1 scores using Tukey's HSD test. Populations with different capital letters on the top of the error bars in indicate significant pairwise differences using PERMANOVA and pairwise permutation MANOVAs on all traits simultaneously.
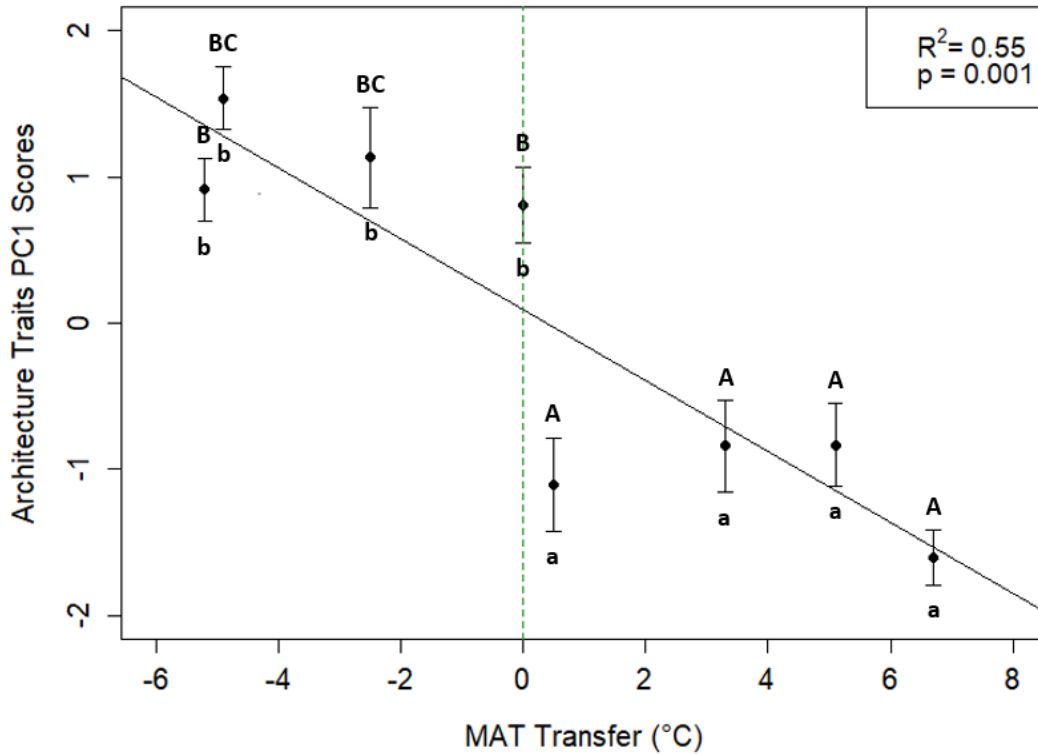
215

Figure S2.2. Relationship of the 8-source population mean annual temperature transfer with Principal component 1 loadings of the within architecture traits spectrum PCA. Vertical bars represent standard errors (i.e., variation of genotypes within populations) and vertical dotted lines indicate the mean annual temperature (MAT °C) of the garden. Populations with different lowercase letters next to the data points indicate significant pairwise differences in PC1 scores using Tukey's HSD test. Populations with different capital letters left to the data points indicate significant pairwise differences using PERMANOVA and pairwise permutation MANOVAs on all architecture traits simultaneously.
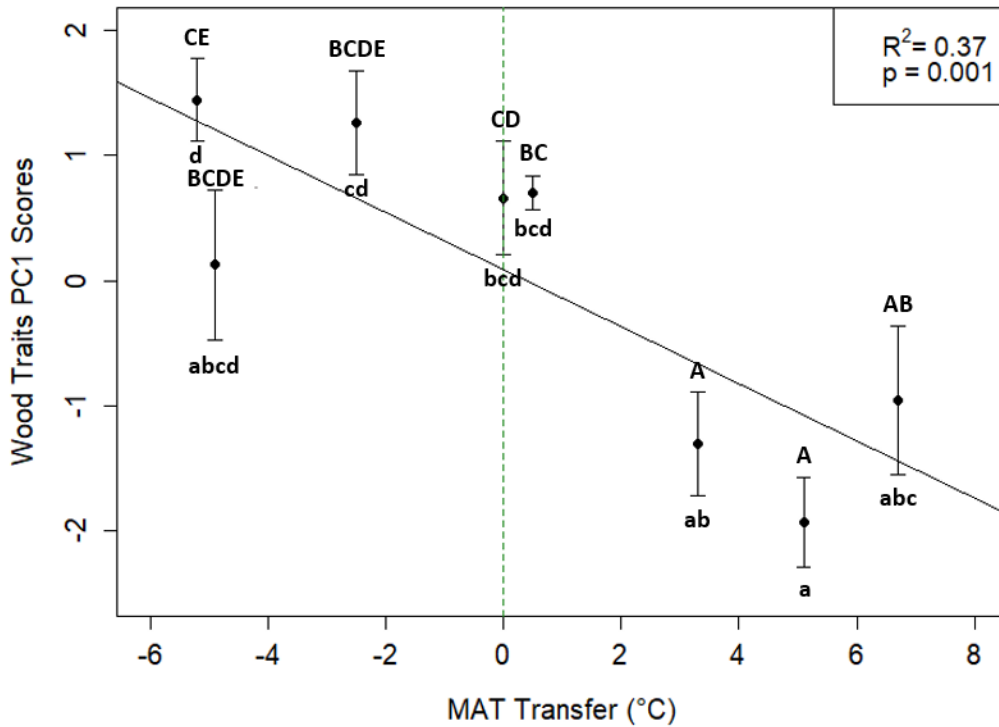
Figure S2.3. Relationship of the 8-source population mean annual temperature transfer with Principal component 1 loadings of the within wood traits spectrum PCA. Vertical bars represent standard errors (i.e., variation of genotypes within populations) and vertical dotted lines indicate the mean annual temperature (MAT °C) of the garden. Populations with different lowercase letters indicate significant pairwise differences in PC1 scores using Tukey's HSD test. Populations with different capital letters indicate significant pairwise differences using PERMANOVA and pairwise permutation MANOVAs on all wood traits simultaneously.
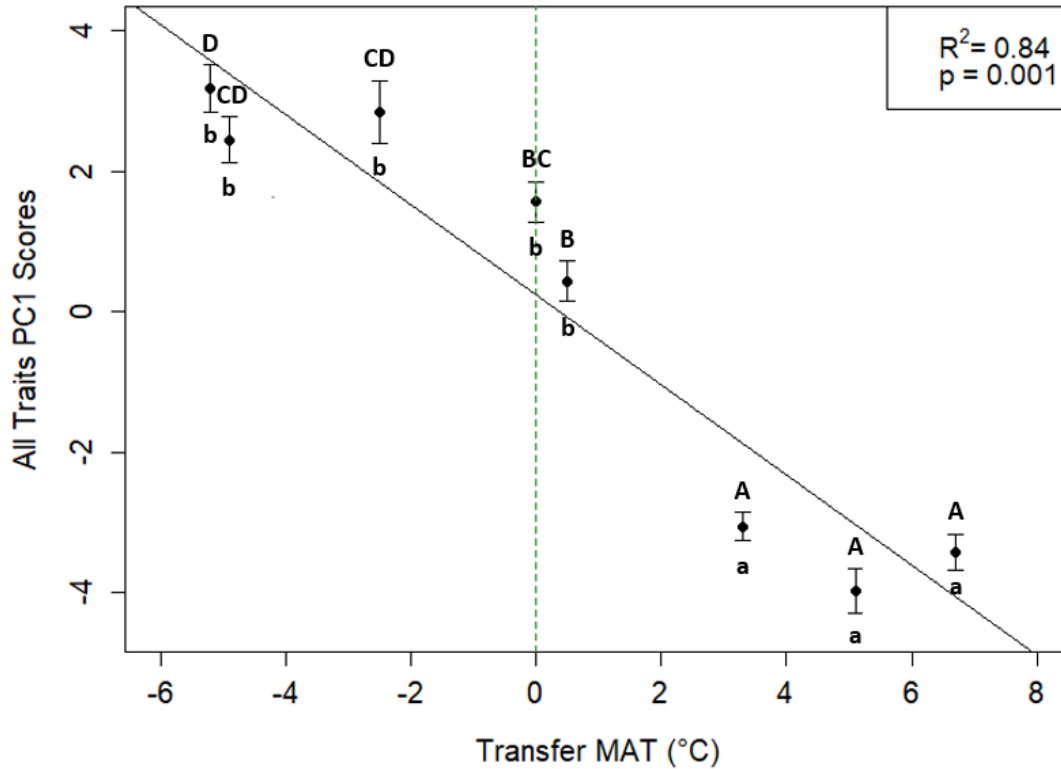
Figure S2.4. Relationship of the 8 source population elevations with PC1 loadings of all 27 traits spectrum PCA. Vertical bars represent standard errors (i.e., variation of genotypes within populations) and vertical dotted lines indicate the mean annual temperature (MAT °C) of the garden. Populations with different lowercase letters indicate significant pairwise differences in PC1 scores using Tukey's HSD test. Populations with different capital letters indicate significant pairwise differences using PERMANOVA and pairwise permutation MANOVAs on all traits simultaneously.

APPENDIX B

SUPPLEMENTAL TABLES AND FIGURES FOR CHAPTER 3

Table S3.1. Mixed-model repeated measures ANOVA results of mid-day water potential (Ψ_{md}, MPa) in *Populus fremontii* trees occurring at an experimental common garden at the Agua Fria National Monument in 2017 growing season. Data was collected on June 6 (day 157), June 29 (day 180), July 27 (day 208), and August 24 (day 236).

	Df	Sum Sq	Mean Sq	F value	Pr(>F)
Between-subject effects					
Population	1	1.350	1.3499	11.626	0.0015**
Month	1	0.067	0.0673	0.579	0.4510
Residuals	40	4.644	0.1161		
Within-subject effect					
Month	4	39.59	9.898	105.431	< 2e-16 ***
Population:Month	4	0.49	0.123	1.313	0.267
Residuals	159	14.93	0.094		

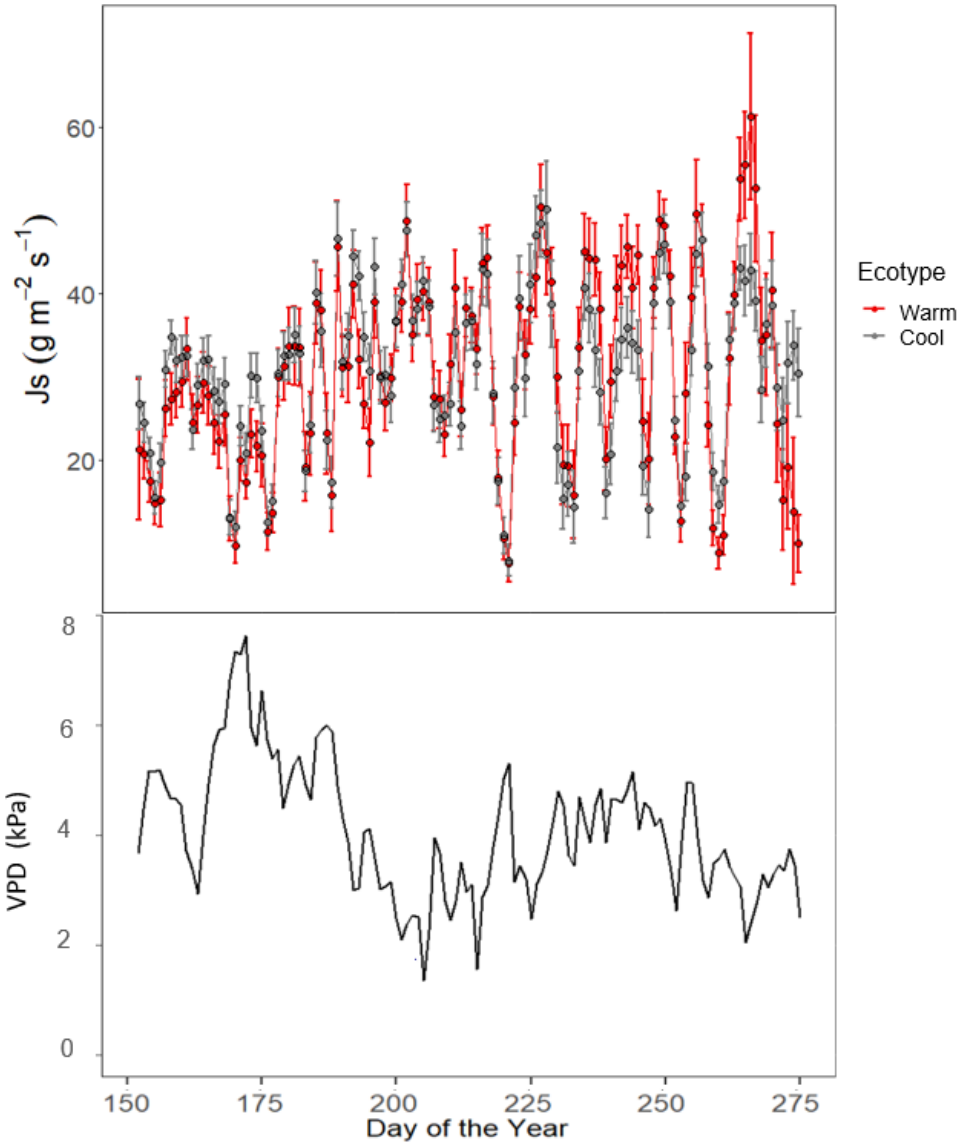† Signif. codes: 0 *** 0.001 ** 0.01 * 0.05 . 0.1 1

Figure S3.1. Mean daily sap-flux scaled measured between the hours of 1,100 and 1,900 from day of year 158 (June 7th) to day of year 275 (October 2nd) of the 2017 growing season on 24 warm- adapted genotypes and 32 cool adapted genotypes occurring in a common garden in central Arizona. Error bars represent the standard errors of the mean. Warm-adapted ecotypes were sourced from cuttings of mature *Populus fremontii* trees occurring along the species warmest edge of its thermal distribution (n=24 genotypes). Cool-adapted ecotypes were sourced from cuttings of mature *P.fremontii* trees occurring along the species colder edge of its thermal distribution (n = 32 genotypes).
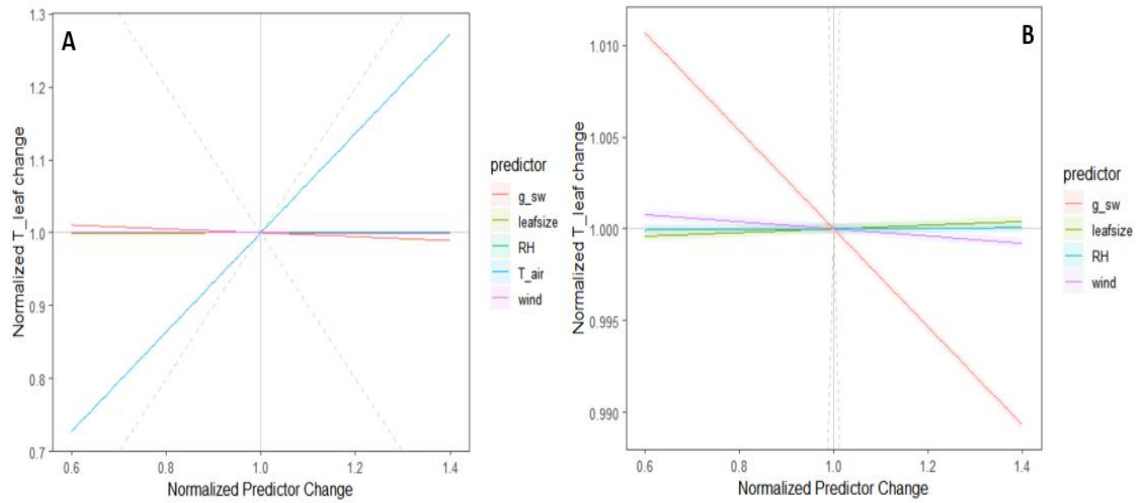
Figure S3.2. (a) Representation of the effect of the temperature of the air (T_air), stomata conductance (g_sw), leaf size (leafsize), relative humity (RH), and wind speed (wind) on energy balanced estimations of changes in leaf temperature. (b) Representation of the effect of stomata conductance (g_sw), leaf size (leafsize), and relative humity (RH) on energy balanced estimations of changes in leaf temperature.
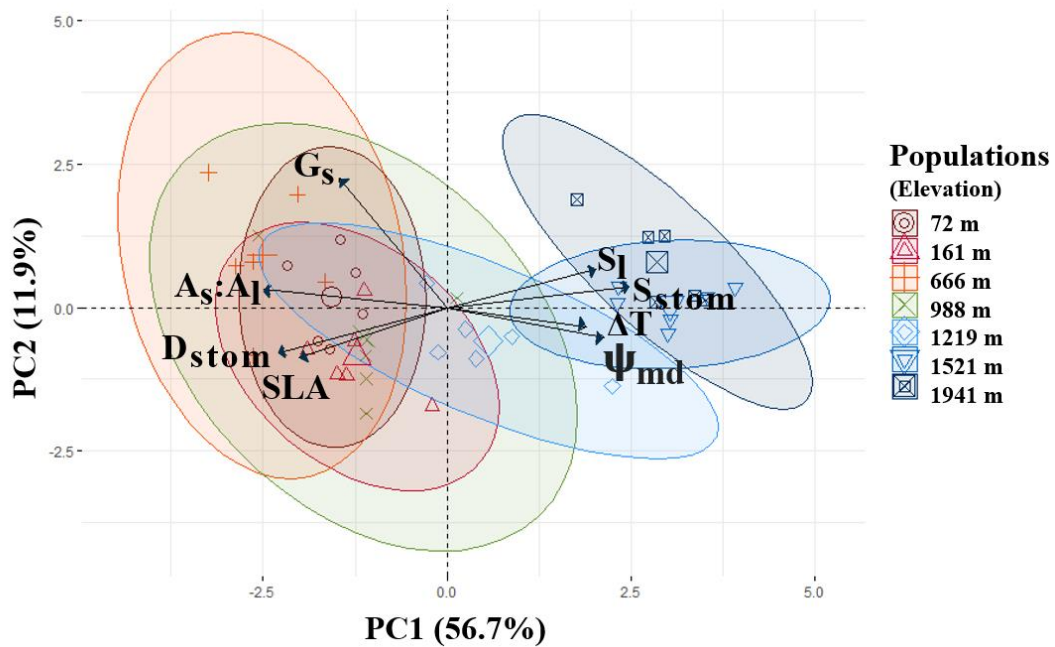
Figure S3.3. Principal component analysis (PCA) summarizing the relationship between seven morphophysiological traits (A_{il}, A_s:A_l, D_{stom}, G_s, Ψ_{md}, SLA and S_{stom}) and the leaf-to-air temperature differences at genotype level. 95% prediction ellipses represent the 7 source populations that collectively represent the entire elevational range of *Populus fremontii*. X and Y axis show principal component 1 and principal component 2 that explain 57.3% and 13.6% of the total variance, respectively.

APPENDIX C

SUPPLEMENTAL TABLES AND FIGURES FOR CHAPTER 4

Table S4.1. Annual environmental parameters in the PVER garden: mean annual maximum temperature (MAMT$_{PVER}$) and mean annual vapor pressure deficit (VPD$_{PVER}$).

Year	Mean annual maximum temperature (MAMT$_{PVER}$) (°C)	Vapor pressure deficit (VPD$_{PVER}$) (hPa)
2011	30.1	36.4
2012	30.9	38.8
2013	30.7	37.4
2014	30.8	38.6

APPENDIX D

STATEMENT OF CO-AUTHOR PERMISSION

STATEMENT OF CO-AUTHOR PERMISSION

The information in Chapter 2-4 of my dissertation has been or will be submitted for review in peer-reviewed journals. Each journal submission has been or will be co-authored by Dr. Kevin Hultine. Chapter 2 and 3 were additionally co-authored by Dan F. Koepke, Dr. Kevin C. Grady, Dr. Gerard J. Allan, Dr. Catherine A. Gehring, Dr. Thomas G. Whitham. Additionally, Chapter 2 was coauthored by Dr. Samuel A. Cushman and chapter 3 by Dr. Susan E. Bush, and Dr. Thomas A. Day. Chapter 4 will be co-authored by Dr. John Roden and Dr. Drew Peltier.